

University of Nottingham

UK | CHINA | MALAYSIA

The role of the vitamin D axis in skeletal muscle physiology: a multi-modal approach

Shelby Erika Bollen

BSc. (2017), MSc (2018)

This thesis is submitted to the University of Nottingham for the degree of Doctor of Philosophy

April 2024

Abstract

Despite vitamin D deficiency clinically presenting with myopathy, muscle weakness, and atrophy, the mechanisms by which vitamin D exerts its regulatory effects upon skeletal muscle remain to be fully established. Recent studies have shown that the receptor by which 1α,25-dihydroxyvitamin D_3 ($1,25(OH)_2D_3$) exerts its biological actions (i.e., the vitamin D receptor, VDR) elicits both genomic and non-genomic effects, i.e. modulation of proteostasis, mitochondria and signalling cascades, within skeletal muscle. Relative to more well-studied targets such as the skeleton, the impact of genetic variation within key vitamin D-related genes upon skeletal muscle is unclear. Identifying genetic variants capable of influencing musculoskeletal physiology may allow identification of those genetically predisposed to perturbed muscle mass and function. Therefore, this thesis aimed to explore the impact of genetic variation within the vitamin D system upon skeletal muscle function and to investigate the potential underlying mechanisms *in vitro*.

This thesis begins with **Chapter 1**, which presents a narrative literature review of vitamin D physiology and the evidence suggesting a regulatory role for this endocrine system in skeletal muscle. In **Chapter 2**, a systematic review was conducted that examines the impact of genetic variance in key targets of the vitamin D pathway upon skeletal muscle function. This chapter revealed that, within the vitamin D system, the *VDR* gene is the primary gene of which associations between single nucleotide polymorphisms (SNPs) and muscle function have been investigated and, of all SNPs investigated, only A1012G was consistently associated with higher handgrip strength.

Based on the results of **Chapter 2**, six *VDR* and two vitamin D binding protein (DBP; *Gc*) gene SNPs were selected and their potential relationship with neuromuscular performance and musculoskeletal characteristics was evaluated in a cohort of elite male master athletes (MA) and non-athletic controls in **Chapter 3.** The results confirmed an association between A1012G and greater muscle/physical function and highlighted novel links between the vitamin D system and sex hormones in muscle. According to the current literature, this was the first study to explore the impact of the two key *GC* SNPs, rs4588 and rs7041, upon multiple parameters of musculoskeletal physiology. It appears that the two SNPs studied here had differing effects, as carriers of rs4588 displayed higher knee extensor strength and peak quadriceps cross-sectional area (CSA), whereas individuals carrying rs7041 had reduced bone mineral density (BMD) than non-carriers.

To explore and provide potential mechanisms underlying *VDR* SNPs, RNA interference (RNAi) was used to silence the *Vdr* gene in C2C12 myotubes in **Chapter 4**. For the first time, VDR-KD myotubes were also exposed for 24 hours to conditions that are frequent to skeletal muscle: insulin growth factor 1 (IGF-1), dexamethasone (Dex), and lipopolysaccharides (LPS; from *E.coli*). VDR-KD resulted in altered myogenic signalling, downregulation of anabolic targets, and impaired mitochondrial respiratory activity. In the absence of VDR, IGF-1 was unable to activate the PI3K/Akt/mTOR pathway and it appears that VDR is not involved in IGF-1 regulation of autophagy. For the first time, Dex was found to upregulate *Vdr* expression, as demonstrated in NC myotubes. In addition, *Vdr* expression and DBP protein levels were downregulated following LPS exposure which may contribute to the pro-

inflammatory environment generated by LPS in skeletal muscle. Finally, exposure of VDR-KD myotubes to each of the three conditions increased mitochondrial respiratory activity in Complex I and Complexes I and II combined. As a novel relationship was demonstrated between two SNPs of the gene encoding DBP (*Gc*) and musculoskeletal parameters in **Chapter 3,** this was explored further by silencing DBP (DBP-KD) in C2C12 myotubes in **Chapter 5.** Loss of DBP resulted in the formation of dysmorphic myotubes, altered myogenic signalling, and perturbed expression of α- and β-tubulin. In addition, anabolic signalling was impaired by DBP-KD with perturbation of GLUT1 and GLUT4 expression and, finally, downregulation of *Vdr* and *Cubn* mRNA expression.

Publications

Bollen SE, Bass, JJ, Wilkinson, DJ, Hewison, M, Atherton, PJ. The Impact of Genetic Variation within the Vitamin D Pathway Upon Skeletal Muscle Function: A Systematic Review. *Journal of Steroid Biochemistry and Molecular Biology*. 2023; 229.

Bollen SE, Bass, JJ, Fujita, S, Wilkinson, DJ, Hewison, M, Atherton, PJ. The Vitamin D/Vitamin D receptor (VDR) axis in muscle atrophy and sarcopenia. *Cellular Signalling*. 2022; 96.

Bollen SE, Atherton, PJ. Myogenic, genomic and non-genomic influences of the vitamin D axis in skeletal muscle. *Cell Biochemistry and Function*. 2020; 39(1).

Presentations

Oral Presentations

Bollen SE, Bass JJ, Crossland, H, Piasecki, J, McPhee, JS, Piasecki, M, Wilkinson DJ, Hewison M, Atherton PJ. Vitamin D receptor and vitamin D binding protein polymorphisms are associated with skeletal muscle function and physiology in elite master athletes. (2022). Vitamin D Workshop, Austin, USA.

Bollen SE, Bass JJ, Crossland, H, Piasecki, J, McPhee, JS, Piasecki, M, Wilkinson DJ, Hewison M, Atherton PJ. The Impact of Genetic Variation Within the Vitamin D Pathway Upon Skeletal Muscle Function: A Systematic Review & Validation Study. (2022). Sue Watson Research Event, University of Nottingham.

Bollen SE, Crossland, H, Bass, JJ, Wilkinson, DJ, Hewison, M, Atherton, PJ. Validation and Optimisation of a Tetra-Primer Amplification Refractory System (Tetra-ARMS) Assay for Rapid and Cost-Effective Detection of Single Nucleotide Polymorphisms of the VDR. (2021) Society of Endocrinology, Physical Activity and the Endocrine System.

Poster Presentations

Bollen SE, Bass JJ, Crossland, H, Piasecki, J, McPhee, JS, Piasecki, M, Wilkinson DJ, Hewison M, Atherton PJ. The association of vitamin D binding protein gene (GC) single nucleotide polymorphisms with skeletal muscle function and performance in master athletes. (2022). The Physiological Society, Europhysiology, Copenhagen, Denmark.

Bollen SE, Bass JJ, Crossland, H, Piasecki, J, McPhee, JS, Piasecki, M, Wilkinson DJ, Hewison M, Atherton PJ. The Impact of Genetic Variation Within the Vitamin D Pathway Upon Skeletal Muscle Function: A Systematic Review & Validation Study. (2022) The Physiological Society, The Biomedical Basis of Elite Performance, Nottingham, UK. Poster Presentation.

Bollen SE, Bass JJ, Wilkinson DJ, Hewison M, Atherton PJ. 'The Impact of Genetic Variation Within the Vitamin D Pathway Upon Skeletal Muscle Function: A Systematic Review' (2021). Vitamin D Workshop, Online Poster Presentation.

Awards

2022 Vitamin D Workshop, Ron Horst Presentation Award
2022 The Physiological Society, Professional Development Award
2022 Sue Watson Research Event, First Prize
2021 Vitamin D Workshop, Trainee Scholarship

COVID-19 Impact Statement

Given the widespread impact of the COVID-19 pandemic, it is important to consider its influence upon the research conducted throughout my PhD studies. Following the initial COVID-19 outbreak, The University of Nottingham closed in March 2020 with all access to laboratories being prohibited until October 2020. Initially, the plan was to conduct a clinical trial investigating vitamin D supplementation in older humans, but the nationwide restrictions put in place made recruitment impossible. To counteract this, I designed and received ethical approval for a clinical trial investigating the efficacy of vitamin D supplementation in individuals experiencing long-term symptoms post COVID-19 infection. While recruitment was initially promising, human research was then, again, put on hold until Summer 2021, at which point local GP-lead research prevented us from recruiting anyone who was already within the NHS pathway. The subsequent impact on recruitment was enormous and lead to us having too low participant numbers for the data to be included in this final thesis. In addition, a large component of this thesis uses cellular models and this work unfortunately experienced lengthy delays on reagents due to the prioritisation of vaccine development and synthesis. Some reagents took up to 6 months to arrive, which caused significant delays to experimental timelines. To add to this, despite laboratories re-opening in October 2020, strict restrictions around out-of-hours research meant that it took a considerable amount of time for my out-of-hours to be approved by the school, so I was unable to start any cell-based work until I received the approval (early 2021). However, given these difficulties, the work presented in this final thesis represents the progress achieved despite the circumstances faced.

Acknowledgments

First and foremost, I would like to express my utmost gratitude to my supervisors, Professor Philip Atherton, Professor Martin Hewison, and Dr Daniel Wilkinson. There are no words to express how grateful I am for all of your support and guidance, and the opportunities that you all made possible for me. The experiences I gained during my PhD were above and beyond anything I could have ever dreamed of, so I will be forever thankful for you all giving me the opportunity to work on this research.

I would also like to thank all of the COMAP group at Derby, past and present. My time spent working with you all has genuinely been amazing, and it is difficult to relay just how thankful I am for all your advice, support, and friendship. A special thanks has to go to Dr Joseph Bass and Dr Hannah Crossland for putting up with my constant stream of questions and queries. When I started out on this PhD journey it seemed like I had a mountain to climb, but you both helped me to grow into the researcher I am today.

A million thank yous to my incredible family for the lifetime of support you have given me. I will always be eternally grateful to have gone through this process knowing that I have you all rooting for me the whole way through. Piers, you were what got me through the loneliness of the pandemic, the failed experiments, and the thesis writing. I am forever grateful for you being there to vent to, even when you had no idea what a cell or a western blot was.

Finally, this thesis is dedicated to my 18-year-old self. None of this would be possible without your determination, resilience, and sheer stubbornness. Science is hard and brain injuries are really hard, so together they may seem like an impossible combination, but you got us here (somehow).

Declaration

DNA samples for the study in **Chapter 3** were provided from a previous study completed at the University of Nottingham by Dr Hannah Crossland and Dr Mathew Piasecki. All participant data presented in **Chapter 3** was collected in a previous study and was provided by Dr Mathew Piasecki. The data in this thesis was collected and analysed by myself unless otherwise acknowledged. I declare that this thesis has been constructed by myself and that all the data presented are my own work unless otherwise stated. All published literature within this thesis has been appropriately referenced. None of the data presented in this thesis has been submitted towards the assessment of a higher degree previously. Elements of this thesis have been published as peer-reviewed papers:

Chapter 1:

Bollen SE, Bass, JJ, Fujita, S, Wilkinson, DJ, Hewison, M, Atherton, PJ. The Vitamin D/Vitamin D receptor (VDR) axis in muscle atrophy and sarcopenia. *Cellular Signalling*. 2022; 96. [1]

Bollen SE, Atherton, PJ. Myogenic, genomic and non-genomic influences of the vitamin D axis in skeletal muscle. *Cell Biochemistry and Function*. 2020; 39(1). [2]

Chapter 2:

Bollen SE, Bass, JJ, Wilkinson, DJ, Hewison, M, Atherton, PJ. The Impact of Genetic Variation within the Vitamin D Pathway Upon Skeletal Muscle Function: A Systematic Review. *Journal of Steroid Biochemistry and Molecular Biology*. 2023; 229. [3]

Shelby Bollen,

April 2024

List of Abbreviations

$1\alpha,25(OH)_2D_3$	1,25-dihydroxyvitamin D_3
$1\alpha,24,25(OH)_3D_3$	1,24,25-trihydroxyvitamin D_3
$24,25(OH)D_2D_3$	24,25-dihydroxyvitamin D_3
$25(OH)D_3$	25-hydroxyvitamin D_3
4EBP1	eukaryotic translation initiation factor 4E-binding protein
7-DHC	7-dehydrocholesterol
AA	amino acid
ADL	activities of daily life
ADP	adenosine diphosphate
AFFM	appendicular fat-free mass
AKI	acute kidney injury
Akt	AKT serine/threonine kinase 1
ALM	appendicular lean mass
AMPK	adenosine monophosphate-activated protein kinase
ANOVA	analysis of variance
ASM	appendicular skeletal muscle mass
Asp	aspartate
ATP	adenosine triphosphate
β-Gal	β-galactosidase
BMC	bone mineral content
BMD	bone mineral density
BMI	body mass index
bp	base pairs
BrdU	bromodeoxyuridine
Ca^{2+}	calcium
$[Ca^{2+}]_i$	intracellular calcium
CBB	coomassie brilliant blue
CDK	cyclin dependent kinase
CDKI	CDK inhibitor
cDNA	complementary DNA

CI	complex I
CI+II	complexes I+II combined
CII	complex II
Cl^-	chloride
cm	centimetres
CO_2	carbon dioxide
COPD	chronic obstructive pulmonary disease
CS	citrate synthase
CSA	cross-sectional area
c-Src	proto-oncogene tyrosine-protein kinase Src
CYP2R1	25-hydroxylase
CYP24A1	24-hydroxylase
CYP27B1	1α-hydroxylase
DBD	DNA-binding domain
DBP	vitamin D binding protein
DBP-MAF	macrophage activating factor
Dex	dexamethasone
DHCR7	7-dehydrocholesterol reductase
DHEA	dehydroepiandrosterone
DHEAS	DHEA sulphate
DHT	dihydrotestosterone
DMEM	dulbecco's modified eagle medium
DNA	deoxyribonucleic acid
DXA	dual-energy X-ray absorptiometry
E2	oestradiol
EASS	extracellular actin scavenging system
EDTA	ethylenediaminetetraacetic acid
EE	elbow extension
EF	elbow flexion
EGTA	ethylene-bis(oxyethylenenitrilo)tetraacetic acid
EIF4E	eukaryotic translation initiation factor 4E

ERK	extracellular signal-related kinase
ET	maximal respiratory capacity
ETC	electron transport chain
F-actin	filamentous actin
FBS	fetal bovine serum
FCCP	carbonyl cyanide p-trifluoromethoxyphenylhydrazone
FGF23	fibroblast growth factor 23
FOXO	forkhead box protein
FFM	fat-free mass
F_{max}	maximum force
g	gram
g	g force
G	glutamate
GA	gastrocnemius
G-actin	globular actin
GAPDH	glyceraldehyde 3-phosphate dehydrogenase
Gc	group-specific component
Glu	glutamine
GSK3β	glycogen synthase kinase 3β
GTP	guanosine triphosphate
GWAS	genome wide association study
HDAC9	histone deacetylase 9
HGS	handgrip strength
H_{max}	maximum jump height
HRP	horseradish peroxidase
Hz	hertz
ICU	intensive care unit
IFM	interfibrillar mitochondria
IGF-1	insulin-like growth factor1
IL-1β	interleukin 1β
IL-6	interleukin 6

IVE	*in vivo* electrotransfer
KD	knock-down
kDa	kilodalton
KE	knee extension
KF	knee flexion
kg	kilogram
KO	knock out
L	litre
LBD	ligand-binding domain
LC3B-II	light chain 3B-II
LC-MS/MS	liquid chromatography-tandem mass spectrometry
LD	linkage disequilibrium
LPS	lipopolysaccharides
Lys	Lysine
M	molar
M	malate
MA	master athlete
MAFbx	muscle atrophy F-box protein
MAPK	mitogen activated protein kinase
MBR	muscle-to-bone ratio
mg	milligram
MHC	myosin heavy chain
MiR05	mitochondrial respiration media
mL	millilitre
mm	millimetres
MMP	matrix metalloproteinase
MPB	muscle protein breakdown
MPS	muscle protein synthesis
MRF	myogenic regulatory factor
MRI	magnetic resonance imaging
mRNA	messenger RNA

MT	microtubule
mtDNA	mitochondrial DNA
mTOR	mechanistic target of rapamycin
MuRF1	muscle RING-finger protein 1
MVC	maximal voluntary contraction
mVDR-KO	myocyte specific VDR knock out
Myf5	myogenic factor 5
MyoD1	myoblast determination protein 1
MyoG	myogenin
NAD	nicotinamide adenine dinucleotide
NaF	sodium fluoride
NaGal	N-acetyl-galactosamine
Na_3VO_4	sodium orthovanadate
NC	negative control
NF-kB	nuclear factor kappa B
ng	nanogram
NICE	National Institute for Health & Care Excellence
nm	nanometres
nM	nanomolar
NPB	net protein balance
NR	nuclear receptor
O_2	oxygen
OCR	oxygen consumption rate
OE	overexpression
OXPHOS	oxidative phosphorylation
P	pyruvate
P_i	phosphate
p70S6K	ribosomal protein S6 kinase β-1
PAGE	polyacrylamide gel electrophoresis
PCNA	proliferating cell nuclear antigen
PCR	polymerase chain reaction

PI3K	phosphatidylinositol 3-kinase
PKC	protein kinase C
PKCα	protein kinase C α
P_{max}	absolute vertical jump power
P_{max}Rel	absolute vertical jump power relative to body weight
pmol	picomolar
PTH	parathyroid hormone
PTM	post-translational modification
PVDF	polyvinylidene fluoride
qRT-PCR	quantitative reverse transcriptase PCR
Raf-1	proto-oncogene serine/threonine-protein kinase
RCT	randomised controlled trial
RNA	ribonucleic acid
RNAi	RNA interference
RNAseq	RNA sequencing
ROS	reactive oxygen species
rpm	revolutions per minute
rps6	ribosomal protein S6
RTP	room temperature and pressure
RXRα	retinoid X receptor-α
SA-β-Gal	senescence associated β-galactosidase
SDS	sodium dodecyl sulphate
Ser	serine
Serca	sarcoplasmic reticulum calcium transport ATPase
SHBG	sex hormone binding globulin
shRNA	short hairpin RNA
siRNA	small interfering RNA
SIRT1	sirtuin-1
SMI	skeletal muscle index
SNP	single nucleotide polymorphism
SOCE	store-operated calcium entry

SPPB	short physical performance battery
SSM	subsarcolemmal mitochondria
STS5	five times sit-to-stand test
TA	tibialis anterior
TBST	Tris buffered saline with Tween 20
TCA	tricarboxylic acid
TD	terminally differentiated
TE	trunk extension
tetra-ARMS	tetra-primer amplification refractory mutation system
TF	trunk flexion
THEM4	thioesterase superfamily member 4
Thr	threonine
TNFα	tumour necrosis factor α
Tris-HCl	tris-hydrochloride
TRP-C	transient receptor potential-canonical
TSC2	tuberous sclerosis complex 2
TUG	timed up and go
ULK1	uncoordinated 51-like kinase 1
UPP	ubiquitin-proteasomal pathway
UTR	untranslated region
UVB	ultraviolet B
V	volts
VDCC	L-type voltage-dependent calcium channel
VDR	vitamin D receptor
VDRE	vitamin D response element
VIBE	Vertical Impact on Bone Health in Elderly
VL	vastus lateralis
v/v	volume/volume
W	watts
WT	wildtype
µg	microgram

µl	microlitres
µM	micromolar

Throughout this thesis, the following gene nomenclature was used:

- Humans – all letters upper case (e.g. *GAPDH*)
- Mice/rats – first letter upper case and all the rest lower case (e.g. *Gapdh*)

Table of Contents

ABSTRACT **2**

PUBLICATIONS **5**

PRESENTATIONS **5**

AWARDS **6**

COVID-19 IMPACT STATEMENT **7**

ACKNOWLEDGMENTS **8**

DECLARATION **10**

LIST OF ABBREVIATIONS **11**

TABLE OF CONTENTS **19**

LIST OF TABLES **25**

CHAPTER 1: LITERATURE REVIEW **27**

1.1 Vitamin D Physiology 27
1.1.1 Sources of Vitamin D *27*
1.1.2 Vitamin D Metabolism *28*
1.1.4 Vitamin D Binding Protein *30*
1.1.3. Effects of Race and Differences in Ethnicity Upon Vitamin D Metabolism *33*
1.2 Mechanisms of Action of Vitamin D/VDR Axis 34
1.2.1 Vitamin D Receptor *34*
1.2.2 Genomic Mechanism of Action *35*
1.2.3 Non-Genomic Mechanism of Action *37*
1.3 The Vitamin D/VDR Axis and the Musculoskeletal System 39
1.3.1 Evidence from Human Studies *40*
1.3.2 VDR expression and skeletal muscle *42*
1.3.3 The Vitamin D/VDR Axis and Myogenesis *44*
1.3.4 Genomic Action of the Vitamin D/VDR Axis in Skeletal Muscle *49*
1.3.5 Non-genomic Regulation of Skeletal Muscle by the Vitamin D/VDR Axis *51*
1.3.5.1 Catabolic Pathways 52
1.3.5.2 Anabolic Pathways 55
1.3.5.3 Intracellular Calcium Homeostasis 58
1.3.5.4 Mitochondrial Function 60
1.3.6 DBP and Skeletal Muscle *62*
1.4 Thesis Aims 65

CHAPTER 2: THE IMPACT OF GENETIC VARIATION WITHIN THE VITAMIN D PATHWAY UPON SKELETAL MUSCLE FUNCTION: A SYSTEMATIC REVIEW **66**

2.1 Introduction 66
2.2 Materials and Methods 68
2.2.1 Search Strategy & Study Selection *68*
2.2.2 Inclusion Criteria *69*
2.2.3 Data Extraction *69*
2.2.4 Quality Assessment *69*
2.3 Results 71
2.3.1 Demographics of Included Participants *81*
2.3.2 Quality of Included Studies *81*
2.3.2.1 VDR 81
2.3.2.2 Other Studied Genes of the Vitamin D System 84
2.4 Discussion 85
2.5 Future Directions and Conclusions 89

CHAPTER 3: THE ASSOCIATION OF VITAMIN D RECEPTOR (*VDR)* AND VITAMIN D BINDING PROTEIN GENE (*GC*) SINGLE NUCLEOTIDE POLYMORPHISMS WITH SKELETAL MUSCLE FUNCTION AND PERFORMANCE IN ELITE MASTER ATHLETES – A CANDIDATE GENE ASSOCIATION STUDY..... 91

3.1 INTRODUCTION 91
3.2 METHODS 95
3.2.1 Participants & Ethical Approval *95*
3.2.2 Anthropometric Measurements *95*
3.2.3 Muscle Strength and Physical Performance *96*
3.2.4 Jumping Mechanography. *98*
3.2.5 Biochemical Parameters *98*
3.2.6 Genetic DNA Extraction *98*
3.2.7 Genotyping - Primer Design *99*
3.2.8 Genotyping - Tetra-primer ARMS PCR & DNA Gel Electrophoresis *99*
3.2.9 Statistical Analyses. *100*
3.3 RESULTS 104
3.3.1 Study Population *104*
3.3.2 VDR & GC SNP Frequencies *105*
3.3.3 General Characteristics, body composition and VDR/GC single nucleotide polymorphisms *108*
3.3.4 Physical performance and VDR/GC polymorphisms. *110*
3.3.5 Muscle strength/function and VDR/GC polymorphisms *110*
3.3.6 Biochemical parameters and VDR/GC polymorphisms *112*
3.4 DISCUSSION 139
3.4.1 VDR SNPs. *139*
3.4.2 GC (DBP) SNPs *144*
3.4.3 Limitations *149*
3.5 CONCLUSIONS 151

CHAPTER 4: VDR REGULATES MYOGENIC/PROTEOLYTIC SIGNALLING AND MITOCHONDRIAL RESPIRATION IN RESPONSE TO ANABOLIC, CATABOLIC, AND PRO-INFLAMMATORY CONDITIONS IN C2C12 MYOTUBES. 152

4.1 INTRODUCTION 152
4.2 METHODS 158
4.2.1 Cell Culture *158*
4.2.2 RNA Interference *158*
4.2.3 Treatment of Cells *159*
4.2.4 High-Resolution Respirometry *159*
4.2.5 qRT-PCR *161*
4.2.7 Western Blotting *164*
4.2.8 Statistical Analysis. *165*
4.3 RESULTS 166
4.3.1 Successful generation of VDR-KD C2C12 myotubes. *166*
4.3.2 VDR knockdown in C2C12 myotubes results in altered mRNA and protein expression of key metabolic targets. *166*
4.3.3 Changes in gene expression & protein content of key metabolic targets in VDR-KD myotubes following exposure to hypertrophic, atrophic, and pro-inflammatory condiitions.. *171*
4.3.3.1 Altered Vdr levels following 24-hour stimulation of NC myotubes. 171
4.3.3.2 Hypertrophy – IGF-1 171
4.3.3.3 Atrophy - Dexamethasone 176
4.3.3.4 Inflammation - LPS 180
4.3.4 Changes in mitochondrial respiration following VDR knockdown in C2C12 myotubes... *184*
4.3.5 Changes in mitochondrial respiration in VDR-KD myotubes following exposure to hypertrophic, atrophic, and inflammatory conditions. *186*
4.3.5.1 Hypertrophy – IGF-1 187
4.3.5.2 Atrophy - Dexamethasone 189
4.3.5.3 Inflammation - LPS 191
4.4 DISCUSSION 193

4.4.1 Effects of VDR-KD *193*
4.4.2. Treatment of VDR-KD myotubes with the hypertrophic, atrophic, and pro-inflammatory conditions *201*
4.4.2.1. IGF-1 201
4.4.2.2. Dexamethasone 206
4.4.2.3. Lipopolysaccharide 210
4.4.2.4. Mitochondrial Function 216
4.4.3 Limitations *219*
4.5 CONCLUSIONS 223

CHAPTER 5: CHARACTERISATION OF LOSS OF THE VITAMIN D BINDING PROTEIN (DBP) GENE (*GC*) IN C2C12 MYOTUBES – A PRELIMINARY STUDY. **224**

5.1 INTRODUCTION 224
5.2 METHODS 228
5.2.1 Cell Culture *228*
5.2.2 RNA Interference *228*
5.2.3 Light Microscopy *229*
5.2.5 qRT-PCR *229*
5.2.6 Western Blotting *233*
5.2.8 Statistical Analysis. *234*
5.3 RESULTS 235
5.3.1 Successful generation of DBP-KD C2C12 Myotubes. *235*
5.3.2 Effect of DBP-KD upon C2C12 myotube morphology *235*
5.3.3 Effect of DBP knockdown in C2C12 myotubes upon mRNA and protein expression of key metabolic targets. *236*
5.3.3.1 Targets Related to Anabolism/Catabolism 237
5.3.3.2 Metabolic-Related Targets 237
5.3.3.3 Myogenic-Related Targets 238
5.3.3.4 Cytoskeletal & Sarcomeric-Related Targets 238
5.3.3.5 Glucose Trafficking-Related Targets 238
5.3.3.6 Vitamin D Axis-Related Targets 238
..... 240
5.4 DISCUSSION 242
5.4.1 Effects of DBP-KD *242*
5.4.2. Limitations *251*
5.4 CONCLUSIONS 253

CHAPTER 6: GENERAL DISCUSSION **254**

6.1 OVERVIEW OF AIMS 254
6.2 SUMMARY OF RESULTS 254
6.2.1. Chapter 2 – The impact of genetic variation within the vitamin D pathway upon skeletal muscle function: a systematic review. *254*
6.2.2. Chapter 3 – The association of vitamin D receptor (VDR) and vitamin D binding protein gene (GC) single nucleotide polymorphisms with skeletal muscle function and performance in elite master athletes – a candidate gene association study. *255*
6.2.3. Chapter 4 – VDR regulates myogenic/proteolytic signalling and mitochondrial respiration in response to anabolic, catabolic, and pro-inflammatory conditions in C2C12 myotubes. ... *256*
6.2.4 Chapter 5 – Characterisation of loss of the vitamin D binding protein (DBP) gene (Gc) in C2C12 myotubes – a preliminary study. *257*
6.3 FUTURE DIRECTIONS 258
6.3.1 Genetic Association Studies *258*
6.3.2 Mechanistic Studies *259*

REFERENCES **262**

List of Figures

Chapter 1

Figure 1.1: The genomic mechanism of vitamin D ($1,25(OH)_2D_3$). p36

Figure 1.2: The proposed non-genomic mechanisms of vitamin D ($1,25(OH)_2D_3$). p38

Figure 1.3: The proposed effects of $1,25(OH)_2D_3$ at the main stages of myogenesis. p45

Figure 1.4: Internalisation of DBP into skeletal muscle. p64

Chapter 2

Figure 2.1: A flow chart depicting the process of identifying and selecting articles for review. P71

Figure 2.2: The vitamin D system and key genes. P90

Chapter 4

Figure 4.1: Successful generation of VDR-KD C2C12 myotubes. p166

Figure 4.2: Effect of VDR-KD upon mRNA expression of key metabolic and myogenic targets as measured by qRT-PCR. p168

Figure 4.3: Effect of VDR-KD upon protein expression of key metabolic and myogenic targets as measured by western blotting. p169

Figure 4.4: Effect of 24-hour exposure to IGF-1, dexamethasone (Dex) and lipopolysaccharides (LPS) upon mRNA expression of *VDR* in NC myotubes, as measured by qRT-PCR. p171

Figure 4.5: Effect of 24-hour IGF-1 treatment upon mRNA expression of key metabolic and myogenic targets in NC and VDR-KD C2C12 myotubes, as measured by qRT-PCR. p173

Figure 4.6: Effect of 24-hour IGF-1 treatment upon protein expression of key metabolic and myogenic targets in NC and VDR-KD C2C12 myotubes, as measured by western blotting. p175

Figure 4.7: Effect of 24-hour dexamethasone (Dex) treatment upon mRNA expression of key metabolic and myogenic targets in NC and VDR-KD C2C12 myotubes, as measured by qRT-PCR. p177

Figure 4.8: Effect of 24-hour dexamethasone (Dex) treatment upon protein expression of key metabolic and myogenic targets in NC and VDR-KD C2C12 myotubes, as measured by western blotting. p179

Figure 4.9: Effect of 24-hour lipopolysaccharide (LPS) treatment upon mRNA expression of key metabolic and myogenic targets in NC and VDR-KD C2C12 myotubes, as measured by qRT-PCR. p181

Figure 4.10: Effect of 24-hour lipopolysaccharide (LPS) treatment upon protein expression of key metabolic and myogenic targets in NC and VDR-KD C2C12 myotubes, as measured by western blotting. p183

Figure 4.11: Representative high resolution respirometry trace for quantification of cellular respiration in permealised C2C12 myotubes. p185

Figure 4.12: Examination of cellular respiration in VDR-KD and NC C2C12 myotubes. p186

Figure 4.13: Examination of cellular respiration in VDR-KD and NC C2C12 myotubes following 24-hour IGF-1 treatment. p188

Figure 4.14: Examination of cellular respiration in VDR-KD and NC C2C12 myotubes following 24-hour Dex treatment. p190

Figure 4.15: Examination of cellular respiration in VDR-KD and NC C2C12 myotubes following 24-hour LPS treatment. p192

Chapter 5

Figure 5.1: Successful generation of DBP-KD C2C12 myotubes. p235

Figure 5.2: Light microscopy images of NC and DBP-KD C2C12 myotubes at day 5 differentiation displaying myotube disorganisation, branching, and overlapping in the DBP-KD group. p236

Figure 5.3: Effect of DBP-KD upon mRNA expression of key metabolic and myogenic targets as measured by qRT-PCR. p239

Figure 5.4: Effect of DBP-KD upon protein expression of key metabolic and myogenic targets as measured by western blotting. p240

List of Tables

Chapter 2

Table 2.1: Cross-sectional studies on associations of polymorphisms of vitamin D-related genes with muscle phenotypes. p72

Table 2.2: Longitudinal studies on associations of *VDR* polymorphisms with muscle phenotypes. p79

Chapter 3

Table 3.1: Characteristics and allele information for DBP (GC) isoforms. p94

Table 3.2: *VDR* SNP primer information for tetra-primer ARMS PCR. p102

Table 3.3: *GC (*DBP*)* SNP primer information for tetra-primer ARMS PCR. p103

Table 3.4: Characteristics of the Study Population. p104

Table 3.5: Genotype frequencies of *VDR* SNPs in MA and controls. p107

Table 3.6: Genotype & isoform frequencies of GC (DBP) SNPs in MA and controls. p108

Table 3.7: Participant characteristics (body composition, muscle strength/function, physical function, and biochemical data) in relation to BsmI. p113

Table 3.8: Participant characteristics (body composition, muscle strength/function, physical function, and biochemical data) in relation to TaqI. p116

Table 3.9: Participant characteristics (body composition, muscle strength/function, physical function, and biochemical data) in relation to FokI. p119

Table 3.10: Participant characteristics (body composition, muscle strength/function, physical function, and biochemical data) in relation to Cdx2. p122

Table 3.11: Participant characteristics (body composition, muscle strength/function, physical function, and biochemical data) in relation to ApaI. p124

Table 3.12: Participant characteristics (body composition, muscle strength/function, physical function, and biochemical data) in relation to A1012G. p127

Table 3.13: Participant characteristics (body composition, muscle strength/function, physical function, and biochemical data) in relation to rs7041. p130

Table 3.14: Participant characteristics (body composition, muscle strength/function, physical function, and biochemical data) in relation to rs4588. p133

Table 3.15: Participant characteristics (body composition, muscle strength/function, physical function, and biochemical data) in relation to DBP isoforms. p136

Chapter 4

Table 4.1: Primers used in qRT-PCR. p163

Chapter 5

Table 5.1: Primers used in qRT-PCR. p231

Chapter 1: Literature Review

1.1 Vitamin D Physiology

1.1.1 Sources of Vitamin D

In humans, vitamin D can be attained through two sources: dietary intake and epidermal synthesis. Reports have suggested that ~90% of an individual's intake is obtained by the latter, although this may vary depending on lifestyle, clothing, skin pigmentation, use of sunscreens, and dietary/supplementation habits [4]. Within our diets, two dietary forms of vitamin D exist: vitamin D_2 (ergocalciferol) and vitamin D_3 (cholecalciferol). Ergocalciferol is present in certain types of plants and fungi where it is converted from ergosterol, whilst cholecalciferol can be found in dairy and meat products and fortified foods [5].

Food sources richest in vitamin D include eggs, fatty fish, and sun-exposed mushrooms but in some countries, vitamin D can also be attained via fortified foods. Breads and cereals are among common food types to be fortified, along with dairy products (such as milk and butter), but their contribution to the vitamin D intake of the UK adult population remains to be very low (0.8 μg/day) [6]. As the interest in the biological benefits of vitamin D has grown, so has the volume of sales of over-the-counter vitamin D supplementation. These supplements provide a cheap alternative for those who may not be able to obtain optimal vitamin D levels, especially during the winter months.

1.1.2 Vitamin D Metabolism

Upon exposure to sunlight, solar ultraviolet B (UVB) photons (with a wavelength (λ) of 290-315 nm) penetrate the epidermal layer of skin and cause a rearrangement of the 5,7-diene in the B ring of 7-dehydrocholesterol (7-DHC), thereby causing a B ring break and formation of the 9,10-secosterol, previtamin D_3 [7,8]. Pre-vitamin D_3 is a biologically inert and thermodynamically unstable compound that must undergo isomerisation to form vitamin D_3 [9]. Sunlight itself can regulate synthesis of vitamin D_3 as UVB can cause pre-vitamin D_3 to isomerise into two photoisomers that are biologically inactive: tachysterol and lumisterol. In addition to this regulatory mechanism, vitamin D_3 can be isomerised by UVB photons into at least three other biologically inert photoisomers (namely suprasterols I and II, and 5,6-transcholecalciferol). The remaining unisomerised vitamin D_3 (~10-15%) can enter the circulation bound to vitamin D binding protein (DBP) for further metabolic alterations [10]. Ingested vitamin D is absorbed in the small intestine as a fat-soluble vitamin alongside long-chain triglycerides and incorporated into chylomicrons [11,12]. These vitamin D-containing chylomicrons are subsequently transported into venous circulation via the lymphatic system.

Upon reaching the liver, both DBP-bound vitamin D and vitamin D within chylomicrons is hydroxylated at position 25 (C-25) by 25-hydroxylase (CYP2R1) to form 25-hydroxyvitamin D ($25(OH)D_3$; calcidiol) before conversion to 1,25-dihydroxyvitamin D ($1,25(OH)_2D_3$; calcitriol) in the kidneys by hydroxylation of C-1 by 25-hydroxyvitamin D-1-α-hydroxylase (CYP27B1). 1α-hydroxylation is

regulated by parathyroid hormone (PTH) as raised levels of PTH have a positive effect on this hydroxylation, whilst hypoparathyroidism inhibits the conversion of $25(OH)D_3$ to $1,25(OH)_2D_3$ [13]. Whilst this secondary 25-hydroxylation step was initially believed to occur exclusively in the kidneys, extra-renal sites of CYP27B1 have since been identified [14]. $1,25(OH)_2D_3$ is the biologically active form of vitamin D yet, due to its relatively short half-life of 15 hours, vitamin D status is clinically based upon serum measurements of $25(OH)D_3$ which circulates at concentrations approximately 1000 times higher than $1,25(OH)_2D_3$ and has a half-life of 2-3 weeks [15].

In the kidney, $1,25(OH)_2D_3$ levels are tightly controlled with synthesis being regulated by the parathyroid glands, serum calcium (Ca^{2+}) levels, and fibroblast growth factor-23 (FGF23) [16,17]. Low serum Ca^{2+} levels, or hypocalcaemia, stimulate release of PTH by the parathyroid gland which stimulates CYP27B1 activity with a subsequent rise in $1,25(OH)_2D_3$ synthesis [16]. Acting through a negative feedback loop, increased levels of $1,25(OH)_2D_3$ suppress PTH release by upregulation of Ca^{2+}-sensing receptors, causing a subsequent increase in serum Ca^{2+} levels [16]. Conversely, serum $1,25(OH)_2D_3$ levels are negatively regulated by a bone-kidney feedback loop in which high phosphate serum (P_i) levels, or hyperphosphatemia, induce FGF23 release from osteoblasts and osteocytes in bone [18]. FGF23 stimulates renal excretion of P_i which, in turn, inhibits CYP27B1, increases expression of the enzyme 24-hydroxylase (CYP24A1), and, therefore, reduces serum $1,25(OH)_2D_3$ levels [19].

In addition, $1,25(OH)_2D_3$ can also self-regulate via its own negative feedback loop in which $1,25(OH)_2D_3$ directly induces expression of CYP24A1 which hydroxylates both $25(OH)D_3$ and $1,25(OH)_2D_3$ at C-24, subsequently resulting in the synthesis of the less potent metabolites, 24,25-dihydroxyvitamin D_3 ($24,25(OH)_2D_3$) and 1,24,25-trihydroxyvitamin D_3 ($1,24,25(OH)_3D_3$), respectively [20,21]. Due to recent developments within the field of liquid chromatography-tandem mass spectrometry (LC-MS/MS), research has demonstrated a potential clinical application for the ratio of $25(OH)D_3$ to $24,25(OH)_2D_3$ as a marker of vitamin D status ($25(OH)D_3$) relative to its catabolism [22,23] . Several studies have also successfully used this ratio to more effectively define the serum status of $25(OH)D_3$ following vitamin D supplementation [24,25].

1.1.4 Vitamin D Binding Protein

As mentioned in **Section 1.1.2**, vitamin D metabolites are transported in circulation by the carrier protein, vitamin D binding protein (DBP). First identified as Group-specific component (Gc), DBP belongs to the albuminoid protein family that also includes α-fetoprotein, afamin, and albumin, and it has remained well conserved throughout evolution of vertebrates [26]. It is primarily synthesised by the liver but gene and protein expression of DBP has also been detected in other tissues, such as stomach, gall bladder, pancreas, and cardiac muscle [27–29]. In humans the DBP gene (*GC*) is located on the long arm of chromosome 4 (4q11-q13) and codes for a 458 amino acid (AA) secreted protein with the characteristic triple-domain modular structure of an

albuminoid protein [30,31]. Domain A possesses a single cleft that acts as a binding site for vitamin D metabolites, while an actin binding site spans across domains B and C with some involvement from domain A also [32]. Due to the high number of DBP in circulation (200-600 mg/L), only ~5% of vitamin D metabolite binding sites are occupied at any time, and DBP is able to bind all metabolites of vitamin D but with varying affinity, namely: $25(OH)D_3$ = $24,25(OH)_2D_3$ > $1,25(OH)_2D_3$ > vitamin D > $1,24,25(OH)_3D_3$ [33].

The DBP-locus is one of the most highly polymorphic known with over 120 identified human variants of which two particular exon 11 missense variants (also known as single nucleotide polymorphisms, SNPs) have been most frequently researched, rs4588 (T436K; c.1307C>A) and rs7041 (D432E; c.1296T>G) [34,35]. Three common DBP isoforms exist that depend on what alleles of rs4588 and rs7041 an individual possesses. Gc1f (rs7041-T/rs4588-C) is the most frequent isoform and is commonly referred to as the wild-type (WT), followed by Gc1s (rs7041-G/rs4588-C) and, finally, Gc2 (rs7041-T/rs4588-A) [31]. Gc1s and Gc2 are distinguishable from Gc1f as the AA substitutions lead to altered post-translational glycosylation which can be demonstrated experimentally by differences in their isoelectric points [36]. In addition, it appears that the isoform carried can influence serum levels of $25(OH)D_3$, with Gc2 homozygotes displaying the lowest circulating $25(OH)D_3$ concentration across several different cohorts [37–39]. Why Gc2 leads to reduced serum $25(OH)D_3$ levels is currently unclear but previous suggestions have included

lower hepatic synthesis, increased rate of clearance, and reduced affinity for $25(OH)D_3$ [26,40].

Despite its name, DBP is actually a multi-functional protein with several roles beyond the transport of vitamin D metabolites. As DBP possesses an actin binding site it allows DBP to act as an extracellular actin-binding protein in the extracellular actin scavenging system (EASS) [41,42]. In the event of a major clinical event, such as sepsis or major trauma, an influx of actin into the circulation from damaged tissue/cells occurs [43,44]. Upon release into the circulation, actin polymerises into filamentous actin (F-actin) that, if uncleared, can lead to microcirculatory occlusions, a hypercoagulable profile and, ultimately, multi-organ failure [43]. The EASS is comprised of DBP and gelsolin with gelsolin depolymerising F-actin to globular actin (G-actin) and, due to its high affinity for G-actin, DBP preventing repolymerisation by binding and clearing it from circulation [45]. As such, DBP is considered as an acute phase reactant, as its serum levels are significantly altered following trauma and/or in inflammatory states [46]. Like all other albuminoid proteins, DBP can also bind fatty acids [47,48]. While it has been demonstrated that high concentrations of polyunsaturated fatty acids (e.g. linoleic acid and arachidonic acid) can reduce the affinity of DBP for $25(OH)D_3$ and $1,25(OH)_2D_3$, it is unclear whether this also occurs at more physiologically relevant concentrations [49].

In addition, reports have suggested a role for DBP in inflammation, but whether this is direct or indirect is currently a matter of speculation. DBP has been

implicated in complement-mediated recruitment of neutrophils but DBP itself lacks chemotactic activity [50,51]. Thus, it has been proposed that DBP associates with a binding site complex on the cell surface in order to mediate the chemotactic cofactor effect [52]. Finally, as involvement of DBP has also been documented in macrophage activation, it is also often referred to as macrophage-activating factor (DBP-MAF) [53]. Deglycosylation of the threonine that is substituted for lysine in the rs4588 SNP has been shown to convert DBP to active DBP-MAF [54]. DBP-MAF has been demonstrated to facilitate differentiation of monocytes into osteoclasts and stimulate bone resorption in a rat model of osteopetrosis [55,56].

1.1.3. Effects of Race and Differences in Ethnicity Upon Vitamin D Metabolism

There is a growing body evidence to suggest that the prevalence of vitamin D deficiency (serum 25(OH)D_3 <25 nmol/L) is greater in Black individuals and other people of colour than White individuals [57–59]. Several hypotheses have been suggested in an attempt to explain these observations. Firstly, Black individuals have a higher concentration of melanin which, as it absorbs UVB radiation, is believed to result in impaired cutaneous synthesis of pre-vitamin D_3 due to reduced availability of UVB photons for photochemical conversion of 7-DHC to pre-vitamin D_3 [60]. Secondly, it is possible that the differences could be due to genetic variability in genes encoding certain enzymes and proteins that are key in the vitamin D metabolic pathway [61]. Indeed, recent reports have indicated that SNPs in the *Gc* gene can account for a greater proportion of variation in 25(OH)D_3 serum levels between Black and White Americans than

other well-known factors (e.g. season, BMI, and calcium intake) [61]. Based on this information, when considering the vitamin D system as a whole, it is sensible to wonder whether this relationship between genetics and our physiology can be applied to other genes related to vitamin D metabolism. For example, activity of CYP27B1 appears to be increased while CYP24A1 activity is lower in Black individuals relative to White, as suggested by differences in the ratios of $1,25(OH)_2D_3$:$25(OH)D_3$ and $24,25(OH)_2D_3$:$25(OH)_2D_3$, respectively [62]. It is entirely possible that this variation in the activities of CYP27B1 and CYP24A1 can be influenced by SNPs located in their encoding genes and that the SNP frequencies may vary across different populations but confirming this would require large population-based genetic association studies that fully encompass global diversity.

1.2 Mechanisms of Action of Vitamin D/VDR Axis

As a steroid hormone, $1,25(OH)_2D_3$ exerts its biological effects via two mechanisms: i) Genomic - binding of $1,25(OH)_2D_3$ to an intracellular receptor subsequently activates gene transcription, and ii) non-genomic - binding of $1,25(OH)_2D_3$ to an intracellular receptor triggers intracellular signalling pathways that, ultimately, lead to events that occur independently of gene transcription.

1.2.1 Vitamin D Receptor

Following identification of the active metabolite, $1,25(OH)_2D_3$, there was a significant push to uncover the underlying mechanistic machinery or pathways.

This eventually led to the discovery and characterisation of the vitamin D receptor (VDR), a cell membrane receptor belonging to the superfamily of nuclear receptors (NRs) [63]. Whilst highest levels of VDR can be found in bone, intestine, kidney, and the parathyroid gland, the tissue distribution of VDR is vast with its expression also being documented in the majority of human tissues, therefore demonstrating the broad scope of the effects of $1,25(OH)_2D_3$ [64].

The human *VDR* gene maps to the centromeric region of chromosome 12 (12cen-q12) and codes for a 427 AA protein [65,66]. Whilst the 427 AA protein is the standard-length protein (WT, or VDR-A), the presence of a common SNP, FokI, alters the location of the translation initiation codon, resulting in a VDR protein that is 3 AA shorter but displays higher transcriptional activity [67]. As a member of the NR superfamily, the structure of VDR is the same as that of its fellow NRs, in which it is comprised of a short N-term domain, a DNA-binding domain (DBD), a ligand-binding domain (LBD), and a hinge region that connects the DBD to the LBD [68]. The LBD permits the interaction between VDR and $1,25(OH)_2D_3$, as VDR binds with an affinity of 0.1 nM, which is much higher than the affinity of other NRs for their respective ligands [69].

1.2.2 Genomic Mechanism of Action

Upon entry into the cell, $1,25(OH)_2D_3$ binds to VDR resulting in conformational change in the receptor and subsequent nuclear translocation. In the nucleus the VDR associates with its heterodimeric partner, retinoid X receptor (RXR),

forming a 1,25(OH)$_2$D$_3$-VDR-RXR complex that is able to modulate gene expression by binding vitamin D response elements (VDREs) in DNA (**Figure 1.1**) [70]. Identification of multiple genes that are under transcriptional regulation of the vitamin D system, roughly 3% of the human genome, exemplifies the sheer breadth of potential explanations for vitamin D$_3$ mechanisms of action within normal biological function, e.g. cellular adhesion, cell cycle and cytoskeletal maintenance [71,72].

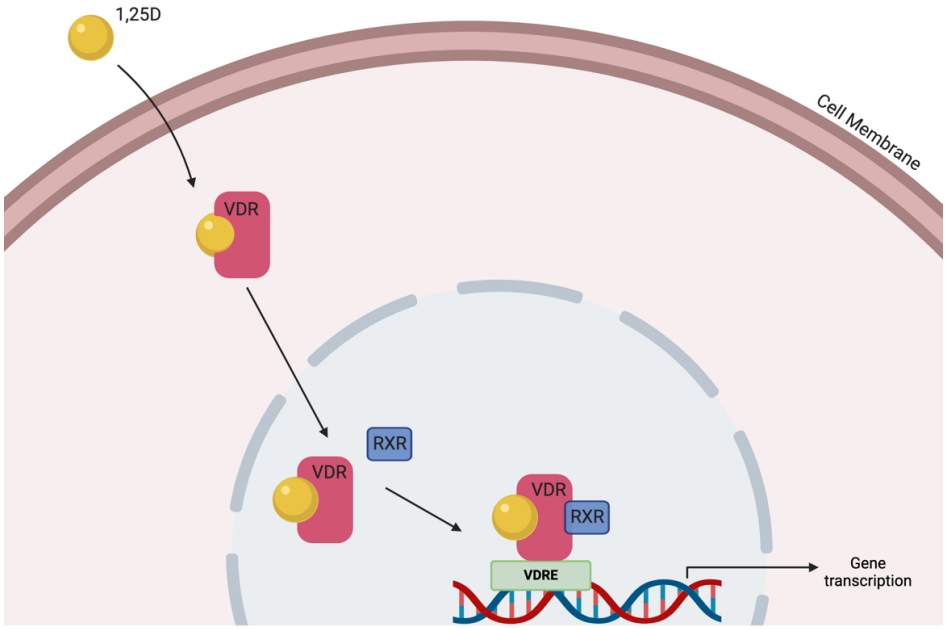


Figure 1.1. The genomic mechanism of vitamin D (1,25(OH)$_2$D$_3$).

Upon entry into the cell, 1,25(OH)$_2$D$_3$ binds to the VDR causing conformational changes in the receptor and subsequent nuclear translocation. In the nucleus, VDR associates with RXR (its heterodimeric partner) to form a 1,25D-VDR-RXR complex that modulates gene expression by binding VDREs in DNA. Abbreviations: *1,25D,* 1,25-dihydroxyvitamin D$_3$; *VDR*, vitamin D receptor; *RXR*, retinoid X receptor; *VDRE*, vitamin D response element. Created with BioRender.com.

1.2.3 Non-Genomic Mechanism of Action

$1,25(OH)_2D_3$ is also able to exert its influence via non-genomic actions, which include the modulation of intracellular calcium ion concentration ($[Ca^{2+}]_i$), stimulation of intracellular signalling cascades (e.g. mitogen activated protein kinases (MAPKs)), and induction of Ca^{2+} and chloride (Cl^-) channel activity (**Figure 1.2)** [73]. Unlike the genomic effects, non-genomic responses occur rapidly (within seconds or minutes) indicating the occurrence of transcription-independent events following $1,25(OH)_2D_3$ stimulation [74].

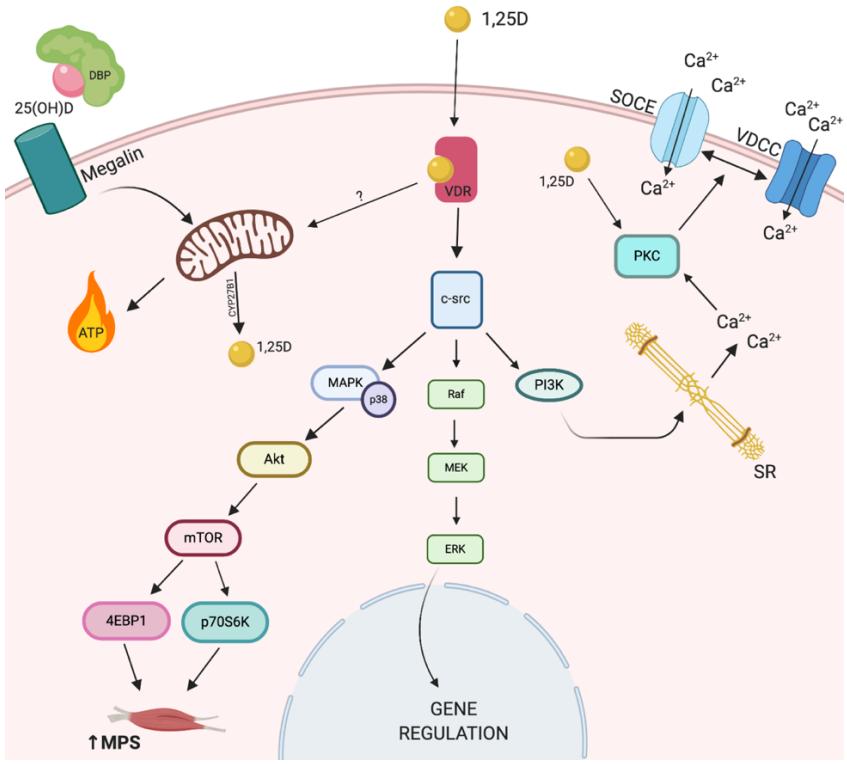


Figure 1.2. The proposed non-genomic mechanisms of vitamin D (1,25(OH)$_2$D$_3$).

1,25(OH)$_2$D$_3$ has been demonstrated to play a role in intracellular signalling and calcium homeostasis. It is likely that c-Src acts as a gateway to cell signalling for 1,25(OH)$_2$D$_3$ as it is a key upstream regulator of the MAPK/ERK pathways and PI3K. The relationship of vitamin D and mitochondrial function is unclear but proposed effects involve influences on energy production. Abbreviations: *25(OH)D$_3$*, 25-hydroxyvitamin D$_3$; *1,25D$_3$*, 1,25-dihydroxyvitamin D$_3$; *SR*, sarcoplasmic reticulum; *DBP*, vitamin D binding protein; *VDR*, vitamin D receptor; *MPS*, muscle protein synthesis; *ATP*, adenosine triphosphate; *CYP27B1*, 1α-hydroxylase; *c-Src*, proto-oncogene tyrosine-protein kinase Src; *MAPK*, mitogen-activated protein kinase; *mTOR*, mechanistic target of rapamycin; *4EBP1*, eukaryotic translation initiation factor 4E-binding protein; *p70S6K*, ribosomal protein S6 kinase β-1; *Raf*, proto-oncogene serine/threonine-protein kinase; *PI3K*, phosphatidylinositol-3-kinase; *PKC*, protein kinase C; *Ca^{2+}*, calcium ion; *SOCE*, store-operated calcium entry; *VDCC*, voltage-dependent calcium channel; *MEK*, MAPK-kinase; *ERK*, extracellular signal-regulated kinase; *Akt,* AKT serine/threonine kinase 1. Created with BioRender.com

1.3 The Vitamin D/VDR Axis and the Musculoskeletal System

Skeletal muscle accounts for almost 40% of an individual's body weight, is fundamental for locomotion, breathing, lipid and glucose homeostasis, and is the primary protein reservoir of the human body [75]. As such, extant muscle atrophy is a clinical problem across the life course, irrespective of the underlying aetiology, e.g. post-trauma or disease. In terms of increasing age, the incipient loss of muscle mass (and sometimes increase in fat mass) and function, is termed sarcopenia [76]. Maintenance of skeletal muscle mass relies on a strictly regulated balance of muscle protein synthesis (MPS) and breakdown (MPB) - or proteostasis. Muscle atrophy occurs when the rate of MPB exceeds that of MPS, so there is understandably great interest in elucidating the mechanisms underlying atrophy and any key factors that may influence the process [77–79].

Muscle atrophy is influenced via genetic, epigenetic, and behavioural mechanisms, but environmental and nutritional factors also play a key role, with vitamin D being a prominent factor. It is estimated that vitamin D deficiency affects approximately 1 billion people globally and these individuals typically present with bone pain, fatigue, muscle pain (myalgia), muscle atrophy and weakness, and an increased risk of sarcopenia [80]. While these muscle symptoms are among some of the key features of hypovitaminosis D, the relationship between vitamin D and skeletal muscle is still not fully understood.

1.3.1 Evidence from Human Studies

As an individual ages, the need for optimal maintenance of muscle mass and strength is imperative due to the impact sarcopenia can have on functional independence and, ultimately, quality of life. Multiple human studies have indicated a relationship between vitamin D deficiency (low serum $25(OH)D_3$), reduced muscle function, and an increased risk of sarcopenia [81]. In the United Kingdom, NICE guidelines state that serum $25(OH)D_3$ levels of less than 25 nmol/L should be considered as vitamin D deficiency (hypovitaminosis D), 25-50 nmol/L as insufficiency, and over 50 nmol/L as sufficient [82]. Risk of vitamin D deficiency and dysregulated vitamin D function increases with age. This may be attributed to reduced sensitivity to $1,25(OH)_2D_3$ due to a combined effect of age-related decline in VDR expression within skeletal muscle, impairment of cutaneous vitamin D synthesis, or altered expression of vitamin D metabolic enzymes [83–86]. In addition, poor nutrition and reduced exposure to sunlight are commonly seen in institutionalised individuals - a population at a particularly high risk of deficiency [87]. It has been well-established that low serum $25(OH)D_3$ levels are associated with reduced muscle strength [88–95] and impaired physical function [96–102]. Longitudinal studies indicate that deficiency may exacerbate the age-related decline in strength and physical performance [101,103–109] whilst also potentially acting as an independent risk factor for sarcopenia [107,110,111].

Vitamin D deficiency-related muscle dysfunction may be partly explained by alterations to skeletal muscle morphology, particularly type II muscle fibres (fast-twitch) [112–114] . Degenerative changes, such as muscle opacity, fibrosis, fibre atrophy, and enlarged interfibrillar spaces have been seen in patients with osteomalacic myopathy (a condition associated with vitamin D deficiency) [115]. Sarcopenia has similar morphological manifestations in skeletal muscle to vitamin D deficiency, and its effects are, again, also more prominent in type II fibres [116]. Given that preservation of fast-twitch type II muscle fibres is crucial for maintaining posture due to their role in generating rapid forces, it is perhaps unsurprising that low $25(OH)D_3$ levels are associated with an increased risk and prevalence of falls [117–121]. Vitamin D supplementation has been shown to increase the percentage of type II muscle fibres in both males and females, but further investigations are needed to confirm these results [122,123].

Given the volume of evidence supporting an association between vitamin D deficiency and impaired musculoskeletal function, there has been great focus on the therapeutic potential of the hormone, particularly in elderly populations. Multiple studies have demonstrated that restoration of serum $25(OH)D_3$ levels can improve measures of strength and physical function [124–132]. However, a significant number of trials have failed to show any benefits of vitamin D supplementation upon muscle strength and/or mass, therefore generating a degree of uncertainty regarding its benefits [133–140]. The potential reasons for these disparities are numerous but may include differences in the form of

the supplement and its dosage, the study duration, and heterogeneity of participant demographics. Furthermore, whilst the common ideology is that higher vitamin D levels will provide optimal physical function, this may not be correct in terms of the musculoskeletal response to vitamin D supplementation. A dose-dependent response has been proposed in the form of a U-shaped curve, as several studies have demonstrated that both those with the lowest and highest quartiles of serum 25(OH)D_3 levels display impaired muscle strength and an increased risk of fractures and frailty [103,141]. Further research is required to fully comprehend the reasoning behind these observations, but the possibility for a potential therapeutic threshold of vitamin D in the musculoskeletal system is clear.

In view of the age-related reduction in muscle VDR expression and vitamin D synthesis and metabolism, the deficiency-associated morphological alterations of fast-twitch type II fibres and impairment of muscle strength/mass, it is of no surprise that a biological link has been hypothesised between the vitamin D system and muscle atrophy. Human studies have highlighted the phenotypical and clinical alterations that result from vitamin D deficiency, but there is a lack of understanding of the underlying molecular mechanisms.

1.3.2 VDR expression and skeletal muscle

Early studies reported a positive association between VDR content of classical tissue targets of vitamin D, e.g. bone and intestine, and the level of biological activity as a response to treatment with vitamin D_3 [142]. It has since been

demonstrated, that upon treatment with $1,25(OH)_2D_3$, VDR expression is also upregulated in skeletal muscle cells [143–145]. However, confirmed expression of VDR in skeletal muscle has been subject to controversy. Initial animal studies used immunohistochemistry as a means for detection, but selectivity of the widely used anti-VDR antibody 9A7 was questionable in cross-reacting with unrelated proteins on Western blots [146]. More recent data confirming the presence of VDR in both human and murine skeletal muscle cells has been generated through studies using multiple VDR antibodies [122,143,147]. However, in fully differentiated murine and human muscle, VDR levels have been detected at extremely low levels or not at all, whereas VDR expression is higher in cell-cycling myoblasts than differentiated cells [143,148,149]. One potential explanation for these observations is that VDR levels are dynamic in nature, being highest during immaturity followed by an age-related decline. This hypothesis is supported by the fact that VDR is displayed to be upregulated in regenerating muscle of mice that have undergone muscular injuries or exercise [150–152]. This raises an important question – is VDR expression enriched in satellite cells? In postnatal muscle fibres, this population of muscle stem cells represents approximately 30-35% of the total muscle cell population, before declining to 5% in healthy adult muscle [153]. As satellite cells normally exist in a quiescent state, unless stimulated to differentiate into myocytes by exercise or muscular damage, this could explain the difficulties of detecting VDR in adult muscle [154]. Nonetheless, DNA-bound VDR may also represent a challenge for detection using standard extraction techniques.

1.3.3 The Vitamin D/VDR Axis and Myogenesis

The majority of studies investigating the vitamin D axis and muscle cell function have adopted *in vitro* cultures of muscle cells. Myogenesis, the means by which skeletal muscle is generated, is a multi-step process and can be largely broken down into 4 stages: 1. Activation of satellite cells, 2. Proliferation of myoblasts, 3. Myoblast differentiation, and 4. Formation of myotubes. This process is displayed in **Figure 1.3**.

Studies using the C2C12 murine skeletal muscle cell line have demonstrated $1,25(OH)_2D_3$ as being anti-proliferative, but stimulatory of differentiation [144,155]. Treatment of myoblasts with 100nM $1,25(OH)_2D_3$ for 1-week resulted in a 75% reduction in proliferating cell nuclear antigen (PCNA - a biomarker of cellular proliferation) [156], whilst significant reductions in cells positive for bromodeoxyuridine ($BrdU^+$ - a thymidine analog that labels proliferating cells) were also observed following 2-day treatments at the same dosage [143,151]. It is important to note that, while a dosage of 100nM $1,25(OH)_2D_3$ is commonly used for *in vitro* studies, it is highly unlikely to occur *in vivo* at this concentration. Future studies should aim to optimise dosages of *in vitro* $1,25(OH)_2D_3$ treatments to better reflect that of physiologically relevant dosages.

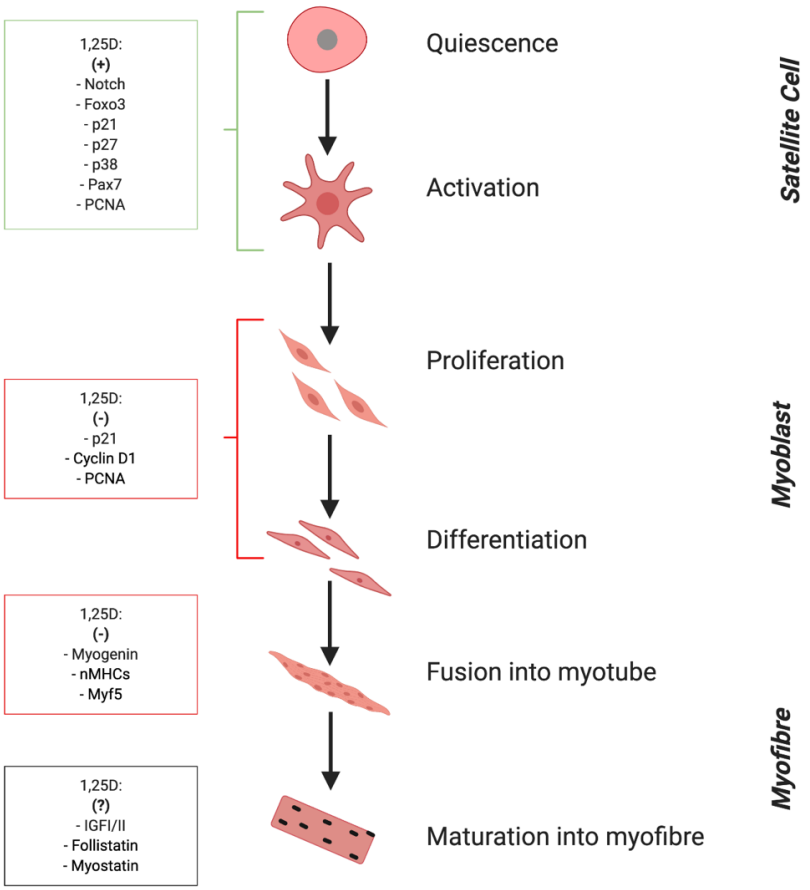


Figure 1.3. The proposed effects of 1,25(OH)$_2$D$_3$ at the main stages of myogenesis. 1,25(OH)$_2$D$_3$ appears to exert differential effects that are dependent on the stage of myogenesis that the cell is in. The effects of 1,25(OH)$_2$D$_3$ in satellite cells is believed to be stimulatory, whereas it evokes inhibitory effects in myoblasts. These effects are summarised here. Stimulatory effects (+), inhibitory effects (-), and uncertain effects (?) are illustrated. Abbreviations: *1,25D*, 1,25-dihydroxyvitamin D$_3$; *FOXO3*, Forkhead box protein 3; *p21,* cyclin dependent kinase inhibitor 1B; *p27,* cyclin dependent kinase inhibitor 1B; *p38,* mitogen activated protein kinase; *Pax7*, paired box protein 7; *PCNA*, proliferating cell nuclear antigen; *nMHC*, neonatal myosin heavy chain; *Myf5*, myogenic factor 5; *IGFI/II*, insulin-like growth factor 1/2. Created with BioRender.com.

At onset of differentiation, expression of the majority of cyclins are downregulated, as this is the stage at which cells arrest in the G_0/G_1 phases of cell division. Expression of cyclin D3 is associated with permanent cell cycle withdrawal and induction of early myogenesis, whereas cyclin D1 is seen to be highly expressed in proliferating myoblasts [157,158]. Treatment of C2C12 myoblasts with 1nM $1,25(OH)_2D_3$ increases cyclin D3 expression, supporting observations that $1,25(OH)_2D_3$ causes cellular arrest in G_0/G_1 phase [143,157,159]. It appears that this effect occurs simultaneously with induction of the cyclin-dependent kinase inhibitors (CDKIs) p21 and p27 [157], and data from studies using VDR knockdown (VDR-KD) cell lines indicate that these cell-cycle influences are VDR-dependent [158].

Fusion of myoblasts into multinucleated myotubes is a strictly controlled process. The first wave occurs during embryogenesis and is responsible for generating the myotubes of the preliminary muscular system, whereas the secondary wave takes place later in a vertebrate's lifespan. It is this second wave that is responsible for the addition of secondary myotubes/myofibres that increase muscle mass, so the impact of vitamin D on this process is of particular interest [160]. Myotube formation can occur spontaneously in high serum media and is believed to rely primarily on myogenin. In culture, C2C12 myoblasts can be induced to exit the cell cycle and differentiate into myotubes through switching "growth culture" medium (10% foetal bovine serum, FBS) to "differentiation medium" (2% FBS). This method of differentiation induction via serum starvation is primarily driven by insulin-like growth factor-1 (IGF-1) and

has been used to examine the differences that occur when myoblasts are treated with vitamin D_3 either at the point of differentiation initiation or when they are fully differentiated [161].

Interestingly, $1,25(OH)_2D_3$ appears to stimulate myotube formation when high-sera medium is used for both C2C12 and primary muscle cell cultures [156,162], yet it has the opposing effect in cases of differentiation via serum starvation [143,163]. Thus, it is possible to suggest that vitamin D elicits differential effects depending on the model of myogenesis used. When C2C12 myoblasts are treated with 100nM $1,25(OH)_2D_3$ during the early differentiation phases (i.e. day 0 and day 4), myogenin and neonatal myosin heavy chain (nMHC) isoforms were downregulated, but this effect wasn't present in the fully differentiated group (day 8) [157]. In fact, treatment with $1,25(OH)_2D_3$ at day 8 post-differentiation appeared to have an opposing effect as myosin heavy chain type IIa expression was upregulated with an additional protective role against cellular detachment [157]. The inhibitory influence of $1,25(OH)_2D_3$ upon myotube formation has been supported further as C2C12 myoblasts also treated at day 4 differentiation were only able to fuse partially, resulting in abnormally shaped myotubes that possessed an increased number of myonuclei [145].

The results from these aforementioned *in vitro* studies have been translated in vivo through use of vitamin D deficient and/or VDR null animals. These animals possess similar phenotypes, namely presenting with smaller muscle fibres,

reduced muscle strength, higher fatigue, fibre hyper-nuclearity, and abnormal gait [163–166]. In rats, vitamin D deficiency causes cell cycle arrest which, whilst initially seeming undesirable for muscle function, it is possible that this action of $1,25(OH)_2D_3$ promotes entry of myoblasts into a quiescent state [167]. Notch signalling is considered a master regulator of myoblast quiescence and, whilst expression of full-length Notch is unaffected by deficiency, a decrease in the cleaved form of Notch is present, indicating reduced activation of the Notch pathway in vitamin-D deficient rats [167,168]. $1,25(OH)_2D_3$ has been demonstrated to influence the enzymes responsible for proteolytic processing of Notch, a γ-secretase complex and an ADAM protease, in neuroblastoma cells but further investigations are required to evaluate this hypothesis in skeletal muscle cells [167,169]. As this pro-myogenic pathway is involved in the proliferation of satellite cells, and deficiency of vitamin D leads to a blunted Notch response within skeletal muscle, it may be possible to place this relationship as a potential aggravator for age-related decline in myoregenerative capacities.

The development of a genetically modified mouse model lacking the gene encoding *Vdr* (VDR-KO) has allowed investigators to study the impact of loss of VDR [170,171]. Whilst VDR-KO mice display an aberrant muscle phenotype, the phenotypic alterations of this VDR-KO mouse model are not only limited to the muscular system as these animals also display alterations to other physiological systems e.g. the cardiovascular and gastrointestinal systems [172]. Due to the confounding systemic impact caused by the absence of the *Vdr* gene, it has

become difficult to draw final conclusions from results produced from the total-body VDR-KO mice. Tissue-specific VDR-KO animal models have been generated in an attempt to bypass this problem, and work using mice with a myocyte-specific *Vdr* deletion (mVDR-KO) has demonstrated the importance of VDR in muscle function [147]. Stark differences can be seen between these mice and the whole-body knockout animals, as the mVDR-KO mice were of a normal body size, yet their muscle fibres were marginally larger in diameter [147]. Thus, efforts should be focused on clarifying conclusions drawn from whole-body models using this new tissue-specific model, whilst also yielding novel information regarding the biological activity of vitamin D.

1.3.4 Genomic Action of the Vitamin D/VDR Axis in Skeletal Muscle

PCR array analysis studies using human muscle biopsies have identified a number of myogenic genes where expression correlates with $1,25(OH)_2D_3$ [173], whilst RNA sequencing has (RNAseq) demonstrated alterations to expression levels of over 1900 mRNAs following treatment of human skeletal muscle cells with $1,25(OH)_2D_3$ [174]. With regards to myogenic-related genes, several have been found to possess VDREs. Forkhead box protein 1 (FOXO1), a transcription factor belonging to the forkhead/winged helix family, has a VDRE in its promoter and regulates muscle atrophy through its influences upon MPS and cellular differentiation [72,175]. VDR signalling has been shown to inhibit both expression and nuclear translocation of FOXO1, but upon VDR-KD, this suppressive effect is abolished, suggesting FOXO1 as a chief target in the altered signalling demonstrated in VDR-KO skeletal muscle [176,177].

The insulin-like growth factor (IGF) system comprises multiple ligands (IGF-I, IGF-II, and insulin), receptors, and six binding proteins (IGFBPs), several of which possess VDREs within their genes. Within skeletal muscle, IGFBP-5 is the primary secreted IGFBP, and, through its activation of the IGF-II auto-regulation loop, it promotes myogenic differentiation [178,179]. IGFBP-5 interacts directly with VDR and seemingly prevents heterodimerization with RXR, thereby impairing $1,25(OH)_2D_3$ induced cell-cycle progression and gene transcription [180,181]. Similarly, the gene encoding thioesterase superfamily member 4 (THEM4; also known as carboxyl-terminal modulator protein, CTMP) also possesses a VDRE in its promoter region. THEM4 inhibits the phosphorylation and subsequent activation of Akt, resulting in MPB due to cessation of Akt's inhibition and activation of members of the FOXO family and mechanistic target of rapamycin (mTOR), respectively [182]. Treatment with $1,25(OH)_2D_3$ caused upregulation of THEM4 which, paired with the fact that it has been found to be elevated in atrophic C2C12 cells, further suggests a role for the vitamin D system in the maintenance of muscle proteostasis [183,184].

Despite being primarily implicated in skeletal health, recent studies have implicated the bone-derived hormone osteocalcin in the regulation of muscle function [185,186]. The presence of a VDRE in the osteocalcin promoter indicates that $1,25(OH)_2D_3$ is able to directly regulate this gene, an effect that has been demonstrated *in vitro* by upregulation following $1,25(OH)_2D_3$ treatment [187]. As osteocalcin has been shown to influence muscular mitochondrial function, myofibre uptake and catabolism of glucose/fatty acids,

and insulin sensitivity [186,188,189], it is sensible to suggest this genomic relationship as one potential explanation for the aberrant muscle phenotype seen in VDR-KO mice. Similar to the VDR, expression levels of the osteocalcin gene have been shown to decline as an individual ages [190].

Lastly, expression of integrinβ3 is also recognised to be under the control of a VDRE, and deficiency of this integrin in myoblasts results in impaired myoblast migration and fusion [191]. The integrins are a major family of transmembrane receptors that act to provide connections between the extracellular matrix and the cytoskeleton [192]. It seems that vitamin D increases expression of integrinβ3, thereby inducing the formation of focal adhesions that are crucial for cellular adhesion, whilst also potentially initiating the differentiation process in satellite cells [191,193]. Currently, uncertainty exists with regards to the directly impacted target genes of $1,25(OH)_2D_3$ in myogenic cells. The use of transcriptomics and RNAseq following treatment of myogenic cells, i.e. satellite cells, myoblasts, and/or myotubes, with $1,25(OH)_2D_3$ would provide further data that may clarify the issue, whilst also elucidating any differences that occur at each stage of the myogenic pathway.

1.3.5 Non-genomic Regulation of Skeletal Muscle by the Vitamin D/VDR Axis

Muscle proteostasis is tightly regulated by an intrinsic balance between the rates of MPS (anabolism) and MPB (catabolism). If the net rate of MPS exceeds that of MPB, then the net muscle protein balance (NPB) is considered to be positive, and growth of muscle fibres is achieved; alternatively, muscle atrophy

occurs when the NPB is negative due to rate of MPB being higher than MPS [194,195].

1.3.5.1 Catabolic Pathways

Of the various proteolytic systems existing in skeletal muscle, vitamin D has been mainly implicated in one in particular, the ubiquitin-proteasomal pathway (UPP) [196,197]. In rats, deficiency of vitamin D resulted in increased levels of MPB, significantly elevated expression of both the ubiquitin conjugating enzyme E2 and its ubiquitin conjugates, but no alterations to either calpain or lysosomal enzymes were observed [196]. At the heart of the UPP lies the 26S proteasome, a large complex comprised of two smaller subcomplexes: the 20S core peptidase and the 19S regulatory unit [198,199]. Proteasomal activity of the 20S subunit was seen to be upregulated in biopsies from the vitamin D-deficient mouse model, thereby indicating an increase in nonlysosomal proteolysis and a place for the vitamin D system in skeletal muscle protein degradation [196].

Further to this, expression of both muscle ring finger protein 1 (MuRF1) and muscle atrophy F-box protein (MaFbx, also known as Atrogin-1) has been seen to be higher in both the vitamin-deficient and VDR-KO mice when compared with control animals [147,196], a result similar to that observed in sarcopenic muscle of aged rats [200]. Expression of both MuRF1 and atrogin-1 is controlled by the phosphorylation state of the FOXO family. Basally, FOXO proteins are phosphorylated by Akt, sequestering them in the cytoplasm, and preventing

their nuclear translocation and downstream transcription of MuRF1 and atrogin-1 [201]. In cellular models, treatment of fully differentiated human myotubes and C2C12 models of stress (e.g., glucocorticoid and oxidative) with $1,25(OH)_2D_3$ inhibited expression of atrogin-1 and MuRF1 but increased levels of FOXO1 [197,202,203]. Paraspinal muscle biopsies from patients with chronic lower back pain supplemented with vitamin D demonstrated increased Akt and reduced FOXO3a in comparison to baseline [204]. Vitamin D deficient rats display elevated levels of total protein breakdown and atrogin-1/MuRF1, and repletion of vitamin D levels also normalised atrogin-1/MuRF1 expression levels in the *gastrocnemius* (GA) muscle of a deficient cachexic mouse model [196,205]. MuRF1 is upregulated in the *tibialis anterior* (TA) muscle of VDR-KO mice, but no significant differences were seen with control WT mice in the *soleus* muscle [206]. This reinforces the type II muscle fibre specificity observed in vitamin D deficient patients, as TA and GA are considered fast muscles whilst *soleus* is slow.

Another key regulator of proteostasis is adenosine monophosphate-activated protein kinase (AMPK). Functioning as a nutrient sensor, AMPK is activated in states of metabolic stress, such as low ATP levels, and acts by activating ATP-producing pathways whilst inhibiting those that are ATP-consuming [207]. For example, activated AMPK phosphorylates mTOR and uncoordinated 51-like kinase 1 (ULK1), thereby inhibiting the positive influence of mTOR upon MPS yet promoting autophagy via ULK1. The impact of older age upon AMPK expression is uncertain, but a large body of evidence suggests AMPK expression

decreases with age, and this decline may be augmented by inactivity/unloading (common features of increasing age) [208]. An age-related loss of AMPK would be detrimental as this impairs the ability for the cell to respond to states of metabolic dysregulation, thereby increasing oxidative stress. In cellular models of atrophy and stress, $1,25(OH)_2D_3$ treatment seems to increase AMPK activity and vitamin D deficient rats display reduced activation of sirtuin-1 (SIRT1), a key activator of AMPK [209–211]. Muscle of VDR-KO mice display higher AMPK levels, which may initially appear paradoxical due to the pro-catabolic influences of AMPK, but it is likely that this is a compensatory mechanism for the diminished ATP levels also seen in these animals [212]. Whilst there is evidently much more to be understood regarding this relationship, it is sensible to question whether age-related declines in vitamin D serum levels exacerbate the effects of reduced skeletal muscle AMPK activity that have been proposed to occur with increasing age.

Whilst the link between proteolytic signalling pathways and vitamin D has been well-documented, evidence exploring the relationship between the autophagy lysosomal pathway and the vitamin D system in skeletal muscle is notably much sparser. Expression of Cathepsin L, a lysosomal cysteine protease, was higher in VDR-KO rats versus controls and treatment with $1,25(OH)_2D_3$ suppressed glucocorticoid-induced expression of Cathepsin L in C2C12 myotubes [203,213]. As discussed previously, $1,25(OH)_2D_3$ stimulates AMPK activity, which is pivotal in activating autophagy via phosphorylation of ULK1, plus markers of autophagy (namely Beclin-1 and light chain 3B-II (LC3B-II)) are heightened in

various cell types (e.g. macrophages and neurones) treated with $1,25(OH)_2D_3$ [214,215]. Recent RNAseq data has also highlighted key autophagy-related gene sets that are upregulated in VDR-KO rats, thereby providing a solid platform for researchers to devise and plan future research upon [213].

1.3.5.2 Anabolic Pathways

Conversely, hypertrophy (an increase in size of muscle cells) is largely governed via intracellular signalling cascades, and several attempts have been made in order to try and clarify the relationship between these myogenic processes and $1,25(OH)_2D_3$. Potential explanations have stemmed from studies that investigated influences upon cellular signalling, particularly post-translational modifications (PTMs) as they can be imperative to normal signalling, as exemplified by the effects exerted by $1,25(OH)_2D_3$ upon altered phosphorylation of certain members of the MAPK pathway [216]. In its phosphorylated state, Raf-1 (proto-oncogene serine/threonine-protein kinase) is able to initiate a protein kinase cascade that results in gene transcription being induced via MAPK. When C2C12 myoblasts are treated with $1,25(OH)_2D_3$, a rapid rise in serine phosphorylation of Raf-1 is seen alongside a steep rise in dephosphorylation of the Ras-GTPase-activating protein [216].

In line with these results, it has also been demonstrated that $1,25(OH)_2D_3$ can activate the cellular sarcoma kinase (c-Src), a major transcription factor that lies upstream of Raf-1, thereby also promoting gene transcription through downstream activation of MAPK [217]. Studies using VDR-KD cell lines have

confirmed that activation of MAPK signalling is dependent on VDR, as both c-Src and p38 MAPK were significantly downregulated in its absence [217]. Furthermore, reports have revealed that $1,25(OH)_2D_3$ treatment of rats undergoing high-intensity exercise reduces expression of key components of the MAPK signal cascade, namely extracellular signal-regulated kinases 1 and 2 (ERK1/2), in comparison to the placebo group [218]. Due to previous demonstrations that inhibition of ERK1/2 in myocytes leads to the induction of muscle atrophy and upregulation of MuRF1 and MaFbx, the idea of $1,25(OH)_2D_3$ reducing MPS via diminishing ERK1/2 expression levels seems rather paradoxical [219]. It is possible that this effect of vitamin D is dependent on what developmental stage the myogenic cell is in at time of study because, as discussed, its effects can be anti-proliferative. Under basal conditions, c-Src is colocalised with caveolin-1 in close proximity to the plasma membrane but, upon treatment of $1,25(OH)_2D_3$, VDR translocation to the plasma membrane occurs followed by disruption of the colocalization [220,221]. It seems that association with caveolin-1 suppresses kinase activity of c-Src, meaning it's possible to hypothesise that $1,25(OH)_2D_3$-induced translocation of VDR permits activation of c-Src signalling, therefore suggesting that c-Src acts as a gateway to cell signalling for vitamin D.

As c-Src is under positive regulation by vitamin D_3 and is also known to be an upstream regulator of Akt, it is therefore possible that the hormone is able to have some element of control over mTOR and p70kDa S6 kinase (p70S6K) signalling. The Akt/mTOR signalling pathway is deemed to be one of the

principal regulators of muscle mass in skeletal muscle, and myogenesis is seen to be impaired when mTOR is inhibited following muscle injury [222]. Akt is able to positively control MPS via its relationship with mTOR, whilst also repressing MPB through its inhibitive phosphorylation of members of the FOXO family of transcription factors [223]. Vitamin D deficiency is associated with downregulation of mTOR and subsequent suppression of its phosphorylation of eIF4E-binding protein 1 (4EBP1) and p70S6K, implying an overall decrease in MPS [224]. This was supported by demonstration of sensitization of the mTOR/Akt pathway by $1,25(OH)_2D_3$ in C2C12 myoblasts to the effects of insulin and leucine through upregulation of phosphorylation, and consequent inhibition, of glycogen synthase kinase 3β (GSK3β) by Akt [225].

Upstream of Akt lies myostatin, a negative regulator of muscle mass whose absence in both KO animal models, and human loss-of-function mutations leads to muscular hypertrophy and hyperplasia (an increased number of muscle cells) [226,227]. *In vitro* studies using the C2C12 cell line have revealed that $1,25(OH)_2D_3$ treatment at the myoblast stage induces a transition from cell proliferation to differentiation by reducing the expression of myostatin and upregulating its antagonist, Follistatin [156]. Paradoxically, these results confute previous work reporting a decrease in expression levels of promyogenic factors upon myoblast treatment with $1,25(OH)_2D_3$ compared to skeletal muscle obtained from VDR-KO mice [163]. When taking the experimental protocols used into consideration, it is possible that these contradictions may be due to time-dependent and/or dosage effects. A single

dose of $1,25(OH)_2D_3$ treatment lasting 48-96 hours [163], may have elicited an acute response resulting in diminished myogenesis, whereas prolonged exposure (i.e. 7 daily doses) could be considered as chronic and brings about pro-myogenic influences [156].

1.3.5.3 Intracellular Calcium Homeostasis

Recent data has suggested that it may be the relationship between vitamin D_3 and intracellular calcium (Ca^{2+}) homeostasis that drives certain observations. Normal healthy skeletal muscle cells have low $[Ca^{2+}]_i$ levels (100-120 nM) that are strictly controlled as perturbations of calcium homeostasis can result in activation of proteases, impaired energy production and muscular contraction, and even cellular death [228].

The response of protein kinase C (PKC) to $1,25(OH)_2D_3$ treatment was investigated *in vitro* using chick myoblasts and myotubes [229]. Vitamin D-induced translocation of PKC from the cytosol to the cell membrane was markedly higher in myotubes, as was the rise in Ca^{2+} concentration [229]. This intracellular influx of Ca^{2+} is notably reduced in antisense PKC knockdown models [230], but it appears to be VDR independent as no change is seen to the increase in PKC translocation following $1,25(OH)_2D_3$ treatment in VDR-KO models [231]. PKC modulates Ca^{2+} homeostasis via its activation of L-type voltage-dependent calcium channels (VDCCs) and store-operated calcium entry (SOCE) [232], hence it is possible to propose that the vitamin D-induced Ca^{2+} influx is mediated by these actions of PKC. Structurally, SOCE channels are

constituted of various members of the transient receptor potential-canonical (TRPC) protein family, of which TRPC3 has been identified as a primary mediator of SOCE induced by $1,25(OH)_2D_3$ [233]. In addition, TRPC1 is required for fusion of myoblasts into myotubes [234], which may partly explain conclusions made by Zhang et al. regarding the positive influence of $1,25(OH)_2D_3$ upon the influx of Ca^{2+} in myotubes, but not myoblasts, when in a calcium sufficient environment [235].

It is well recognised that calcium is required for fusion of myoblasts during their differentiation process [236,237], thus it is sensible to theorise that the suppressive influences upon myoblast-to-myotube formation may be partly due to a reduction in cytosolic calcium. Finally, it has been documented that the perturbed Ca^{2+} uptake that accompanies vitamin D deficiency alters the kinetics of muscle contraction, thereby extending the relaxation phase of contraction [238,239]. Under basal conditions, mitochondrial uptake of Ca^{2+} occurs during the twitch and tetanic responses of muscle contraction [240], but when the cell is in a vitamin D deficient state it seems that oxidative phosphorylation (OXPHOS) is impaired, and mitochondria are unable to retain Ca^{2+} [241]. If contraction kinetics are altered by this perturbed Ca^{2+} then it may be possible that this is the underlying mechanism for the muscle weakness that is a classic clinical manifestation of vitamin D deficiency.

1.3.5.4 Mitochondrial Function

Several reports have indicated a relationship between the vitamin D/VDR axis and mitochondrial physiology in skeletal muscle [242–244]. Since mitochondrial translocation of VDR was first described [245], two key questions remain unanswered: 1. What is the general role of vitamin D in mitochondria, and 2. How does this relationship specifically translate into skeletal muscle? Indeed, *in vitro* models of primary human skeletal muscle cells demonstrate improved mitochondrial bioenergetics in response to active $1,25(OH)_2D_3$ [246,247], increasing oxygen consumption rates and fission/fusion dynamics [174]. Interestingly, while CYP27B1-mediated intracrine synthesis of $1,25(OH)_2D_3$ appears to be a feature of skeletal muscle, vitamin D_3 metabolites lacking the 1α-hydroxyl group (i.e. $25(OH)D_3$ and $24R,25(OH)_2D_3$) do not elicit the same muscle bioenergetic response as $1,25(OH)_2D_3$ [174]. Thus, the muscle CYP27B1-VDR intracrine pathway may have a selective impact on muscle function. Conversely, diet-induced $25(OH)D_3$ deficiency in mice elicits reduced mitochondrial function and these changes were not mediated through alterations in mitochondrial protein content including electron transport chain (ETC) expression or citrate synthase (CS) activity [243].

Recent supplementation studies in humans have indicated that $1,25(OH)_2D_3$ results in improved mitochondrial function within skeletal muscle [248], but the mechanism for this beneficial effect has yet to be fully elucidated. Potential explanations may be that $1,25(OH)_2D_3$ can directly influence energy production (e.g. ATP synthesis) by eliciting its genomic effects on mechanisms such as

OXPHOS or the tricarboxylic acid (TCA) cycle [249]. This theory has been explored by several research groups, all of which have demonstrated upregulation of expression levels of genes associated with the TCA cycle and ETC [174,250]. Additionally, studies using VDR-KD cell lines have shown that the rate of ATP synthesis derived from OXPHOS is reduced by 20% versus a short hairpin RNA (shRNA) scrambled control [244], and that this absence of VDR is also associated with increased production of reactive oxygen species (ROS) [251]. Whilst evidence does exist to indicate a relationship between mitochondria and the vitamin D system it is clear that further investigations are required for concise conclusions to be made.

Separate from mediating $1,25(OH)_2D_3$ induced effects in muscle, the VDR seems to have an independent role upon mitochondrial function. VDR-KD *in vitro* impairs mitochondrial function, through as yet undefined mechanisms, however dysregulation of membrane permeability or Ca^{2+} handling, and raised levels of ROS may offer a potential means [244,251]. Further, in response to VDR-KO *in vivo*, multiple mitochondrial related gene sets are downregulated [213], suggesting the VDR may be necessary for mitochondrial bioenergetic function though the regulation of key mitochondrial gene sets. However, recent investigations have determined that VDR-KO mice display decreased intramuscular ATP despite showing no reductions in ETC protein expression [212]. It is postulated this may be due to changes in nutrient utilisation and efficiency rather than impaired mitochondrial function, however these aspects

and the surrounding role of the vitamin D/VDR axis upon mitochondrial function require further investigation.

1.3.6 DBP and Skeletal Muscle

As discussed in **Section 1.1.2**, 25(OH)D_3 has a remarkably long residence time in circulation of around 2-3 weeks [15]. Considering that the majority of 25(OH)D_3 circulates tightly bound to DBP, it would be sensible to consider whether this could contribute to the unusually long half-life of 25(OH)D_3, yet the turnover of DBP is, comparatively, much more rapid (1-3 days) as it is being consistently discarded and replenished hepatically [26]. Therefore, two theories have been proposed: 1. 25(OH)D_3 must either be transferred from one molecule of DBP to another or, 2. it is passed on and stored in an extravascular site.

Evidence has demonstrated that muscle cells are able to take up DBP as C2C12 myotubes have been shown to possess megalin and cubilin, the transmembrane proteins involved in DBP internalisation, and DBP-actin complexes have been found in rabbit skeletal muscle [252,253]. In addition, when pregnant rats were treated with radioactively labelled vitamin D_3, the majority of the radioactivity was recovered in the skeletal muscle of the offspring but in the form of 25(OH)D_3 [254]. When considered collectively, this evidence led to the suggestion that perhaps DBP-25(OH)D_3 complexes are internalised into muscle cells by an endocytic mechanism mediated by megalin and cubilin and, once in the cell, the DBP-25(OH)D_3 complex binds actin

filaments [255]. Subsequent proteolytic degradation of DBP in skeletal muscle would release bound 25(OH)D_3, allowing it to diffuse out of the cell, back into the circulation where it can immediately bind to another DBP molecule, therefore providing an explanation for its variable and unusually lengthy half-life. In addition, as discussed in **Section 1.2.5.4**, CYP27B1 is also expressed in mitochondria, so an intracellular store/supply of 25(OH)D_3 would permit intracrine synthesis of 1,25$(OH)_2D_3$. **Figure 1.4** provides a schematic for this process. Beyond this newly defined role for DBP, there is a significant absence of research into its relationship with skeletal muscle.

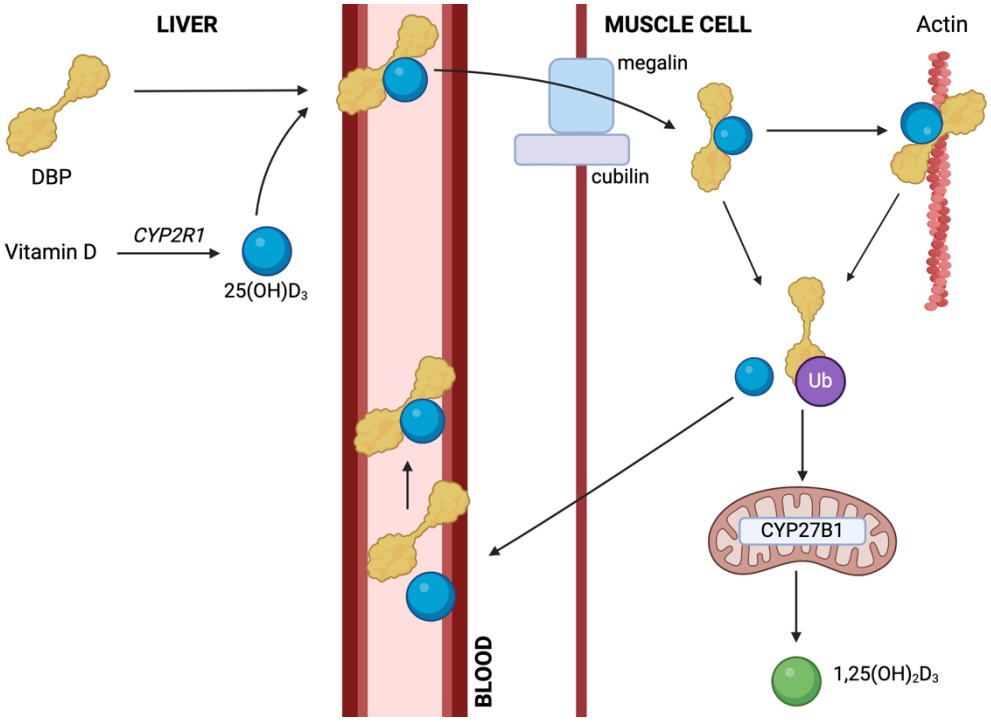


Figure 1.4. Internalisation of DBP into skeletal muscle.

DBP binds $25(OH)D_3$ (and other vitamin D metabolites) to form DBP-$25(OH)D_3$ complexes which are transported in circulation. These DBP-$25(OH)D_3$ complexes can be internalised into skeletal muscle cells via an endocytic mechanism mediated by megalin and cubilin. DBP binds actin and is proteolytically degraded, thereby releasing $25(OH)D_3$ to either diffuse back into circulation to bind another DBP molecule or to be utilised by mitochondria for synthesis of $1,25(OH)_2D_3$. Abbreviations: *DBP,* vitamin D binding protein; *CYP2R1,* 25-hydroxylase; *$25(OH)D_3$,* 25-hydroxyvitamin D_3; *Ub*, ubiquitin; *CYP27B1*, 1α-hydroxylase; *$1,25(OH)_2D_3$*, 1,25-dihydroxyvitamin D_3. Created with BioRender.com.

1.4 Thesis Aims

As demonstrated throughout this introductory chapter, there is a sufficient body of evidence to place confidence in the hypothesis of the vitamin D axis having a direct regulatory role in skeletal muscle. However, the understanding of the mechanisms underlying this relationship remains unclear, thus highlighting a need for further research.

Therefore, the three primary aims of this thesis are to:

i) Determine the current state of knowledge with regards to the impact of genetic variation within vitamin D axis-related genes upon skeletal muscle function and physiology.

ii) Investigate the impact of key single nucleotide polymorphisms (SNPs) identified and selected from (i) upon skeletal muscle function and physiology in a cohort of elite master athletes.

iii) Provide a mechanistic basis for these vitamin D axis-related SNPs by conducting gene knockdown experiments in C2C12 myotubes.

Chapter 2: The impact of genetic variation within the vitamin D pathway upon skeletal muscle function: a systematic review

2.1 Introduction

Skeletal muscle function is highly influenced by both environmental and genetic factors. While the study of environmental factors, e.g., diet and exercise type, encompass the majority of research in this area, recent evidence suggests heritability rates of 45-82% for muscle-related traits [256]. Progressive loss of muscle and muscle function (sarcopenia) is a common feature of aging, but it is associated with an increased risk of adverse outcomes, e.g., frailty, fall prevalence, functional decline, and mortality [76]. Given the growing volume of evidence demonstrating that muscle health and function can be significantly influenced by genetics, particularly certain genetic variants [257,258], enhancement of our understanding of how an individual's genetics can influence this process is of upmost importance, plus it may provide further information with regards to prognosis and response to treatment interventions.

Considering the importance of the vitamin D axis in the general functioning of several physiological systems, the impact of genetic variation within key genes of this axis has become a particular area of interest. Indeed, SNPs of the *VDR* gene have been demonstrated to alter biological activity of the $1,25(OH)_2D_3$-VDR complex, thereby raising the possibility that, not only vitamin D status, but also VDR structure and expression can govern molecular actions [259–261]. As

discussed in depth throughout **Chapter 1**, *in vitro* studies have highlighted a key molecular role for $1,25(OH)_2D_3$ in skeletal muscle function and several hallmark symptoms of vitamin D deficiency include negative muscle outcomes [2]. This *in vitro* data has been translated further *in vivo*, as the muscle atrophy seen in murine VDR-KO models further exemplifies a fundamental regulatory role for VDR [262]. Thus, it is sensible to hypothesise that SNPs within vitamin D-related genes could influence various parameters of muscle function [2].

Therefore, here, the aim was to conduct a systematic literature review examining the role of genetic variance in members of the vitamin D pathway upon skeletal muscle function, including muscle power, strength, and mass. SNPs for the following genes were researched: *VDR, DHCR7, RXRA, GC, CYP27B1, CYP2R1, CYP24A1, LRP2, and CUBN*.

2.2 Materials and Methods

2.2.1 Search Strategy & Study Selection

Following PRISMA guidelines, a systematic literature review was conducted, and it was registered on PROSPERO [263]. PubMed, Web of Knowledge (WoK), and EMBASE were searched up to week 1, June 2022. A search was conducted for studies published between 2000 and 2022, that investigated the association of muscle outcomes and genetic factors known to be linked with the vitamin D pathway and metabolism. To minimise bias, this search was conducted on two separate occasions.

The following common variants of the vitamin D receptor (*VDR*) were searched: FokI, rs2228570, TaqI, rs731236, BsmI, rs1544410, ApaI, rs7975232, and Cdx2, rs11568820. Variants in other genes involved in synthesis, transport, or metabolism of vitamin D were also included: *DHCR7*, 7-dehydrocholesterol reductase, *CYP2R1*, 25-hydroxylase, *CYP27B1*, 1α-hydroxylase, *CYP24A1*, 24-hydroxylase, *LRP2*, megalin, *CUBN*, cubilin, *RXR*, retinoid X receptor, *GC,* and vitamin D binding protein. Papers were included if they investigated association between the aforementioned SNPs and muscle function parameters, e.g., hand grip strength (HGS), timed up and go test (TUG), and knee flexion/extension (KF/KE). All human research articles regardless of language and article type were considered, whilst bibliographies of retrieved papers and previous reviews were also hand-searched to identify other relevant studies.

2.2.2 Inclusion Criteria

PICO criteria for study inclusion were as follows: (1) participants – individuals of any age, (2) intervention or exposure – assessment of vitamin D genetic factors known to affect vitamin D metabolism, pathways, and concentration, (3) comparators – studies reporting a quantitative association between muscle function outcomes and genetic variation/gene expression in normal tissue, and (4) outcome – muscle specific parameters, including muscle strength, power, and mass.

2.2.3 Data Extraction

Data extraction was performed by a single investigator (SB) using a tailored data extraction form that included the following information: authors, publication year, study type, participants (number, sex, age, ethnicity), gene name, polymorphism, muscle phenotype/outcomes, and primary findings of study.

2.2.4 Quality Assessment

Quality and bias risk of included studies was assessed by using the Quality of Genetic Association Studies (Q-Genie) tool [264]. This tool is comprised of 11 items covering the following areas:

1. Rationale for study
2. Selection & definition of outcome of interest
3. Selection & comparability of comparison groups
4. Technical classification of the exposure

5. Non-technical classification of the exposure
6. Other sources of bias
7. Sample size & power
8. A priori planning of analyses
9. Statistical methods & control for confounding
10. Testing for assumptions & inferences for genetic analyses
11. Appropriateness of inferences drawn from results

Each item was scored on a 7-point Likert scale (1 = poor, 3 = good, 5 = very good, 7 = excellent) and overall quality of the included study was classified by collating the total scores from each item. For studies that included a control group, a total score of <35 indicated poor quality, 35-45 indicated a study of moderate quality, and >45 meant a good quality study. Comparatively, studies that lacked a control group were considered poor quality if they had a score of <32, moderate quality if the score lied between 32-40, and good quality if they scored >40. Corresponding authors were contacted in the event of missing details to ensure accuracy of scores given.

2.3 Results

The process of study selection is depicted as a flowchart in **Figure 2.1**. The systematic search of three online databases identified an overall total of 1848 papers. Following removal of duplicates and screening of titles/abstracts for eligibility, 21 studies remained. Of the 21 studies included in this review, 17 were cross-sectional and 4 were longitudinal. The main characteristics of the 17 cross-sectional studies are summarised in **Table 2.1**, whilst **Table 2.2** represents a summary of the 4 longitudinal studies. Publication dates of included articles ranged from 2002 to 2020. The majority of the studies were conducted in Europe (11 studies from France, Sweden, Italy, Belgium, UK, and Hungary), followed by China and the USA (3 studies each).

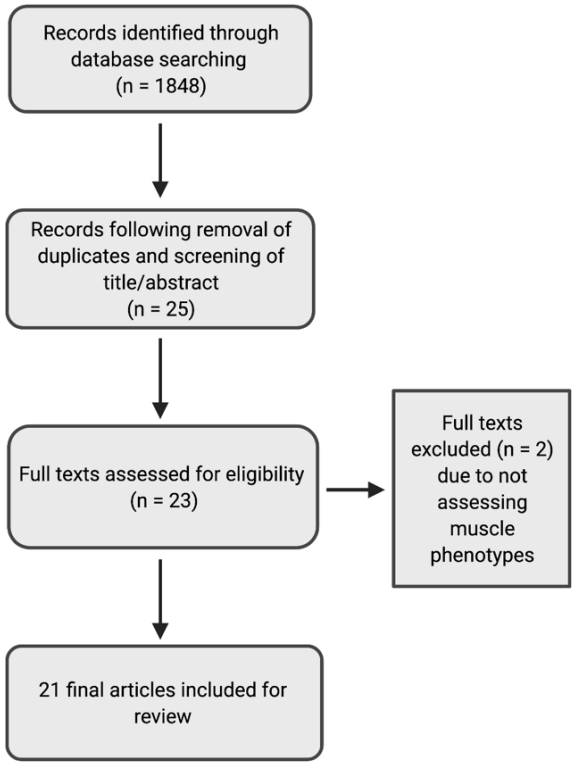


Figure 2.1. A flow chart depicting the process of identifying and selecting articles for review. Created with BioRender.com

Table 2.1. Cross-sectional studies on associations of polymorphisms of vitamin D-related genes with muscle phenotypes.

[REF]; Region	*Gene*/ SNP	Sample Population	Study Outcome	Results	Q-Genie Score
[265]; USA	***VDR*** A1012G, FokI, DdeI, BsmI, TaqI	**Cohort - AIMMY** N=273 (102M & 171F) Average Age: 21.25±2.22yr	HGS	**FokI** Caucasian females carrying ≥1 F allele displayed significantly greater right HGS versus ff homozygotes (*p*=0.035). **A1012G** Black GG females displayed significantly greater left HGS (*p*=0.046).	36
[266]; Sweden	***VDR*** BsmI, 3' UTR poly A repeat	N=175F Average Age: 29.6±5.9yr	KF & KE; HGS; lean & fat mass	**BsmI** BB homozygotes displayed significantly higher hamstring strength than bb (*p*=0.03). **3' UTR poly A repeat** Individuals carrying ss genotype had significantly higher hamstring strength and fat mass than LL (*p*=0.02 & 0.04, respectively).	42
[267]; Turkey	***VDR*** FokI, BsmI, TaqI	**Cases** N=120M Average Age: 69±6.9yr **Controls** N=60M Average Age: 34±5yr	KF & KE; FFM	**BsmI** BB homozygotes displayed significantly higher KE strength versus Bb/bb (*p*=0.038).	43

[268]; Italy	***VDR*** FokI, BsmI	N=259 (87M & 172F) Average Age: 85.0±4.5yr	HGS; SPPB score	No significant differences in muscle strength or physical performance were found between genotypes.	43
[269]; China	***VDR*** FokI, BsmI	**Cases** N=205 (94M & 111F) Average Age: 68.77±6.86yr **Controls** N=410 (183M & 227F) Average Age: 67.92±7.43yr	HGS; gait speed; ASM; SMI	**FokI** Both male and female ff homozygotes displayed lower HGS than F allele carriers (*p*=0.013 & 0.047, respectively). f allele increased risk of sarcopenia compared to F allele (OR = 1.310, 95% CI: 1.032, 1.663). **BsmI** Bb males displayed lower HGS but higher SMI than BB (*p*=0.006 & 0.036, respectively). Bb heterozygotes were more likely to have lower HGS than BB individuals (β = -0.05, 95% CI: -0.10, 0.01).	55
[270]; Hungary	***VDR*** A102G, FokI, DdeI, BsmI, TaqI, rs10783215	N=706 (360M & 346F) Average Age: 9.8±1.2yr	HGS	**BsmI** bb homozygotes displayed significantly lower HGS than BB (*p*=0.010). **A1012G** GG homozygotes displayed significantly higher HGS than AA (*p*=0.009). **TaqI** CC homozygote displayed significantly higher HGS than TT (*p*=0.038).	48

[271]; Sweden	***VDR*** Cdx2, rs9729, rs10735810, rs17882106, rs7136534, rs11574024, rs4516035,	N=2844M Average Age: 75.4±3.2yr	HGS; STS5; 6m walk; 20cm narrow walk	No significant differences in muscle strength or physical performance were found between genotypes.	50
[272]; UK	***VDR*** FokI, BsmI	**Cases** N=107 (75M & 32F) Average Age: 63.5±9.5yr **Controls** N=104 (48M & 56F) Average Age: 61.8±8.5yr	HGS (controls only); Quads MVC; FFM	**FokI** In both whole group and COPD patients only, FF homozygotes displayed significantly lower KE strength than f allele carriers (*p*=0.01 & 0.02, respectively).	48
[261]; USA	***VDR*** FokI, BsmI	N=302M Age: 58-93yr	Quads ASM; SMI; total FFM	**FokI** FF males had significantly lower AFFM, FFM and SMI compared to f allele carriers (*p*=0.009, 0.002, 0.001, respectively), and a 2.17-fold higher risk of sarcopenia (*p*=0.03).	46
[273]; USA	***VDR*** FokI, BsmI, TaqI	N=864 (489M & 375F) Age: 22-90yr	HGS; KE peak torque; AFFM; total FFM	**FokI** FF had modestly lower peak KE torque than Ff/ff (p=0.04). **BsmI** b allele carriers had higher peak torque at 180° and 30° than BB homozygotes (p=0.02 & 0.01, respectively).	49

[274]; China	***VDR*** FokI, BsmI	N=785 (275M & 510F) Age: 63.1-72.5yr	HGS; gait speed; SMI; FFM; total fat mass	**FokI** HGS and SMI were significantly higher in ff males versus those carrying ≥1 F allele (*p*=0.03 & 0.04 respectively) and their risk of sarcopenia was lower (*p*=0.03). **BsmI** bb homozygotes displayed greater HGS than carriers of ≥1 B allele (*p*=<0.01).	49
[275]; France, UK, Germany,	***VDR*** FokI, BsmI	**OPUS cohort** N=1970F Average Age: 66.9±7.0yr	HGS; rise from chair test	**BsmI** B allele carriers performed better on rise from chair test both with and without arms in comparison to bb homozygotes (*p*=0.008 & 0.03, respectively). These individuals also displayed significantly lower maximum power (*p*=0.044).	49
[276]; Italy	***VDR*** FokI, BsmI, TaqI, ApaI	**Centenarians** N=102M Average Age: 102.3±0.3yr **Septuagenarians** N=163M Average Age: 73.0±0.6yr	HGS	**FokI** In centenarians, FF homozygotes had higher left HGS than f allele carriers (*p*=0.021).	51

[277]; Taiwan	***VDR*** ApaI, BsmI, DdeI, rs2239185	**Cases** N=103 (36M & 67F) Average Age: 76yr **Controls** N=369 (215M & 154F) Average Age: 72.7yr	HGS	**ApaI** AC females displayed significantly lower HGS than CC homozygotes (p<0.05). Presence of the minor allele of each SNP and physical inactivity were jointly associated with increased risk of low HGS in both females and males.	45
[278]; Belgium	***VDR*** BsmI, TaqI, FokI	N=493 (253M & 240F) Average Age: 48.2yr	HGS; KE & KF; FFM	**FokI** Female ff homozygotes displayed significantly higher isometric KE strength at 90°. B**smI-TaqI Haplotype** Male BtBt homozygotes displayed significantly greater isometric KE strength at 150° than bT carriers (p=0.01).	51
[279]; Belgium	***VDR*** TaqI, ApaI	**Cases** N=271M Age: 71-86yr **Controls** N=135M Age: 20-50yr	HGS; EF; STS5	No significant differences in muscle strength or physical performance were found between genotypes.	52
[280]; China	***VDR*** TaqI, ApaI, BsmI	N=109F Average age: 19.82yr	KF & KE; EF & EE	**BsmI** B allele carriers displayed significantly higher KF at 180° than bb homozygotes (p=0.030). **ApaI** AA homozygotes displayed significantly lower KE at 120° than Aa & aa carriers (p=0.004 & 0.003, respectively). These individuals also displayed lower EE and EF at 120° and 30° than aa homozygotes (p=0.0029 & 0.0039, respectively.)	39

[281]; UK	***CYP3A4*** – rs2740574 ***CUBN*** – rs3740165 ***RXRA*** – rs7861779, rs9409929 ***CYP24A1*** – rs6013897, rs2762934, rs2762939, rs2248137 ***GC*** – rs16846876, rs7041, rs12512631, rs4588, rs2070741, rs2298849 ***CYP27A1*** – rs17470271 ***CYP27B1*** – rs4646536, rs4646537 ***LRP2*** – rs3755166 ***DHCR7*** – rs12785878, rs3829251 ***VDR*** – TaqI, Cdx2, A1012G, ApaI, BsmI, FokI, rs4334089, rs10783219, rs7976091, rs2238136, rs2853539, rs7970314,	N=278 (169M & 109F) Age: 41-92yr	Quads strength	No significant differences in muscle strength were found between genotypes.	46

Abbreviations: *[REF],* reference; *SNP,* single nucleotide polymorphism; *M*, male; *F*, female; *USA,* United States of America; *UK,* United Kingdom; *VDR*, vitamin D receptor; *yr,* years; *m,* metre; *cm,* centimetre; *OR,* odds ratio; *CI,* confidence interval; *HGS*, handgrip strength; *MVC*, maximum voluntary contraction; *FFM*, fat-free mass; *AFFM*, appendicular FFM; *SMI*, skeletal

muscle index; *ASM*, appendicular skeletal muscle mass; *TUG*, timed up and go; *STS5*, five times sit-to-stand test; *SPPB*, short physical performance battery; *KE*, knee extension; *KF*, knee flexion, *EE*, elbow extension; *EF*, elbow flexion; *TE*, trunk extension; *TF*, trunk flexion; *COPD,* chronic obstructive pulmonary disease; *AIMMY,* Assessing Inherited Markers of Metabolic Syndrome in the Young; *OPUS,* the Osteoporosis and Ultrasound Study.

Table 2.2 Longitudinal studies on associations of *VDR* polymorphisms with muscle phenotypes.

[REF]; Region	*Gene/* SNP	Study Design	Sample Population	Study Outcome	Results	Q-Genie Score
[282]; France	BsmI, TaqI, ApaI	Followed prospectively for 11 years	N=589F Average Age: 62yr	HGS	No significant differences in muscle strength were found between genotypes	45
[283]; Japan	TaqI, ApaI	Followed prospectively for 4 years	N=119F Average Age: 60.1±6.6yr	HGS; KF & KE; TF & TE	No significant differences in muscle strength were found between genotypes.	45
[265]; USA	***VDR*** A1012G, FokI, DdeI, BsmI, TaqI	12-week unilateral resistance training of non-dominant arm	**Cohort - FAMuSS** N=436 (167M & 269F) Average Age: 23.5yr	Bicep MVC; whole-muscle volume	**FokI** Males carrying ≥1 F allele displayed significantly greater baseline biceps strength (p=0.049). These individuals displayed smaller changes in whole muscle volume at 12 weeks than ff homozygotes (p=0.034).	36

[284]; Japan	***VDR*** BsmI, TaqI, FokI, ApaI	12-week intervention of low-resistance training twice/week	N=63 (24M & 39F) Average Age: 76.7±9.65yr	HGS; TUG; brain-grip reaction time; 6-minute walk; one leg stand with eyes open; anterior bending at sitting; 32m walk; 2 minutes of stepping; muscle boundary length	**BsmI** bb homozygotes had greater changes in muscle boundary length of right thigh (*p*=<0.05). **ApaI** Those carrying ≥1 A allele displayed greater changes in muscle boundary length of upper and forearms, and right thigh (both *p*=<0.05 & <0.05). **FokI** Those carrying ≥1 f allele displayed greater changes in muscle boundary length of right forearm and left upper and forearm (both *p*=<0.05 & <0.05).	38

Abbreviations: *[REF]*, reference; *SNP,* single nucleotide polymorphism; *USA,* United States of America; *M*, male; *F*, female; *yr,* year; *HGS*, handgrip strength; *MVC*, maximum voluntary contraction; *FFM*, fat-free mass; *TUG*, timed up and go test; *ADL*, activities of daily life; *KE*, knee extension; *KF*, knee flexion; *TE*, trunk extension; *TF*, trunk flexion; *m*, metre; *FAMuSS,* Functional SNPs Associated with Muscle Size and Strength.

2.3.1 Demographics of Included Participants

In total, 12,414 subjects participated across the 21 studies. Of these, 6574 (52.96%) were men and 5840 (47.04%) were women, and 81% of included articles only included participants aged ≥50 years. Of the 21 studies, 15 included Caucasians, 7 assessed Asian subjects, and only 2 studies also included Black participants. All 21 studies included muscle strength testing, but only 6 reported physical function outcomes and 9 described body composition. Muscle mass and size was only investigated in 3 studies.

2.3.2 Quality of Included Studies

All included articles were assessed as being of either moderate or good quality.

2.3.2.1 VDR

Of the twenty-one articles that were included for final analysis, 20 only studied genetic variation of the *VDR* gene. Across the studies, a total of 20 different *VDR* SNPs were investigated in relation to muscle function, with multiple studies identifying associations with muscle outcomes and BsmI (rs1544410), FokI (rs2228570), ApaI (rs7975232), and A1012G (rs4516035).

A study conducted in 2004 in Swedish women demonstrated a significant association between the BsmI and poly A *VDR* genotypes and muscle strength [266]. Carriers of the shorter poly A genotype (ss) and/or the linked BsmI restriction site (BB) displayed greater hamstring strength than subjects possessing the long allele of poly A (LL) and bb genotypes ($P = 0.02$ and $P = 0.03$,

respectively). However, following adjustment for confounding factors, i.e., age, fat, and lean mass, this significance was lost [266]. The observation of higher muscle strength in BB individuals has since been replicated, as it was seen that those with higher knee extensor (KE) and quadriceps strength were carriers of the B allele [267,280]. However, results among the studies are also rather conflicting. One study found that B allele carriers had a significantly higher fall risk and demonstrated a poorer performance on rise from chair and power tests than bb homozygotes (P = 0.03 and P = 0.044, respectively) [275]. bb homozygotes have also been shown to have higher handgrip (HGS) and KE strength – a trait also seen in bb COPD patients [269,272,273,285]. Whilst the previously discussed studies identified significant associations between BsmI and muscle function and strength, 7 of the 17 studies that investigated BsmI failed to find any differences at all [261,268,271,276,277,281,282].

Comparatively, despite being included in 12 studies, only one study is yet to have found a significant association for the TaqI SNP, as Bozsodi et al. highlighted that homozygous tt schoolchildren had higher handgrip strength in their dominant hand than their TT counterparts (P = 0.010) [285]. Due to the strong linkage disequilibrium (LD) that exists between BsmI and TaqI, several studies have opted to include BsmI-TaqI haplotypes in their analyses [273,278]. Whilst Walsh et al. failed to demonstrate any significant associations between the haplotypes and muscle parameters, they did find that the bT/bT haplotype was significantly associated with a higher fat free mass (FFM) in males [273]. Additionally, the bT/bT haplotype has also been linked with higher muscle

strength, as carriers displayed higher concentric and isometric KE strength (P = 0.01) [278].

15 of the 21 included articles investigated FokI, and 10 reported significant differences between genotypes. Individuals carrying at least 1 copy of the mutant F allele of FokI have been shown to display higher baseline muscle strength (i.e., MVC and HGS) [265,269,276] but, in contrast, other studies reported an opposing relationship in which the F allele is instead associated with poorer muscle strength [261,272–274,278]. Several studies have described associations between the FokI polymorphism and physical function, but the results conflicted. Indeed, elderly FF homozygotes display reduced gait speed, yet younger FF homozygotes perform better on the timed up and go (TUG) test [269,279]. Only two studies reported associations between body composition parameters and FokI. Roth et al. reported that FF carriers have significantly lower appendicular muscle mass and total FFM (P= 0.009 & 0.002, respectively), whilst Xia et al. described an association between the ff genotype and increased skeletal muscle index (SMI) (P = 0.04) [261,274]. Two studies reported that FF homozygotes carried an increased risk of sarcopenia [261,273] but, comparatively, it has also been reported that those homozygous for the f allele possess a higher sarcopenic risk [269].

Of the 8 studies that included the ApaI polymorphism in their investigations, only 3 reported significant associations [277,280,284]. For every mutant A allele, the risk of low HGS was reported to increase 2.05-fold [277], and AA

homozygotes displayed reduced KE and EE strength (P = 0.003 & 0.004, respectively) [280]. Additionally, the aa genotype was reported to significantly influence change of boundary lengths of upper- and forearm muscles, but the paper failed to report whether the change was positive or negative (P = <0.05) [284]. The C allele of the DdeI polymorphism was reported to increase the risk of low HGS in physically inactive elders [277]. Whereas individuals carrying the A1012G SNP displayed the highest HGS in two studies [265,285].

2.3.2.2 Other Studied Genes of the Vitamin D System

The only included article that investigated genes of the vitamin D pathway other than that encoding the vitamin D receptor (*VDR*) was published in 2018 by Jolliffe et al [281]. This study genotyped for 35 SNPs across 11 genes (*CYP3A4, CUBN, RXRA, CYP24A1, GC, CYP27A1, CYP27B1, CYP2R1, LRP2, DHCR7 & VDR*) in a small (n = 134) cohort of COPD patients. No significant associations were found between any of the studied SNPs and quadriceps strength [281].

2.4 Discussion

At time of writing (Summer 2024), the systematic review conducted in this chapter provides the most up to date and extensive overview of research into associations between genetic variation of the vitamin D system and skeletal muscle. The literature search displayed that this research has been primarily restricted to one gene, the gene for the vitamin D receptor (*VDR*). At time of writing this thesis, Spring 2024, there remains to only be a single study investigating associations between genetic variance of *RXRA, GC, CYP27B1, CYP2R1, CYP24A1, LRP2, and CUBN* with muscle function [281].

Our search generated a total of 21 articles; 20 of which were exclusively focused on the *VDR* gene. The two most frequently studied SNPs were BsmI (rs1544410) and FokI (rs2228570), but inconsistencies were found across these studies, and many failed to replicate earlier findings. For example, 6 studies demonstrated that the BsmI SNP was significantly associated with lower muscle strength and poor performance on physical function tests [269,272–275] yet, comparatively, 3 studies displayed carriers of BsmI had higher muscle strength than those not carrying the SNP [266,267,285]. Inconsistencies between results is also an issue with the FokI SNP (also known as the start codon polymorphism (SCP)), a SNP of particular interest due to being the only known *VDR* polymorphism resulting in structural changes within the VDR protein. FokI is associated with a T-to-C substitution in the first 5' ATG start codon of the *VDR* gene. This change of ATG to ACG abolishes the start codon and forces translation to initiate at the second initiation site located three

codons downstream, thereby resulting in the production of a protein that is 3 AA shorter than the WT (424 AA as opposed to 427 AA) [286]. Whilst very few studies exist that have investigated the functional consequences of this SNP, it appears that the resulting shorter protein possesses increased biological activity which would subsequently influence its transcriptional activity and activation of genes containing VDREs [287]. Of the 15 articles that included FokI in their investigations, 10 found significant associations with outcomes related to muscle function and physical performance but, like BsmI, the findings conflict. 7 of the 10 studies found that ff genotype carriers (WT; the longer isoform) performed better across a range of muscle phenotypes/outcomes and that those carrying a mutant F allele had a greater risk of sarcopenia [261,265,272–274,278,284]. rs4516035 (A1012G) was the only SNP to be consistently associated with greater HGS [265,285]. This SNP is located in the 1A promoter region at the 5' end of the *VDR* gene and is the result of an A-to-G transition. Similar to FokI, the functional impact of this SNP is unclear, but it has been proposed that the G variant (mutant) has reduced affinity of GATA3 for its promoter [288]. Furthermore, it is possible that A1012G is a determinant of where transcription begins from, either exon 1a or 1d. If transcription starts in exon 1a (A allele; WT), then it would lead to the production of a normal length VDR protein, but if it starts in 1d (G allele; mutant), then a longer mutant VDR protein would result [288].

The reasons for disparities between findings are most likely multifactorial due to the varying methodologies, study design, population demographics, and

ethnicities that span across the included studies. All 21 articles measured muscle strength, but methods differed, as 48% determined strength via HGS only. Measurement of HGS is a cheap and useful indicator of strength and is one of the four factors required in sarcopenia diagnosis, yet variations can arise by differences in dynamometer type, participant position during testing, and reference values used for cut-offs [289].

Articles were included regardless of the health status of included participants to provide a complete overview of current research so inclusion of a mixture of healthy and disease cohorts (e.g., COPD) may contribute to the variable results seen here. However, a previous systematic review that only included articles with healthy cohorts also reported variable results, so it would seem that the mixture of healthy/disease states contributed minimally to result variability in this instance [290]. Similarly, no criteria were set with regards to age of included participants, as the aim was to capture as much of the available literature as possible. However, it should be noted that this approach does have its limitations as it is possible that co-factors associated with age may affect skeletal muscle function and performance to a greater extent than that of the SNP. This raises an important question of would the effects of these SNPs still be seen if studied in younger participants where the influence of age-related factors on skeletal muscle are removed? While this question cannot be answered herein, it represents a potentially interesting line of research moving forwards.

Finally, and likely the most extreme disparity, only two of the 21 studies included Black participants [265,281]. This racial bias isn't restricted to research of genetic variation of the vitamin D system; in fact, individuals of African and Latin American descent only make up 1-2% of participants in genome-wide association studies (GWAS), whilst white Europeans constitute 78% [291]. Exclusion of Black individuals and other people of colour from genetic research prevents research from capturing global genetic diversity and impedes our ability to fully understand the genetic basis of human physiology and disease. Until these populations are better represented in genetic research, results will remain poorly representative of the global population and will only exacerbate health disparities further.

2.5 Future Directions and Conclusions

This systematic review provides a comprehensive and up-to-date view on the current understanding with regards to research into genetic variation within the vitamin D axis and its impact upon skeletal muscle. Research was found to have primarily focused on the *VDR* gene and there is a large amount of variability between results; only one SNP was consistently associated with greater HGS (A1012G; rs4516035). While the lack of definitive evidence and study heterogeneity makes it difficult to draw conclusions, the findings of this review highlight a need for improvements with regards to the use of more diverse study populations, i.e., inclusion of Black individuals and other people of colour, and expanding research scope beyond the *VDR* gene. Moving forward, efforts should be made to try and provide explanations for the genetic-phenotypic associations that exist between *VDR* variants and muscle, as this could provide further information on the genetic basis of *VDR.* Additionally, exploration of other genes within the vitamin D system (**Figure 2.2**) in relation to skeletal muscle, e.g., vitamin D binding protein (DBP; *GC*) and megalin (*LRP2*), may synthesise novel relationships and mechanisms that will contribute to the overall understanding of vitamin D physiology in relation to muscle health. Finally, there has been a distinct absence of GWASs focused on variants of *VDR* and other genes within the vitamin D system in relation to traits such as HGS. Given the volume of large databases possessing relevant musculoskeletal function data for large cohorts (>10,000 individuals) it is therefore reasonable to suggest a GWAS as the next investigation moving forwards.

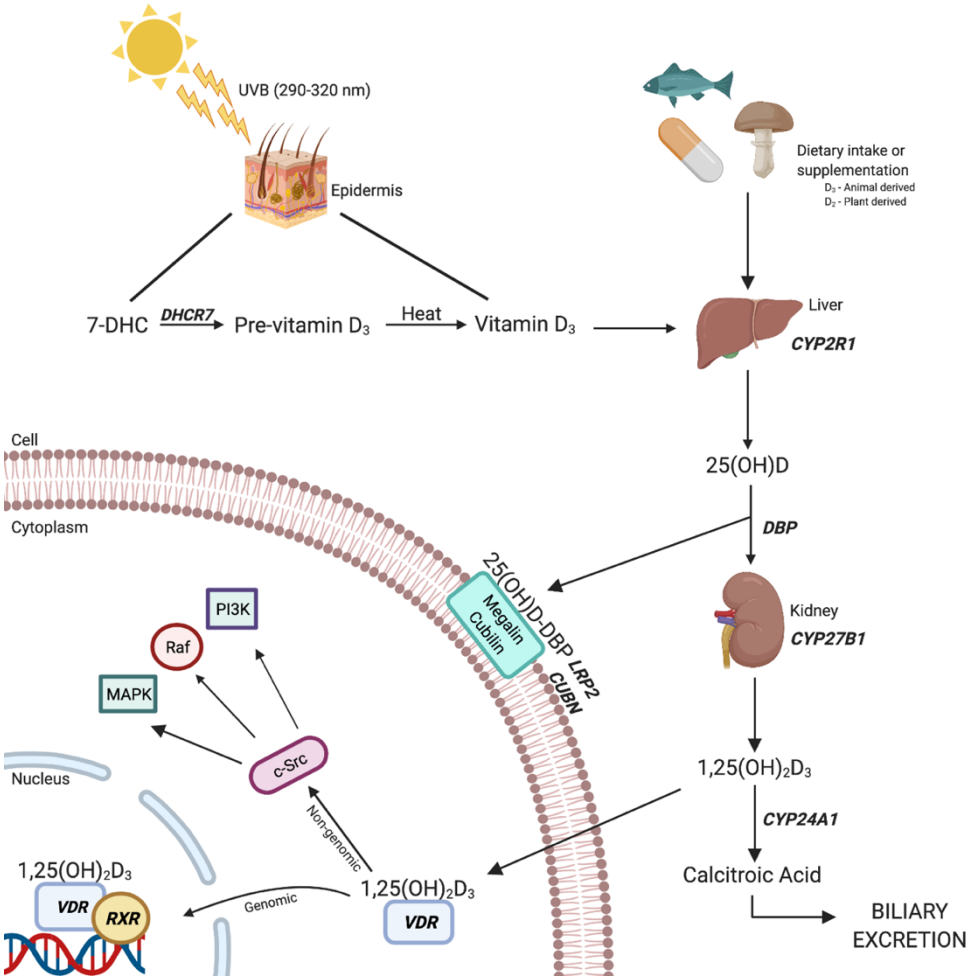


Figure 2.2. The vitamin D system and key genes. Genes are highlighted in bold italics. Abbreviations: *7-DHC;* 7-dehydrocholesterol; *7-DHCR7*, 7-dehydrocholesterol reductase; *25(OH)D$_3$*, 25-hydroxyvitamin D$_3$; *1,25(OH)$_2$D$_3$*, 1,25-dihydroxyvitamin D$_3$; *CYP2R1*, 25-hydroxylase; *DBP*, vitamin D binding protein; *CYP27B1*, 1α-hydroxylase; *VDR*, vitamin D receptor; *RXR*, retinoid X receptor; *LRP2*, megalin; *CUBN*, cubilin; *CYP24A1*, 24-hydroxylase; *nm*, nanometre; *UVB*, ultraviolet B; *D$_2$,* ergocalciferol; *D$_3$,* cholecalciferol; c-*Src*, proto-oncogene tyrosine-protein kinase; *MAPK*, mitogen-activated protein kinase; *Raf,* proto-oncogene serine/threonine-protein kinase; *PI3K*, phosphatidylinositol-3-kinase. Created with BioRender.com

Chapter 3: The association of vitamin D receptor (*VDR)* and vitamin D binding protein gene (*GC*) single nucleotide polymorphisms with skeletal muscle function and performance in elite master athletes – a candidate gene association study

3.1 Introduction

Commonly considered a geriatric syndrome, sarcopenia is the term given to define an age-related decline in muscle mass and function [292]. The functional consequences of sarcopenia can be vast, ranging from an increased risk of falls to impaired quality of life and, ultimately, increased mortality. Whilst sarcopenia is most frequently observed in individuals over the age of 70, declines in muscle mass and function have also been documented in younger groups, thereby warranting investigations into potential mechanisms and interventions [293]. It is difficult to define the definitive driving forces for sarcopenia onset as it appears to be a multifactorial syndrome. A multitude of hypotheses have been suggested, including environmental, hormonal, neurological factors, nutrition, and genetics [294].

One factor that encompasses several of these hypotheses is vitamin D, whose physiology and synthetic pathways have been described in great detail throughout **Chapter 1**. As a steroid hormone, vitamin D primarily acts via its receptor, vitamin D receptor (VDR). VDR expression has been documented in

human skeletal muscle and appears to decline with age but studies in rat models have demonstrated that it is positively responsive to a single bout of exercise [83,150,295]. *VDR* knockout (VDR-KO) and/or *VDR* overexpression (VDR-OE) animal and cellular models have exemplified the mechanistic importance for VDR in skeletal muscle [213,296]. Located in the centromeric region of chromosome 12 (12cen-q12), the *VDR* gene is 100kb long and >100 SNPs have been reported [297]. BsmI (rs1544410), TaqI (rs731236), and FokI (rs2228570) are among the most frequently studied *VDR* SNPs and have all been found to be associated with differences in muscle strength and function [266,270,272]. However, the systematic review conducted in **Chapter 2** exemplified that results conflict across the literature with some studies failing to report any differences at all, which may be a consequence of variable study design, methodologies, and population demographics [3]. A1012G, a SNP occurring in the 5' 1e promoter region of the *VDR* gene, has been consistently found to have an association with higher HGS [265,285]. Whilst the functional impact of this SNP hasn't been defined, it is possible that the differences in muscle strength stem from altered VDR transcriptional activity and mRNA stability due to the SNPs location in the *VDR* 5' promoter [288,298].

In circulation, the majority of 25(OH)D_3 is bound to a member of the albuminoid family, vitamin D binding protein (DBP). Encoded by the *GC* gene located on chromosome 4q11-13, DBP has several functions other than transporting vitamin D metabolites, including actin scavenging, binding of fatty acids (particularly unsaturated), and activation of the complement C5 system [26].

The missense variants rs4588 (T436K; c.1307C>A) and rs7041 (D432E; c.1296T>G) are both located in exon 11 of the *GC* gene and are two of the most frequently studied *GC* SNPs. Three common DBP isoforms exist that depend on what alleles of rs4588 and rs7041 an individual possesses. Gc1f (rs7041-T/rs4588-C) is the most frequent isoform, followed by Gc1s (rs7041-G/rs4588-C) and, finally, Gc2 (rs7041-T/rs4588-A) (**Table 3.1**) [40]. Both the presence of an actin binding site on DBP and the discovery that, in rats, maternal 25(OH)D_3 is transported from the placenta directly to the foetal skeletal muscle where it accumulates, has led to the hypothesis of a functional relationship existing between muscle and DBP, particularly in the conservation of vitamin D status [254,299]. Several candidate gene studies have investigated the relationship between *GC* SNPs and vitamin D status, yet there is a distinct absence of studies investigating the functional impact of variance within the *GC* gene upon skeletal muscle [300–302].

Thus, the aim of this chapter was to evaluate the potential relationship of SNPs of genes encoding vitamin D receptor (*VDR*) and, for the first time, vitamin D binding protein (DBP; *GC*) with neuromuscular performance and musculoskeletal characteristics in a cohort of elite master athletes (MA) and non-athletic controls. The cohort of MA used herein represents a physiologically distinct population of older individuals with diverse muscle mass, function, and performance compared to that of age-matched controls. Therefore, they offer a unique population to study the impact of genetic variation upon muscular outcomes but in an aged cohort.

Table 3.1. *Characteristics and allele information for DBP (GC) isoforms.*

Haplotype	Alleles rs7041/rs4588	AA 432/436
Gc1f	**T/C**	**Asp/Thr**
Gc1s	**G/C**	**Glu/Thr**
Gc2	**T/A**	**Asp/Lys**

Abbreviations: *T*, thymine; *C,* cytosine; *G,* guanine; *A,* adenine; *AA*, amino acid; *Asp*, aspartic acid; *Thr,* threonine; *Glu*, glutamine; *Lys*, lysine.

3.2 Methods

3.2.1 Participants & Ethical Approval

The study was conducted in accordance with the Declaration of Helsinki, except for registration in a database. The study was approved by the University Research Ethics Committee (14/NW0275) and the National Research Ethics Service Committee Northwest (15/NW/0426). All participants provided written informed consent.

N = 47 male MA were recruited as part of the Vertical Impact on Bone Health in Elderly (VIBE) multiple cohort study [303,304] through two national MA competitions and adverts placed in a national athletics magazine. N = 45 male controls were recruited from the local community. To be included, MA had to be actively competing in their respective disciplines and completing 5 or more hours of training per week at time of testing. 12 MA were sprinters (those competing in events <800m) and 36 were endurance athletes (≥800m).

3.2.2 Anthropometric Measurements

Participant body mass and height were measured on calibrated scales and stadiometry, respectively, and were used to calculate body mass index (BMI). Total body fat percentage was quantified by dual-energy X-ray absorptiometry (DXA; Lunar Prodigy Advance, version EnCore 10.50.086; GE Healthcare, Little Chalfont, United Kingdom) in which the participant was in a supine position with their arms and legs fully extended. Bone mineral density (BMD; g/cm^2) was taken from full body scans. Cross-sectional area (CSA) of the right *vastus*

lateralis (VL) was determined via magnetic resonance imaging (MRI) using a T1-weighted turbo 3D sequence on a 0.25-T G-scan. An external reference easily identifiable on the MRI scan was taped to the skin to mark the motor point (approximately mid muscle belly). A series of transverse-plane slices (6mm thick) were collected before images were exported and analysed using Osirix imaging software (Osirix medical imaging, Osirix, Atlanta, GA, United States) [305].

3.2.3 Muscle Strength and Physical Performance

Upper limb strength was measured via HGS in both MA and controls with a Jamar dynamometer handle (Model 5030 J1, Sammons Preston Rolyon, Bolingbrook, IL, USA). Measurements were taken whilst the participant was stood upright with their arm fully extended beside the body, with a ~5cm gap between the hip/upper leg and the wrist to ensure that the hand was not resting against the body. Participants performed three maximum contractions with both hands and results were recorded in kilograms (kg), to the nearest 0.1kg. The best of three attempts was included for statistical analysis.

Right KE strength was assessed in the controls only. Participants were told to sit in the testing chair with both knee and hip joints flexed at 90° and an isometric force dynamometer (calibrated strain gauge, RS Components Ltd, Corby, UK) was fastened 30 cm below the centre of the knee to measure forces generated. A belt was placed across the pelvis to minimise any movement from the upper trunk. Before maximal contractions were attempted, participants

were permitted to perform several submaximal contractions as a warm-up practise. Subsequently, the participant was asked to perform contractions at maximum effort whilst the investigator provided verbal encouragement. This was repeated three times, each with a 60 second rest interval between, and the best of these three attempts was included in statistical analysis as the maximum voluntary contraction (MVC).

For assessment of physical performance, timed-up-and-go (TUG) testing was performed. Participants were asked to stand from a standardised armless chair without using their hands, walk to and around an obstacle three metres away, and then return to their original seated position. The time taken to complete the task was measured in seconds via a handheld stopwatch. Three attempts were performed by each participant and the average value was taken for statistical analysis.

Balance was assessed in the control group only by asking participants to perform standing balance tests. Participants were instructed to stand with their arms parallel to the ground and extended horizontally. Three attempts were given, each separated by intervals of 30 seconds, to achieve 30 seconds without touching external supports or taking any attempts in the following two foot-placements: 1. One-leg standing with eyes open, and 2. One-leg standing with eyes closed. The best attempt of the three attempts was taken for statistical analysis.

3.2.4 Jumping Mechanography

Lower limb power (absolute (W) and relative (W/kg)) was assessed using a Leonardo Jump Mechanography Platform (Leonardo Software version 4.2: Novotiec Medical GmbH, Pforzheim, Germany), as previously described [306]. In brief, participants were instructed to perform a two-footed countermovement jump with maximal effort. Three jumps were performed with a minute between each effort and force was sampled at 800Hz. The best of the three attempts was included for statistical analysis. All jumps were performed in the presence of a trained assistant.

3.2.5 Biochemical Parameters

All hormone measurements were conducted using a fasted venous blood sample collected between 8.30-9.30 AM in controls only. Blood samples were centrifuged immediately for 20 minutes at 3200rpm at 4°C before being aliquoted and stored at -80°C until further use. Serum concentrations of dihydrotestosterone (DHT), dehydroepiandrosterone (DHEA), DHEA sulphate (DHEAS), total oestradiol (E2), and $1,25(OH)_2D_3$ were all quantified using a validated LC-MS system. Concentrations of serum sex hormone binding globulin (SHBG) and albumin were determined via chemiluminescence and bromocresol purple, respectively.

3.2.6 Genetic DNA Extraction

Genomic DNA was extracted for use in previous work published by the group [307]. Briefly, genomic DNA was extracted from buffy coat with the QIAamp

blood mini-DNA kit (Qiagen) following manufacturer's instructions. Isolated DNA was quantified on the NanoDrop 2000 (Thermo Fisher Scientific) and stored at -80°C until further use.

3.2.7 Genotyping - Primer Design

Primers were designed using the default settings of the PRIMER1 program: http://primer1.soton.ac.uk/primer1.html. The sequences of the primers used in this study and the size of their PCR products are listed in **Table 3.2** and **3.3** (*VDR* and *GC* SNPs, respectively).

3.2.8 Genotyping - Tetra-primer ARMS PCR & DNA Gel Electrophoresis

Genotyping for four *VDR* SNPs (BsmI, Cdx2, ApaI and A1012G) and two *GC* SNPs (rs4588 and rs7041) was performed with the tetra-primer amplification refractory mutation system (tetra-ARMS) PCR technique [308]. Each PCR reaction was performed with a final volume of 16 µl, containing SYBR Green (Applied Biosystems), 30 ng of genomic DNA, and primers (SNP-specific primer ratios can be found in **Table 3.2**). Optimal annealing temperatures for each primer set were determined by initially performing a gradient PCR with the outer primers only. Successive validation steps involved incorporating the inner primers in variable concentrations to produce clear definite bands when visualised via DNA gel electrophoresis. PCR conditions were as follows: an initial denaturation step of 95°C for 2 minutes, 35 cycles of 95°C for 30 seconds, annealing at n°C (see **Tables 3.2** and **3.3** for SNP-specific annealing conditions) for 45 seconds and 72°C for 45 seconds, followed by a final extension step of

72°C for 5 minutes. Amplification was performed using a Viia 7 real-time PCR machine (Applied Biosystems). The amplified PCR products were mixed with 4 µl gel-loading buffer (New England Biolabs) and separated electrophoretically on a 2-3% agarose gel containing SYBR Safe (Invitrogen) at 100V. Gels were visualised using a ChemiDoc XRS.

Genotyping - TaqMan Assay

TaqI and FokI were both genotyped via TaqMan assays (Thermo Fisher Scientific). This was performed on a Viia 7 real-time PCR machine (Applied Biosystems) in a 384-well format. All genotyping was conducted by a single investigator (SB) who was blinded to subject status. Samples were randomised prior to genotyping and were genotyped simultaneously. Negative controls were used as a measure for quality control, and samples would be randomly selected for repeated detection.

3.2.9 Statistical Analyses

Hardy-Weinberg equilibrium (HWE) was calculated using Chi-square analysis to compare genotype frequencies. D'Agostino and Pearson testing was first performed to assess for normality. One-way ANOVA or Kruskal-Wallis test with post-hoc Tukey's for multiple comparisons were used to analyse differences in physical characteristics and outcomes between genotypes and groups. Due to small numbers in the Cdx2 AA group (n=2 for MA and controls), the AA and GA groups were combined, and either a Student T-test (for parametric factors) or Mann Whitney U test (for non-parametric factors) were performed to assess

differences between genotypes (GG vs GA/AA). Results are reported as mean ± SD and statistical significance was set at $P < 0.05$. All statistical analyses were performed using GraphPad Prism Software (Version 10.0.2; San Diego, California, USA).

Table 3.2. *VDR* SNP primer information for tetra-primer ARMS PCR

***VDR* SNP**	**Primer Sequence**	**Primer Ratio (Inner:Outer)**	**Annealing Temperature (°C)**	**Product Size**
BsmI	FI: GCAAGAGCAGAGCCTGAGTATTGGGAAGGC FO: GTCAAGGGTCACTGCACATTGCCTCCAAA RI: GTTCCTGGGGCCACAGACAGGCCTTCA RO: CTGAGGTGCCCCTCACTGCCCTTAGCTC	5:1	67	Control: 276bp G allele: 144bp A allele: 189bp
ApaI	FI: AAGGCACAGGAGCTCTCAGCTGGACC FO: ACTGCTTGGAGTGCTCCTCATTGAGGCT RI: GGGGTGGTGGGATTGAGCAGTGAAGT RO: CCCATGGAAGGACCTAGGTCTGGATCCT	2:1	55	Control: 356bp C allele: 215bp A allele: 192bp
Cdx2	FI: AGGATAGAGAAAATAATAGAAAACATT FO: TCCTGAGTAAACTAGGTCACAA RI: AACCCATAATAAGAAATAAGTTTTTAC RO: ACGTTAAGTTCAGAAAGATTAATTC	2:1	55	Control: 297bp G allele: 235bp A allele: 110bp
A1012G	FI: CGATGACCTCCTTTAGCCAGGGAATAC FO: TGGGGTTCCCTCTTCTTAGAACTCACTG RI: TTCCTCCTCTGTAAGAGGCGAATAGCACTA RO: CTCAGAAATGGTTCAGAGACCATTGCAC	1:1	65	Control: 316bp A allele: 208bp G allele: 165bp

Abbreviations: *VDR,* vitamin D receptor; *SNP,* single nucleotide polymorphism; *°C,* Celsius; *T*, thymine; *C,* cytosine; *G,* guanine; *A,* adenine; *bp,* base pairs; *FI,* forward inner; *FO,* forward outer; *RI,* reverse inner; *RO,* reverse outer.

Table 3.3. *GC (*DBP*)* SNP primer information for tetra-primer ARMS PCR

***GC* SNP**	**Primer Sequence**	**Primer Ratio (Inner:Outer)**	**Annealing Temperature (°C)**	**Product Size**
rs4588 (T436K)	FI: GCTTGTTAACCAGCTTTGCCAGTTTCG FO: AACACCAGGAAAAGCCTGTCACATAATGG RI: AGCAAAATTGCCTGATGCCACACCTAA RO: TCGAAGAGGCATGTTTCACTTTCTGATCTC	2:1	65	Control: 446bp C allele: 265bp A allele: 235bp
rs7041* *D432E	FI: GCTTTGCCAGTTCCGTGGGTGTGACC FO: TGTTTCTTACTTTCATTGCAAAGACAGCCA RI: GAGCGACTAAAAGCAAAATTGCCTAAT RO: CTCGAAGAGGCATGTTTCACTTTCTGATCT	1:1	65	Control: 486bp G allele: 254bp T allele: 285bp

Abbreviations: *GC,* vitamin D binding protein; *SNP,* single nucleotide polymorphism; *°C,* Celsius; *T*, thymine; *C,* cytosine; *G,* guanine; *A,* adenine; *bp,* base pairs; *FI,* forward inner; *FO,* forward outer; *RI,* reverse inner; *RO,* reverse outer.

3.3 Results

3.3.1 Study Population

Demographic data, physical function, muscle strength, and biochemical data for the 47 elite male MA and 45 male controls included in this study are summarised in **Table 3.4.** Controls (75.80±6.14yr) were significantly older than MA (70.66±5.99yr; P = <0.0001). Individuals in the control cohort displayed a higher weight, BMI, and higher percentage of fat mass than the MA group (P = <0.0001), whilst they also performed worse on the timed up and go (TUG) test and displayed a lower percentage of lean mass (P = <0.0001).

Table 3.4. Characteristics of the Study Population.

Variable	***MA (n=47)***	***Controls (n=45)***	***P***
Age (yr)	70.66±5.99	75.80±6.14	***<0.0001***
Height (m)	1.72±0.06	1.73±0.07	*0.6644*
Weight (kg)	66.88±8.44	78.59±14.56	***<0.0001***
BMI (kg/cm^2)	22.69±2.27	26.45±4.34	***<0.0001***
HGS (kg)	38.91±9.23	35.35±9.32	*0.0701*
TUG (s)	5.547±0.66	8.254±3.44	***<0.0001***
Hmax (m)	0.2584±0.16	0.2082±0.1	*0.3054*
Fmax (N)	1.467±0.33	1.731±0.37	*0.0014*
Pmax (kW)	2.159±0.79	2.217±0.69	*0.4200*
Pmax/mass (W/kg)	32.28±10.40	28.54±9.64	*0.1727*
Percentage Fat Mass (%)	15.62±6.11	29.76±9.21	***<0.0001***

Total Body Lean Mass (kg)	53.60±7.13	53.10±6.02	*0.7148*
Percentage Lean Mass (%)	80.28±6.30	67.86±8.61	***<0.0001***
BMD (g/cm^2)	1.200±0.17	1.242±0.13	*0.3961*
BMC (g)	29.98±5.51	32.10±6.26	*0.0880*

[1]Abbreviations: *MA,* master athletes; *yr,* year; *m,* metre; *kg,* kilogram; *cm,* centimetre; *s,* second; *N,* newton; *W,* watt; *kW,* kilowatt; *%,* percent; *g,* gram; *HGS*, handgrip strength; *TUG*, Timed Up & Go; *Hmax*, maximum jump height; *Fmax*, maximum force; *Pmax*, absolute vertical jump power; *PmaxRel*, absolute vertical jump power relative to body weight; *BMD*, bone mineral density; *BMC*, bone mineral content (whole body); *BMI,* body mass index. [2]Data shown as mean ± SD.

3.3.2 VDR & GC SNP Frequencies

Genotype frequencies for *VDR* and *GC* SNPs are shown in **Tables 3.5** and **3.6**, respectively. No significant differences in frequency were found between MA and controls for any of the *VDR* and *GC* SNPs studied and there was no deviation from Hardy Weinberg equilibrium as determined by Chi-square analyses. In addition, no significant differences in DBP haplotype frequencies were seen between MA and controls (**Table 3.6**).

VDR - For BsmI, 57.45% of MA were AA homozygotes, 29.79% AG heterozygotes, and 12.77% GG homozygotes, compared with 40% AA homozygotes, 46.67% AG heterozygotes, and 13.33% GG homozygotes in the controls. In the MA cohort for FokI, 17.02% were TT homozygotes, 46.81% TC heterozygote, and 36.17% CC homozygote whereas, for the control group,

15.56% were TT, 60% TC, and 26.67% CC. 46.81% of MA were homozygous AA, 34.04% heterozygous AG, and 19.15% homozygous GG for TaqI, compared to 44.44% AA, 44.44% AG, and 11.11% GG in controls. For ApaI, 23.40% of MA were CC homozygous, 42.55% CA heterozygous, and 34.04% AA homozygous whilst, in the controls, 15.56%, 55.56% and 28.89% were CC, CA, and AA, respectively. 74.47% of individuals in the MA cohort were AA homozygous, 21.28% AG heterozygous, and 4.26% GG homozygous for Cdx2, compared with 62.22% AA homozygotes, 33.33% AG heterozygotes, and 4.44% GG homozygotes in the controls. 19.15% of MA were homozygous AA, 53.19% heterozygous AG, and 27.66% homozygous GG for A1012G whereas, 20%, 48.89%, and 31.11% of the controls were AA, AG, and GG, respectively.

GC (DBP) - In the MA cohort, 53.19% were homozygous CC, 38.30% heterozygous CA, and 8.51% homozygous AA for rs4588 (T-K) whilst 48.89% of controls were CC homozygotes, 37.78% CA heterozygotes, and 13.33% AA homozygotes. For rs7041 (D-E), 23.40%, 44.68%, and 31.91% of MA were TT homozygous, TG heterozygous, and 31.91% GG homozygous, respectively. In comparison, 22.22% of controls were TT homozygotes, 40% TG heterozygotes, and 37.78% GG homozygotes. With regards to haplotype frequencies, 74.5% of MA possessed Gc1f, 19.1% Gc1s, and 6.4% Gc2, whereas 64% of controls carried Gc1f, 27% Gc1s, and 9% Gc2.

Table 3.5. *Genotype frequencies of VDR SNPs in MA and controls.*

SNP	*Genotype*	*MA (n=47)*	*Controls (n=45)*	*Significance*
BsmI	AA	27	18	$\chi2 = 3.158$
	AG	14	21	$p=0.2062$
	GG	6	6	
TaqI	AA	22	20	$\chi2 = 1.640$
	AG	16	20	$p=0.4405$
	GG	9	5	
Cdx2	AA	35	28	$\chi2 = 1.735$
	AG	10	15	$p=0.4200$
	GG	2	2	
ApaI	CC	11	7	$\chi2 = 1.712$
	CA	20	25	$p=0.4248$
	AA	16	13	
FokI	TT	8	7	$\chi2 = 1.428$
	TC	22	27	$p=0.4896$
	CC	17	12	
A1012G	AA	9	9	$\chi2 = 0.1851$
	AG	25	22	$p=0.9116$
	GG	13	14	

Abbreviations: *SNP,* single nucleotide polymorphism; *MA,* master athletes; χ^2, chi squared.

Table 3.6. *Genotype & isoform frequencies of GC (DBP) SNPs in MA and controls.*

SNP	*Genotype*	*MA (n=47)*	*Controls (n=45)*	*Significance*
rs4588 (T436K)	CC	25	22	χ2 = 0.5769
	CA	18	17	*p*=0.7494
	AA	4	6	
rs7401 (D432E)	TT	11	10	χ2 = 0.3601
	TG	21	18	*p*=0.8352
	GG	15	17	
	rs7041/rs4588			
Gc1f	T/C	35	29	χ2 = 1.09
Gc1s	G/C	9	12	*p*=0.5796
Gc2	T/A	3	4	

Abbreviations: *SNP,* single nucleotide polymorphism; *MA,* master athletes; χ^2, chi squared.

3.3.3 General Characteristics, body composition and VDR/GC single nucleotide polymorphisms

General Characteristics & Body Composition - Controls homozygous for the mutant CC genotype of FokI were significantly taller than the wildtype TT homozygotes (CC 1.77±0.08 metres vs TT 1.69±0.06 metres, P = 0.0497) (**Table 3.9**). MA carrying one or two G alleles of the Cdx2 *VDR* SNP weighed significantly more than AA homozygotes (AA 65.3±8.21 kg vs AG/GG 71.6±7.54 kg, P = 0.023) (**Table 3.10**).

In the controls, those homozygous for the GG genotype of the *GC* SNP rs7041 (D-E) displayed significantly higher quadriceps cross sectional area (CSA) than

TT homozygotes (TT 51.1±11.8 cm^2 vs GG 66.6±11.3 cm^2, P = 0.0018) (**Table 3.13**). Total body fat percentage was significantly greater in controls in possession of the Gc2 DBP isoform than those carrying Gc1s (Gc2 40.0±6.21% vs Gc1s 24.5±10.2%, P = 0.0075). Additionally, Gc1s controls displayed significantly higher CSA of the quadriceps than Gc1f (Gc1s 69.5±12.1 cm^2 vs Gc1f 56.4±9.17 cm^2, P = 0.0027) (**Table 3.15**).

Bone Densitometry - Whole body bone mineral content (BMC) was significantly higher in MA carrying one or two G alleles of Cdx2 (AA 29.0±5.62 grams vs AG/GG 32.8±4.16 grams, P = 0.036) (**Table 3.10**). In addition, the muscle-to-bone ratio (MBR) was significantly lower in controls homozygous for the T allele of the *GC* SNP, rs7041 (D-E) compared to GG homozygotes (TT 7.62±3.54 vs GG 10.3±1.17, P = 0.0369) (**Table 3.13**). MA carrying one or two A alleles of the GC SNP, rs4588 (T-K) displayed significantly lower bone mineral density (BMD) than those carrying two C alleles (CA 1.17±0.117 g/cm^2 vs AA 0.946±0.428 g/cm^2; P = 0.0299; CC 1.26±0.103 vs AA, P = 0.0013) (**Table 3.14**). Differences were also seen between DBP isoforms as Gc1s carrying controls had a significantly greater MBR than those in possession of the Gc1f isoform (Gc1s 10.8±0.842 vs Gc1f 8.76±1.98, P = 0.0313) (**Table 3.15**).

Lean Mass - Appendicular lean mass (ALM) was significantly higher in MA carrying one or two G alleles of Cdx2 compared to AA homozygotes (AA 24.4±3.89 kg vs AG/GG 28.1±3.68 kg, P = 0.008). In addition, Cdx2 A allele

carrying MA (AG/GG) had greater total body lean mass than their AA carrying counterparts (AA 52.1±6.81 kg vs AG/GG 57.9±6.50 kg, P = 0.020) (**Table 3.10**). No significant differences were seen between DBP SNPs and outcomes related to lean mass, yet controls carrying the Gc1s DBP isoform had a significantly higher percentage of total lean body mass than Gc2 carriers (Gc1s 72.5±9.69% vs Gc2 58.6±5.92%, P = 0.0112) (**Table 3.15**).

3.3.4 Physical performance and VDR/GC polymorphisms

There were no significant differences in TUG test performance and any of the *VDR* and *GC* SNPs investigated. Controls carrying the CC genotype of ApaI were able to stand on one leg with their eyes closed for significantly longer than those carrying one or two A alleles (CC 10.0±12.6 seconds vs CA 2.68±2.50 seconds, P = 0.0096; CC vs AA 2.74±1.95 sec, P = 0.0191) (**Table 3.11**).

3.3.5 Muscle strength/function and VDR/GC polymorphisms

Muscle Strength - HGS was higher in MA homozygous for the mutant GG alleles for A1012G compared to AA individuals (AA 32.8±10.5 kg vs GG 42.3±8.24 kg, P = 0.0453). (**Table 3.12**). No significant differences were found in knee extensor MVC (KE-MVC) and any of the *VDR* SNPs studied. Interestingly, controls carrying one or two G alleles of the *GC* SNP rs7041 (D-E) displayed significantly higher KE-MVC than TT homozygous controls (TT 229±86.0 N vs TG 337±89.4 N, P = 0.0121; TT vs GG 342±94.8 N, P = 0.0092, respectively) (**Table 3.13**).

Muscle Function - Jump mechanography was used to determine muscle function via measurements of lower limb power. MA carrying of one or two G alleles of the Cdx2 SNP displayed significantly higher absolute power (P_{max}) compared to those homozygous for the AA genotype (AA 1.96±0.61 kW vs AG/GG 2.73±0.99 kW, P = 0.009). The same observation was also seen with regards to relative power and MA carrying Cdx2 (P_{max}Rel; AA 30.3±9.02 W/kg vs AG/GG 37.9±12.3 W/kg, P = 0.027) (**Table 3.10**). Intriguingly, in the control cohort, possession of one or two copies of the mutant G allele of A1012G was related to significantly higher maximal jump velocity (V_{max}; AA 1.37±0.40 m/s vs AG 1.87±0.43, P = 0.0144; AA vs GG 1.90±0.29 m/s, P = 0.0145) and significantly higher P_{max}Rel (AA 21.1±7.03 W/kg vs AG 30.4±9.41, P = 0.0460; AA vs GG 32.6±8.94 W/kg, P = 0.0198) (**Table 3.12**).

No significant differences were found in muscle function and the two *GC* SNPs studied but differences were found between DBP isoforms. Controls carrying the Gc1s isoform displayed significantly greater V_{max} than Gc2 carrying controls (Gc1s 2.08±0.405 m/s vs Gc2 1.28±0.545 m/s, P = 0.0169). In addition, compared to controls carrying Gc2, Gc1s controls also displayed significantly greater maximal jump height (H_{max}; Gc1s 0.266±0.115 m vs Gc2 0.0998±0.0717 m, P = 0.0283) and P_{max}Rel (Gc1s 35.9±9.39 W/kg vs 19.1±8.50 W/Kg, P = 0.0250) (**Table 3.15**).

3.3.6 Biochemical parameters and VDR/GC polymorphisms

Biochemical data was available in the control cohort only. Serum levels of sex hormone binding globulin (SHBG) were significantly higher in controls homozygous for the mutant GG genotype of A1012G than those carrying one or two A alleles (GG 66.1±25.6 nmol/L vs AG 43.4±17.3 nmol/L,P = 0.0048; GG vs AA 44.1±13.1 nmol/L, P = 0.0323) (**Table 3.12**).

Whilst no differences were seen between either of the *GC* SNPs in relation to any of the biochemical markers measured, a significant difference was seen between the DBP isoforms and serum levels of $1,25(OH)_2D_3$ in controls (P = 0.0423). However, after adjusting for multiple comparisons, this was found to be non-significant (Gc1f 54.9±24.6 nmol/L vs Gc1s 75.7±33.2 nmol/L, P = 0.0780; Gc1s vs Gc2 41.8±12.7 nmol/L, P = 0.0816) (**Table 3.15**).

Table 3.7. Participant characteristics (body composition, muscle strength/function, physical function, and biochemical data) in relation to BsmI.

Variable	*All MA (n=47)*			*P*	*All Controls (n=45)*			*P*
	AA	**AG**	**GG**		**AA**	**AG**	**GG**	
Age (yr)	70.4± 6.2	69.9± 6.1	72.9± 5.4	*0.566*	74.5± 5.8	76.7± 6.3	76.0± 6.8	*0.498*
Height (m)	1.7± 0.064	1.7± 0.071	1.7± 0.037	*0.423*	1.7± 0.085	1.7± 0.068	1.7± 0.058	*0.588*
Weight (kg)	68.0± 9.2	64.1± 8.6	67.7± 3.3	*0.390*	75.9± 12	80.9± 13	85.9± 24	*0.307*
BMI (kg/cm^2)	23.1± 2.4	21.3± 2.0	22.2± 1.2	*0.061*	25.1± 3.5	27.2± 4.0	29.3± 6.4	*0.088*
Percentage Fat Mass (%)	17.1± 6.0	13.4± 6.2	14.0± 5.3	*0.141*	26.5± 8.6	31.9± 8.7	32.2± 12	*0.153*
Percentage Lean Mass (%)	78.6± 6.5	82.7± 5.5	82.0± 5.5	*0.110*	70.3± 8.1	66.5± 8.2	65.4± 11	*0.309*
Total Body Lean Mass (kg)	53.4± 7.9	52.9± 7.0	55.4± 3.5	*0.757*	52.8± 6.5	53.0± 5.6	54.2± 7.0	*0.895*
Appendicular Lean Mass (kg)	2.46± 0.43	2.59± 0.45	2.75± 0.15	*0.241*	2.43± 0.40	2.41± 0.30	2.33± 0.35	*0.833*
BMD (g/cm^2)	1.2± 0.11	1.1± 0.28	1.2± 0.12	*0.312*	1.2± 0.13	1.3± 0.13	1.2± 0.13	*0.802*
BMC (g)	30.4± 5.1	29.4± 7.0	29.4± 4.3	*0.847*	31.5± 6.2	32.8± 6.7	31.1± 5.5	*0.758*
MBR	-	-	-	-	9.4± 2.1	8.9± 1.7	11.7± 0.84	*0.147*
Quads CSA (cm^2)	-	-	-	-	58.2± 12	60.1± 9.2	64.6± 17	*0.553*
HGS (kg)	37.8± 9.04	41.7± 10.2	38.2± 8.17	*0.448*	36.0± 9.81	34.1± 9.37	37.9± 8.42	*0.642*
KE MVC (N)	-	-	-	-	307± 122	325± 89.2	302± 68.0	*0.808*
TUG (s)	5.7± 0.656	5.5± 0.52	5.3± 0.876	*0.441*	7.6± 3.28	8.4± 3.15	9.7± 4.86	*0.409*
1 leg EO (s)	-	-	-	-	19.0± 12.4	13.0± 12.5	6.15± 4.31	*0.085*

1 leg EC (s)	-	-	-	-	3.2± 2.33	4.9± 7.95	1.8± 2.87	*0.484*
Vmax (m/s)	-	-	-	-	1.9± 0.476	1.7± 0.365	1.6± 0.476	*0.321*
Hmax (m)	0.25±0 .12	0.26± 0.21	0.31± 0.19	*0.653*	0.24± 0.12	0.19± 0.08	0.17± 0.07	*0.223*
Fmax (N)	1.5± 0.32	1.4± 0.36	1.46± 0.37	*0.560*	1.8± 0.42	1.7± 0.29	1.6± 0.49	*0.515*
Pmax (kW)	2.02±0 .73	2.4± 1.01	2.22± 0.54	*0.375*	2.5± 0.84	2.06± 0.47	1.94± 0.62	*0.143*
Pmax/mass (W/kg)	29.8± 8.93	36.9± 12.6	33.1± 9.24	*0.127*	32.8± 11.3	25.9± 6.93	25.2± 9.75	*0.116*
DHEA (µmol/L)	-	-	-	-	4.59± 2.59	3.55± 2.81	4.62± 3.42	*0.469*
DHEAS (µmol/L)	-	-	-	-	2.23± 1.28	1.52± 0.58	2.4± 1.22	*0.056*
Albumin (g/L)	-	-	-	-	41.7± 2.11	39.4± 4.47	41.3± 3.72	*0.131*
SHBG (nmol/L)	-	-	-	-	51.3± 22.6	47.0± 16.4	61.8± 34.5	*0.351*
$1,25(OH)_2D_3$ (nmol/L)	-	-	-	-	56.4± 28.1	61.0± 25.0	59.8± 39.3	*0.881*
DHT (nmol/L)	-	-	-	-	1.67± 0.91	1.25± 0.69	1.99± 1.28	*0.139*
E2 (pmol/L)	-	-	-	-	85.9± 48.3	76.6± 22.5	83.0± 31.6	*0.723*

[1] Abbreviations: *MA,* master athletes; *yr,* year; *m,* metre; *kg,* kilogram; *BMI,* body mass index; *cm,* centimetre; *%,* percent; *HGS*, handgrip strength; *TUG,* Timed Up & Go; *Vmax*, maximum jump velocity; *Hmax*, maximum jump height; *Fmax*, maximum force; *Pmax*, absolute vertical jump power; *PmaxRel*, absolute vertical jump power relative to body weight; *BMD*, bone mineral density; *BMC*, bone mineral content (whole body); *MBR,* muscle-to-bone ratio; *Quads CSA*, quadriceps cross-sectional area; *KE-MVC*, knee extensor maximal voluntary contraction; *N,* Newton; *s,* seconds; *EO*, eyes open; *EC*, eyes closed; *W,* watt; *kW,* kilowatt; *DHEA*, dehydroepiandrosterone; *DHEAS*, *DHEA* sulphate; *SHBG*, sex hormone binding globulin; *$1,25(OH)_2D_3$*, 1,25-dihydroxyvitamin D_3, *DHT*, dihydrotestosterone; *E2*, oestradiol; *µmol*, micromole; *nmol,* nanomole; *pmol,* picomole; *L,* litre.

[2]Significance taken as P <0.05. [a] <0.05 compared with both AG and GG genotypes. [b] <0.05 compared with GG genotype only. [c] <0.05 compared with AG genotype only. [d] <0.05 compared with both AA and AG genotypes. [e] no significant differences after adjusting for multiple comparisons. [3]Data shown as mean ± SD.

Table 3.8. Participant characteristics (body composition, muscle strength/function, physical function, and biochemical data) in relation to TaqI.

Variable	*All MA (n=47)*			*P*	*All Controls (n=45)*			*P*
	AA	**AG**	**GG**		**AA**	**AG**	**GG**	
Age (y)	71.1± 6.31	69.8± 5.63	71.2± 6.28	*0.762*	74.7± 5.54	76.8± 6.53	76.6± 7.37	*0.542*
Height (m)	1.71± 0.07	1.73± 0.07	1.74± 0.05	*0.517*	1.73± 0.08	1.73± 0.07	1.72± 0.06	*0.891*
Weight (kg)	67.9± 9.22	65.3± 8.13	67.3± 7.38	*0.639*	76.1± 11.7	82.1± 16.7	83.7± 15.5	*0.357*
BMI (kg/cm^2)	23.1± 2.41	21.7± 2.13	22.3± 1.96	*0.186*	25.3± 3.45	27.5± 4.78	28.4± 4.96	*0.173*
Percentage Fat Mass (%)	17.0± 6.38	13.8± 5.68	15.5± 6.00	*0.304*	27.3± 8.61	32.3± 9.40	29.3± 9.94	*0.230*
Total Body Lean Mass (kg)	53.6± 7.84	52.8± 6.24	53.6± 7.26	*0.925*	52.6± 6.19	52.8± 6.24	56.2± 4.27	*0.478*
Appendicular Lean Mass (kg)	2.50± 0.41	2.55± 0.46	2.61± 0.38	*0.784*	2.43± 0.38	2.38± 0.34	2.44± 0.17	*0.900*
Percentage Lean Mass (%)	79.1± 6.66	82.2± 5.08	79.7± 7.26	*0.336*	69.8± 7.95	65.8± 9.02	68.4± 9.38	*0.342*
BMD (g/cm^2)	1.23± 0.98	1.18± 0.27	1.16± 0.11	*0.446*	1.23± 0.13	1.24± 0.14	1.30± 0.11	*0.595*
BMC (g)	30.6± 4.86	30.4± 6.72	27.8± 4.63	*0.434*	31.8± 6.12	31.7± 6.35	35.1± 7.02	*0.539*
MBR	-	-	-	-	9.23± 1.96	9.16± 1.73	10.1± 2.86	*0.765*
Quads CSA (cm^2)	-	-	-	-	58.0± 10.9	60.3± 9.56	66.5± 18.5	*0.396*
HGS (kg)	37.4± 9.09	42.3± 9.39	36.5± 8.44	*0.188*	37.0± 9.79	32.4± 8.99	40.8± 4.93	*0.116*
KE MVC (N)	-	-	-	-	310± 117	312± 94.6	348± 35.0	*0.744*
TUG (s)	5.66± 0.70	5.47± 0.53	5.43± 0.80	*0.586*	7.51± 3.12	9.16± 3.92	7.63± 1.96	*0.295*
1 leg EO (s)	-	-	-	-	17.4± 12.7	13.8± 12.5	5.99± 4.67	*0.225*
1 leg EC (s)	-	-	-	-	3.10± 2.24	4.95± 8.22	2.24± 3.11	*0.531*
Vmax (m/s)	-	-	-	-	1.85± 0.47	1.67± 0.38	1.59± 0.50	*0.402*

Hmax (m)	0.26± 0.13	0.25± 0.19	0.27± 0.18	*0.954*	0.23± 0.11	0.19± 0.08	0.18± 0.06	*0.369*
Fmax (N)	1.50± 0.33	1.41± 0.35	1.49± 0.35	*0.696*	1.81± 0.39	1.64± 0.34	1.74± 0.41	*0.5050*
Pmax (kW)	2.10± 0.77	2.31± 0.93	2.02± 0.62	*0.613*	2.45± 0.80	2.02± 0.54	2.01± 0.52	*0.197*
Pmax/mass (W/kg)	31.0± 9.28	35.2± 12.0	30.2± 9.74	*0.390*	32.0± 10.7	25.9± 7.35	24.9± 9.98	*0.163*
DHEA (µmol/L)	-	-	-	-	4.85± 2.70	3.63± 3.00	3.09± 1.81	*0.276*
DHEAS (µmol/L)	-	-	-	-	2.22± 1.21	1.47± 0.56	2.50± 1.34	***0.034*** [e]
Albumin (g/L)	-	-	-	-	**41.8± 2.07** [c]	38.9± 4.45	42.2± 3.42	***0.027***
SHBG (nmol/L)	-	-	-	-	49.4± 22.2	51.1± 23.4	55.2± 18.7	*0.870*
$1,25(OH)_2D_3$ (nmol/L)	-	-	-	-	58.0± 27.1	59.6± 24.7	60.1± 45.3	*0.979*
DHT (nmol/L)	-	-	-	-	1.61± 0.88	1.29± 0.82	2.06± 1.11	*0.195*
E2 (pmol/L)	-	-	-	-	83.3± 46.7	76.2± 22.4	92.8± 29.2	*0.627*

[1] Abbreviations: *MA,* master athletes; *yr,* year; *m,* metre; *kg,* kilogram; *BMI,* body mass index; *cm,* centimetre; *%,* percent; *HGS*, handgrip strength; *TUG,* Timed Up & Go; *Vmax*, maximum jump velocity; *Hmax*, maximum jump height; *Fmax*, maximum force; *Pmax*, absolute vertical jump power; *PmaxRel*, absolute vertical jump power relative to body weight; *BMD*, bone mineral density; *BMC*, bone mineral content (whole body); *MBR,* muscle-to-bone ratio; *Quads CSA*, quadriceps cross-sectional area; *KE-MVC*, knee extensor maximal voluntary contraction; *N,* Newton; *s,* seconds; *EO*, eyes open; *EC*, eyes closed; *W,* watt; *kW,* kilowatt; *DHEA*, dehydroepiandrosterone; *DHEAS*, *DHEA* sulphate; *SHBG*, sex hormone binding globulin; *$1,25(OH)_2D_3$*, 1,25-dihydroxyvitamin D_3, *DHT*, dihydrotestosterone; *E2*, oestradiol; *µmol*, micromole; *nmol,* nanomole; *pmol,* picomole; *L,* litre.

[2]Significance taken as P <0.05. [a] <0.05 compared with both AG and GG genotypes. [b] <0.05 compared with GG genotype only. [c] <0.05 compared with AG genotype only. [d] <0.05 compared

with both AA and AG genotypes. [e] no significant differences after adjusting for multiple comparisons.

[3]Data shown as mean ± SD.

Table 3.9. Participant characteristics (body composition, muscle strength/function, physical function, and biochemical data) in relation to FokI.

Variable	*All MA (n=47)*			*P*	*All Controls (n=45)*			*P*
	TT	**TC**	**CC**		**TT**	**TC**	**CC**	
Age (y)	72.9± 4.26	70.2± 6.27	70.2± 6.36	*0.526*	75.7± 4.19	75.9± 6.25	75.7± 7.32	*0.997*
Height (m)	1.70± 0.07	1.73± 0.06	1.73± 0.06	*0.539*	**1.69± 0.06[b]**	1.72± 0.07	1.77± 0.08	***0.043***
Weight (kg)	66.1± 10.4	66.4± 8.75	67.9± 7.45	*0.828*	78.5± 18.1	80.4± 15.0	80.2± 11.6	*0.726*
BMI (kg/cm^2)	22.9± 3.38	22.2± 2.34	21.3± 5.72	*0.646*	26.7± 5.02	27.1± 4.69	25.4± 2.83	*0.567*
Percentage Fat Mass (%)	15.6± 6.80	15.0± 6.38	16.4± 5.71	*0.777*	31.7± 9.01	29.3± 9.96	29.5± 7.96	*0.831*
Total Body Lean Mass (kg)	52.6± 7.10	53.5± 6.93	54.2± 7.75	*0.878*	49.7± 6.35	53.6± 6.21	54.0± 5.08	*0.275*
Appendicular Lean Mass (kg)	2.36± 0.44	2.54± 0.42	2.65± 0.41	*0.274*	2.23± 0.33	2.42± 0.37	2.50± 0.26	*0.243*
Percentage Lean Mass (%)	80.0± 6.69	80.9± 6.44	79.6± 6.27	*0.835*	67.5± 9.08	67.9± 9.13	68.1± 7.73	*0.990*
BMD (g/cm^2)	1.22± 0.09	1.17± 0.24	1.22± 0.07	*0.668*	1.25± 0.10	1.22± 0.12	1.29± 0.15	*0.296*
BMC (g)	29.8± 5.12	30.3± 5.97	29.6± 5.36	*0.930*	30.8± 5.32	30.9± 5.41	35.8± 7.69	*0.074*
MBR	-	-	-	-	9.23± 3.36	9.24± 1.87	9.42± 1.66	*0.977*
Quads CSA (cm^2)	-	-	-	-	59.0± 14.2	60.5± 12.4	59.0± 5.89	*0.918*
HGS (kg)	35.8± 5.83	38.6± 9.73	40.8± 9.83	*0.443*	31.3± 5.76	34.9± 9.90	39.0± 9.05	*0.227*
KE MVC (N)	-	-	-	-	296± 77.0	302± 88.8	359± 131.0	*0.245*
TUG (s)	5.57± 0.74	5.50± 0.53	5.61± 0.78	*0.887*	7.28± 2.28	8.73± 3.50	7.71± 3.95	*0.524*
1 leg EO (s)	-	-	-	-	16.2± 15.1	13.5± 11.2	16.7± 14.2	*0.753*
1 leg EC (s)	-	-	-	-	3.19± 3.29	3.48± 4.42	4.95± 8.95	*0.764*

Vmax (m/s)	-	-	-	-	1.61± 0.45	1.73± 0.48	1.83± 0.38	*0.674*
Hmax (m)	0.25± 0.07	0.26± 0.19	0.26± 0.15	*0.987*	0.19± 0.09	0.20± 0.10	0.22± 0.10	*0.836*
Fmax (N)	1.55± 0.30	1.47± 0.30	1.43± 0.39	*0.701*	1.87± 0.36	1.64± 0.31	1.83± 0.46	*0.289*
Pmax (kW)	2.24± 0.64	2.05± 0.61	2.26± 1.05	*0.706*	2.11± 0.57	2.17± 0.72	2.36± 0.71	*0.727*
Pmax/mass (W/kg)	33.9± 8.18	31.5± 9.91	32.5± 12.2	*0.854*	27.0± 10.3	28.0± 9.61	30.3± 10.2	*0.786*
DHEA (µmol/L)	-	-	-	-	3.00± 1.42	4.41± 3.00	4.12± 2.93	*0.502*
DHEAS (µmol/L)	-	-	-	-	2.09± 1.43	1.96± 1.07	1.85± 0.89	*0.914*
Albumin (g/L)	-	-	-	-	40.6± 2.37	40.0± 4.14	42.3± 2.58	*0.243*
SHBG (nmol/L)	-	-	-	-	47.0± 10.8	50.5± 23.7	54.1± 24.1	*0.810*
$1,25(OH)_2D_3$ (nmol/L)	-	-	-	-	67.0± 43.6	61.6± 24.6	46.2± 20.5	*0.233*
DHT (nmol/L)	-	-	-	-	1.25± 0.94	1.50± 0.96	1.79± 0.64	*0.470*
E2 (pmol/L)	-	-	-	-	67.9± 37.1	**75.5± 29.8**[b]	106± 41.4	***0.034***

[1] Abbreviations: *MA,* master athletes; *yr,* year; *m,* metre; *kg,* kilogram; *BMI,* body mass index; *cm,* centimetre; *%,* percent; *HGS*, handgrip strength; *TUG,* Timed Up & Go; *Vmax*, maximum jump velocity; *Hmax*, maximum jump height; *Fmax*, maximum force; *Pmax*, absolute vertical jump power; *PmaxRel*, absolute vertical jump power relative to body weight; *BMD*, bone mineral density; *BMC*, bone mineral content (whole body); *MBR,* muscle-to-bone ratio; *Quads CSA*, quadriceps cross-sectional area; *KE-MVC*, knee extensor maximal voluntary contraction; *N,* Newton; *s,* seconds; *EO*, eyes open; *EC*, eyes closed; *W,* watt; *kW,* kilowatt; *DHEA*, dehydroepiandrosterone; *DHEAS*, *DHEA* sulphate; *SHBG*, sex hormone binding globulin; *$1,25(OH)_2D_3$*, 1,25-dihydroxyvitamin D_3, *DHT*, dihydrotestosterone; *E2*, oestradiol; *µmol*, micromole; *nmol,* nanomole; *pmol,* picomole; *L,* litre.

[2]Significance taken as P <0.05. [a] <0.05 compared with both TC and CC genotypes. [b] <0.05 compared with CC genotype only. [c] <0.05 compared with TC genotype only. [d] <0.05 compared

with both TT and TC genotypes. [e] no significant differences after adjusting for multiple comparisons.

[3]Data shown as mean ± SD.

Table 3.10. Participant characteristics (body composition, muscle strength/function, physical function, and biochemical data) in relation to Cdx2.

Variable	*All MA (n=47)*		*P*	*All Controls (n=45)*		*P*
	AA	**AG/GG**		**AA**	**AG/GG**	
Age (y)	71.2± 5.86	69.1± 6.32	*0.223*	75.6± 6.41	76.1± 5.84	*0.689*
Height (m)	1.71± 0.07	1.75± 0.04	*0.059*	1.74± 0.08	1.72± 0.06	*0.380*
Weight (kg)	65.3± 8.21	71.6± 7.54	***0.023***	80.0± 14.7	79.0± 14.7	*0.821*
BMI (kg/cm^2)	22.2± 2.34	23.3± 1.93	*0.167*	26.6± 4.26	26.7± 4.58	*0.928*
Percentage Fat Mass (%)	15.7± 6.65	15.3± 4.41	*0.849*	30.6± 9.00	28.4± 9.66	*0.4361*
Total Body Lean Mass (kg)	52.1± 6.81	57.9± 6.50	***0.020***	53.0± 6.38	53.3± 5.57	*0.849*
Appendicular Lean Mass (kg)	24.4± 3.89	28.1± 3.68	***0.008***	24.1± 3.62	24.2± 3.16	*0.905*
Percentage Lean Mass (%)	80.1± 6.71	80.9± 5.14	*0.703*	67.2± 8.22	68.9± 9.38	*0.544*
BMD (g/cm^2)	1.18± 0.20	1.24± 0.09	*0.430*	1.25± 0.12	1.23± 0.14	*0.564*
BMC (g)	29.0± 5.62	32.8± 4.16	***0.036***	32.7± 6.32	31.1± 6.23	*0.425*
MBR	-	-	-	8.80± 1.65	10.0± 2.10	*0.094*
Quads CSA (cm^2)	-	-	-	58.6± 9.57	62.0± 13.4	*0.338*
HGS (kg)	37.7± 9.18	42.4± 8.83	*0.100*	34.6± 9.23	36.6± 9.62	*0.498*
KE MVC (N)	-	-	-	323± 104	301± 95.1	*0.474*
TUG (s)	5.53± 0.66	5.59± 0.68	*0.788*	8.73± 3.95	7.47± 2.28	*0.387*
1 leg EO (s)	-	-	-	14.4± 12.7	15.3± 12.0	*0.795*
1 leg EC (s)	-	-	-	4.17± 6.95	3.18± 2.31	*0.502*
Vmax (m/s)	-	-	-	1.67± 0.44	1.88± 0.43	*0.204*

Hmax (m)	0.24± 0.14	0.31± 0.21	*0.167*	0.20± 0.10	0.22± 0.09	*0.473*
Fmax (N)	1.44± 0.35	1.55± 0.27	*0.330*	1.77± 0.39	1.66± 0.33	*0.375*
Pmax (kW)	1.96± 0.61	2.73± 0.99	***0.009***	2.15± 0.68	2.36± 0.71	*0.421*
Pmax/mass (W/kg)	30.3± 9.02	37.9± 12.3	***0.027***	26.9± 9.07	31.9± 10.3	*0.163*
DHEA (µmol/L)	-	-	-	4.16± 2.92	4.05± 2.62	*0.958*
DHEAS (µmol/L)	-	-	-	1.83± 1.03	2.10± 1.11	*0.498*
Albumin (g/L)	-	-	-	40.5± 4.10	40.9± 2.85	*0.927*
SHBG (nmol/L)	-	-	-	46.7± 15.4	57.9± 29.6	*0.106*
$1,25(OH)_2D_3$ (nmol/L)	-	-	-	57.7± 28.4	61.1± 27.4	*0.704*
DHT (nmol/L)	-	-	-	1.49± 0.76	1.57± 1.12	*0.776*
E2 (pmol/L)	-	-	-	82.3± 26.6	79.5± 49.0	*0.526*

[1] Abbreviations: *MA,* master athletes; *yr,* year; *m,* metre; *kg,* kilogram; *BMI,* body mass index; *cm,* centimetre; *%,* percent; *HGS*, handgrip strength; *TUG,* Timed Up & Go; *Vmax*, maximum jump velocity; *Hmax*, maximum jump height; *Fmax*, maximum force; *Pmax*, absolute vertical jump power; *PmaxRel*, absolute vertical jump power relative to body weight; *BMD*, bone mineral density; *BMC*, bone mineral content (whole body); *MBR,* muscle-to-bone ratio; *Quads CSA*, quadriceps cross-sectional area; *KE-MVC*, knee extensor maximal voluntary contraction; *N,* Newton; *s,* seconds; *EO*, eyes open; *EC*, eyes closed; *W,* watt; *kW,* kilowatt; *DHEA*, dehydroepiandrosterone; *DHEAS*, *DHEA* sulphate; *SHBG*, sex hormone binding globulin; *$1,25(OH)_2D_3$*, 1,25-dihydroxyvitamin D_3, *DHT*, dihydrotestosterone; *E2*, oestradiol; *µmol*, micromole; *nmol,* nanomole; *pmol,* picomole; *L,* litre.

[2]Significance taken as $P < 0.05$ & data shown as mean ± SD.

Table 3.11. Participant characteristics (body composition, muscle strength/function, physical function, and biochemical data) in relation to ApaI.

Variable	*All MA (n=47)*			*P*	*All Controls (n=45)*			*P*
	CC	**CA**	**AA**		**CC**	**CA**	**AA**	
Age (y)	71.0± 5.31	20.4± 6.47	20.8± 6.13	*0.953*	72.4± 4.43	77.2± 6.38	75.0± 5.97	*0.170*
Height (m)	1.76± 0.04	1.72± 0.07	1.71± 0.07	*0.121*	1.73± 0.07	1.72± 0.07	1.74± 0.09	*0.703*
Weight (kg)	68.0± 6.55	65.8± 9.44	67.5± 8.61	*0.740*	84.6± 22.1	79.3± 13.4	77.5± 12.5	*0.588*
BMI (kg/cm^2)	22.1± 1.78	22.2± 2.26	23.2± 2.56	*0.352*	28.2± 6.70	26.8± 3.93	25.5± 3.54	*0.397*
Percentage Fat Mass (%)	13.6± 5.14	16.0± 6.42	16.5± 6.39	*0.463*	30.0± 12.6	30.3± 9.46	28.6± 7.15	*0.867*
Total Body Lean Mass (kg)	55.7± 4.52	52.6± 8.33	53.4± 7.03	*0.499*	55.0± 5.37	52.9± 5.64	52.5± 7.23	*0.652*
Appendicular Lean Mass (kg)	2.76± 0.29	2.51± 0.42	2.41± 0.44	*0.094*	2.41± 0.21	2.41± 0.32	2.41± 0.45	*0.999*
Percentage Lean Mass (%)	82.2± 5.06	79.9± 6.75	79.4± 6.59	*0.513*	67.5± 12.2	67.8± 8.66	68.3± 6.90	*0.979*
BMD (g/cm^2)	1.11± 0.29	1.22± 0.12	1.23± 0.11	*0.164*	1.26± 0.10	1.25± 0.13	1.22± 0.14	*0.680*
BMC (g)	30.5± 4.85	29.5± 6.50	30.3± 4.83	*0.858*	31.9± 4.49	32.3± 6.64	31.8± 6.72	*0.968*
MBR	-	-	-	-	10.1± 1.96	9.46± 1.84	8.49± 2.03	*0.382*
Quads CSA (cm^2)	-	-	-	-	64.2± 15.1	61.3± 9.83	54.9± 10.6	*0.182*
HGS (kg)	37.9± 9.62	40.8± 8.95	37.3± 9.46	*0.486*	41.7± 4.17	33.4± 8.53	35.7± 11.5	*0.115*
KE MVC (N)	-	-	-	-	344± 49.3	318± 95.7	294± 127	*0.566*
TUG (s)	5.38± 0.69	5.54± 0.65	5.69± 0.65	*0.500*	8.03± 4.62	8.28± 3.15	8.32± 3.60	*0.984*
1 leg EO (s)	-	-	-	-	13.8± 13.1	13.4± 12.2	17.5± 12.7	*0.657*
1 leg EC (s)	-	-	-	-	**10.0± 12.6**[a]	2.68± 2.5	2.74± 1.95	***0.010***
Vmax (m/s)	-	-	-	-	1.81± 0.44	1.75± 0.45	1.68± 0.47	*0.855*

Hmax (m)	0.28± 0.16	0.34± 0.27	0.21± 0.07	*0.185*	0.21± 0.07	0.21± 0.11	0.20± 0.10	*0.918*
Fmax (N)	1.48± 0.30	1.45± 0.39	1.48± 0.30	*0.943*	1.63± 0.42	1.73± 0.29	1.80± 0.52	*0.696*
Pmax (kW)	2.46± 1.02	2.18± 0.76	1.93± 0.62	*0.245*	2.17± 0.42	2.23± 0.68	2.23± 0.92	*0.981*
Pmax/mass (W/kg)	35.9± 12.8	33.3± 10.2	28.6± 8.10	*0.179*	28.5± 8.51	28.9± 10.3	27.7± 10.0	*0.957*
DHEA (µmol/L)	-	-	-	-	4.62± 3.12	3.53± 2.58	4.94± 2.95	*0.308*
DHEAS (µmol/L)	-	-	-	-	2.41± 1.04	1.65± 0.75	2.20± 1.42	*0.133*
Albumin (g/L)	-	-	-	-	39.1± 7.34	40.2± 2.60	42.2± 2.03	*0.157*
SHBG (nmol/L)	-	-	-	-	58.0± 22.8	50.4± 23.4	47.5± 19.3	*0.604*
$1,25(OH)_2D_3$ (nmol/L)	-	-	-	-	65.1± 35.3	58.6± 24.8	56.3± 30.6	*0.800*
DHT (nmol/L)	-	-	-	-	1.96± 1.18	1.34± 0.79	1.63± 0.89	*0.235*
E2 (pmol/L)	-	-	-	-	90.1± 29.0	81.1± 36.1	76.8± 40.1	*0.739*

[1] Abbreviations: *MA,* master athletes; *yr,* year; *m,* metre; *kg,* kilogram; *BMI,* body mass index; *cm,* centimetre; *%,* percent; *HGS*, handgrip strength; *TUG,* Timed Up & Go; *Vmax*, maximum jump velocity; *Hmax*, maximum jump height; *Fmax*, maximum force; *Pmax*, absolute vertical jump power; *PmaxRel*, absolute vertical jump power relative to body weight; *BMD*, bone mineral density; *BMC*, bone mineral content (whole body); *MBR,* muscle-to-bone ratio; *Quads CSA*, quadriceps cross-sectional area; *KE-MVC*, knee extensor maximal voluntary contraction; *N,* Newton; *s,* seconds; *EO*, eyes open; *EC*, eyes closed; *W,* watt; *kW,* kilowatt; *DHEA*, dehydroepiandrosterone; *DHEAS*, *DHEA* sulphate; *SHBG*, sex hormone binding globulin; *$1,25(OH)_2D_3$*, 1,25-dihydroxyvitamin D_3, *DHT*, dihydrotestosterone; *E2*, oestradiol; *µmol*, micromole; *nmol,* nanomole; *pmol,* picomole; *L,* litre.

[2]Significance taken as P <0.05. [a] <0.05 compared with both CA and AA genotypes. [b] <0.05 compared with AA genotype only. [c] <0.05 compared with CA genotype only. [d] <0.05 compared

with both CC and CA genotypes. [e] no significant differences after adjusting for multiple comparisons.

[3]Data shown as mean ± SD.

Table 3.12. Participant characteristics (body composition, muscle strength/function, physical function, and biochemical data) in relation to A1012G.

Variable	*All MA (n=47)*			*P*	*All Controls (n=45)*			*P*
	AA	**AG**	**GG**		**AA**	**AG**	**GG**	
Age (y)	69.8± 5.65	72.0± 6.31	68.8± 5.31	*0.268*	76.2± 7.51	75.6± 6.40	75.8± 5.13	*0.973*
Height (m)	1.70± 0.07	1.72± 0.06	1.74± 0.06	*0.368*	1.73± 0.09	1.72± 0.07	1.74± 0.07	*0.892*
Weight (kg)	62.7± 7.35	66.8± 9.68	70.0± 5.11	*0.133*	80.5± 9.76	**84.2± 16.6[b]**	71.8± 10.5	***0.039***
BMI (kg/cm^2)	21.6± 1.80	22.5± 2.41	23.1± 2.23	*0.287*	26.8± 2.05	**28.3± 5.05[b]**	24.0± 2.79	***0.012***
Percentage Fat Mass (%)	15.3± 6.02	16.1± 6.71	14.9± 5.29	*0.828*	33.0± 6.96	30.3± 11.0	26.8± 6.81	*0.280*
Total Body Lean Mass (kg)	49.9± 6.54	53.3± 8.01	56.8± 4.06	*0.077*	52.0± 4.79	55.1± 5.03	50.7± 7.34	*0.079*
Appendicular Lean Mass (kg)	2.34± 0.30	2.52± 0.25	2.28± 0.44	*0.263*	2.43± 0.40	2.49± 0.48	2.69± 0.23	*0.085*
Percentage Lean Mass (%)	79.7± 6.92	80.0± 6.63	81.3± 5.56	*0.807*	64.9± 5.67	67.1± 10.4	70.9± 6.20	*0.242*
BMD (g/cm^2)	1.14± 0.34	1.22± 0.12	1.20± 0.10	*0.520*	1.29± 0.12	1.23± 0.14	1.22± 0.12	*0.485*
BMC (g)	30.8± 6.35	30.3± 5.42	28.8± 5.35	*0.658*	35.0± 6.95	31.6± 6.92	31.1± 4.26	*0.303*
MBR	-	-	-	-	8.11± 0.81	10.1± 1.33	8.98± 2.60	*0.086*
Quads CSA (cm^2)	-	-	-	-	56.8± 5.36	63.5± 11.7	56.5± 12.0	*0.157*
HGS (kg)	**32.8± 10.5[b]**	39.4± 8.52	42.3± 8.24	*0.054*	31.0± 11.6	36.3± 8.59	36.7± 8.71	*0.300*
KE MVC (N)	-	-	-	-	333± 94.4	328± 82.0	283± 126	*0.356*
TUG (s)	5.58± 0.52	5.47± 0.69	5.68± 0.70	*0.670*	9.47± 4.06	8.32± 3.73	7.37± 2.37	*0.366*
1 leg EO (s)	-	-	-	-	13.3± 12.7	12.2± 11.8	19.2± 12.4	*0.271*

1 leg EC (s)	-	-	-	-	4.99± 10.2	2.98± 2.51	4.27± 5.56	*0.668*
Vmax (m/s)	-	-	-	-	**1.37± 0.40**[a]	1.87± 0.43	1.90± 0.29	***0.008***
Hmax (m)	0.23± 0.14	0.27± 0.17	0.26± 0.16	*0.814*	0.15± 0.08	0.23± 0.10	0.23± 0.08	*0.108*
Fmax (N)	1.38± 0.39	1.45± 0.35	1.55± 0.26	*0.485*	1.79± 0.27	1.69± 0.27	1.73± 0.56	*0.829*
Pmax (kW)	1.88± 0.82	2.16± 0.86	2.35± 0.65	*0.404*	1.75± 0.62	2.34± 0.58	2.46± 0.73	***0.048***[e]
Pmax/mass (W/kg)	29.2± 9.31	32.7± 11.3	33.7± 9.61	*0.600*	**21.1± 7.03**[a]	30.4± 9.41	32.6± 8.94	***0.017***
DHEA (µmol/L)	-	-	-	-	3.92± 2.17	4.37± 3.24	3.87± 2.54	*0.854*
DHEAS (µmol/L)	-	-	-	-	1.86± 1.53	1.98± 0.96	1.90± 0.92	*0.954*
Albumin (g/L)	-	-	-	-	41.8± 2.68	40.9± 2.98	39.7± 4.85	*0.398*
SHBG (nmol/L)	-	-	-	-	44.1± 13.1	43.4± 17.3	**66.1± 25.6**[d]	***0.004***
$1,25(OH)_2D_3$ (nmol/L)	-	-	-	-	57.1± 24.4	62.9± 26.8	54.2± 32.0	*0.657*
DHT (nmol/L)	-	-	-	-	1.22 ±0.54	1.38 ±0.73	1.93 ±1.17	*0.100*
E2 (pmol/L)	-	-	-	-	73.9± 24.5	78.7± 24.3	89.9± 53.2	*0.529*

[1] Abbreviations: *MA,* master athletes; *yr,* year; *m,* metre; *kg,* kilogram; *BMI,* body mass index; *cm,* centimetre; *%,* percent; *HGS*, handgrip strength; *TUG,* Timed Up & Go; *Vmax*, maximum jump velocity; *Hmax*, maximum jump height; *Fmax*, maximum force; *Pmax*, absolute vertical jump power; *PmaxRel*, absolute vertical jump power relative to body weight; *BMD*, bone mineral density; *BMC*, bone mineral content (whole body); *MBR,* muscle-to-bone ratio; *Quads CSA*, quadriceps cross-sectional area; *KE-MVC*, knee extensor maximal voluntary contraction; *N,* Newton; *s,* seconds; *EO*, eyes open; *EC*, eyes closed; *W,* watt; *kW,* kilowatt; *DHEA*, dehydroepiandrosterone; *DHEAS*, *DHEA* sulphate; *SHBG*, sex hormone binding globulin; *$1,25(OH)_2D_3$*, 1,25-dihydroxyvitamin D_3, *DHT*, dihydrotestosterone; *E2*, oestradiol; *µmol*, micromole; *nmol,* nanomole; *pmol,* picomole; *L,* litre.

[2]Significance taken as P <0.05. [a] <0.05 compared with both AG and GG genotypes. [b] <0.05 compared with GG genotype only. [c] <0.05 compared with AG genotype only. [d] <0.05 compared with both AA and AG genotypes. [e] no significant differences after adjusting for multiple comparisons.

[3]Data shown as mean ± SD.

Table 3.13. Participant characteristics (body composition, muscle strength/function, physical function, and biochemical data) in relation to rs7041.

Variable	*All MA (n=47)*			*P*	*All Controls (n=45)*			*P*
	TT	**TG**	**GG**		**TT**	**TG**	**GG**	
Age (y)	70.4± 5.49	71.3± 6.39	70.7± 6.75	*0.904*	78.7± 5.44	74.9± 5.96	75.0± 6.52	*0.242*
Height (m)	1.71± 0.07	1.72± 0.07	1.74± 0.05	*0.383*	1.73± 0.06	1.74± 0.07	1.71± 0.08	*0.436*
Weight (kg)	66.7± 8.15	65.6± 9.59	68.0± 8.35	*0.778*	77.5± 12.3	80.9± 12.3	79.5± 18.2	*0.838*
BMI (kg/cm^2)	22.8± 2.41	22.2± 2.12	22.3± 2.53	*0.701*	25.8± 3.82	26.9± 4.24	26.9± 4.87	*0.799*
Percentage Fat Mass (%)	16.1± 6.73	16.2± 6.07	14.5± 5.63	*0.736*	31.2± 6.33	29.6± 8.48	29.1± 11.5	*0.845*
Total Body Lean Mass (kg)	53.5± 8.20	52.2± 8.23	54.9± 4.39	*0.632*	50.2± 5.94	55.0± 5.53	52.8± 6.18	*0.130*
Appendicular Lean Mass (kg)	2.60± 0.42	2.43± 0.44	2.58± 0.41	*0.461*	**2.21± 0.30^c**	2.53± 0.31	2.41± 0.36	*0.054*
Percentage Lean Mass (%)	80.2± 7.15	79.6± 6.51	81.2± 4.78	*0.804*	65.3± 5.38	68.8± 7.96	68.4± 10.7	*0.581*
BMD (g/cm^2)	1.22± 0.13	1.20± 0.14	1.15± 0.29	*0.615*	1.27± 0.16	1.23± 0.11	1.23± 0.14	*0.699*
BMC (g)	30.3± 5.69	29.0± 6.08	30.1± 6.02	*0.775*	33.3± 7.53	32.3± 5.21	31.2± 6.71	*0.682*
MBR	-	-	-	-	**7.62± 3.54^b**	9.02± 1.35	10.3± 1.17	***0.037***
Quads CSA (cm^2)	-	-	-	-	**51.1± 11.8^b**	59.1± 6.31	66.6± 11.3	***0.003***
HGS (kg)	39.3±10.1	40.0±8.12	36.9±10.1	*0.666*	**30.9± 6.57^c**	39.4± 9.21	33.7± 9.55	***0.042***
KE MVC (N)	-	-	-	-	**229± 86.0^a**	337± 89.4	342± 94.8	***0.006***
TUG (s)	5.58± 0.71	5.65± 0.69	5.36± 0.48	*0.527*	9.50± 4.89	7.46± 2.04	8.36± 3.62	*0.329*
1 leg EO (s)	-	-	-	-	11.7± 12.8	15.0± 12.7	16.2± 12.1	*0.692*

1 leg EC (s)	-	-	-	-	1.98± 2.00	5.28± 8.33	3.32± 2.70	*0.353*
Vmax (m/s)	-	-	-	-	1.69± 0.42	1.74± 0.36	1.78± 0.57	*0.910*
Hmax (m)	0.26± 0.11	0.25± 0.16	0.28± 0.23	*0.870*	0.19± 0.08	0.22± 0.07	0.20± 0.13	*0.750*
Fmax (N)	1.49± 0.33	1.37± 0.37	1.55± 0.29	*0.309*	1.67± 0.37	1.82± 0.44	1.64± 0.25	*0.430*
Pmax (kW)	2.23± 0.76	1.90± 0.62	2.40± 1.10	*0.214*	2.11± 0.72	2.28± 0.57	2.20± 0.85	*0.867*
Pmax/mass (W/kg)	32.9± 8.72	29.3± 9.46	35.2± 14.2	*0.306*	27.3± 10.9	28.3± 7.55	29.3± 12.0	*0.893*
DHEA (µmol/L)	-	-	-	-	4.56± 2.86	3.84± 2.76	4.16± 2.92	*0.814*
DHEAS (µmol/L)	-	-	-	-	2.47± 1.40	1.86± 0.98	1.68± 0.82	*0.161*
Albumin (g/L)	-	-	-	-	41.4± 1.43	39.7± 4.66	41.1± 3.32	*0.409*
SHBG (nmol/L)	-	-	-	-	52.4± 22.4	48.4± 21.1	52.4± 23.8	*0.842*
$1,25(OH)_2D_3$ (nmol/L)	-	-	-	-	57.5± 33.6	53.6± 19.8	65.8± 31.7	*0.446*
DHT (nmol/L)	-	-	-	-	1.54± 0.84	1.42± 0.89	1.63± 0.98	*0.792*
E2 (pmol/L)	-	-	-	-	89.0± 57.9	73.8± 27.8	84.9± 25.9	*0.505*

[1] Abbreviations: *MA,* master athletes; *yr,* year; *m,* metre; *kg,* kilogram; *BMI,* body mass index; *cm,* centimetre; *%,* percent; *HGS*, handgrip strength; *TUG,* Timed Up & Go; *Vmax*, maximum jump velocity; *Hmax*, maximum jump height; *Fmax*, maximum force; *Pmax*, absolute vertical jump power; *PmaxRel*, absolute vertical jump power relative to body weight; *BMD*, bone mineral density; *BMC*, bone mineral content (whole body); *MBR,* muscle-to-bone ratio; *Quads CSA*, quadriceps cross-sectional area; *KE-MVC*, knee extensor maximal voluntary contraction; *N,* Newton; *s,* seconds; *EO*, eyes open; *EC*, eyes closed; *W,* watt; *kW,* kilowatt; *DHEA*, dehydroepiandrosterone; *DHEAS*, *DHEA* sulphate; *SHBG*, sex hormone binding globulin; *$1,25(OH)_2D_3$*, 1,25-dihydroxyvitamin D_3, *DHT*, dihydrotestosterone; *E2*, oestradiol; *µmol*, micromole; *nmol,* nanomole; *pmol,* picomole; *L,* litre.

[2]Significance taken as P <0.05. [a] <0.05 compared with both TG and GG genotypes. [b] <0.05 compared with GG genotype only. [c] <0.05 compared with TG genotype only. [d] <0.05 compared with both TT and TG genotypes. [e] no significant differences after adjusting for multiple comparisons.

[3]Data shown as mean ± SD.

Table 3.14. Participant characteristics (body composition, muscle strength/function, physical function, and biochemical data) in relation to rs4588.

Variable	*All MA (n=47)*			*P*	*All Controls (n=45)*			*P*
	CC	**CA**	**AA**		**CC**	**CA**	**AA**	
Age (y)	70.3± 6.03	70.0± 5.63	75.8± 6.40	*0.205*	77.0± 6.17	74.5± 5.99	75.2± 6.71	*0.466*
Height (m)	1.73± 0.06	1.72± 0.07	1.75± 0.07	*0.622*	1.74± 0.06	1.72± 0.08	1.74± 0.01	*0.679*
Weight (kg)	69.0± 7.67	64.6± 9.47	64.2± 5.98	*0.194*	80.8± 12.6	75.1± 14.1	88.1± 19.9	*0.148*
BMI (kg/cm^2)	23.2± 2.26	21.9± 2.25	21.0± 0.58	*0.065*	26.8± 4.10	25.7± 4.45	29.1± 4.59	*0.258*
Percentage Fat Mass (%)	16.7± 6.27	15.0± 6.29	12.1± 2.55	*0.334*	30.6± 7.19	26.2± 10.2	**36.5± 9.89[c]**	***0.048***
Total Body Lean Mass (kg)	54.7± 7.43	52.1± 7.14	53.5± 5.00	*0.515*	53.0± 6.19	53.2± 6.17	53.2± 6.03	*0.989*
Appendicular Lean Mass (kg)	2.61± 0.43	2.48± 0.39	2.35± 0.43	*0.394*	2.41± 0.35	2.42± 0.34	2.39± 0.38	*0.983*
Percentage Lean Mass (%)	79.3± 6.90	81.0± 5.92	83.4± 2.44	*0.414*	66.2± 6.75	72.1± 8.94	**61.8± 9.34[c]**	***0.015***
BMD (g/cm^2)	1.26± 0.10	1.17± 0.12	**0.95± 0.43[d]**	***0.001***	1.27± 0.14	1.23± 0.10	1.16± 0.15	*0.253*
BMC (g)	31.3± 5.43	28.4± 5.74	28.7± 3.25	*0.204*	33.2± 6.62	31.2± 5.41	30.6± 7.50	*0.507*
MBR	-	-	-	-	9.05± 2.44	9.33± 1.46	9.88± 1.75	*0.768*
Quads CSA (cm^2)	-	-	-	-	56.7± 10.5	62.0± 9.77	66.0± 15.4	*0.164*
HGS (kg)	39.8± 8.68	40.0± 9.12	28.3± 8.29	*0.053*	34.9± 7.72	37.7± 9.92	30.3± 12.2	*0.240*
KE MVC (N)	-	-	-	-	310± 117	320± 84.2	315± 89.6	*0.954*
TUG (s)	5.45± 0.63	5.65± 0.75	5.76± 0.19	*0.519*	8.42± 3.62	7.39± 2.52	10.1± 4.71	*0.243*
1 leg EO (s)	-	-	-	-	15.5± 12.8	14.3± 12.6	13.0± 12.0	*0.905*
1 leg EC (s)	-	-	-	-	3.01± 2.09	5.57± 8.99	2.29± 2.78	*0.343*
Vmax (m/s)	-	-	-	-	1.83± 0.37	1.76± 0.45	1.43± 0.53	*0.203*

Hmax (m)	0.25± 0.14	0.28± 0.20	0.18± 0.08	*0.558*	0.23± 0.09	0.22± 0.10	0.12± 0.08	*0.072*
Fmax (N)	1.51± 0.31	1.40± 0.36	1.52± 0.38	*0.567*	1.80± 0.44	1.64± 0.35	1.78± 0.16	*0.500*
Pmax (kW)	2.25± 0.67	2.16± 0.98	1.63± 0.43	*0.366*	2.42± 0.71	2.14± 0.59	1.85± 0.81	*0.251*
Pmax/mass (W/kg)	32.6± 8.37	33.3± 13.2	25.3± 5.33	*0.370*	30.5± 9.37	28.7± 9.31	22.5± 10.8	*0.285*
DHEA (µmol/L)	-	-	-	-	3.85± 2.93	4.21± 2.41	4.81± 3.63	*0.758*
DHEAS (µmol/L)	-	-	-	-	1.98± 1.17	2.06± 1.05	1.41± 0.45	*0.431*
Albumin (g/L)	-	-	-	-	40.9± 2.08	39.4± 4.65	43.3± 3.83	*0.064*
SHBG (nmol/L)	-	-	-	-	49.0± 22.8	54.5± 22.4	46.5± 19.2	*0.666*
1,25$(OH)_2D_3$ (nmol/L)	-	-	-	-	62.9± 30.0	54.3± 22.1	58.2± 36.4	*0.642*
DHT (nmol/L)	-	-	-	-	1.44± 0.96	1.69± 0.82	1.34± 0.95	*0.616*
E2 (pmol/L)	-	-	-	-	84.5± 47.4	78.6± 23.2	77.4± 14.5	*0.851*

[1] Abbreviations: *MA,* master athletes; *yr,* year; *m,* metre; *kg,* kilogram; *BMI,* body mass index; *cm,* centimetre; *%,* percent; *HGS*, handgrip strength; *TUG,* Timed Up & Go; *Vmax*, maximum jump velocity; *Hmax*, maximum jump height; *Fmax*, maximum force; *Pmax*, absolute vertical jump power; *PmaxRel*, absolute vertical jump power relative to body weight; *BMD*, bone mineral density; *BMC*, bone mineral content (whole body); *MBR,* muscle-to-bone ratio; *Quads CSA*, quadriceps cross-sectional area; *KE-MVC*, knee extensor maximal voluntary contraction; *N,* Newton; *s,* seconds; *EO*, eyes open; *EC*, eyes closed; *W,* watt; *kW,* kilowatt; *DHEA*, dehydroepiandrosterone; *DHEAS*, *DHEA* sulphate; *SHBG*, sex hormone binding globulin; *1,25(OH)$_2D_3$*, 1,25-dihydroxyvitamin D_3, *DHT*, dihydrotestosterone; *E2*, oestradiol; *µmol*, micromole; *nmol,* nanomole; *pmol,* picomole; *L,* litre.

[2]Significance taken as P <0.05. [a] <0.05 compared with both CA and AA genotypes. [b] <0.05 compared with AA genotype only. [c] <0.05 compared with CA genotype only. [d] <0.05 compared

with both CC and CA genotypes. [e] no significant differences after adjusting for multiple comparisons.

[3]Data shown as mean ± SD.

Table 3.15. Participant characteristics (body composition, muscle strength/function, physical function, and biochemical data) in relation to DBP isoforms.

Variable	*All MA (n=47)*			*P*	*All Controls (n=45)*			*P*
	Gc1f	**Gc1s**	**Gc2**		**Gc1f**	**Gc1s**	**Gc2**	
Age (y)	70.5± 5.87	**68.6± 5.27[b]**	78.7± 3.21	***0.035***	76.4± 5.92	74.4± 6.65	75.3± 7.14	*0.628*
Height (m)	1.72± 0.07	1.75± 0.04	1.74± 0.08	*0.399*	1.74± 0.06	1.70± 0.06	1.75± 0.14	*0.202*
Weight (kg)	66.5± 8.69	69.2± 8.15	64.0± 7.31	*0.599*	80.0± 12.1	74.4± 15.6	92.4± 23.1	*0.098*
BMI (kg/cm^2)	22.5± 2.25	22.7± 2.67	21.0± 0.70	*0.508*	26.6± 4.02	25.7± 4.60	29.9± 5.44	*0.256*
Percentage Fat Mass (%)	16.1± 6.33	14.7± 6.16	12.8± 2.59	*0.600*	30.5± 7.79	**24.5± 10.2[b]**	40.0± 6.21	***0.008***
Total Body Lean Mass (kg)	53.1± 7.87	55.8± 3.65	52.9± 5.98	*0.608*	53.2± 5.95	52.9± 6.29	53.1± 7.54	*0.990*
Appendicular Lean Mass (kg)	2.54± 0.41	2.62± 0.42	2.23± 0.43	*0.369*	2.41± 0.33	2.43± 0.35	2.34± 0.48	*0.913*
Percentage Lean Mass (%)	79.9± 6.77	81.1± 5.30	82.7± 2.55	*0.685*	67.2± 7.34	**72.5± 9.69[b]**	58.6± 5.92	***0.012***
BMD (g/cm^2)	1.22± 0.12	1.15± 0.33	1.16± 0.04	*0.526*	1.24± 0.13	1.25± 0.12	1.23± 0.17	*0.967*
BMC (g)	30.0± 5.51	30.9± 6.42	27.3± 1.84	*0.635*	32.4± 6.12	31.3± 6.33	32.5± 8.63	*0.871*
MBR	-	-	-	-	**8.76± 1.98[b]**	10.8± 0.84	8.65± 0.65	***0.036***
Quads CSA (cm^2)	-	-	-	-	**56.4± 9.17[b]**	69.5± 12.1	58.9± 49.9	***0.004***
HGS (kg)	39.5± 9.12	39.2± 9.77	31.0± 7.83	*0.310*	35.9± 9.31	36.6± 8.16	27.5± 11.4	*0.213*
KE MVC (N)	-	-	-	-	300± 100	353± 94.8	306± 113	*0.316*
TUG (s)	5.60± 0.70	5.25± 0.47	5.79± 0.21	*0.332*	8.22± 3.34	7.30± 2.55	11.4± 5.39	*0.119*
1 leg EO (s)	-	-	-	-	13.4± 12.6	17.6± 11.9	16.4± 13.2	*0.637*
1 leg EC (s)	-	-	-	-	3.93± 6.79	4.26± 2.56	1.79± 2.14	*0.755*
Vmax (m/s)	-	-	-	-	1.70± 0.38	**2.08± 0.41[b]**	1.28± 0.55	***0.017***

Hmax (m)	0.25± 0.14	0.31± 0.24	0.18± 0.09	*0.453*	0.21± 0.08	**0.27± 0.12[b]**	0.09± 0.07	***0.035***
Fmax (N)	1.44± 0.35	1.52± 0.25	1.59± 0.44	*0.686*	1.77± 0.41	1.57± 0.28	1.85± 0.11	*0.408*
Pmax (kW)	2.08± 0.68	2.62± 1.11	1.69± 0.51	*0.107*	2.19± 0.61	2.53± 0.77	1.67± 0.88	*0.180*
Pmax/mass (W/kg)	31.3± 9.10	38.0± 14.2	26.2± 6.15	*0.130*	27.5± 8.62	**35.9± 9.39[b]**	19.1± 8.50	***0.022***
DHEA (µmol/L)	-	-	-	-	4.03± 2.74	3.59± 2.47	6.21± 3.76	*0.270*
DHEAS (µmol/L)	-	-	-	-	2.04± 1.16	1.78± 0.93	1.56± 0.49	*0.609*
Albumin (g/L)	-	-	-	-	40.5± 3.95	40.5± 3.05	41.8± 3.77	*0.816*
SHBG (nmol/L)	-	-	-	-	50.0± 20.9	58.1± 26.1	36.5± 10.6	*0.233*
$1,25(OH)_2D_3$ (nmol/L)	-	-	-	-	54.9± 24.6	75.7± 33.2	41.8± 12.7	***0.042[e]***
DHT (nmol/L)	-	-	-	-	1.46± 0.84	1.88± 0.98	1.00± 0.87	*0.197*
E2 (pmol/L)	-	-	-	-	79.1± 40.0	87.7± 29.6	79.3± 18.2	*0.796*

[1] Abbreviations: *MA,* master athletes; *yr,* year; *m,* metre; *kg,* kilogram; *BMI,* body mass index; *cm,* centimetre; *%,* percent; *HGS*, handgrip strength; *TUG,* Timed Up & Go; *Vmax*, maximum jump velocity; *Hmax*, maximum jump height; *Fmax*, maximum force; *Pmax*, absolute vertical jump power; *PmaxRel*, absolute vertical jump power relative to body weight; *BMD*, bone mineral density; *BMC*, bone mineral content (whole body); *MBR,* muscle-to-bone ratio; *Quads CSA*, quadriceps cross-sectional area; *KE-MVC*, knee extensor maximal voluntary contraction; *N,* Newton; *s,* seconds; *EO*, eyes open; *EC*, eyes closed; *W,* watt; *kW,* kilowatt; *DHEA*, dehydroepiandrosterone; *DHEAS*, *DHEA* sulphate; *SHBG*, sex hormone binding globulin; *$1,25(OH)_2D_3$*, 1,25-dihydroxyvitamin D_3, *DHT*, dihydrotestosterone; *E2*, oestradiol; *µmol*, micromole; *nmol,* nanomole; *pmol,* picomole; *L,* litre.

[2]Significance taken as P <0.05. [a] <0.05 compared with both Gc1s and Gc2 isoforms. [b] <0.05 compared with Gc2 isoform only. [c] <0.05 compared with Gc1s genotype only. [d] <0.05 compared

with both Gc1f and Gc1s isoforms. [e] No significant differences after adjusting for multiple comparisons.

[3]Data shown as mean ± SD.

3.4 Discussion

In this candidate gene study conducted in a cohort of elite MA and controls, associations were reported between several *VDR* SNPs and outcomes of skeletal muscle strength and performance, and a novel link between the vitamin D system and SHBG. For the first time, this chapter also demonstrates a relationship between SNPs of the vitamin D binding protein gene (*GC*) and skeletal muscle strength/function and body composition.

3.4.1 VDR SNPs

The relationship between genetic variance of the *VDR* gene and skeletal muscle function has already been investigated in multiple studies and the systematic review conducted in **Chapter 2** provides a comprehensive outline of their results and findings. Of the six *VDR* SNPs investigated in this study, differences were found in muscular function and strength in carriers of ApaI, Cdx2, and A1012G. Comparatively, no notable differences were demonstrated in MA or controls carrying FokI, BsmI, and TaqI.

ApaI is a SNP located close to the 3' untranslated region (UTR) in intron 8 of the *VDR* gene that is the result of a nucleotide change of C to A (C>A) [309]. Due to its location, it is unlikely that ApaI results in a VDR protein with a functionally altered structure but it's possible that it affects mRNA stability as the 3' UTR is key for mRNA translocation and localisation [310]. In relation to muscle strength, data suggesting a relationship with ApaI conflicts across the literature. Multiple articles have failed to demonstrate any differences at all

[276,279,281,282] and, whilst others report greater HGS and quadriceps strength, there is conflict on what is to be regarded as the "beneficial" genotype [277,280]. Like other groups, no significant differences were found in muscle strength between genotypes, but carriers of the WT CC ApaI genotype did display significantly better balance. Balance is a key aspect of motor function and, the time that an individual is able to stand on one leg with their eyes closed is considered as an index of static steady-state balance ability [311]. Until now, ApaI has only been investigated in relation to balance in one other study and no significant differences were found [284]. However, the sample size used in this study was small (n=63) making it possible that the study lacked statistical power and the inclusion of participants with hemi-paralysis makes it highly probable that their results were confounded to some degree [284]. In the investigations, balance tests were only conducted in the control group so it would be interesting to repeat them in the MA cohort to see how this data translates across groups. In addition, performing these investigations in a younger cohort would be valuable as there is a large volume of interest into the use of balance as an indicator of future physical function and identification of balance influencing SNPs may provide information clinically to identify at risk individuals [312].

Getting its name from its location in the Cdx2 binding site within the 1e promoter region of the *VDR* gene, Cdx2 involves an A to G nucleotide change (A>G) [313]. While it doesn't result in any alterations to the AA sequence, reports have suggested that the G allele is associated with increased VDR

transcriptional activity due to an altered binding affinity of VDR for the Cdx2 transcription factor [314]. Only 2 studies have investigated Cdx2 in relation to skeletal muscle strength and function, both of which reported no significant differences [271,281]. Interestingly, in the work conducted here, differences between Cdx2 genotypes were only found in the MA cohort and, in line with the literature, no differences were seen with regards to skeletal muscle strength. Comparatively, the data demonstrated that MA carrying one or two copies of the mutant G allele weighed significantly more, displayed significantly greater absolute and relative power, and had significantly higher whole body bone mineral content (BMC) and lean mass (appendicular and total body) than GG homozygotes. Weight is infrequently reported in studies that have previously investigated Cdx2, and they tend to report BMI instead making it difficult to draw direct comparisons with the data presented here. Given that total body lean mass was also significantly higher in MA carrying one or two G alleles and that muscle is denser than fat, the observation that these individuals also weighed significantly more is unsurprising. However, these observations conflict with the literature, as several studies have reported no differences at all [315,316] whilst others have found that carriers of the GG genotype possess increased fat mass compared to G allele carriers [317]. As jumping is a natural movement that is also physiologically complex, jump mechanography acts as a novel validated technique that can measure both muscle and neuromuscular function [318]. Here, it was demonstrated that MA in possession of one or two G alleles of the Cdx2 SNP displayed significantly higher lower limb power, both absolute and relative (P_{max} and P_{max}Rel, respectively), than those carrying the

AA genotype. P_{max} represents the ability of the muscle to produce force at a given velocity, and reports suggest that it is correlated with the percentage of type II muscle fibres [319,320]. Whilst it is possible that Cdx2 may affect the contractile properties of muscle fibres, it is unlikely through a direct affect upon skeletal muscle given that expression of the Cdx2 transcription factor has not been documented in skeletal muscle and its influence upon VDR expression is, in fact, intestine-specific [321]. Instead, it is wholly possible that the Cdx2 SNP is in linkage disequilibrium (LD) with one or more functional SNPs within the *VDR* gene that are yet to be discovered. However, whilst the Cdx2 SNP may not have direct effects upon skeletal muscle, the specificity of the Cdx2 transcription factor to the intestine may have influence upon skeletal parameters due to the calciotropic function of vitamin D. *In vitro* studies conducted in Cdx2 transfected Caco-2 cells, a colonic derived cell line, have demonstrated that transcriptional activity of the *VDR* promoter in AA cells was 70% of those carrying the GG genotype [314]. This observation has been translated clinically, as several articles have shown associations between the Cdx2 SNP and bone mineral density (BMD) [314,322,323]. In the investigations conducted here, no significant differences were seen in BMD for Cdx2, but it was demonstrated that AA homozygous MA had significantly lower bone mineral content (BMC) than those carrying one or two G alleles. Only one other study exists investigating Cdx2 in relation to BMC (all other articles only included BMD) and it reported that no significant differences were seen between genotypes in a cohort of patients with juvenile idiopathic arthritis [324]. As this was conducted in a patient cohort with a mean age of 10.96±4.6

years, it is clearly difficult to draw comparisons with this cohort of older healthy elite male MA, which only indicates a need for further investigations including study populations inclusive of a wide range of age groups and disease/healthy states.

An A to G transition (A>G) at position -1210 to the transcription start site in the *VDR* gene results in a SNP known as A1012G. This SNP is relatively novel in comparison to others, but it is the only SNP to be consistently associated with greater HGS throughout the literature, as demonstrated by the systematic review conducted in **Chapter 2** [265,285]. Here, the data was in support of the literature as it was also found that MA carrying the mutant GG genotype displayed significantly greater HGS than AA homozygotes. For the first time, significant differences were demonstrated in relative power and maximal velocity (V_{max}) between GG homozygous controls and those carrying one or two A alleles, indicating that the benefits of the mutant G allele of A1012G aren't only limited to the upper limbs. Interestingly, a relationship was found between the vitamin D system and sex hormones, as GG control homozygotes had significantly higher serum levels of the protein responsible for transporting sex hormones, sex hormone binding globulin (SHBG). Multiple studies, conducted in both men and women, have reported positive correlations between serum 25(OH)D_3 and SHBG levels [325–328] and, whilst A1012G has never been studied in relation to SHBG before, associations have been found between SHBG levels and both FokI and BsmI [329,330]. Currently, the functional consequence of A1012G isn't wholly understood. Due to its location in the 1a

promoter region, it appears that A1012G negatively modifies the binding ability of the *VDR* promoter to the zinc-finger transcription factor, GATA-3 [288]. It has been demonstrated that the GATA-3 binding site is present in the AA genotype of A1012G whereas it is absent in GG homozygotes [331]. The impact of this is unclear, particularly in skeletal muscle, as the majority of functional A1012G research has been conducted in immune cells due to the direct role of GATA-3 upon polarisation of naïve T cells into Th2 cells [332]. One study conducted in peripheral blood mononuclear cells (PBMC) isolated from psoriasis patients genotyped for A1012G demonstrated that the SNP influences *VDR* mRNA expression as a dose dependent increase in *VDR* expression was seen across genotypes (AA<AG<GG) [333]. Another potential hypothesis is that A1012G determines where transcription starts in the *VDR* gene and, therefore, what VDR protein isoform an individual possesses. If transcription begins in exon 1a (AA), then the WT VDRA isoform is produced, whereas initiating transcription in exon 1d (GG) produces a protein with a longer N-term and greater transactivation potential, VDRB1 [334]. As these functional studies have never been conducted in skeletal muscle cells, further research is imperative to clarify and confirm whether the hypotheses presented are valid in skeletal muscle, or whether there are other potential underlying mechanisms present.

3.4.2 GC (DBP) SNPs

At time of writing (Spring 2024), this is the only work to have investigated and report relationships between two SNPs of the vitamin D binding protein (DBP;

GC) gene and musculoskeletal outcomes. The impact of genetic variation within the *GC* gene upon circulating 25(OH)D_3 levels has been well-researched, relative to skeletal muscle function and performance, and several studies have reported associations between two *GC* SNPs in particular, rs7041 and rs4588 [335–338]. rs7041, is a SNP occurring in exon 11 of the *GC* gene that results in an AA substitution of aspartate (Asp) to glutamine (Glu)) caused by a nucleotide change of T to G (T>G) [36]. Comparatively, rs4588 is also located in exon 11, involves a C to A transition (C>A), and results in the substitution of threonine (Thr) for lysine (Lys) [36]. As displayed in **Table 3.1**, three isoforms of DBP exist: Gc1f (rs7041-T/rs4588-C), Gc1s (rs7041-G/rs4588-C), and Gc2 (rs7041-T/rs4588-A).

DBP & Muscle Outcomes

In the physiological scenario of skeletal muscle, the data suggests that rs7041 may be a SNP with positive influences as GG homozygous controls displayed greater quadriceps CSA and KE-MVC than those carrying one or two WT T alleles. Additionally, carriers of the Gc1s isoform of DBP possessed greater lower limb muscle power and function, as demonstrated by jump mechanography, compared to those carrying Gc2. As *GC* SNPs and DBP isoforms have never been explored before in relation to skeletal muscle outcomes, no other studies exist to allow for comparison of the data presented here. The longstanding hypothesis for the potential functional mechanism underlying rs7041 has been that it influences vitamin D status due to altered

binding affinity of DBP for vitamin D metabolites, thereby subsequently altering vitamin D bioavailability for target tissues [339]. However, this hypothesis is currently a matter of debate within the field due to several conflicting articles that either showed no differences in affinity between isoforms or differences that appear to be dependent on the population studied and/or the assay kit utilised to quantify DBP [339–342]. Another possible hypothesis is that the SNP affects glucose control as it appears that DBP is involved in insulin dynamics. Several groups have demonstrated negative correlations between serum levels of DBP and insulin levels in both men and women, whilst mice lacking the *Gc* gene (DBP-KO) possess elevated insulin sensitivity and reduced glucagon secretion compared to their WT littermates [343–345]. Given this information and paired with the fact that skeletal muscle is a major regulator of glucose homeostasis, it is perhaps sensible to consider whether altered insulin dynamics contributed to the beneficial effects of the rs7041 GG genotype that were seen in the control cohort.

Since the discovery that DBP is also key in macrophage activation, it is often also known as, macrophage-activating factor (DBP-MAF) [53]. DBP is converted to active DBP-MAF via deglycosylation of the threonine that is substituted for lysine in the rs4588 SNP. Galactose and sialic acid are removed by β-galactosidase and sialidase, respectively, leaving just N-acetyl-galactosamine (NaGal) bound to threonine, thereby forming DBP-MAF [54]. Whilst both Gc1f and Gc1s DBP isoforms are glycosylated, Gc2 is unglycosylated due to having a lysine in place of threonine, thus potentially impairing DBP-MAF formation and

activity [346]. Macrophages play a major role in skeletal muscle plasticity (particularly in response to damage/increasing age), lipid dysregulation, and insulin resistance, so it is possible to hypothesise that the positive effects upon skeletal muscle that were associated with Gc1s here may be due to the Gc2 isoform possessing diminished macrophage activation and conversion [347,348]. In addition, activated macrophages have been documented to regulate bioavailability of $1,25(OH)_2D_3$ by expression of high levels of 1α-hydroxylase (CYP27B1), so the hypothesised diminished macrophage activation could contribute further to a reduction in bioavailability of macrophage-derived $1,25(OH)_2D_3$ [349]. Unfortunately, there is a distinct absence of experimental studies exploring these theories, especially in skeletal muscle, but further research should endeavour to validate these speculations. Finally, one other potential mechanism lies in the actin-binding ability of DBP. The extracellular actin scavenging system (EASS) is key in an individual's response to trauma, as tissue damage leads to a large efflux of actin into the circulation, forming polymerised filamentous actin (F-actin) [43]. If not removed, this pool of F-actin can lead to intravascular coagulation and, ultimately, multiorgan failure [43]. To avoid this, the EASS employs gelsolin to depolymerise F-actin into globular actin (G-actin), which DBP can bind with high affinity, thereby preventing its repolymerisation [45]. The DBP-actin complex is then cleared from circulation at multiple sites, primarily the liver, but also the lungs and spleen [40]. A previously held common misconception was that this function of DBP was only relevant to extracellular actin, until the discovery that DBP strongly co-localises with cytoskeletal actin filaments in skeletal muscle

[350]. It has since been demonstrated that DBP can be internalised into skeletal muscle via megalin/cubilin, bind cytoplasmic actin and, subsequently, intracellular $25(OH)D_3$ that can be released into circulation following proteolytic degradation of DBP [252]. The functional consequence of different DBP isoforms/SNPs upon actin binding is unclear as very few experimental studies exist exploring this, but two early studies report no differences in affinity for actin between the three isoforms [42,351]. Comparatively, when affinity was measured via capillary electrophoresis by another group, differences between isoforms were detected; the methodological differences have not since been clarified nor validated, therefore representing an attractive topic for future research [352]. Finally, loss of the *Gc* gene in murine pancreatic α cells generated abnormalities in the actin cytoskeleton, suggesting involvement of DBP in normal cytoskeletal maintenance [345]. It would be intriguing to explore whether similar observations occur in skeletal muscle cells, as the cytoskeleton is crucial for fusion of myoblasts into myotubes.

DBP & Skeletal Outcomes

Whilst there is an absence of research in relation to skeletal muscle and genetic variation of DBP, a greater volume of information exists relating to its impact upon skeletal physiology comparatively. In the work conducted herein, it was found that the mutant A allele of rs4588 was associated with reduced BMD compared to the WT CC genotype. Like the effects in skeletal muscle, rs7041 appeared to provide a positive effect upon the muscle-to-bone ratio (MBR), as this was higher in controls carrying the mutant GG genotype than TT individuals.

This was supported further by the fact MBR was also higher in controls possessing the Gc1s DBP isoform when compared to Gc1f. These results are not unique to the investigations conducted in this chapter, as similar observations have been described in the literature. An article by Rivera-Paredz et al. also reported that, within their cohort of Mexican women, the A allele of rs4588 was associated with higher BMD and DBP serum levels than the CC genotype [353]. Furthermore, women carrying the G allele of rs7041 possessed lower serum levels of DBP and also had reduced BMD in comparison to those with the wildtype TT genotype [353]. Fortunately, the knowledge of the mechanisms underlying these observations is far less speculative than that of skeletal muscle as the stimulatory nature of DBP-MAF is not just restricted to macrophages - it also has a stimulatory effect upon osteoclasts. In fact, osteoclast activity is actually greater when treated with *ex-vivo* synthesised DBP-MAF compared to that of traditional stimulators (e.g., $1,25(OH)_2D_3$ and PTH) [55]. Additionally, DBP-MAF treatment of rats with osteopetrosis, a condition in which bones are excessively dense, increased osteoclastic activity and number and resulted in a subsequent reduction in bone mass [56].

3.4.3 *Limitations*

Studying a cohort as unique as the MA comes with associated difficulties, particularly with regards to attaining large sample sizes, so future genetic association studies conducted in MA should seek to use much larger sample sizes. Additionally, some outcomes were only conducted in the control cohort, e.g., the biochemical parameters, and it would be useful to have this data for

the MA to allow for comparisons between the two groups. The participant data for ethnicity or previous medical history, such as previous surgeries, comorbidities, or joint replacements was not available. This data would have provided further information about the population being studied, as it's well known that SNP frequency can differ across different populations, and it also could have highlighted any potential confounders. In addition, no data was collected with regards to activity levels in the controls, which would have been useful as if some were sedentary then this could have confounded their performance on certain outcomes. Having dietary questionnaire data, such as calcium intake or details of any supplements routinely taken, would have been beneficial as it could aid interpretation of the bone densitometry results. As the participant data used in this chapter was collected for another study, the investigator (SB) did not have full control over how certain data is described. For example, serum levels of $25(OH)D_3$ states whether they were above or below 10 ng/mL (> or <10), and no exact values were provided, thus only providing a very general view of the data. Exact values were provided for $1,25(OH)_2D_3$ yet, of the two, this is arguably the least useful value.

3.5 Conclusions

Based on the literature, it appears the work conducted in this chapter is the first to explore the impact of two key *GC* SNPs, rs4588 and rs7041, upon multiple parameters of musculoskeletal physiology in a cohort of elite master athletes. Like several other groups, no differences were found in those carrying the *VDR* SNPs BsmI, TaqI, and FokI. However, the results did support an association between A1012G and greater muscle/physical function, whilst highlighting novel links between the vitamin D system and sex hormones in muscle. Future research should further explore the relationship between the vitamin D binding protein and skeletal muscle physiology, whilst also attempting to clarify the functional mechanisms underlying the SNPs investigated here.

Chapter 4: VDR regulates myogenic/proteolytic signalling and mitochondrial respiration in response to anabolic, catabolic, and pro-inflammatory conditions in C2C12 myotubes.

4.1 Introduction

The focus of this thesis so far has been the role of the vitamin D system in skeletal muscle physiology, particularly the impact of genetic variation within this pathway. Vitamin D biology, e.g., synthesis, metabolism, and genomic/non-genomic mechanisms of action, have been discussed in depth in **Chapter 1.** The physiological effects of vitamin D are the result of $1,25(OH)_2D_3$ binding to its receptor, vitamin D receptor (VDR). This $1,25(OH)_2D_3$-VDR complex translocates to the nucleus where it forms a trimeric complex with retinoid x receptor (RXR), a nuclear receptor that can recruit both corepressors and coactivators. It is through this liganded complex that VDR is able to perform its function as a transcriptional co-activator controlling ~3% of the human genome [71,72].

In relation to skeletal muscle, the role of VDR has historically been a matter of debate. For over a decade, there was a degree of uncertainty surrounding whether VDR was actually expressed in skeletal muscle, but it was discovered that this was the result of using unreliable antibodies that cross-reacted with unrelated proteins [148,354]. Since this controversy, multiple studies using

different VDR antibodies have confirmed that the VDR protein is indeed present in both human and murine skeletal muscle [122,143,355]. Currently, the exact role of vitamin D and VDR in skeletal muscle physiology is unclear but several lines of evidence suggest a regulatory function upon myogenesis and myogenic cell function. VDR-KO mice display smaller muscle fibres and have persistently high expression of key myogenic factors, e.g., myogenin and Myf5 [163]. Additionally, work conducted in mice carrying a myocyte-specific deletion of *Vdr* (mVDR-KO) displayed that loss of *Vdr* results in a sarcopenic phenotype and altered expression of genes related to calcium-handling (e.g. Serca-2b & -3) and cell cycle control (e.g. cyclin-D1, -D2 and -D3) [147]. In support of this data, overexpression (OE) of VDR in skeletal muscle results in muscular hypertrophy and a rise in muscle protein synthesis (MPS) paired with upregulation of mTOR signalling [296]. These observations have also been translated *in vitro,* as VDR-KD C2C12 myoblasts were unable to differentiate normally, resulting in fewer myotubes, and also had reduced MPS [213]. Whilst these existing studies support a putative relationship between the vitamin D system and skeletal muscle, there remains to be a notable gap in the knowledge of the mechanistic underpinnings of this connection.

Based on recent evidence, it appears that the vitamin D system has a key regulatory role in skeletal muscle mitochondrial function. To date, the majority of research has focused upon investigating the influence of vitamin D deficiency, and several articles have demonstrated that supplementation of deficient humans and rodents results in improvements in both mitochondrial

function and density [224,248,356]. These observations have been replicated *in vitro* as treatment of human skeletal muscle cells with $1,25(OH)_2D_3$ resulted in an increase in mitochondrial volume and oxygen consumption rate (OCR) [174]. Loss of the *Vdr* gene in C2C12 myoblasts via lentiviral short hairpin RNA (shRNA) silencing was associated with blunted mitochondrial respiration from oxidative phosphorylation (OXPHOS) in both proliferating myoblasts and differentiated myotubes [244]. However, the mechanisms underlying this mitochondrial regulatory function of vitamin D is unknown, as it appears that vitamin D has no impact upon mitochondrial protein content, such as activity of citrate synthase (CS) or expression of electron transport chain (ETC) machinery [243].

Intriguingly, whilst multiple studies exist examining the influence of perturbed *VDR* expression upon basal myogenic cellular function *in vitro,* there is a distinct lack of investigations that challenge *VDR* silenced skeletal muscle cells with conditions frequent to skeletal muscle, such as atrophy or inflammation. These types of investigations would be particularly useful as they could provide further information about the involvement of VDR in cellular responses to these types of physiological scenarios, particularly in skeletal muscle.

Skeletal muscle atrophy is regarded as the loss of muscle mass and development of muscle weakness that occurs when the protein net balance (NPB) is negative due to the rate of muscle protein breakdown (MPB) exceeding that of muscle protein synthesis (MPS). Clinically, atrophy is a

common negative outcome of certain catabolic pathological scenarios, such as infections, prolonged periods of immobilisation (e.g., bedrest), and cancer (also termed cachexia). So, understandably, there is a large volume of research focused upon furthering our understanding of the underlying mechanisms and investigating potential interventions. Whilst a plethora of randomised clinical trials (RCTs) exist investigating the efficacy and efficiency of vitamin D supplementation in the prevention and/or restoration of muscle atrophy, *in vitro* mechanistic studies are lacking. Dexamethasone (Dex) is a glucocorticoid commonly used in the treatment of a range of diseases, e.g., rheumatoid arthritis or SARS-CoV-2, due to its anti-inflammatory properties [357,358]. When used in high doses or long-term, Dex treatment can result in muscle atrophy [359], and it is because of these side effects that Dex is frequently used *in vivo* and *in vitro* to generate a model of glucocorticoid-induced skeletal muscle atrophy. VDR-KO mice were injected daily with 25 mg/kg Dex for 10 days to induce muscle atrophy and the skeletal muscle injuries that these mice developed were much more severe than their WT counterparts [360]. Dex treatment caused a decrease in the density of type I and IIa muscle fibres, but type IIb fibre density increased; an effect that was far more profound in the VDR-KO mice versus WT [360].

On the opposite side of the scale, skeletal muscle hypertrophy occurs when the NPB is positive due to the rate of MPS exceeding that of MPB. Common inducers of hypertrophy *in vivo* include resistance training and certain hormones (i.e., testosterone and insulin-like growth factor-1, IGF-1) [361,362],

some of which can be exploited experimentally and be used to generate *in vitro* hypertrophic models. Unlike muscle atrophy, VDR has been scarcely researched in relation to skeletal muscle hypertrophy. Work previously conducted by Bass et al. exemplified that VDR-OE in the *Tibialis anterior* (TA) of rats induced hypertrophy as marked by a significant increase in global total protein and RNA content plus a larger myofibre CSA [296]. In addition, several studies in which C2C12 myotubes were treated with $1,25(OH)_2D_3$ and/or $25(OH)D_3$ have shown increases in myotube diameter [143,144,156]. Skeletal muscle hypertrophy is accompanied by an increase in expression of the growth factor, IGF-1. IGF-1 can be used *in vitro* as a model of hypertrophy as when added to differentiated myotubes, it results in activation of the phosphatidylinositol 3-kinase (PI3K)/Akt pathway; a pathway considered one of the principal regulators of mTOR [363,364]. As mentioned previously, no articles exist examining muscular hypertrophy *in vitro* in the scenario of perturbed VDR signalling, thus representing an attractive area to explore experimentally.

Finally, a significant field of vitamin D research has focused upon its anti-inflammatory and immunoregulatory properties. Lipopolysaccharide (LPS) is an endotoxin derived from bacterial outer-membranes and its administration *in vivo* and *in vitro* is a well-established model of skeletal muscle inflammation [365,366]. Unfortunately, little data exists investigating vitamin D and inflammation in relation to skeletal muscle with only one study demonstrating that pre-treatment of C2C12 myotubes with $1,25(OH)_2D_3$ was able to inhibit

LPS-induced IL-6 production [367]. This protective effect of 1,25$(OH)_2D_3$ against LPS-induced inflammation has also been demonstrated in other cell types, such as alveolar basal epithelial cells and oral keratinocytes [368,369]. In addition, markers of renal inflammation, e.g., creatinine accumulation and tubular cell apoptosis, were significantly greater in VDR-KO mice with LPS-induced acute kidney injury (AKI) in comparison to WT mice [370]. When this information is considered collectively, it is sensible to hypothesise that loss or impairment of VDR signalling in skeletal muscle would pre-dispose to heightened inflammation in response to either LPS treatment or other pro-inflammatory conditions.

Here, the aim of this chapter was to use RNA interference (RNAi) to knockdown *Vdr* expression (VDR-KD) in C2C12 myotubes to investigate the involvement of the vitamin D/VDR axis in mitochondrial respiration and myogenic signalling in response to atrophic, hypertrophic, and pro-inflammatory conditions (dexamethasone, IGF-1, and LPS).

4.2 Methods

4.2.1 Cell Culture

Murine C2C12 myoblasts (ECACC, Salisbury, UK) were cultured and maintained in Dulbecco's Modified Eagle Medium (DMEM; Thermo Fisher Scientific) supplemented with 10% (v/v) fetal bovine serum (FBS), 1% (v/v) antibiotic-antimycotic solution, and 4mM L-Glutamine (all Sigma-Aldrich, UK) at 37°C with 5% CO_2. Cells (passage 8) were seeded onto 6-well plates (Nunclon™ Delta: Thermo Fisher Scientific) and upon reaching 70-80% confluency, differentiation was induced by switching to DMEM with reduced serum (2% FBS (v/v)). The day on which differentiation was induced is referred to as day 0. Media changes were performed every 48 hours.

4.2.2 RNA Interference

A small-interfering RNA (siRNA) sequence targeting vitamin D receptor (*VDR*) was used (Sigma Aldrich; EHU010441) and all knockdown experiments were performed in parallel with cells transfected with a Universal Negative Control siRNA (Sigma Aldrich; SIC001). At day 2 post-differentiation, cells were transfected with 25 pmol VDR or negative control (NC) siRNAs using the Lipofectamine RNAiMAX Transfection Reagent (Invitrogen) diluted in OptiMEM (Gibco) following manufacturer's instructions.

The VDR eSIRNA sequence was as follows:

CCAGTTCGTGTGAATGATGGTGGAGGGAGCCATCCTTCCAGGCCCAACTCCAGACACACTCCCAGCTT

CTCTGGGGACTCCTCCTCCTCCTGCTCAGATCACTGTATCACCTCTTCAGACATGATGGACTCGTCCAG

CTTCTCCAATCTGGATCTGAGTGAAGAAGATTCAGATGACCCTTCTGTGACCCTAGAGCTGTCCCAGCT

CTCCATGCTGCCCCACCTGGCTGACCTGGTCAGTTACAGCATCCAAAAGGTCATTGGCTTTGCTAAGAT
GATACCAGGATTCAGAGACCTCACCTCTGAGGACCAGATCGTACTGCTGAAGTCAAGTGCCATTGAG
GTCATCATGTTGCGCTCCAATGAGTCCTTCACCATGGACGACATGTCCTGGACCTGTGGCAACCAAGA
CTACAAGTACCGCGTCAGTGACGTGACCAAAGCCGGACACAGCCTGGAGCTGATTGAGCCCCTCATC
AAGTTCCAGGTGGGACTGAAGAAGCTGAACTTGCATGAGGAGGAGC

4.2.3 Treatment of Cells

At 5 days post-differentiation, cells were incubated in the presence of selected treatments known to influence muscle protein synthesis (anabolism), breakdown (catabolism), and inflammation for 24 hours. Treatments were either 20 ng/mL insulin-like growth factor-1 (IGF-1), 1 μM dexamethasone (Dex), or 0.1 μg/mL lipopolysaccharide (LPS; from Escherichia coli O26:B6). All were purchased from Sigma Aldrich.

4.2.4 High-Resolution Respirometry

Mitochondrial oxidative phosphorylation (OXPHOS) was quantified in permealised myotubes by performing high-resolution respiratory in a two-channel titration injection respirometer (Oxygraph-2 k; Oroboros Instruments, Innsbruck, Austria) with the SUIT-008_O2_ce-pce_D025 protocol as designed by Oroboros. Oxygen concentration (μM), as well as oxygen flux per cell (pmol $O_2.s^{-1}\cdot cell^{-1}$), was recorded in real time using DatLab software.

In brief, following a 24-hour incubation period with LPS, IGF-1 or Dex, C2C12 myotubes (day 6 post-differentiation) were trypsinised and centrifuged for 5 minutes at 300 *g*. The cell pellet was resuspended in mitochondrial respiration

media (MiR05; Oroboros) before being placed in the oxygraph chamber with 10 µg/ml digitonin for myotube permealisation. The chamber had been pre-equilibrated with 2 mL MiR05 stirring at 750 rpm at 37°C. To generate NADH for Complex I, 5 mM pyruvate and 2 mM malate were added simultaneously in the absence of adenosine diphosphate (ADP) to measure leakage respiration. Malate acts to maintain pyruvate metabolism by providing a source of oxaloacetate for citrate synthesis. 2.5 mM ADP was added to quantify OXPHOS capacity followed by 10 µM cytochrome c to test mitochondrial outer membrane integrity. Next, 10 mM glutamate was added as a substrate for Complex I whilst the OXPHOS capacity of Complex II was quantified as the difference in oxygen flux after addition of 10 mM succinate. Uncoupling of phosphorylation and oxidation was achieved by performing a titration with 0.5 µM carbonyl cyanide p-trifluoromethoxyphenylhydrazone (FCCP) until maximal respiration was reached. FCCP transports protons across the inner mitochondrial membranes, thereby disrupting adenosine triphosphate (ATP) synthesis. 0.5 µM rotenone was subsequently injected to inhibit Complex I and test the contribution of Complex II to the electron transport chain (ETC). Finally, residual oxygen consumption was induced via addition of 2.5 µM antimycin A. Oxygen consumption rates (OCR; pmol/ml.s) were calculated using DatLab7 (Oroboros, Innsbruck, Austria) and values were normalised to total protein content. Experiments were performed twice with average values from the two oxygraph chambers (i.e., 4 technical replicates/treatment) taken forward for statistical analyses.

4.2.5 qRT-PCR

RNA was extracted using the phenol-chloroform method [371]. At day 6 post-differentiation, cells were scraped into 200 µl TRI reagent (Sigma Aldrich), and then incubated at room temperature and pressure (RTP) for 10 minutes. For the phase separation step, 40 µl chloroform (Fisher) was added and incubated for a further 10 minutes at RTP before samples were centrifuged at 12,000 rpm for 15 minutes at 4°C. The upper aqueous phase was transferred into a fresh Eppendorf (Eppendorf) and equal volume 100% isopropanol (Sigma) and 1 µl GlycoBlue (Invitrogen) were added to precipitate the RNA. Samples were centrifuged for 5 minutes at 7,000 rpm and 4°C, and the resulting RNA pellet was washed three times with 80% ethanol. Following removal of all ethanol after the third and final wash, the pellet was left to air dry and subsequently resuspended in 20 µl Nuclease Free DEPC-treated water (Invitrogen). Sample concentration and purity (260/280 ratio) was determined using a Nanodrop 1000 (Thermo Scientific), and samples were stored at -80°C until further use.

Reverse transcription was performed using a High-Capacity cDNA Reverse Transcription kit (Applied Biosystems) and quantitative reverse transcriptase PCR (qRT-PCR) was subsequently performed on a ViiA7 Real-Time PCR system (Life Technologies) using SYBR Select Master Mix (Applied Biosystems) and primers designed in-house (**Table 4.1**). Thermal cycling conditions were as follows: 2 minutes at 50°C, 10 minutes at 95°C, 40 cycles of 15 seconds at 95°C, and 1 minute at 60°C. Samples were run in triplicate with two control samples, one without reverse transcriptase and one without cDNA, as negative controls.

Gene expression (relative fold change) was quantified by normalising against GAPDH using the $2^{-\Delta\Delta CT}$ method [372].

Table 4.1. Primers used in qRT-PCR.

Gene Target	Forward Primer (5'-3')	Reverse Primer (5'-3')
Gapdh	**TGGAAGGGCTCATGACCACAG**	**ACCAGTGGATGCAGGGATGA**
Vdr	**TCCCCCATCCCTAGAACCAGC**	**TCCTCATTGCTTGGGCTCTG**
Foxo1	**AACCAAAGCTTCCCACACAGT**	**AAGGACTTTTAAATGTAGCCTGC**
Foxo3	**GAAGGGAAGGAGCCGAGGTAG**	**TCCACTTCGAGCGGAGAGAG**
Mtor	**TTCCTGAACAGCGAGCACAA**	**GTAGCGGATATCAGGGTCAGG**
Tsc2	**GAACTGAGTGGTGAATGCGG**	**CTCCACTGCATGCTCCTCAA**
Akt	**TGAAAACCTTCTGTGGGACC**	**TGGTCCTGGTTGTAGAAGGG**
Cubn	**GGCTCCAAGTCCCATTGTCA**	**AATGTACGTCCACAACGGCT**
Myh8	**CACACCCTATCTCCGCCAAG**	**AGCCGAGGTTTCAGCTATGG**
Myf5	**TCAGGAATGCCATCCGCTAC**	**CCCGGCAGGCTGTAATAGTT**
Mrf4	**GAGATTCTGCGGAGTGCCAT**	**GCTCCTCCTTCCTTAGCAGT**
Myh1	**GCATCCCTAAAGGCAGGCTC**	**CAAACACCGATGACTTGGCG**
Rps6	**CTTTTTCGTGACGCCTCCCA**	**ATCCGGACCACATAACCCTTC**
Hdac9	**CTCACCGAATCCGCATGACT**	**ATTGGCTTTGTGAGGACGGT**
Ppp3ca	**AAAGCGCTACTGTTGAGGCT**	**GTCCGTGCCGTTAGTCTCTG**
Myog	**AGGAGATCATTTGCTCGCGG**	**ATCCTCCACCGTGATGCTGT**
Myod1	**TGCTCTGATGGCATGATGGAT**	**CACTGTAGTAGGCGGTGTCG**
Ccnd1	**TCAAGTGACCCGGACTGC**	**CCTTGGGGTCGACGTTCTG**
Cdkn1a	**TTGTCGCTGTCTTGCACTCT**	**TTTCGGCCCTGAGATGTTCC**

Abbreviations*: Gapdh,* Glyceraldehyde 3-phosphate dehydrogenase; *Vdr,* vitamin D receptor; *Foxo1,* forkhead box protein O1; *Foxo3,* forkhead box protein O3; *Mtor,* mechanistic target of rapamycin; *Tsc2,* tuberous sclerosis complex 2; *Akt,* AKT serine/threonine kinase 1; *Cubn,* cubilin; *Myh8,* myosin heavy chain 8; *Myf5,* myogenic factor 5; *Mrf4,* myogenic regulatory factor 4; *Myh1,* myosin heavy chain 1; *Rps6,* ribosomal protein 6; *Hdac9,* histone deacetylase 9; *PPP3ca,* protein phosphatase 3 catalytic subunit alpha; *Myog,* myogenin; *Myod1,* myoblast determination protein 1; *Ccnd1,* Cyclin D1; *Cdkn1a,* cyclin dependent kinase inhibitor 1a.

4.2.7 Western Blotting

At day 6 post-differentiation, cells were homogenised and scraped into ice-cold homogenisation buffer (10 mM β-glycerophosphate disodium salt, 50 mM NaF, 1 mM EGTA, 1 mM EDTA, 1 mM activated Na_3VO_4, and 50 mM Tris·HCl (pH 7.4)) followed by centrifugation of lysates at 11,000 *g* for 10 minutes at 4°C. The supernatant was removed to quantify protein content via Nanodrop. Depending on initial protein concentration, all samples were appropriately diluted in homogenisation buffer and 1x Laemmli buffer to the same concentration.

Samples were loaded onto a Criterion XT Bis-Tris 12% SDS-PAGE gel (BioRad) and ran electrophoretically at 200V for one hour. The resulting separated proteins were then transferred onto a PVDF membrane at 100V for 45 minutes, followed by a one-hour blocking stage using 2.5% milk in 1x Tris buffered saline with 0.1% Tween-20 detergent (1x TBST) with gentle agitation. Membranes were subsequently incubated with their corresponding primary antibody solutions at 4°C overnight after which they were washed for five minutes three times with 1x TBST and incubated at RTP with the HRP-conjugated secondary antibody (anti-rabbit; Cell Signalling Technologies #7074S). After an hour, membranes were washed again three times for five minutes with 1x TBST and subsequently incubated in Millipore HRP reagent (Millipore) for five minutes at RTP. Membrane visualisation was performed with a Chemidoc XRS, and bands were quantified using ImageLab software (Version 6.1). Data was normalised

to total loaded protein as visualised by staining with Coomassie brilliant blue (CBB) R250.

Primary antibodies were all were purchased from Cell Signalling Technologies (unless stated otherwise), diluted 1:2000, and were as follows: Total-ULK1 (T-ULK1; #8054P), Total p70S6K (T-p70S6K; #9202S), Total Akt (T-Akt; #4685S), Total mTOR (T-mTOR; #2972S), phospho-EIF4E (p-EIF4E; #9741S), phospho-AMPKα (p-AMPKα ; #2535S), phospho-4EBP1 (p-4EBP1; #2855S), phospho-Akt (p-Akt; #9271S), phospho-TSC2 (p-TSC2; #3611S), phospho-mTOR (p-mTOR; #2971S), phospho-p70S6K (p-p70S6K; #9234S), phospho-Raptor (p-Raptor; #2083S), and phospho-ULK1 (p-ULK1; #14202S). VDR (ab109234) and DBP (ab65636) were both purchased from Abcam.

4.2.8 Statistical Analysis

For statistical comparisons, the D'Agostino and Pearson test was first performed to assess for normality. Statistical differences between groups were then assessed using a Student T-test (for parametric factors), Mann Whitney U test (for non-parametric factors) for comparing NC and VDR-KD, and a two-way ANOVA with post-hoc Tukey's for multiple comparisons for comparisons between the different experimental conditions for NC and VDR-KD. Results are reported as mean ± standard deviation (SD) and statistical significance was set at $P < 0.05$. All statistical analyses were performed using GraphPad Prism Software (Version 10.0.2; San Diego, California, USA).

4.3 Results

4.3.1 Successful generation of VDR-KD C2C12 myotubes.

To silence *Vdr* signalling, gene knockdown was performed via RNAi in C2C12 myoblasts at day 2 post-induction of differentiation. Following siRNA transfection, *Vdr* mRNA expression was significantly reduced by 43.35% (*P* = 0.0199; **(A)** of **Figure 4.1**), whilst protein levels were also significantly reduced compared to the negative control (NC) by 75.95% (*P* = <0.0001; **(B)** of **Figure 4.1**).

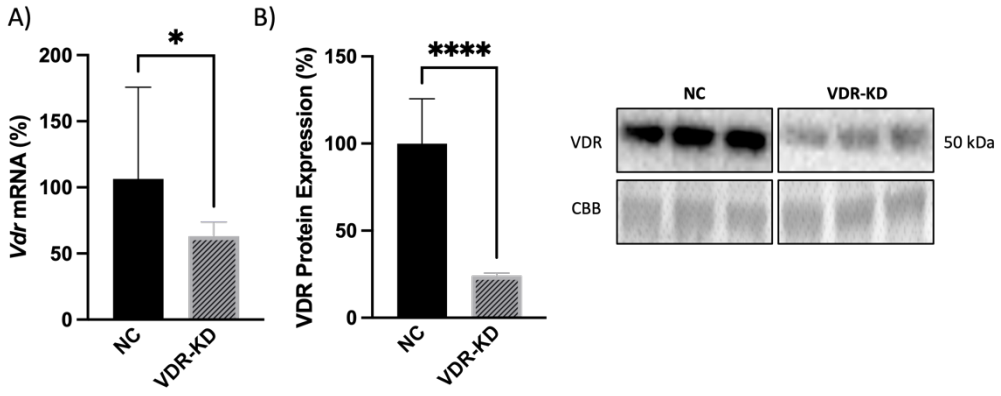


Figure 4.1. Successful generation of VDR-KD C2C12 myotubes. (A) *Vdr* mRNA expression, (B) Representative western blot and quantification of KD (n = 6). Data is shown as mean ± SD. * *P* < 0.05, **** *P* <0.0001. Abbreviations: *Vdr,* vitamin D receptor; *mRNA,* messenger ribonucleic acid; *%,* percent; *KD,* knockdown; *NC,* negative control; *CBB,* coomassie brilliant blue; *kDa,* kilodalton.

4.3.2 VDR knockdown in C2C12 myotubes results in altered mRNA and protein expression of key metabolic targets.

To characterise the effects of VDR-KD alone in C2C12 myotubes, expression levels of key metabolic genes and proteins were quantified via qRT-PCR and

western blotting, respectively. Values are compared to that of the negative control (NC) myotubes (**Figures 4.2 and 4.3**, respectively)**.**

At mRNA level, significant reductions in expression of genes encoding the key anabolic targets were observed, *Mtor* (*P* = 0.0176)*, Rps6* (*P* = 0.0085), and *Tsc2* (*P* = 0.0091) in VDR-KD myotubes (**Figure 4.2**). When quantified at protein level, levels of key anabolic targets were all significantly lower in VDR-KD myotubes compared to the NC; p-mTOR (*P* = <0.0001), T-mTOR (*P* = 0.0012), p-Akt (*P* = 0.0017), T-Akt (*P* = 0.0444), p-TSC2 (*P* = 0.0023), and p-p70S6K (*P* = <0.0001) (**Figure 4.3**). mRNA levels of several key catabolic targets were also significantly downregulated in VDR-KD myotubes compared to the NC including *Foxo1* (*P* = 0.0381) and *Foxo3* (*P* = 0.0043)*,* as was the epigenetic factor *Hdac9* (*P* = <0.0001; **Figure 4.2**). In addition, genes encoding the myogenic regulatory factors (MRFs), *Mrf4* (*P* = 0.0177)*, Myog* (*P* = <0.0001) and *Myod1* (*P* = <0.0001)*,* and the metabolic related targets, *Ppp3ca* (*P* = 0.0006)*, Myh8* (*P* = 0.0197)*, Myh1* (*P* = 0.0022)*,* and *Cdkn1a* (*P* = 0.00177) were all significantly reduced in VDR-KD myotubes compared to the NC (**Figure 4.2**).

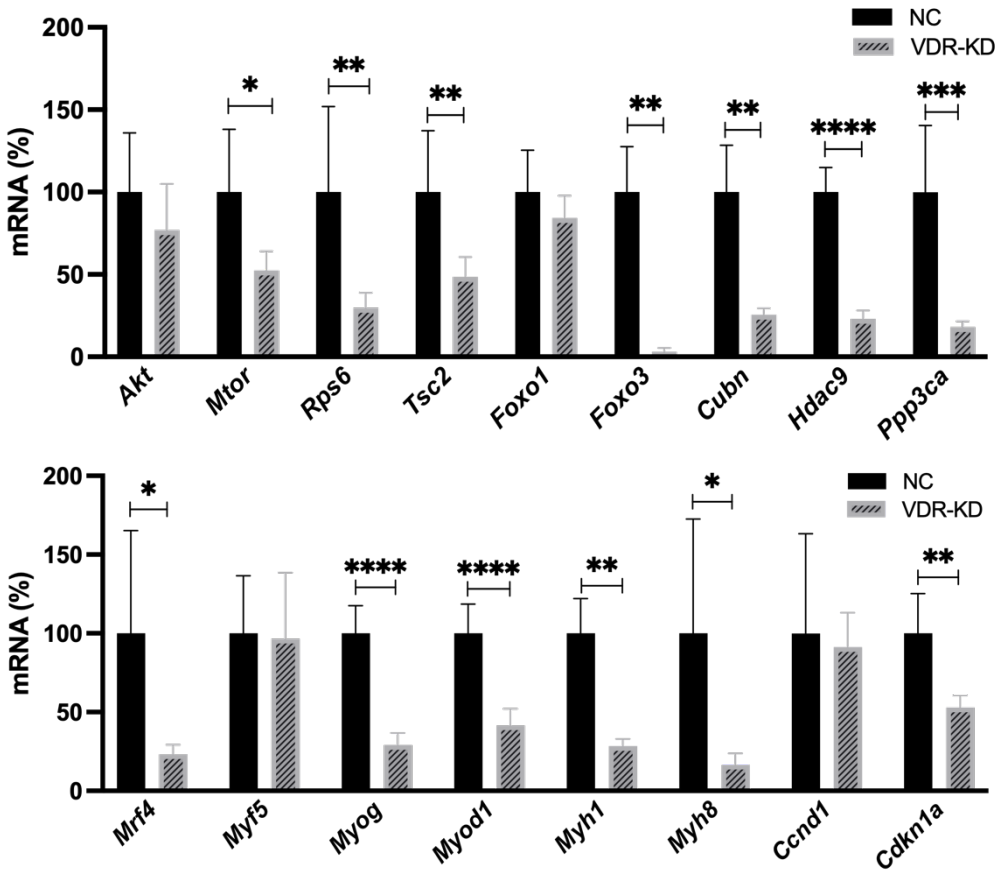


Figure 4.2. Effect of VDR-KD upon mRNA expression of key metabolic and myogenic targets as measured by qRT-PCR. Data is shown as mean ± SD (n = 6). * $P < 0.05$, ** $P < 0.01$, *** $P < 0.001$, **** $P < 0.0001$. Abbreviations: *mRNA,* messenger ribonucleic acid; *%,* percent; *NC,* negative control; *VDR,* vitamin D receptor; *KD,* knockdown; *Foxo1,* forkhead box protein O1; *Foxo3,* forkhead box protein O3; *Mtor,* mechanistic target of rapamycin; *Tsc2,* tuberous sclerosis complex 2; *Akt,* AKT serine/threonine kinase 1; *Cubn,* cubilin; *Myh8,* myosin heavy chain 8; *Myf5,* myogenic factor 5; *Mrf4,* myogenic regulatory factor 4; *Myh1,* myosin heavy chain 1; *Rps6,* ribosomal protein 6; *Hdac9,* histone deacetylase 9; *PPP3ca,* protein phosphatase 3 catalytic subunit alpha; *Myog,* myogenin; *Myod1,* myoblast determination protein 1; *Ccnd1,* Cyclin D1; *Cdkn1a,* cyclin dependent kinase inhibitor 1a.

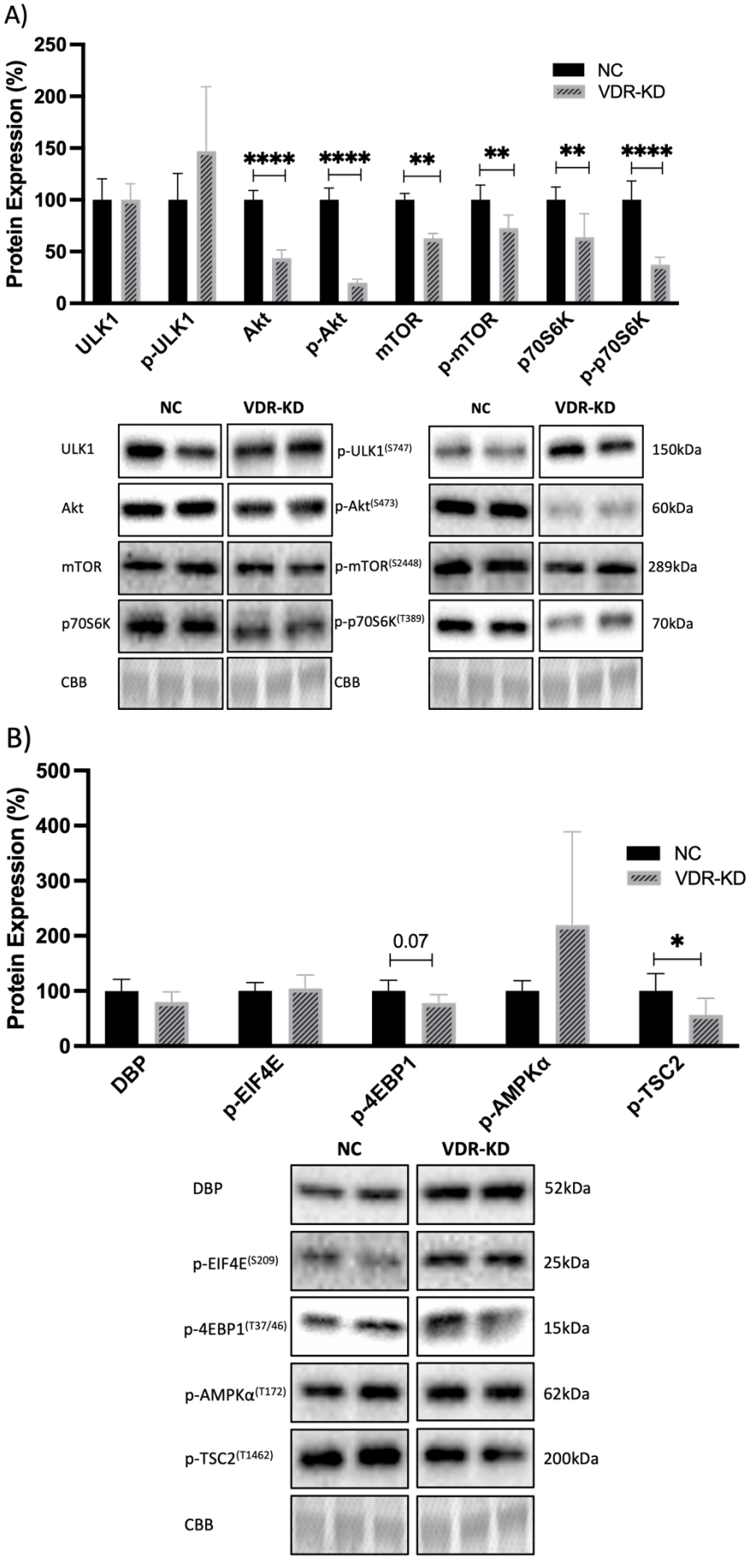

A)
Protein Expression (%)
250
200
150
100
50
0
NC
VDR-KD
****
****
**
**
**
****
ULK1
p-ULK1
Akt
p-Akt
mTOR
p-mTOR
p70S6K
p-p70S6K
NC
VDR-KD
NC
VDR-KD
ULK1
Akt
mTOR
p70S6K
CBB
p-ULK1(S747)
p-Akt(S473)
p-mTOR(S2448)
p-p70S6K(T389)
CBB
150kDa
60kDa
289kDa
70kDa
B)
Protein Expression (%)
500
400
300
200
100
0
NC
VDR-KD
0.07
*
DBP
p-EIF4E
p-4EBP1
p-AMPKα
p-TSC2
NC
VDR-KD
DBP
p-EIF4E(S209)
p-4EBP1(T37/46)
p-AMPKα(T172)
p-TSC2(T1462)
CBB
52kDa
25kDa
15kDa
62kDa
200kDa

Figure 4.3. Effect of VDR-KD upon protein expression of (A) non-phosphorylated and phosphorylated forms of key anabolic and catabolic targets, and (B) key metabolic targets as measured by western blotting. Representative blots are displayed here, and data is shown as mean ± SD (n = 6). * $P < 0.05$, ** $P < 0.01$, *** $P < 0.001$, **** $P < 0.0001$. Abbreviations: *NC,* negative control; *VDR,* vitamin D receptor; *KD,* knockdown; *%,* percent; *p-,* phosphorylated-; *ULK1,* uncoordinated 51-like kinase 1; *Akt,* AKT serine/threonine kinase 1; *mTOR,* mechanistic target of rapamycin; *p70S6K*, p70kDa S6 kinase; *DBP,* vitamin D binding protein; *EIF4E,* eukaryotic translation initiation factor 4E; *4EBP1*, eIF4E-binding protein 1; *AMPKα,* adenosine monophosphate-activated protein kinase catalytic subunit alpha; *TSC2*, tuberous sclerosis complex 2; *CBB*, coomassie brilliant blue; *kDa*, kilodalton.

4.3.3 Changes in gene expression & protein content of key metabolic targets in VDR-KD myotubes following exposure to hypertrophic, atrophic, and pro-inflammatory conditions.

*4.3.*3.1 *Altered Vdr levels following 24-hour stimulation of NC myotubes.*

Vdr mRNA levels were significantly higher in NC myotubes following exposure to IGF-1 (*P* = 0.0145) and Dex (*P* = 0.0022) for 24 hours, whilst, comparatively, 24-hour LPS treatment resulted in significantly lower *Vdr* levels (*P* = 0.0022; **Figure 4.4**).

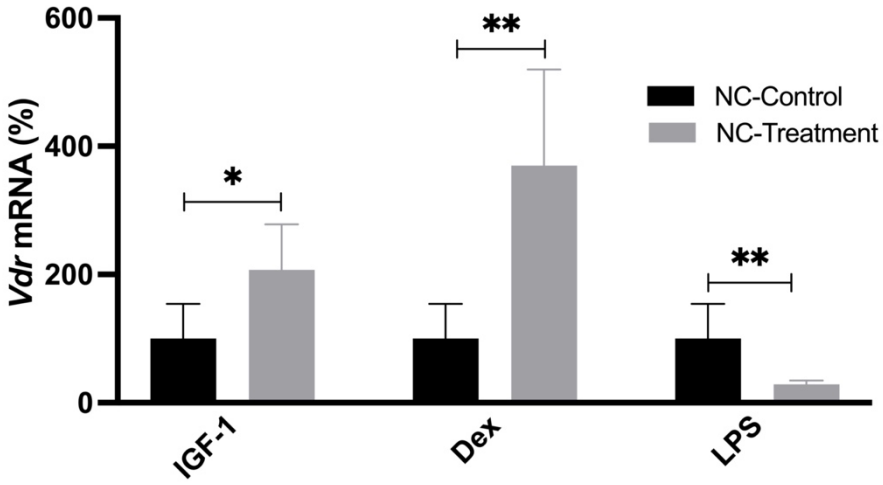


Figure 4.4. Effect of 24-hour exposure to IGF-1, dexamethasone (Dex) and lipopolysaccharides (LPS) upon mRNA expression of *Vdr* in NC myotubes, as measured by qRT-PCR. Data is shown as mean ± SD (n = 6). * *P* < 0.05, ** *P* < 0.01. Abbreviations: *Vdr,* vitamin D receptor; *mRNA,* messenger ribonucleic acid; %, percent; *NC,* negative control; *IGF-1,* insulin-like growth factor 1; *Dex,* dexamethasone; *LPS,* lipopolysaccharides.

*4.3.*3.2 *Hypertrophy – IGF-1*

To induce hypertrophy *in vitro*, VDR-KD and NC myotubes were both exposed to 20 ng/mL IGF-1 for 24 hours. As expected, treatment of NC myotubes with IGF-1 significantly increased gene expression of *Akt* (*P* = 0.0476) and *mTOR* (*P*

= 0.0297) compared to the untreated NC (**Figure 4.5**). This was reinforced further as protein levels of p-Akt (*P* = 0.0163), p-mTOR (*P* = <0.0001), and p-p70S6K (*P* = 0.0164) were significantly higher than the untreated NC in IGF-1 treated myotubes (**Figure 4.6**). Protein levels of T-ULK1 were also significantly reduced by IGF-1 (P = 0.0001). In NC myotubes, IGF-1 treatment also significantly increased gene expression of *Myh1* (*P* = 0.0002; **Figure 4.5**) and pTSC2 protein levels (*P* = 0.0383) (**Figure 4.6**).

Intriguingly, treatment of VDR-KD myotubes with IGF-1 resulted in significantly higher mRNA expression of *Myf5* (*P* = 0.0128; **Figure 4.5**) and T-ULK1 protein levels were significantly lower compared to the VDR-KD untreated control (*P* = 0.0002; **Figure 4.6**).

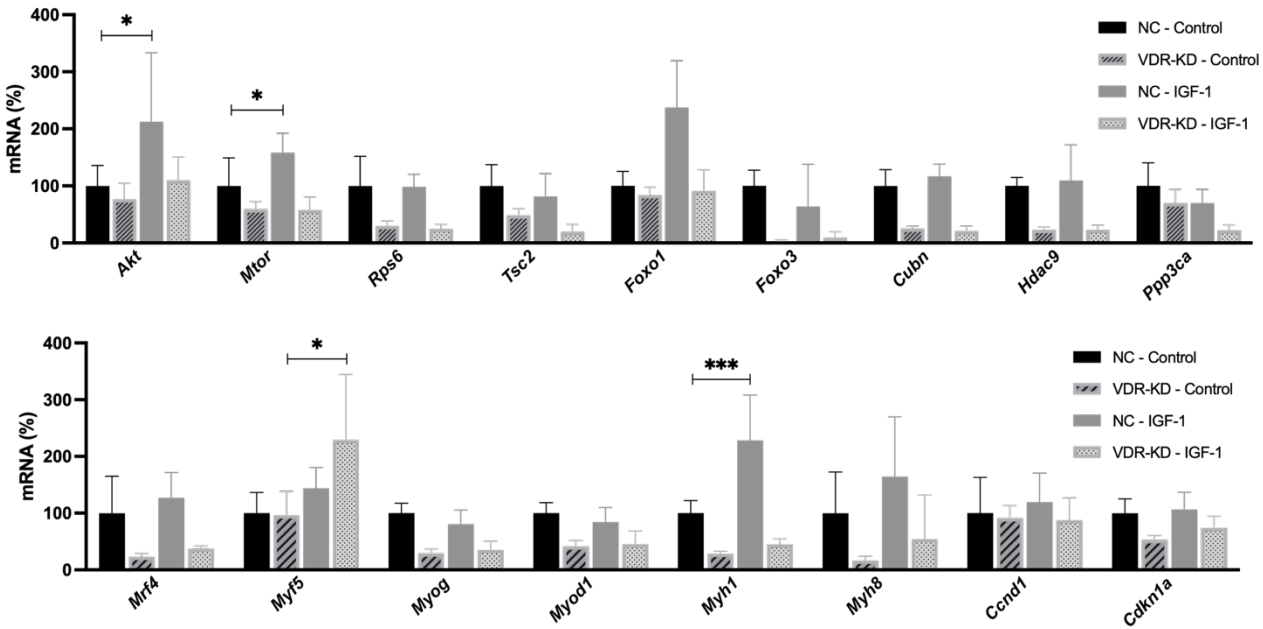
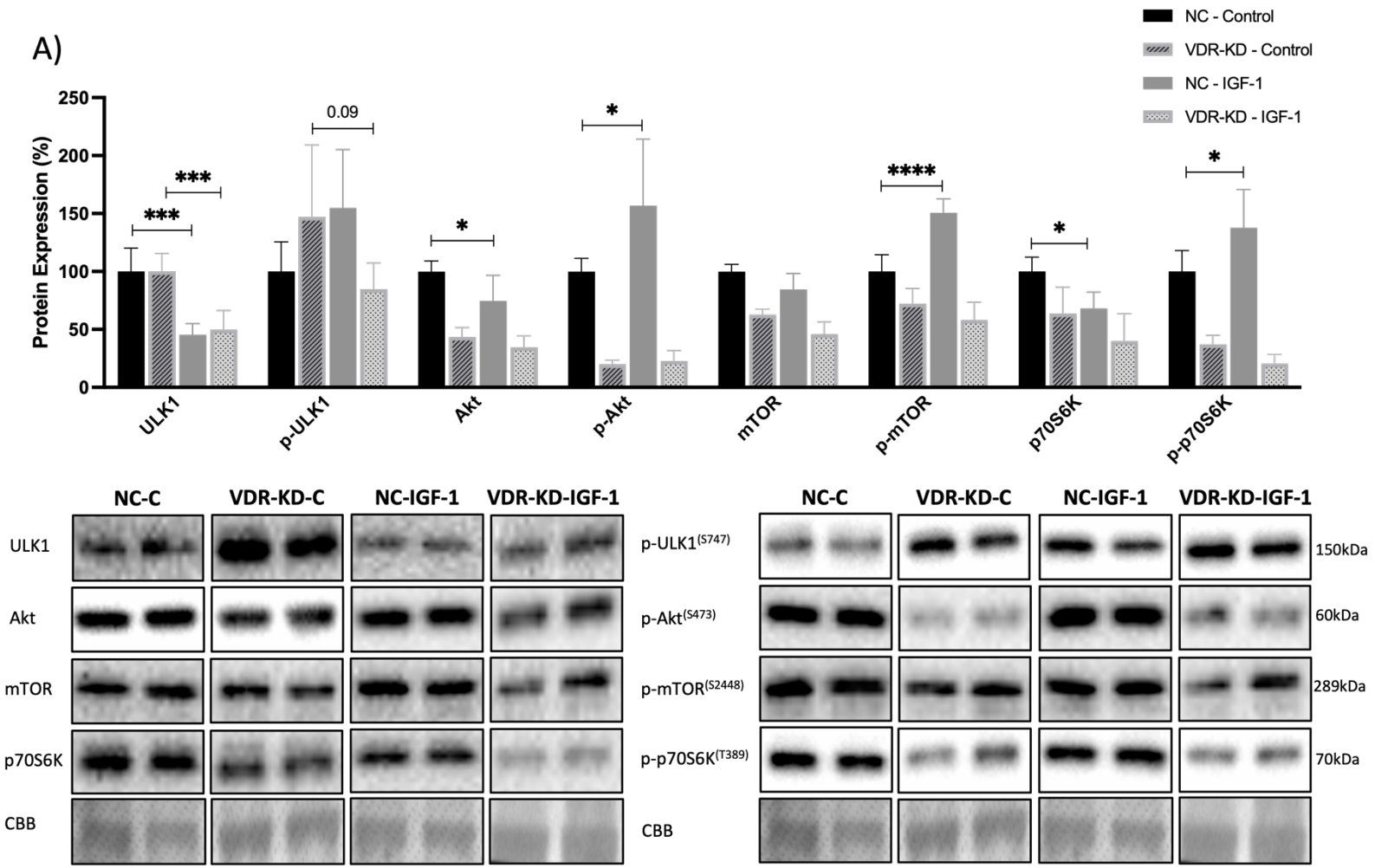


Figure 4.5. Effect of 24-hour IGF-1 treatment upon mRNA expression of key metabolic and myogenic targets in NC and VDR-KD C2C12 myotubes, as measured by qRT-PCR. Data is shown as mean ± SD (n = 6). * $P < 0.05$, ** $P < 0.01$, *** $P < 0.001$, **** $P < 0.0001$. Abbreviations: *mRNA,* messenger ribonucleic acid; *%,* percent; *NC,* negative control; *VDR,* vitamin D receptor; *KD,* knockdown; *Foxo1,* forkhead box protein O1; *Foxo3,* forkhead box protein O3; *Mtor,* mechanistic target of rapamycin; *Tsc2,* tuberous sclerosis complex 2; *Akt,* AKT serine/threonine kinase 1; *Cubn,* cubilin; *Myh8,* myosin heavy chain 8; *Myf5,* myogenic factor 5; *Mrf4,* myogenic regulatory factor 4; *Myh1,* myosin heavy chain 1; *Rps6,* ribosomal protein 6; *Hdac9,* histone deacetylase 9; *PPP3ca,* protein phosphatase 3 catalytic subunit alpha; *Myog,* myogenin; *Myod1,* myoblast determination protein 1; *Ccnd1,* Cyclin D1; *Cdkn1a,* cyclin dependent kinase inhibitor 1a; *IGF-1,* insulin-like growth factor 1.


A)
NC - Control
VDR-KD - Control
NC - IGF-1
VDR-KD - IGF-1
Protein Expression (%)
250
200
150
100
50
0
0.09
***
***
*
*
*
****
*
*
ULK1
p-ULK1
Akt
p-Akt
mTOR
p-mTOR
p70S6K
p-p70S6K
NC-C
VDR-KD-C
NC-IGF-1
VDR-KD-IGF-1
ULK1
Akt
mTOR
p70S6K
CBB
p-ULK1(S747)
p-Akt(S473)
p-mTOR(S2448)
p-p70S6K(T389)
CBB
150kDa
60kDa
289kDa
70kDa

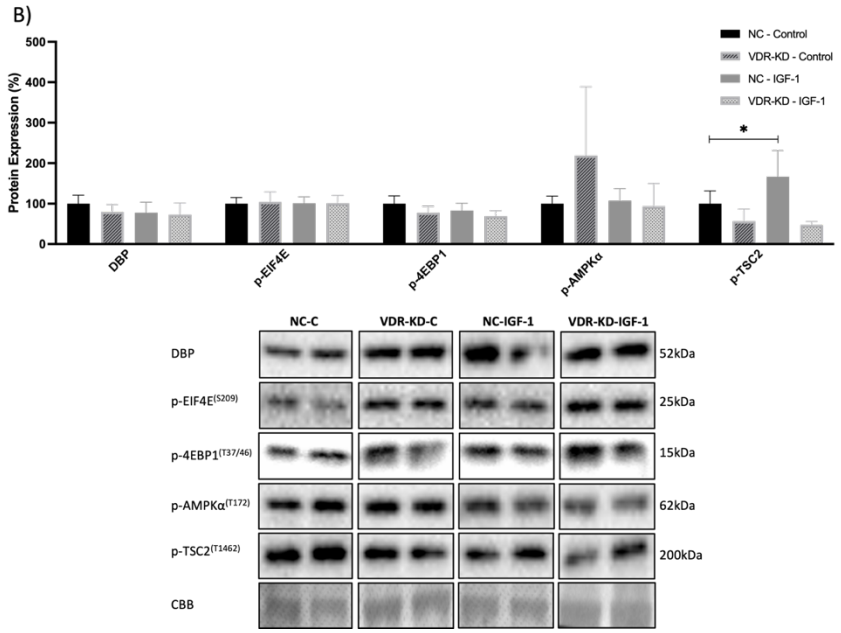


Figure 4.6. Effect of 24-hour IGF-1 treatment upon protein expression of (A) non-phosphorylated and phosphorylated forms of key anabolic and catabolic targets, and (B) key metabolic targets in NC and VDR-KD C2C12 myotubes, as measured by western blotting. Representative blots are displayed here, and data is shown as mean ± SD (n = 6). * $P < 0.05$, ** $P < 0.01$, *** $P < 0.001$, **** $P < 0.0001$. Abbreviations: *NC,* negative control; *VDR,* vitamin D receptor; *KD,* knockdown; *%,* percent; *p-,* phosphorylated-; *ULK1,* uncoordinated 51-like kinase 1; *Akt,* AKT serine/threonine kinase 1; *mTOR,* mechanistic target of rapamycin; *p70S6K*, p70kDa S6 kinase; *DBP,* vitamin D binding protein; *EIF4E,* eukaryotic translation initiation factor 4E; *4EBP1*, eIF4E-binding protein 1; *AMPKα,* adenosine monophosphate-activated protein kinase catalytic subunit alpha; *TSC2*, tuberous sclerosis complex 2; *CBB*, coomassie brilliant blue; *kDa*, kilodalton; *IGF-1,* insulin-like growth factor 1.

4.3.3.3 *Atrophy - Dexamethasone*

Both NC and VDR-KD myotubes were both treated with 1 µM Dex for 24 hours to induce a model of atrophy. Dex treatment had significant impact on gene expression of several key myogenic and metabolic targets. In NC myotubes, Dex significantly lowered mRNA expression of the MRFs, *Myog* (*P* = 0.0006) and *Myod1* (*P* = 0.0002), and a component of the 40S ribosomal subunit, *Rps6* (*P* = 0.0017; **Figure 4.7**). In addition, mRNA expression of the cell cycle regulator, *Cdkn1a,* was significantly lower in Dex treated NC myotubes (*P* = 0.0089), as was mRNA expression of multiple metabolic targets with Dex treatment, i.e., *Hdac9 (P* = <0.0001), *Foxo3 (P* = 0.0005), and *Ppp3ca* (*P* = 0.0130). At protein level, differences were only seen in T-mTOR and p-Akt, as both were reduced in Dex treated NC myotubes (*P* = 0.0143 & <0.0001, respectively; **Figure 4.8**).

In Dex treated VDR-KD myotubes, gene expression of *Myf5* and *Tsc2* were significantly increased (*P* = 0.0012 and 0.0423, respectively; **Figure 4.7**), yet no significant changes were observed in any of the studied targets at protein level.

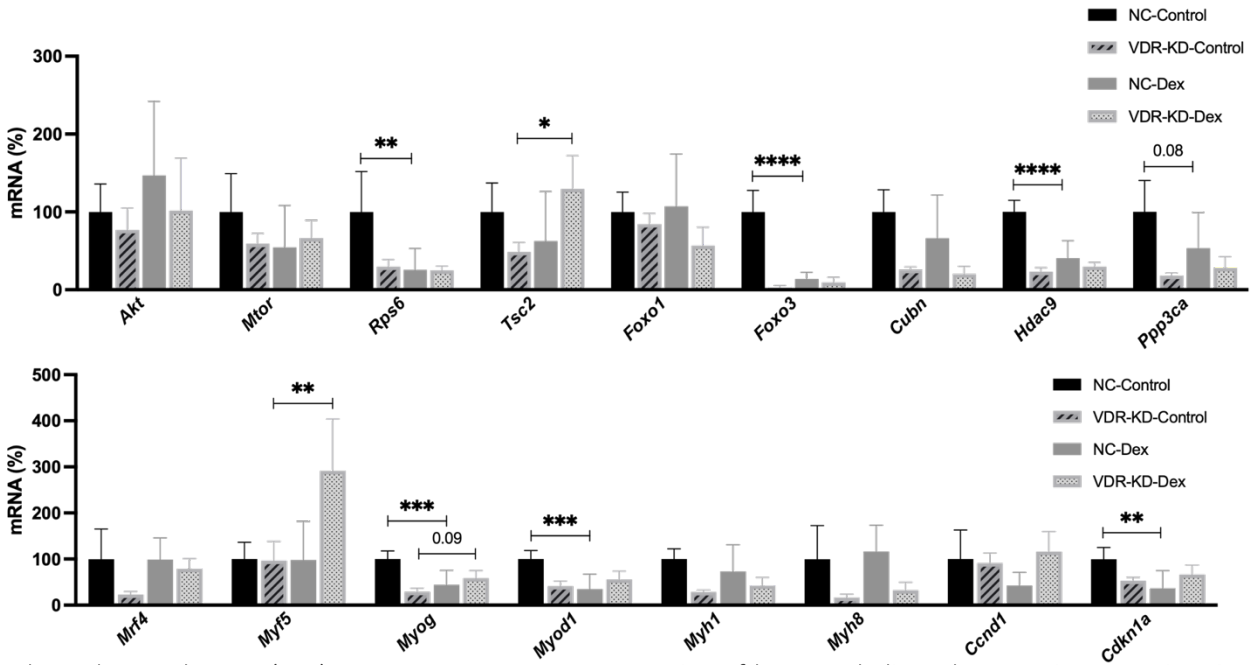
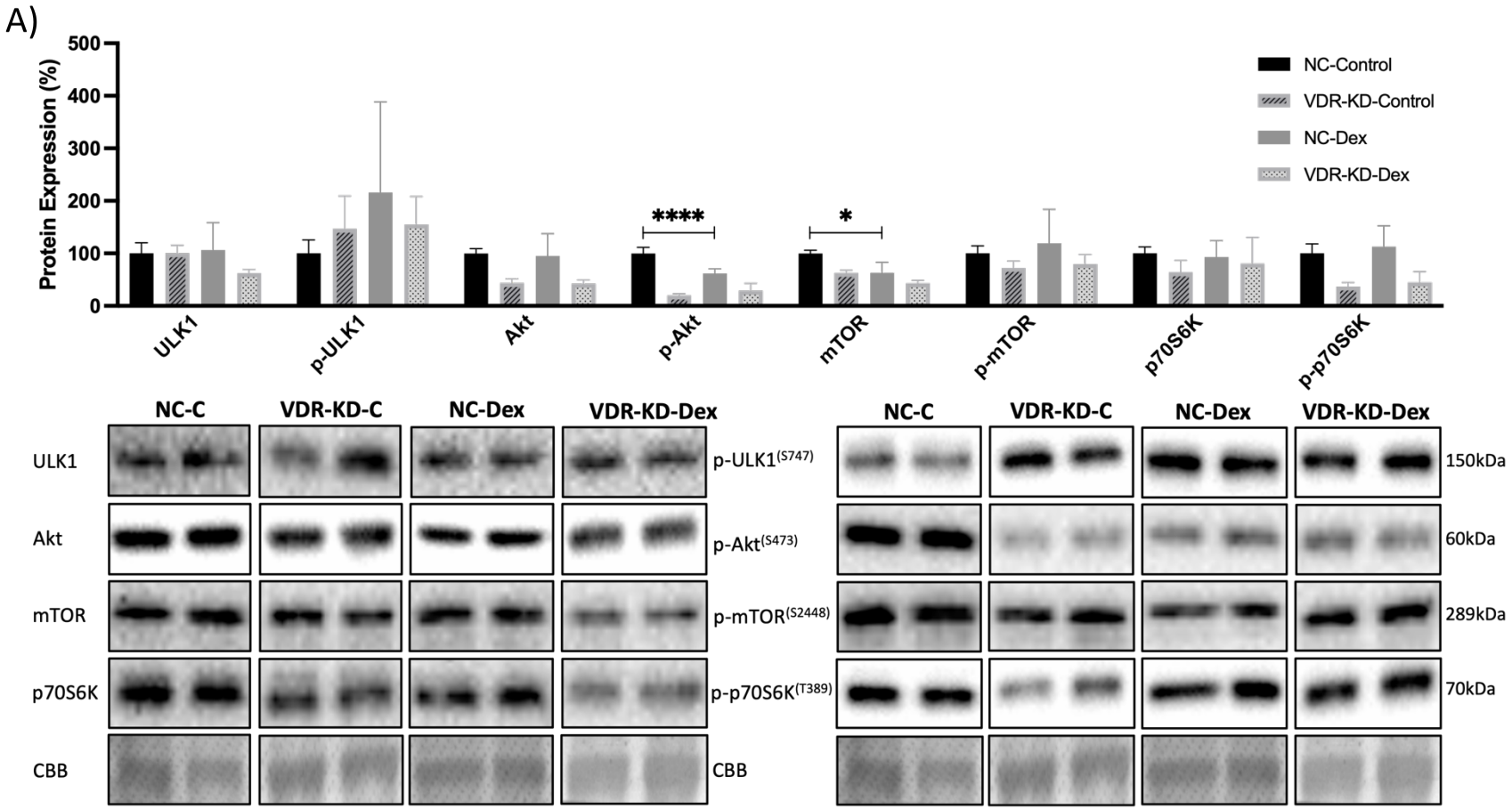


Figure 4.7. Effect of 24-hour dexamethasone (Dex) treatment upon mRNA expression of key metabolic and myogenic targets in NC and VDR-KD C2C12 myotubes, as measured by qRT-PCR. Data is shown as mean ± SD (n = 6). * $P < 0.05$, ** $P < 0.01$, *** $P < 0.001$, **** $P < 0.0001$. Abbreviations: *mRNA,* messenger ribonucleic acid; *%,* percent; *NC,* negative control; *VDR,* vitamin D receptor; *KD,* knockdown; *Foxo1,* forkhead box protein O1; *Foxo3,* forkhead box protein O3; *Mtor,* mechanistic target of rapamycin; *Tsc2,* tuberous sclerosis complex 2; *Akt,* AKT serine/threonine kinase 1; *Cubn,* cubilin; *Myh8,* myosin heavy chain 8; *Myf5,* myogenic factor 5; *Mrf4,* myogenic regulatory factor 4; *Myh1,* myosin heavy chain 1; *Rps6,* ribosomal protein 6; *Hdac9,* histone deacetylase 9; *PPP3ca,* protein phosphatase 3 catalytic subunit alpha; *Myog,* myogenin; *Myod1,* myoblast determination protein 1; *Ccnd1,* Cyclin D1; *Cdkn1a,* cyclin dependent kinase inhibitor 1a; *Dex,* dexamethasone.


A)
Protein Expression (%)
500
400
300
200
100
0
NC-Control
VDR-KD-Control
NC-Dex
VDR-KD-Dex
****
*
ULK1
p-ULK1
Akt
p-Akt
mTOR
p-mTOR
p70S6K
p-p70S6K
NC-C
VDR-KD-C
NC-Dex
VDR-KD-Dex
ULK1
Akt
mTOR
p70S6K
CBB
p-ULK1(S747)
p-Akt(S473)
p-mTOR(S2448)
p-p70S6K(T389)
CBB
NC-C
VDR-KD-C
NC-Dex
VDR-KD-Dex
150kDa
60kDa
289kDa
70kDa

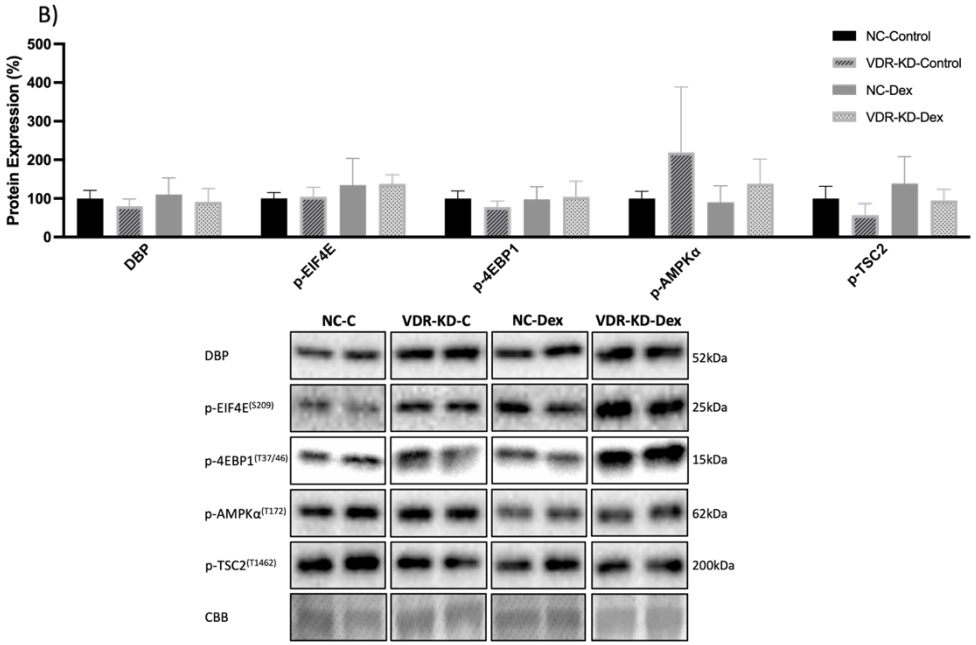


Figure 4.8. Effect of 24-hour dexamethasone (Dex) treatment upon protein expression of (A) non-phosphorylated and phosphorylated forms of key anabolic and catabolic targets, and (B) key metabolic targets in NC and VDR-KD C2C12 myotubes, as measured by western blotting. Representative blots are displayed here, and data is shown as mean ± SD (n = 6). * $P < 0.05$, ** $P < 0.01$, *** $P < 0.001$, **** $P < 0.0001$. Abbreviations: *NC,* negative control; *VDR,* vitamin D receptor; *KD,* knockdown; *%,* percent; *p-,* phosphorylated-; *ULK1,* uncoordinated 51-like kinase 1; *Akt,* AKT serine/threonine kinase 1; *mTOR,* mechanistic target of rapamycin; *p70S6K*, p70kDa S6 kinase; *DBP,* vitamin D binding protein; *EIF4E,* eukaryotic translation initiation factor 4E; *4EBP1*, eIF4E-binding protein 1; *AMPKα,* adenosine monophosphate-activated protein kinase catalytic subunit alpha; *TSC2*, tuberous sclerosis complex 2; *CBB*, coomassie brilliant blue; *kDa*, kilodalton; *Dex,* dexamethasone

4.3.3.4 *Inflammation - LPS*

To generate a model of inflammation, NC and VDR-KD myotubes were both incubated with 0.1 μg/mL LPS for 24 hours. 24-hour treatment of NC myotubes with LPS was accompanied with significantly greater gene expression of *Cdkn1a* (*P* = 0.0115) and significantly lower expression of *Foxo3* (*P* = <0.0001), *Mrf4* (*P* = 0.0005), *Hdac9* (*P* = <0.0001), *Ppp3ca* (*P* = 0.0417), *Rps6* (*P* = 0.0013), *Myh8* (*P* = 0.0025), and *Myh1* (*P* = 0.0311) compared to the untreated NC (**Figure 4.9**). In comparison to the untreated NC, LPS treatment significantly reduced protein levels of DBP (*P* = 0.0173), T-Akt (*P* = <0.0001), p-Akt (*P* = <0.0001), T-ULK1 (*P* = 0.0054), p-p70S6K (*P* = 0.0487), and T-mTOR (*P* = <0.0001; **Figure 4.10**).

Comparatively, 24-hour treatment of VDR-KD myotubes with LPS failed to induce any differences of significance at mRNA level but it was associated with significantly lower protein levels of T-ULK1 compared to the VDR-KD untreated control (*P* = 0.0001; **Figure 4.10**).

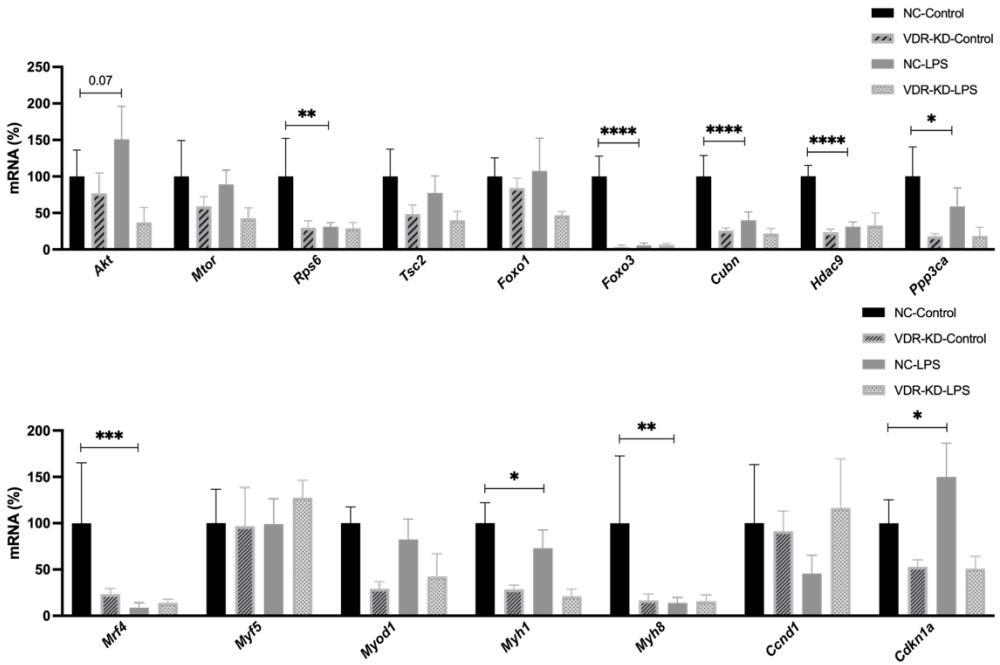
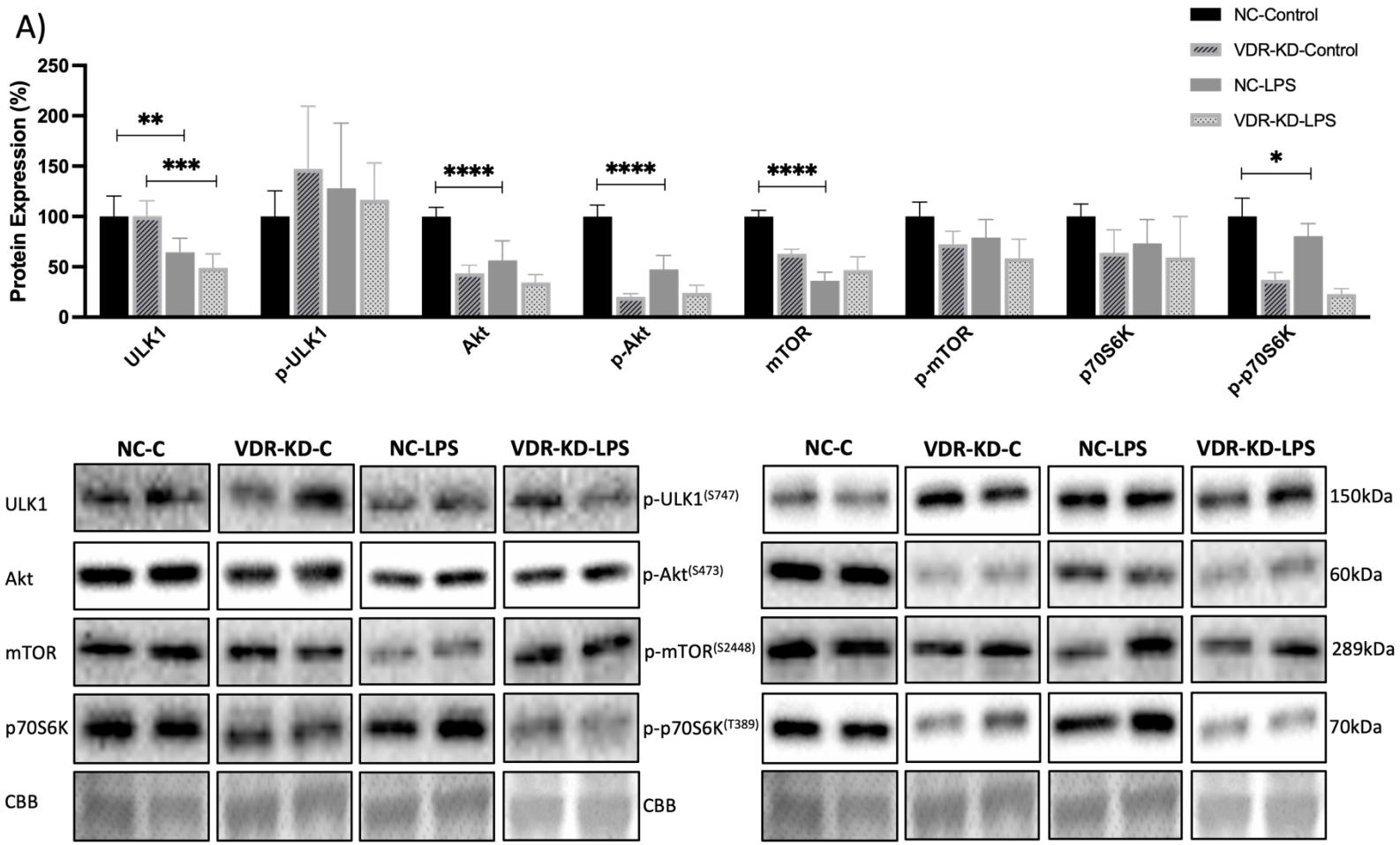


Figure 4.9. Effect of 24-hour lipopolysaccharide (LPS) treatment upon mRNA expression of key metabolic and myogenic targets in NC and VDR-KD C2C12 myotubes, as measured by qRT-PCR. Data is shown as mean ± SD (n = 6). * $P < 0.05$, ** $P < 0.01$, *** $P < 0.001$, **** $P < 0.0001$. Abbreviations: *mRNA,* messenger ribonucleic acid; *%,* percent; *NC,* negative control; *VDR,* vitamin D receptor; *KD,* knockdown; *Foxo1,* forkhead box protein O1; *Foxo3,* forkhead box protein O3; *Mtor,* mechanistic target of rapamycin; *Tsc2,* tuberous sclerosis complex 2; *Akt,* AKT serine/threonine kinase 1; *Cubn,* cubilin; *Myh8,* myosin heavy chain 8; *Myf5,* myogenic factor 5; *Mrf4,* myogenic regulatory factor 4; *Myh1,* myosin heavy chain 1; *Rps6,* ribosomal protein 6; *Hdac9,* histone deacetylase 9; *PPP3ca,* protein phosphatase 3 catalytic subunit alpha; *Myog,* myogenin; *Myod1,* myoblast determination protein 1; *Ccnd1,* Cyclin D1; *Cdkn1a,* cyclin dependent kinase inhibitor 1a; *LPS,* lipopolysaccharide.


A)
NC-Control
VDR-KD-Control
NC-LPS
VDR-KD-LPS
Protein Expression (%)
250
200
150
100
50
0
**
***
****
****
****
*
ULK1
p-ULK1
Akt
p-Akt
mTOR
p-mTOR
p70S6K
p-p70S6K
NC-C
VDR-KD-C
NC-LPS
VDR-KD-LPS
ULK1
Akt
mTOR
p70S6K
CBB
p-ULK1(S747)
p-Akt(S473)
p-mTOR(S2448)
p-p70S6K(T389)
CBB
150kDa
60kDa
289kDa
70kDa

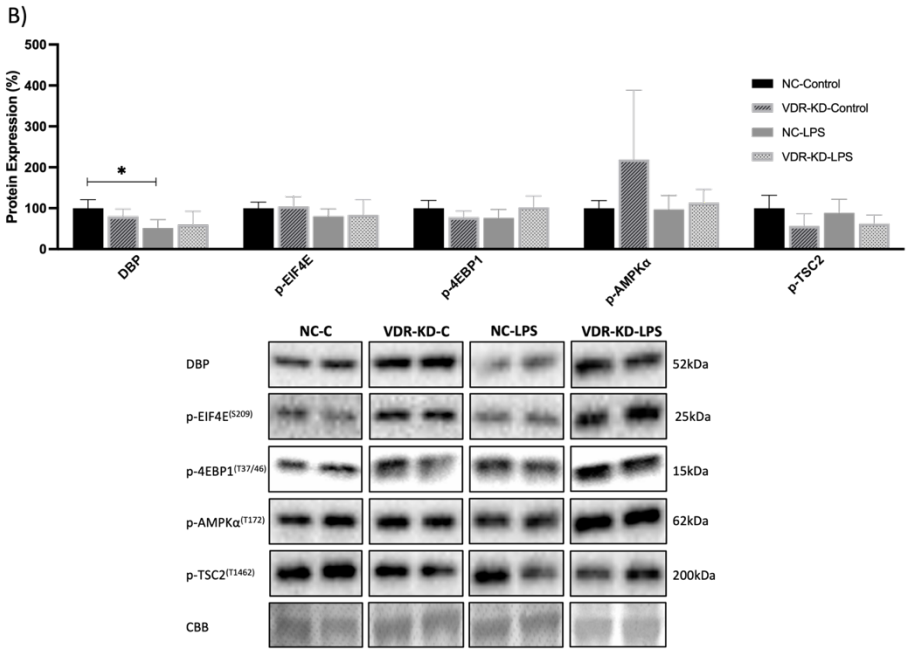


Figure 4.10. Effect of 24-hour lipopolysaccharide (LPS) treatment upon protein expression of (A) non-phosphorylated and phosphorylated forms of key anabolic and catabolic targets, and (B) key metabolic targets in NC and VDR-KD C2C12 myotubes, as measured by western blotting. Representative blots are displayed here, and data is shown as mean ± SD (n = 6). * $P < 0.05$, ** $P < 0.01$, *** $P < 0.001$, **** $P < 0.0001$. Abbreviations: *NC,* negative control; *VDR,* vitamin D receptor; *KD,* knockdown; *%,* percent; *p-,* phosphorylated-; *ULK1,* uncoordinated 51-like kinase 1; *Akt,* AKT serine/threonine kinase 1; *mTOR,* mechanistic target of rapamycin; *p70S6K*, p70kDa S6 kinase; *DBP,* vitamin D binding protein; *EIF4E,* eukaryotic translation initiation factor 4E; *4EBP1*, eIF4E-binding protein 1; *AMPKα,* adenosine monophosphate-activated protein kinase catalytic subunit alpha; *TSC2*, tuberous sclerosis complex 2; *CBB*, coomassie brilliant blue; *kDa*, kilodalton; *LPS,* lipopolysaccharide.

4.3.4 Changes in mitochondrial respiration following VDR knockdown in C2C12 myotubes.

To further evaluate the effects of VDR-KD, mitochondrial respiration was assessed in digitonin permealised NC and VDR-KD myotubes via high-resolution respirometry. A representative trace can be seen in **Figure 4.11**. Across all experiments, addition of cytochrome C did not significantly alter rate of respiration thus indicating that the outer mitochondrial membrane remained intact following permealisation.

No significant differences were found in either the routine or leak state between the NC and VDR-KD (**Figure 4.12**). Reduction of VDR expression resulted in significant reductions in the maximal oxidative phosphorylation (OXPHOS) capacity of complex I as demonstrated by reduced ADP-induced oxygen (O_2) consumption in the presence of pyruvate and malate (PM; P = <0.0001) and glutamate (PMG; P = <0.0001; **Figure 4.12**). Combined OXPHOS of complexes I and II (PMGS), maximal respiratory capacity (ET), and OXPHOS of complex II only (CII) were all significantly reduced by VDR-KD (all P = <0.0001; **Figure 4.12**).

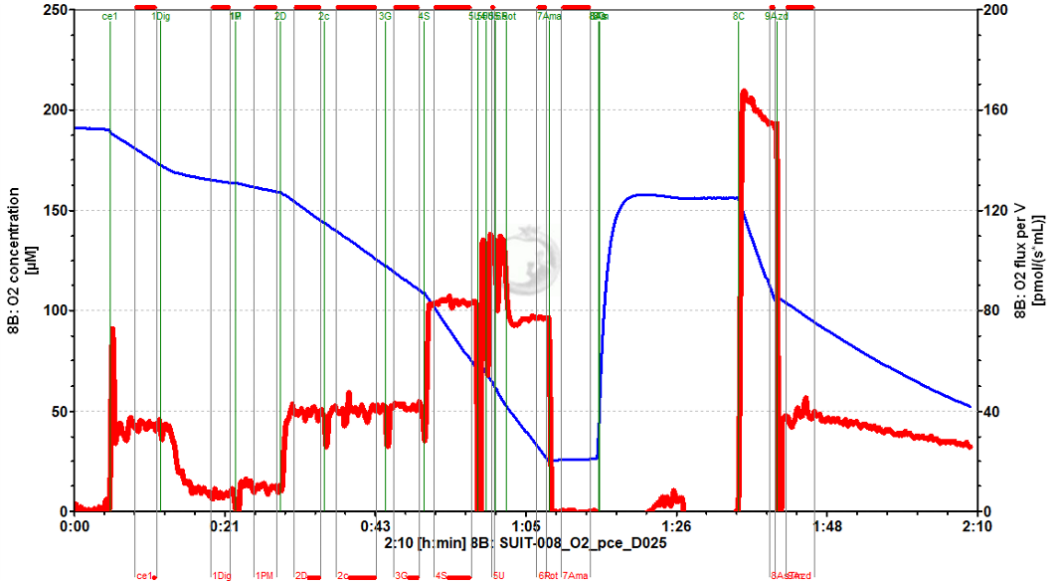


Figure 4.11. Representative high resolution respirometry trace for quantification of cellular respiration in permealised C2C12 myotubes. Taken directly from MitoPedia – BioBlast.com [508].The red line represents the oxygen flux (oxygen being consumed by the cells) and the blue line represents the oxygen concentrations within the oxygraph chamber. In brief, cells were added to the chamber (ce1) followed by 10µg/mL digitonin to permealise cellular membranes (1Dig). 5mM pyruvate and 2mM malate (1PM) were added to generate NADH for Complex I (CI), thus representing the leakage respiration. 2.5mM ADP (2D) was subsequently added to quantify OXPHOS capacity of CI, followed by 10µM cytochrome C (2C) to assess integrity of the outer mitochondrial membrane. 10mM glutamate (3G) was provided as a substrate for CI and addition of 10mM succinate (4S) acted to quantify OXPHOS capacity of Complex II (CII). OXPHOS was uncoupled by titrating 0.5µM carbonyl cyanide p-trifluoromethoxyphenylhydrazone (FCCP; 5U). Finally, CI was inhibited by addition of 0.5µM rotenone (6Rot) followed by 2.5µM antimycin A (7Ama) to induce residual oxygen consumption.

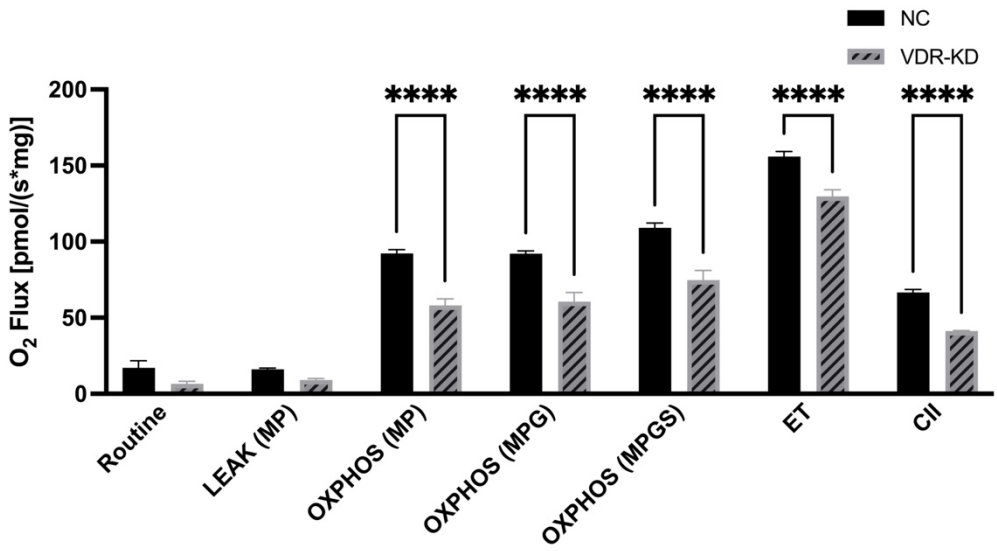


Figure 4.12. Examination of cellular respiration in VDR-KD and NC C2C12 myotubes. Routine state represents oxygen (O_2) consumption rate (OCR) at baseline, before digitonin permealisation. Malate (M) and pyruvate (P) were added together to induce proton leakage (LEAK); addition of ADP stimulates maximal oxidative phosphorylation (OXPHOS). OCR in the presence of N-linked substrates, i.e. M, P, and glutamate (G), represents OXPHOS capacity of Complex I (CI). Succinate (S) addition demonstrates the combined OXPHOS capacity of CI and CII together. Titrated addition of carbonyl cyanide p-trifluoromethoxyphenylhydrazone (FCCP) uncouples OXPHOS and induces maximal respiratory capacity (ET). Addition of rotenone inhibits Complex I, thus demonstrating activity of CII without influence from CI respiration and permitting evaluation of non-mitochondrial respiration. Data expressed as specific flux (oxygen consumption normalised to protein content of sample and after subtraction for non-mitochondrial respiration) and is shown as mean ± SD (n = 4). **** *P* <0.0001.

4.3.5 Changes in mitochondrial respiration in VDR-KD myotubes following exposure to hypertrophic, atrophic, and inflammatory conditions.

To evaluate the impact of VDR knockdown upon mitochondrial function in states of atrophy/hypertrophy, mitochondrial respiration was also measured

in permealised C2C12 myotubes following 24-hour treatments with the different conditions.

4.3.5.1 Hypertrophy – IGF-1

No significant differences were seen in any of the specific flux states in IGF-1-treated NC myotubes compared to untreated (**Figure 4.13**).

Comparatively, IGF-1 treatment of VDR-KD myotubes resulted in significant changes to multiple flux states. Whilst there were no differences in the routine or leak states, IGF1-treatment lead to heightened OXPHOS capacity of complex I (PM and PMG; P = 0.0085 & 0.0137, respectively) and complexes I and II combined (PMGS; P = 0.0029) in VDR-KD myotubes (**Figure 4.13**). Maximal respiratory capacity (ET) was also significantly increased by IGF-1 (P = <0.0001) yet OXPHOS capacity of complex II (CII) was not significantly altered (**Figure 4.13**).

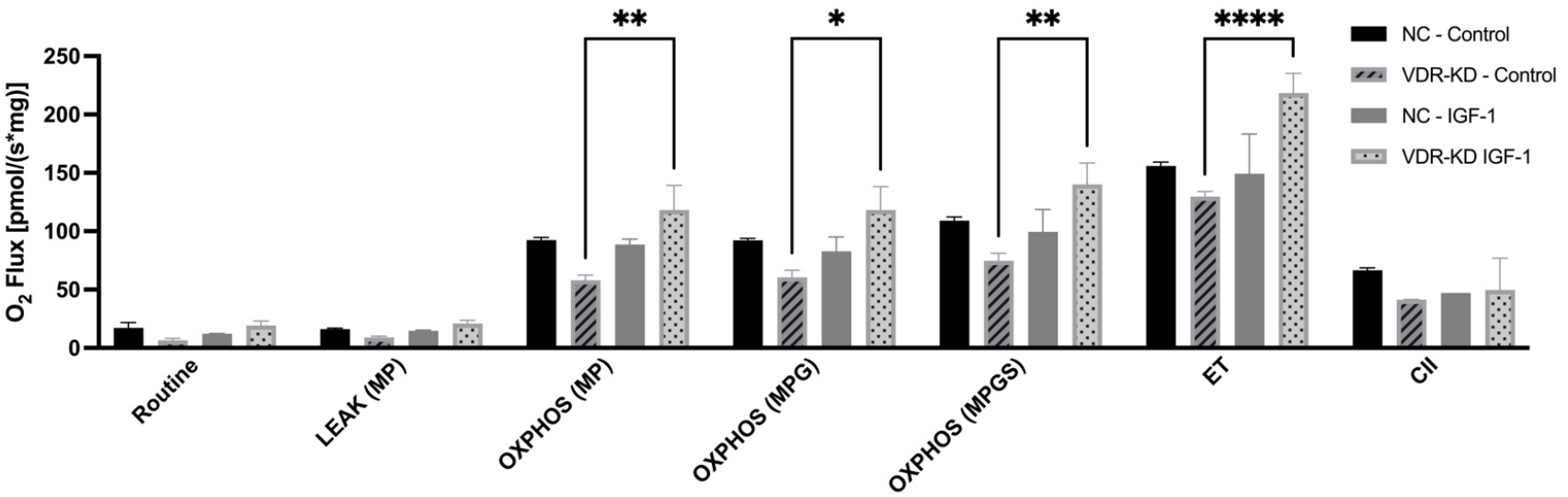


Figure 4.13. Examination of cellular respiration in VDR-KD and NC C2C12 myotubes following 24-hour IGF-1 treatment. Routine state represents oxygen consumption rate at baseline, before digitonin permealisation. Malate (M) and pyruvate (P) were added together to induce proton leakage (LEAK); addition of ADP stimulates maximal oxidative phosphorylation (OXPHOS). OCR in the presence of N-linked substrates, i.e. M, P, and glutamate (G), represents OXPHOS capacity of Complex I (CI). Succinate (S) addition demonstrates the combined OXPHOS capacity of CI and CII together. Titrated addition of carbonyl cyanide p-trifluoromethoxyphenylhydrazone (FCCP) uncouples OXPHOS and induces maximal respiratory capacity (ET). Addition of rotenone inhibits Complex I, thus demonstrating activity of CII without influence from CI respiration and permitting evaluation of non-mitochondrial respiration. Data is expressed as specific flux (oxygen consumption normalised to protein content of sample and after subtraction for non-mitochondrial respiration) and is shown as mean ± SD (n = 4). * $P < 0.05$, ** $P < 0.01$, *** $P < 0.001$, **** $P < 0.0001$.

4.3.5.2 Atrophy - Dexamethasone

No significant differences were seen in both the routine and leak states in Dex-treated NC myotubes compared to untreated (**Figure 4.14**). 24-hour Dex treatment of NC myotubes was associated with significant reductions in the OXPHOS capacity of complex I (PM and PMG; both *P* = <0.0001) and complexes I and II combined (PMGS; *P* = <0.0001; **Figure 4.14**). In addition, both mitochondrial respiratory capacity (ET) and OXPHOS capacity of complex II (CII) were also significantly reduced by Dex treatment (*P* = <0.0001 and 0.0011, respectively; **Figure 4.14**).

In stark comparison, 24-hour Dex treatment had the opposite effect in VDR-KD myotubes. Like the NC, there were no differences in the routine or leak states, but Dex treatment resulted in significantly heightened OXPHOS capacity of complex I (PM and PMG; *P* = 0.0008 and 0.0061, respectively) and complexes I and II combined (PMGS; *P* = 0.0002; **Figure 4.14**). Whilst mitochondrial respiratory capacity (ET) was also significantly higher following Dex treatment (*P* = <0.0001), no differences in the OXPHOS capacity of complex II were found (CII; **Figure 4.14**).

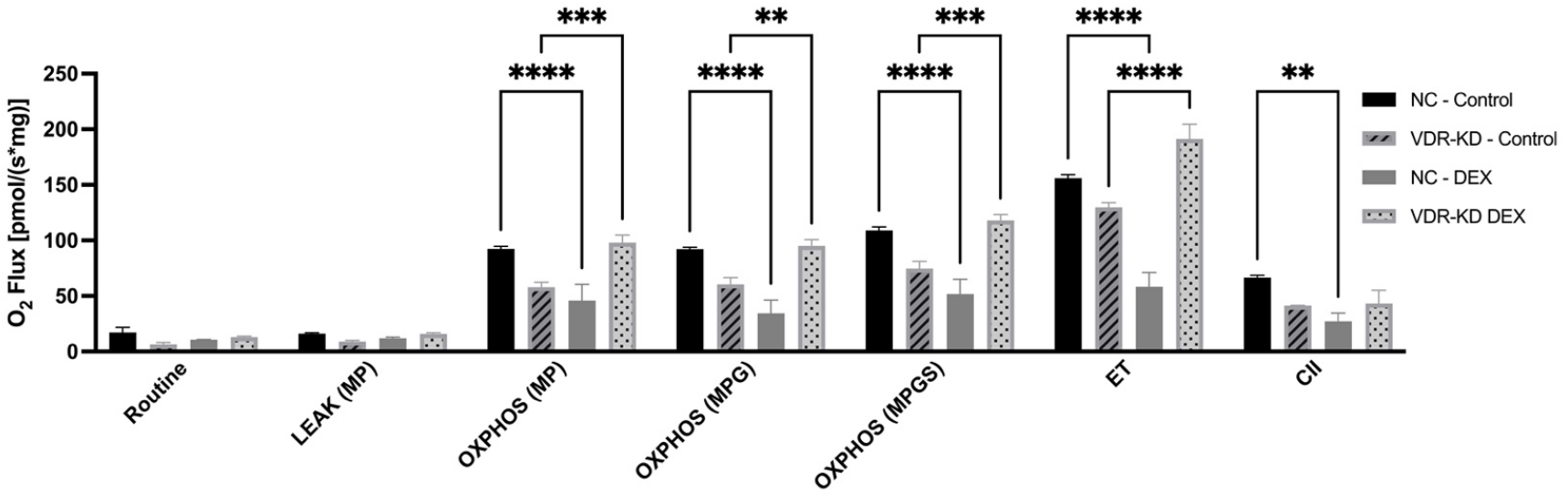


Figure 4.14. Examination of cellular respiration in VDR-KD and NC C2C12 myotubes following 24-hour Dex treatment. Routine state represents oxygen consumption rate at baseline, before digitonin permealisation. Malate (M) and pyruvate (P) were added together to induce proton leakage (LEAK); addition of ADP stimulates maximal oxidative phosphorylation (OXPHOS). OCR in the presence of N-linked substrates, i.e. M, P, and glutamate (G), represents OXPHOS capacity of Complex I (CI). Succinate (S) addition demonstrates the combined OXPHOS capacity of CI and CII together. Titrated addition of carbonyl cyanide p-trifluoromethoxyphenylhydrazone (FCCP) uncouples OXPHOS and induces maximal respiratory capacity (ET). Addition of rotenone inhibits Complex I, thus demonstrating activity of CII without influence from CI respiration and permitting evaluation of non-mitochondrial respiration. Data is expressed as specific flux (oxygen consumption normalised to protein content of sample and after subtraction for non-mitochondrial respiration) and is shown as mean ± SD (n = 4). * $P < 0.05$, ** $P < 0.01$, *** $P < 0.001$, **** $P < 0.0001$.

4.3.5.3 Inflammation - LPS

Like IGF-1, 24-hour treatment of NC myotubes with LPS did not induce any significant changes in any of the specific flux states investigated (**Figure 4.15**). In VDR-KD myotubes, LPS treatment had no significant influence on either the routine or leak states, but it did significantly increase the OXPHOS capacity of complex I (PM and PMG; both P = <0.0001) and complexes I and II combined (PMGS; P = <0.0001; **Figure 4.15**). In addition, LPS treatment resulted in significantly higher mitochondrial respiratory capacity (ET; P = <0.0001) and OXPHOS capacity of complex II (CII; P = 0.0009; **Figure 4.15**).

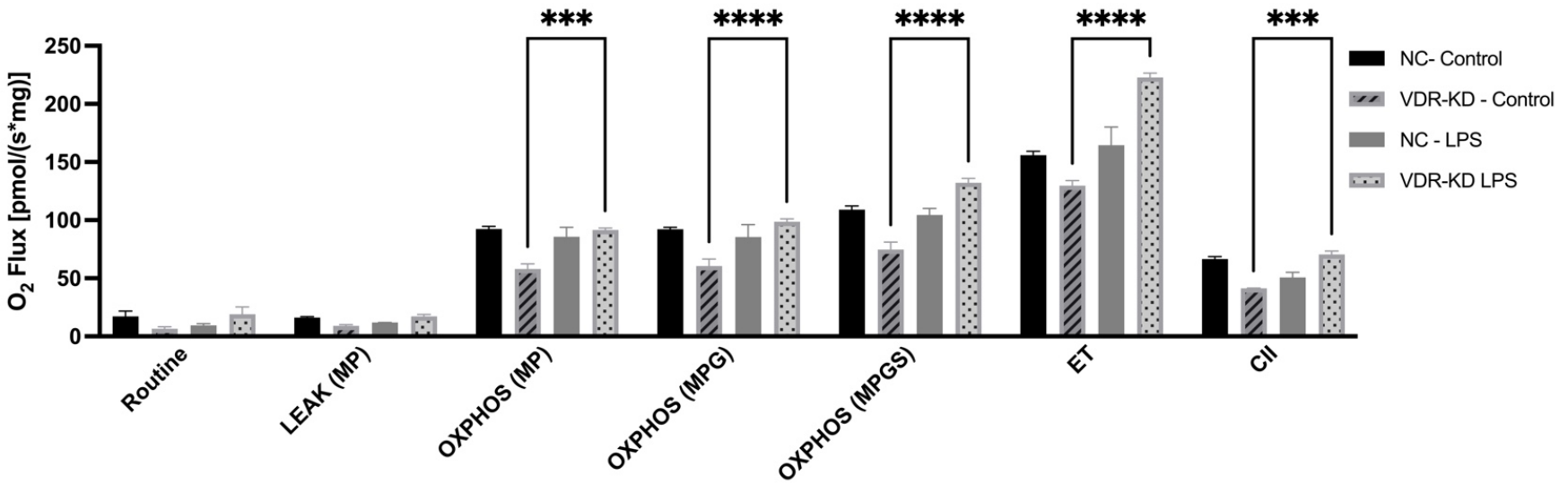


Figure 4.15. Examination of cellular respiration in VDR-KD and NC C2C12 myotubes following 24-hour LPS treatment. Routine state represents oxygen consumption rate at baseline, before digitonin permealisation. Malate (M) and pyruvate (P) were added together to induce proton leakage (LEAK); addition of ADP stimulates maximal oxidative phosphorylation (OXPHOS). OCR in the presence of N-linked substrates, i.e. M, P, and glutamate (G), represents OXPHOS capacity of Complex I (CI). Succinate (S) addition demonstrates the combined OXPHOS capacity of CI and CII together. Titrated addition of carbonyl cyanide p-trifluoromethoxyphenylhydrazone (FCCP) uncouples OXPHOS and induces maximal respiratory capacity (ET). Addition of rotenone inhibits Complex I, thus demonstrating activity of CII without influence from CI respiration and permitting evaluation of non-mitochondrial respiration. Data is expressed as specific flux (oxygen consumption normalised to protein content of sample and after subtraction for non-mitochondrial respiration) and is shown as mean ± SD (n = 4). * $P < 0.05$, ** $P < 0.01$, *** $P < 0.001$, **** $P < 0.0001$.

4.4 Discussion

Whilst the relationship between the vitamin D axis and skeletal muscle has already been studied extensively using both animal and cellular models, the overall understanding of the mechanistic underpinnings of this relationship remains poor. In this chapter, VDR-KD myotubes were successfully generated by performing RNAi in C2C12 myotubes and demonstrated that loss of VDR results in perturbed expression of key metabolic and myogenic related targets at both mRNA and protein level. For the first time, VDR-KD and NC myotubes were exposed to either IGF-1, dexamethasone, or LPS for 24 hours to create *in vitro* models of hypertrophy, atrophy, and inflammation, respectively.

4.4.1 Effects of VDR-KD

Following RNAi, *Vdr* mRNA expression was reduced by 43.35%, whilst protein levels were reduced by 75.95% compared to those transfected with NC siRNA. VDR-KD myotubes demonstrated significant reductions in mTOR, ribosomal protein S6 (rps6), 70kDa ribosomal protein S6 kinase (p70S6K), AKT serine/threonine kinase 1 (Akt), and tuberous sclerosis complex 2 (TSC2; all key regulators of muscle protein synthesis (MPS)) at both mRNA and protein level, thereby indicating a possible decline in MPS. Given that it was demonstrated that VDR-KD lead to downregulation of anabolic targets and that previous studies have demonstrated that catabolic targets were upregulated following VDR-KD *in vivo,* it was anticipated that similar observations would be seen here [373]. However, no differences were seen between VDR-KD and NC myotubes

for any of the catabolic-related targets studied at protein level, but significant reductions were observed in *Foxo3* mRNA expression.

One article previously published by Bass et al. reported that anabolic signalling was unchanged in skeletal muscle following *in vivo* VDR-KO [213]. However, previous studies have shown involvement of the vitamin D axis within regulating MPS, as both deficiency and VDR-KO in rats was associated with reduced levels of anabolic targets whilst $1,25(OH)_2D_3$ treatment of C2C12 myotubes *in vitro* lead to increased p-Akt, p-p70S6K, and p-mTOR [206,224,225]. Intriguingly, VDR overexpression (VDR-OE) also resulted in increased anabolic signalling in rodent skeletal muscle [296]. Overall, the consensus appears to remain that VDR is directly involved in MPS signalling, as demonstrated by previous studies and the data presented herein. In contrast, the results with regards to catabolic signalling between VDR-KD and NC myotubes were surprising and inconsistent with the literature.

Whilst other articles have reported increased proteolytic signalling following VDR-KO and in states of deficiency [88,211,213], no differences in proteolytic related targets were seen at protein level and observed reduced gene expression of certain targets. Forkhead box proteins (FOXO) are a family of transcription factors all possessing significant roles in driving muscle atrophy. mRNA expression of *Foxo3* was lower in VDR-KD but, within the literature, the data conflicts as treatment of human myotubes with $1,25(OH)_2D_3$ upregulated FOXO3 expression whereas vitamin D supplementation decreased levels of FOXO3 in the paraspinal muscle of patients with chronic lower back pain

[204,374]. Additionally, one article reported no differences in FOXO3 protein levels in the skeletal muscle of VDR-KO mice, yet another group suggested that deficiency results in oxidative stress in bone via reductions in the number of FOXO3 positive cells [212,375].

One potential explanation for the observation of no change to catabolic targets following VDR-KD is that muscle atrophy associated with loss of VDR is not the outcome of altered proteolytic signalling, as previously believed, and is instead a consequence of perturbed autophagy. However, no significant differences were found in protein levels of phosphorylated Unc-51-like autophagy activating kinase 1 (p-ULK1) or phosphorylated 5' adenosine monophosphate-activated protein kinase α (p-AMPKα) between VDR-KD and NC myotubes. Phosphorylation and subsequent activation of AMPKα has previously been shown to be upregulated following treatment of C2C12 myotubes with $1,25(OH)_2D_3$, thereby representing induction of autophagosome formation plus skeletal muscle AMPKα activity was reduced in deficient obese and non-obese rats [196,209,211]. On the other hand, the work in this chapter represents the first time that ULK1 has ever been investigated in skeletal muscle in relation to VDR, so it is hard to compare results. Considering no differences were observed in p-AMPKα, it is somewhat unsurprising that p-ULK1 was also unchanged in this instance. Yet, previous research has demonstrated increased levels of other autophagy-related proteins, e.g., Beclin-1, Atg-5 and -7, in not only the skeletal muscle of VDR-KO rats but also VDR-KO vascular smooth muscle cells (VSMCs) and mammary glands [213,376,377]. To ascertain if induction of

autophagy was being prevented via another pathway, histone deacetylase 9 (HDAC9) was investigated, as previous work has demonstrated that increased *Hdac9* expression in hypoxic C2C12 myotubes inhibited autophagic processes by binding the promoters of Beclin-1, Atg-7 and LC3B [378]. However, *Hdac9* gene expression was actually found to be significantly lower in VDR-KD myotubes, so this could not explain the results generated here.

It is possible that the discrepancies between the results presented here, and the literature can be explained by the differences existing between *in vivo* and *in vitro* models. Here, VDR-KD was performed in the early stages of differentiation (day 2) meaning that loss of *Vdr* would primarily impact fusion of myoblasts into mature myotubes and post-differentiation myogenic events. Comparatively, studies that have demonstrated changes in proteolytic signalling either used genetic animal models (either loss of *Vdr* from conception or *in vivo* electrotransfer (IVE)) or chronic models of deficiency [196,197,213]. In addition, the chronic nature of these models means that the systemic whole-body effects that accompany both deficiency and loss of *Vdr*, but are not present *in vitro*, may contribute to the changes seen in proteolysis.

Aside from proteolysis, the influence of VDR-KD upon expression of key myogenic genes was also investigated. A significant body of research has previously focused upon the role of the vitamin D axis within myogenesis, the process by which skeletal muscle is generated (as previously discussed in **Chapter 1**). Here, a reduction in VDR protein levels was found to be

accompanied by a decline in mRNA expression of several myogenic regulatory factors (MRFs). Broadly speaking, myoblast determination protein-1 (MYOD1) and myogenic factor 5 (MYF5) are both deemed as "gatekeepers" in the commitment of stem cells to myogenic lineage, whilst MRF4 (also known as herculin or, in humans, MYF6) and myogenin (MYOG) are responsible for stimulating the transition into multinucleated myofibres. No differences were observed in mRNA expression of *Myf5*, yet *Myod1*, *Mrf4*, and *Myog* were all downregulated following VDR-KD. In addition, the reductions in *Mrf4* (76.69%) and *Myog* (70.88%) gene expression were greater than that of *Myod1* (58.44%). Intriguingly, similar observations have been reported, as VDR-KD in C2C12 myotubes resulted in reduced mRNA expression of *Myog* and *Mrf4* yet no differences were seen in *Myod1* and *Myf5* [379]. In addition, *Cdkn1a* was downregulated by VDR-KD. *Cdkn1a* represents the gene encoding p21, a cyclin dependent kinase (CDK) inhibitor (CDKI) whose expression increases when myoblasts commit to differentiation into myotubes via cell cycle withdrawal [380]. This result is consistent with the literature as p21 levels were also lower following VDR-KD in a mammary tumour cell line whilst 24 hour $1,25(OH)_2D_3$ treatment of C2C12 myoblasts upregulated p21 in a VDR-dependent manner [158,381]. Maintenance of G2 arrest requires p21, so it is possible to speculate whether loss of VDR and its subsequent suppression upon p21 expression renders VDR-KD myotubes unable to completely commit to cell cycle withdrawal [382]. Indeed, depletion of p21 expression has been previously shown to "re-activate" terminally differentiated primary muscle cells and result in apoptosis due to increased levels of DNA damage and incomplete DNA

replication [382]. Thus, if VDR-KD does indeed suppress *Cdkn1a* expression, then any VDR-KD myotubes that may have managed to survive DNA damage-induced apoptosis can enter mitosis with incompletely replicated and damaged DNA, therefore potentially resulting in mitotic catastrophe [382]. This hypothesis could explain previous observations, as myoblasts lacking *Vdr* were unable to fully complete differentiation, with the bulk being in G_0/G_1 phase, and any myotubes that did form were very irregular and large with an increased myonuclei number [213].

Here, gene expression of the fast myosin isoform, myosin heavy chain 1 (*Myh1;* also known as MHC-IIx), was reduced in VDR-KD myotubes. During differentiation, MyH1 is upregulated to aid in initiation and sustainment of myotube fusion, so downregulation of *Myh1* expression, as observed here, would suggest impairment of differentiation by VDR-KD. Furthermore, as MyH1 is the predominant myosin isoform in type II muscle fibres (fast-twitch) [383], this result provides further support for previous observations of type II fibres being the principal target of vitamin D deficiency [115,122,123]. Like MyH1, *Myh8* (perinatal MHC) mRNA expression was also lowered by VDR-KD. As a developmental MHC, MyH8 is expressed in developing and regenerating skeletal muscle [384]. There are inconsistencies throughout the literature surrounding MyH8 and the vitamin D axis, as it has been documented to be both up- and downregulated following treatment of C2C12 and primary human myotubes with $1,25(OH)_2D_3$ [144,374,385,386]. In this instance, the observation of reduced *Myh8* expression appears consistent with the fact that

VDR-KD resulted in impaired expression of differentiation markers, but it highlights a requirement for additional studies to provide further information on this relationship. When viewed collectively, the evidence presented here indicates greater involvement of VDR in the latter stages of differentiation in comparison to the early stages and supports previous evidence suggesting a selective role of the vitamin D axis in type II fibres.

Finally, it was demonstrated that VDR-KD results in impairment of mitochondrial OXPHOS capacity across multiple flux states. Interest into the relationship between skeletal muscle mitochondria and the vitamin D axis has grown substantially over recent years with reports of improvements in mitochondrial function following vitamin D supplementation [224,248,356]. Indeed, this has been confirmed *in vitro* as treatment of both primary human and C2C12 myotubes with $1,25(OH)_2D_3$ increased OCR, indicative of greater mitochondrial metabolism [174,246,247]. Here, no significant differences were observed in mitochondrial respiration in either the routine (baseline) or leak (presence of pyruvate and malate; PM) states in VDR-KD myotubes, but VDR-KD significantly reduced OXPHOS capacity of Complexes I and II (both individually and combined) and maximal respiratory capacity. Previous data suggesting that loss of VDR in C2C12 myotubes results in impairment of basal mitochondrial respiration may suggest that these findings of VDR-KD exerting no influence upon basal respiration are inconsistent with the literature [244]. However, this difference could be explained by several methodological differences, as Ashcroft et al. performed their experiments in a stably

transfected VDR-KD C2C12 cell line possessing lower VDR levels (95% lower than control) than what was achieved herein (75.95% lower than NC), and they measured mitochondrial function via extracellular flux analysis (EFA; Seahorse) [244]. Aside from the baseline data, the remainder of the observations presented here support the notion that loss of VDR results in impaired mitochondrial respiration in myotubes.

The mechanism by which VDR-KD regulates mitochondrial bioenergetics is currently unknown, but several groups have shown that it is not related to mitochondrial volume changes as neither VDR-KO and/or treatment with $1,25(OH)_2D_3$ exert significant effects upon mitochondrial protein content [147,174,213,244]. Intriguingly, the effects of $1,25(OH)_2D_3$ upon OCR are abolished when added directly to isolated mitochondria as opposed to directly treating cells [174], thereby indicating that the underlying mechanism is dependent on extramitochondrial events. To date, several groups have used microarray analyses in an attempt to identify genes that are direct targets of VDR, and evidence suggests that multiple mitochondrial-related gene sets are under VDR-regulation [174,213]. However, it is unclear whether any of these genes possess VDREs and are therefore directly regulated or whether indirect mechanisms are at play. Finally, it is probable that the infamous calciotropic effects of the vitamin D axis also extend to regulating intramitochondrial Ca^{2+} homeostasis. Maintenance of Ca^{2+} levels within mitochondria is tightly regulated and is coupled to the metabolic state of the cell [387]. When avian and human myotubes were treated with $1,25(OH)_2D_3$ an intracellular flux of

Ca^{2+} was observed plus expression levels of the calcium handling gene, sarcoplasmic reticulum calcium transport ATPase (*Serca*), were reduced in the *Quadriceps* of both VDR-KO and deficient mice [147,166,230,235]. Under basal conditions, mitochondrial uptake of Ca^{2+} occurs during the twitch and tetanic responses of muscle contraction [240], but when the cell is in a vitamin D deficient state it seems that oxidative phosphorylation is impaired, and mitochondria are unable to retain Ca^{2+} [241]. Further work is required to improve the overall understanding of this relationship, particularly *in vivo*, as expansion of our knowledge surrounding the vitamin D axis and Ca^{2+} dynamics would further the understanding of not only skeletal muscle and mitochondria, but other tissues also.

4.4.2. Treatment of VDR-KD myotubes with the hypertrophic, atrophic, and pro-inflammatory conditions

Given the evidence implicating VDR in skeletal muscle physiology, as presented in this thesis and within the literature, it is fair to question the extent to which VDR is involved in certain physiological scenarios that are common to skeletal muscle. This was investigated by exposing VDR-KD and NC myotubes to *in vitro* models of hypertrophy, atrophy, and inflammation.

4.4.2.1. IGF-1

Treatment of myotubes with IGF-1 is a commonly used *in vitro* model of hypertrophy as it induces the PI3K/Akt/mTOR pathway [364]. Indeed, as expected, the PI3K/Akt/mTOR pathway was activated following treatment of

NC myotubes with IGF-1 for 24 hours as demonstrated by elevated mRNA expression and protein levels of p-Akt, p-mTOR, and p-p70S6K. In support of this observation, increased protein levels of the phosphorylated form of TSC2 were observed, which is a protein that, when unphosphorylated, forms a mTOR inhibiting complex with TSC1 [388]. In the IGF-1 treated VDR-KD myotubes, the results revealed a very different picture. No changes were seen at mRNA level and there were no significant differences in levels of p-Akt or p-mTOR, therefore implying that, in this instance, IGF-1 treatment was unable to activate the PI3K/Akt/mTOR pathway.

As it was demonstrated that IGF-1 upregulated *Vdr* mRNA expression in NC myotubes, it can be proposed that the previously discussed effects of IGF-1 are VDR-dependent and provide support for previous articles reporting positive correlations between serum IGF-1 and $25(OH)D_3$ levels [389,390]. In line with these observations, VDR-KO mice also display reduced serum IGF-1 levels which can be corrected by feeding the mice a high Ca^{2+} diet [391]. Whilst the underlying mechanisms are yet to be confirmed, particularly in relation to skeletal muscle, several hypotheses have been proposed based on data generated from various other tissue types. The most common suggestion has been that the vitamin D axis influences IGF-1 levels primarily via the liver, as hepatic cells represent a major site of IGF-1 synthesis, express VDR, and respond to $1,25(OH)_2D_3$ *in vitro* [392]. In line with this, an indirect mechanism has been suggested in that the newly synthesised IGF-1 is subsequently transported via the systemic circulation to target tissues, e.g., skeletal muscle,

where it exerts its effects [202]. Whilst it is possible that this hypothesis is correct, it does not explain why the effects of IGF-1 were abolished in the absence of VDR as this result indicates the presence of a direct mechanism. One possibility is that VDR-KD had a direct effect upon certain members of key signalling pathways that IGF-1 acts through. One such example is cellular sarcoma kinase (c-Src), a major transcription factor that has been previously documented to regulate Akt phosphorylation following $1,25(OH)_2D_3$ treatment in C2C12 myotubes [393]. During basal conditions, c-Src is colocalised with caveolin-1 in close proximity to the plasma membrane but, following $1,25(OH)_2D_3$ treatment and translocation of VDR to the plasma membrane, the co-localisation appears to be disrupted [220,221]. As the association with caveolin-1 is inhibitory of c-Src function, it is possible to hypothesize that $1,25(OH)_2D_3$-induced VDR translocation permits activation of c-Src signalling, therefore suggesting that c-Src acts as a gateway to cell signalling for vitamin D. In addition, downregulation of c-Src and several of its downstream targets (e.g., mitogen-activated protein kinase; MAPK) has been previously documented in C2C12 myotubes lacking the *Vdr* gene [217].

As previously discussed, IGF-1 primarily exerts its hypertrophic influences via the PI3K/Akt/mTOR pathway and data from oligodendrocytes suggests that c-Src activity is required for activation of Akt in response to IGF-1 [394]. When viewing the evidence collectively, it is perhaps sensible to propose that, in the model of VDR-KD used herein, two possible theories exist: 1. IGF-1 could not activate the PI3K/Akt/mTOR pathway as c-Src expression is downregulated by

VDR-KD, and/or 2. IGF-1 could not activate the PI3K/Akt/mTOR pathway as, due to absence of VDR, c-Src remains co-localised with caveolin-1 close to the plasma membrane and can therefore not be activated.

In skeletal muscle, the effects of IGF-1 are not limited to MPS regulation only, as it also exerts a regulatory effect upon autophagy [395]. ULK1 is inhibited by phosphorylation via mTOR at Ser 757 and IGF-1 is an activator of mTOR, so an increase in phosphorylation of ULK1 was anticipated to occur following IGF-1 treatment of NC myotubes. However, no significant differences were found in protein levels of p-ULK1 (Ser 757) in either NC or VDR-KD myotubes. Instead, IGF-1 treatment reduced levels of T-ULK1 on a similar magnitude in both VDR-KD (50.26%) and NC (54.69%) myotubes. Intriguingly, this result indicates that VDR is not involved in IGF-1 regulation of autophagy, despite the suppressive effects of VDR-KD upon the PI3K/Akt/mTOR pathway. It is possible to speculate that ULK1 was phosphorylated at other sites (e.g., Ser 317 and Ser 777) by AMPKα but, as protein levels of this phosphorylated form of ULK1 were not measured and p-AMPKα protein levels were not significantly altered by IGF-1 treatment in either cell type, this hypothesis cannot be confirmed.

In NC myotubes only, *Foxo1* mRNA expression was increased by IGF-1 treatment, which initially appears paradoxical considering that IGF-1 and activation of the PI3K/Akt pathway has been demonstrated to inhibit FOXO proteins in skeletal muscle by preventing their nuclear translocation [396,397]. Comparatively, *Foxo1* mRNA expression did not change in VDR-KD IGF-1

treated myotubes, which is perhaps unsurprising, given that it had already been demonstrated that loss of VDR suppressed *Foxo1* gene expression in VDR-KD controls compared to the NC. It is possible that the elevated *Foxo1* gene expression is a compensatory mechanism for the supposed increased phosphorylation of FOXO1 by IGF-1-activated Akt and clearance by ubiquitination but, as protein levels of p-FOXO1 were not measured, this theory remains purely hypothetical. Surprisingly, it appears that stimulation of VDR-KD myotubes with IGF-1 lead to increased mRNA expression of *Myf5.* As previously discussed, *Myf5* is deemed one of the "gatekeepers" of myogenic differentiation along with *Myod1*. As mRNA expression of both *Myf5* and *Myod1* remained unaltered in untreated VDR-KD myotubes, plus IGF-1 has previously been shown to act as a positive regulator of these myogenic factors *in vitro* [398], it raises an interesting question. Does VDR transcriptionally down-regulate *Myf5* expression during differentiation? Evidence from work conducted *in vivo* supports this theory, as persistently high expression levels of *Myf5* were observed in quadriceps of 3-week-old VDR-KO mice [163]. However, whether the *Myf5* gene possesses a VDRE is yet to be established so, until then, a precise mechanism is unable to be definitively confirmed. In line with data published by other groups, IGF-1 treatment increased mRNA expression of *Myh1* in NC myotubes only, but like FOXO1, *Myh1* gene expression was not altered by IGF-1 treatment of VDR-KD myotubes [399,400]. In humans, it appears that MyH1 only increases after periods of inactivity or declined neuromuscular activity, e.g., long-term bed-rest and detraining [401,402], but not following exercise. Whilst this topic is beyond the scope of this thesis, these

observations are supported by previously published *in vitro* data, thus warranting the necessity of further investigations.

4.4.2.2. Dexamethasone

Dexamethasone (Dex) is frequently used *in vitro* to induce a model of physiological atrophy, so using 1 µM Dex, both VDR-KD and NC myotubes were treated for 24 hours before collection and processing for analyses. In NC myotubes, Dex treatment negatively influenced markers of MPS as demonstrated by reductions in mRNA expression of *Rps6* and protein levels of p-Akt and T-mTOR. These observations are consistent with previous studies investigating effects of Dex upon MPS in muscle cells [403–405], however, unlike these other articles, downstream targets of mTOR remained unchanged at protein level. This discrepancy could be due to several experimental differences, such as the length of Dex exposure and the dosage used as, here myotubes were treated for 24 hours with 1 µM Dex whilst others either used varying dosages (0.01-10 µM) and/or longer exposure times (48 hours to 8 days).

Loss of VDR has previously been demonstrated to induce muscle atrophy [88,212,213], so VDR-KD was expected to exacerbate the atrophic effects of Dex, yet this was not the case. Surprisingly, no changes were seen in any MPS or MPB targets in Dex-treated VDR-KD myotubes compared to untreated VDR-KD. As impairment of MPS targets was observed in both Dex-treated NC myotubes and VDR-KD control myotubes, difficulties arise when attempting to

determine the exact mechanisms by which MPS is being impaired. For VDR-KD, confidence can be placed in that in the absence of VDR the PI3K/Akt/mTOR pathway is suppressed, thus providing an explanation for the reductions seen in VDR-KD control myotubes compared to the NC control. However, it raises an interesting question; why didn't Dex reduce MPS target levels further in Dex-treated VDR-KD myotubes? One possibility is that the presence of VDR is a requirement for Dex to perform its MPS-related actions and, indeed, for the first time it was demonstrated that *Vdr* expression was upregulated in NC myotubes following Dex exposure. This is in support of similar observations from studies where squamous cell carcinoma VI cell lines and murine kidneys were also exposed to Dex [406,407], plus *Vdr* gene upregulation has previously been hypothesised to enhance both the effects of Dex action upon cells and also the cellular response to Dex by potentiating the effects of $1,25(OH)_2D_3$ [406,408]. In addition, Dex may suppress MPS via targets that are transcriptionally regulated by VDR and are subsequently downregulated by VDR-KD. Based on data presented in this chapter, this could include FOXO1 as, in skeletal muscle, Dex has previously been documented to suppress MPS via FOXO1 and its mRNA expression was downregulated here by VDR-KD, thus potentially preventing Dex from activating this catabolic pathway [409]. Answering the question of why Dex was unable to reduce MPS targets further in VDR-KD is mechanistically complex and clearly requires further investigations that are beyond the scope of this thesis. Additional research is required to provide further information surrounding the relationship between the vitamin D axis and glucocorticoids, particularly Dex, in relation to MPS/MPB.

Similar to IGF-1, the effects of Dex upon skeletal muscle are not restricted to regulation of proteostasis, and several articles have demonstrated regulatory influences upon myogenesis. However, the data conflicts across the literature, as some argue that Dex acts as negative myogenic regulator [404], whilst others have generated data suggesting the opposite [410,411]. Here, declines were observed in mRNA expression of *Myog* and *Myod1* following Dex treatment of NC myotubes, thereby providing support to the hypothesis of Dex possessing a negative myogenic regulatory role. Like the MPS/MPB targets, Dex treatment of VDR-KD myotubes failed to exert the same changes as in the NC. However, it was noted that in NC myotubes, Dex suppressed *Myog* and *Myod1* expression to levels similar to those seen in VDR-KD untreated myotubes. This observation suggests that reduction of VDR levels induces a state close to that induced by Dex. To add to this, Dex had no influence upon *Myf5* mRNA expression in NC myotubes, but an almost 3-fold increase in its expression was observed in Dex-treated VDR-KD myotubes, similar to that observed in IGF-1. It is possible that Dex treatment induces *Myf5* expression in VDR-KD to compensate for reduced expression and increased degradation of *Myod1* [412]. Yet, if this was the case, then it would also be expected for Dex to increase *Myf5* expression in NC myotubes, thus providing further evidence to support the previously discussed question of whether VDR transcriptionally down-regulates *Myf5* expression during differentiation.

Comparatively, whilst Dex treatment reduced mRNA expression of *Cdkn1a, Hdac9,* and *Foxo3* in NC myotubes*,* no changes were observed in Dex-treated VDR-KD. As previously discussed, p21 (the protein encoded by the *Cdkn1a* gene), is essential for cell cycle withdrawal and commitment to terminal myogenic differentiation [380]. Unfortunately, very few articles exist exploring the influence of Dex upon *Cdkn1a* expression in skeletal muscle, but a 7-fold upregulation of *Cdkn1a* gene expression has been reported in the *triceps surae* complex of Dex-treated mice [413]. This result has been translated clinically as, like in the Dex-treated mice, *Cdkn1a* gene expression was upregulated in *tibialis anterior* biopsies collected from ICU patients with clinical illness myopathy (CIM) [414]. As *Cdkn1a* was already down-regulated in untreated VDR-KD myotubes, it is perhaps unsurprising that Dex treatment was unable to alter its expression further. However, given the evidence, downregulation of *Cdkn1a* in NC myotubes by Dex was unexpected. One possibility is that reduced *Cdkn1a* expression re-activates terminally differentiated (TD) myotubes (as discussed previously in relation to VDR-KD) and could therefore contribute to the pro-atrophic effect of Dex.

As previously demonstrated using different models of muscle atrophy [415,416], *Hdac9* levels were also found to be downregulated by Dex treatment in NC myotubes. This *Hdac9* downregulation has been proposed to occur in atrophic conditions to prevent the inhibitory influence of *Hdac9* upon muscle reinnervation and myogenesis [378,416]. Comparatively, in VDR-KD, Dex treatment had no influence upon *Hdac9* mRNA expression, as levels were

consistent with that of untreated VDR-KD, thus supporting the notion that *Hdac9* expression is VDR-dependent. In addition, *Foxo3* mRNA expression decreased with Dex treatment in NC myotubes, which was an unexpected result given that previous data indicates increased expression in atrophic conditions [417,418]. Comparatively, Dex treatment of the VDR-KD myotubes (which had already shown to have reduced *Foxo3* expression) failed to alter mRNA expression of *Foxo3* further. FOXO3 exerts its pro-atrophic effect by stimulating expression of certain catabolic genes, e.g., Atrogin-1 and muscle RING-finger protein-1 (MuRF1), that are well-documented mediators of atrophy [419]. Why VDR-KD and Dex treatment of NC myotubes reduced *Foxo3* expression in this instance is unclear and, due to time constraints, this result was unable to be explored further. Thus, additional experiments are required to confirm these observations and to provide a mechanistic explanation.

4.4.2.3. Lipopolysaccharide

To create an *in vitro* model of muscle inflammation (e.g., metabolic endotoxemia and/or sepsis) NC and VDR-KD myotubes were exposed to 0.1 µg/mL lipopolysaccharide (LPS) for 24 hours. Following LPS treatment, NC myotubes displayed reductions in key targets of MPS, namely rps6, p70S6K, Akt, and mTOR, yet no changes were observed in any of the catabolic targets investigated. Previous animal studies have shown significant alterations to catabolic targets and MPB rate in skeletal muscle following LPS treatment [420–423], plus *in vitro* data suggests that perturbed catabolic signalling appears to reach a maximal response 8-12 hours after exposure of myotubes

to LPS [422,424]. It is therefore possible that the timepoint of greatest proteolysis was missed as a single time point of 24 hours post LPS exposure was used throughout all experiments conducted in this chapter.

It was initially anticipated that the response to LPS would be more drastic/severe in VDR-KD myotubes, however, this was not the case as no changes were observed in any anabolic or catabolic-related targets following exposure to LPS. Intriguingly, following LPS exposure of NC myotubes, *Vdr* gene expression was reduced by 71.01% compared to the untreated NC. This is in support of previous reports stating LPS as a negative modulator of the vitamin D axis in various cell types, e.g. monocytes and oral keratinocytes [425,426], and provides the first line of evidence suggesting that the same phenomenon occurs in skeletal muscle. As VDR levels are already significantly reduced in the VDR-KD model prior to LPS treatment, LPS is therefore unable to suppress VDR and the PI3K/Akt/mTOR pathway further. One possibility is that LPS downregulates VDR to prevent $1,25(OH)_2D_3$ from exerting its anti-inflammatory and anabolic effects, thus creating an atrophic and inflammatory cellular environment.

Co-treatment of cell and animal models with both $1,25(OH)_2D_3$ and LPS has been demonstrated to inhibit the pro-inflammatory effects of LPS [368,427], while pre-treatment with $1,25(OH)_2D_3$ prior to LPS exposure appears to block LPS-induced nuclear translocation of nuclear factor kappa B (NF-κB) in the placenta [428]. NF-κB is a well-known contributor to muscle inflammation as it

activates MPB whilst inhibiting MPS, and positively regulates several pro-inflammatory cytokines (e.g. tumour necrosis factor alpha (TNF-α), interleukin 6 (IL-6)), and matrix metalloproteinases (MMPs)) [429]. Furthermore, LPS treatment of NC myotubes reduced mRNA expression of *Foxo3* which regulates the anti-inflammatory response via negative regulation of IL-6, IL-1β, and TNF-α [430–432]. VDR-KD also resulted in *Foxo3* down-regulation, but LPS exposure of VDR-KD myotubes resulted in no further changes to *Foxo3* expression. Thus, when this evidence is considered collectively, it can be assumed that in normal conditions, i.e. in the presence of VDR, *Vdr* expression is downregulated by LPS in order to suppress and minimise the anabolic and anti-inflammatory effects of VDR and the vitamin D axis.

Intriguingly, reduced levels of T-ULK1 were observed in both NC and VDR-KD myotubes post LPS exposure, thereby suggesting a VDR-independent mechanism through which LPS regulates ULK1 levels. In addition, when in the absence of LPS, VDR-KD had no effect on T-ULK1 levels compared to the NC which would imply that ULK1 levels are not directly regulated by VDR. Given that T-ULK1 levels were reduced it is sensible to wonder by what means it is being modified, e.g. phosphorylation, but no differences were demonstrated in levels of p-ULK1 (Ser 757). One possibility is that ULK1 is being phosphorylated by MAPK at another site not investigated, such as Ser 504, as previously demonstrated in hepatic stellate cells [433,434]. MAPK phosphorylation inhibits the kinase activity of ULK1 and subsequently disrupts its connections with components of the autophagy initiation complex, e.g.

ATG13 [435]. ULK1 inhibition via MAPK phosphorylation is required for LPS-induced activity of the nucleotide-binding and oligomerisation domain (NOD)-like receptor family pyrin domain containing 3 (NLRP3) inflammasome, which could provide an explanation for why LPS downregulated levels of T-ULK1. To confirm this hypothesis further experiments would be required but it would also expand our knowledge regarding LPS-induced inflammation within skeletal muscle.

Within the literature, previous research has primarily focused upon the catabolic and pro-inflammatory effects of LPS in skeletal muscle, but evidence suggests involvement in key myogenic pathways. In relation to MRFs, upregulation of *Mrf4* expression was observed following LPS exposure in the NC but mRNA expression of *Myod1, Myf5,* and *Myog* all remained unaltered in both LPS treated NC and VDR-KD myotubes. Untreated VDR-KD myotubes displayed reduced *Mrf4* expression compared to the unstimulated NC, but when VDR-KD myotubes were exposed to LPS, no further changes in *Mrf4* were observed. From this, a mechanism can be proposed through which LPS suppresses VDR in order to minimise the inhibitory effect of VDR upon a currently unknown or unidentified factor that is lying downstream of VDR but upstream of *Mrf4*. Very little research exists investigating *Mrf4* and LPS, as most studies appear to focus on the influence of LPS upon levels of *Myod1* and *Myog* [436,437]*,* so any hypotheses generated to explain these results are purely speculative.

Interestingly, *Cdkn1a* mRNA expression was upregulated following LPS exposure of NC myotubes. Similar observations have been reported in dental pulp-derived mesenchymal stem cells (DPMSCs) and murine central nervous system and this rise in *Cdkn1a* has been proposed as a driver for LPS-induced cellular senescence [438,439]. Whilst *Cdkn1a* mRNA expression was the only senescence marker investigated in this chapter, other markers of senescence, e.g. increased activity of senescence-associated beta-galactosidase (SA-β-Gal) and heightened p53 levels, have been previously demonstrated in murine skeletal muscle following LPS treatment [440]. This rise in *Cdkn1a* expression was not present in LPS-treated VDR-KD myotubes which would suggest that without VDR, LPS is unable to upregulate *Cdkn1a*. As LPS suppresses *Vdr* gene expression, it is likely that a mechanism exists similar to that suggested for *Mrf4*, but this would need confirming experimentally.

LPS also downregulated mRNA expression of *Myh1* and *Myh8* in NC myotubes only. As previously discussed in relation to VDR-KD, suppression of these myosin isoforms implies impaired differentiation by LPS, thus supporting previous reports [436]. If LPS does indeed perturb myogenic differentiation, then this could be a contributing factor to LPS-induced muscle atrophy and should be explored in more detail, but this was beyond the scope of this thesis. Like *Mrf4*, *Myh1* and *Myh8* are also downregulated by VDR-KD in the absence of LPS and their mRNA expression remained unchanged following treatment of VDR-KD myotubes with LPS. Furthermore, these observations provide further evidence to support the hypothesis that VDR may act as a positive regulator of

both *Myh1* and *Myh8*. Indeed, treatment of fully differentiated human-derived myotubes and murine satellite cells with $1,25(OH)_2D_3$ upregulates *Myh1* and *Myh8*, and VDR-KO rats display reduced expression of both myosin isoforms [162,224,386].

One particularly interesting result from this chapter is the observation that LPS acts as a negative regulator of vitamin D binding protein (DBP) as DBP protein levels were significantly reduced following exposure of NC myotubes with LPS. This phenomenon has been demonstrated before but only in THLE2 cells (a liver epithelial cell line), so this is the first report of this relationship in C2C12 cells [441]. This raises the question of can VDR regulate DBP levels by either a direct or indirect mechanism? The work conducted in this chapter represents the first time that DBP has ever been explored in relation to skeletal muscle and VDR-KD, making comparisons difficult. From a clinical perspective, lower serum levels of DBP have been associated with poorer outcomes following sepsis, such as multi-organ dysfunction and mortality [441–444]. It is unclear why DBP levels are lowered in these clinical scenarios but, due to the actin-binding capabilities of DBP, it is probable that DBP scavenges actin released from injured tissue. This would prevent polymerisation of monomeric actin into filamentous actin (F-actin) and subsequently avoid formation of polymeric structures that may have potentially led to blockages in the microcirculation [26]. Intriguingly, LPS had no influence upon DBP levels in VDR-KD myotubes. It is possible to speculate that, in these physiological scenarios, the changes in DBP levels are an indirect consequence of direct influences upon VDR, however,

whether the *GC* gene possesses a vitamin D response element (VDRE) is currently unknown. **Chapter 5** discusses the relationship between skeletal muscle and DBP in greater detail, but further research into the regulatory role of VDR upon DBP would be of great interest.

4.4.2.4. Mitochondrial Function

The influence of the three different conditions upon mitochondrial respiration in was also investigated in both NC and VDR-KD myotubes by using high-resolution respirometry. However, the results for VDR-KD were unexpected and very similar for each stimulus so, to avoid repetition, they will be discussed collectively here.

NC IGF-1 - Traditionally, the hypertrophic effects of IGF-1 have been explained primarily by its influence upon MPS, however, some reports have questioned whether effects upon mitochondrial respiration may contribute. Previously published data from work conducted in C2C12 myotubes appeared to suggest that IGF-1 had a positive influence upon mitochondrial biogenesis and respiration [445], yet the results suggest otherwise. In fact, no significant differences in mitochondrial respiration were observed, in any of the investigated flux states, following treatment with IGF-1. This could be due to the length of time of the IGF-1 treatment, as Guan et al. used a 5-day exposure whereas, in this chapter, myotubes were incubated with IGF-1 for 24 hours [445]. However, IGF-1 deficiency in mice has been previously reported to have no effect upon skeletal muscle mitochondrial activity, thus providing support for the result presented here [446]. Definitively defining the influence of IGF-1

upon mitochondrial function in skeletal muscle was beyond the scope of this thesis, however it does represent an attractive area of research moving forwards.

NC Dexamethasone - Several lines of evidence have implicated dysfunctional mitochondria as a major contributor to muscle atrophy so, as anticipated, it was demonstrated that Dex treatment leads to impaired OXPHOS capacity of Complexes I and II (both individually and combined) and maximal respiratory capacity (ET) in NC myotubes [447,448]. In humans, chronic glucocorticoid administration has been associated with several factors of mitochondrial dysfunction, including altered transcription of mitochondrial related genes, mitochondrial enlargement and aggregation, and oxidative damage of mitochondrial DNA (mtDNA) [449]. Mitochondrial dysfunction has also been observed *in vitro* as glucocorticoid exposure resulted in ATP deprivation and declines in mitochondrial respiration in C2C12 myotubes [447].

NC Lipopolysaccharide - Given that impairment of microcirculatory perfusion is a primary pathological event in sepsis, it is logical to propose that LPS treatment would result in dysfunctional mitochondrial function and respiration [450]. To date, research investigating the influence of LPS upon mitochondrial physiology has been primarily focused upon hepatic mitochondria with only a handful of studies investigating this relationship in the context of skeletal muscle. Like IGF-1, no differences were observed in mitochondrial respiration following LPS treatment of NC myotubes. Experimental differences may be to

blame here as previous articles displaying negative effects of LPS upon mitochondrial respiration used different dosages of LPS (e.g. 50 pg/mL and 1 mg/mL), different exposure lengths (e.g. 2-12 hours), isolated mitochondria versus whole tissue, and different models (animal and cells) [451–453].

VDR-KD – Intriguingly, in VDR-KD myotubes the results were very similar across the three different treatments, as increased OXPHOS capacity of Complex I and Complexes I and II combined, and maximal respiratory capacity (ET) was observed in IGF-1, Dex, and LPS-treated myotubes. OXPHOS capacity of Complex II was increased by LPS only.

Initially, these observations appear counterintuitive given that VDR-KD resulted in impaired mitochondrial respiration in the absence of any of the investigated conditions, but it may be that the ideology of increased OCR always equating to improved mitochondrial function may have to be reconsidered. Enhancement of respiratory activity by VDR-KD has been demonstrated previously using the human keratinocyte cell line, HaCaT, and it is believed to be the result of increased generation of reactive oxygen species (ROS) [251]. It may be that, when cells are challenged by an external stimuli in the absence of VDR, elevated mitochondrial OCR represents a compensatory mechanism that acts to protect against the cellular environment induced by VDR-KD and the treatment (i.e. IGF-1, Dex, or LPS). Indeed, it is difficult to be certain on how mitochondria in these challenged VDR-KD myotubes are utilising the increased volume of oxygen that they are consuming, and it is likely

that this adaptive mechanism is transient with mitochondrial function breaking down eventually. Confirming this would require future experiments with time points beyond 24 hours.

All three conditions used in the investigations conducted herein have previously been shown to promote ROS generation in skeletal muscle *in vivo* and/or *in vitro* [452,454–457]. In addition, it appears that VDR acts as a negative regulator of ROS levels as ROS synthesis is increased in the absence of VDR and models of vitamin D deficiency whilst VDR upregulation suppresses ROS generation [251,458,459]. At lower levels, ROS are considered as key regulators of multiple cellular processes, e.g. proliferation and metabolism, but excessive ROS production/accumulation results in mitochondrial damage and, ultimately, mitochondrial-induced apoptosis [460,461]. Following treatment of VDR-KD with all three conditions, an increase in the maximal OXPHOS capacity of Complex I was observed, whose capacity for ROS production is high [462], but as ROS levels were not measured in the investigations conducted in this chapter, it can only be speculated based on previous evidence that a combination of VDR-KD and the conditions used here caused ROS levels to rise, thus requiring a greater OCR.

4.4.3 Limitations

As with any scientific study, it is important to consider the limitations of the work; of which there are several associated with the model and protocols used throughout this chapter.

Firstly, there have been reports of Lipofectamine transfection reagents exerting cytotoxic effects so a vehicle control group (Lipofectamine only) would have been useful to clarify whether transfection-mediated cytotoxicity, if any, may have influenced any of the investigated outcomes [463]. Due to multiple issues in the development and maintenance of a stably transfected VDR-KD cell line, it was decided to use siRNA instead, but this does have its drawbacks as siRNA only provides transient suppression of VDR-mediated signalling while stable transfection would have permitted VDR silencing throughout all stages of myogenesis. In addition, due to the nature of the siRNA technique, off-target effects cannot be eliminated. For the three different conditions, all experiments were conducted 24-hours post-treatment. Whilst this timeframe is routinely used in laboratory protocols, further time points (e.g. at 3- and 12-hours post-treatment) may have provided information on how the cellular response evolved to what was observed at 24 hours. In NC myotubes treated with the three different conditions, data was only available for *Vdr* mRNA expression not protein levels. Having the protein level data for VDR would have given a more accurate picture of how each condition altered VDR levels.

For the investigations into the influence upon mitochondrial physiology, the original plan was to investigate mitochondrial morphology and protein levels of key mitochondrial related proteins, as well as respiratory activity. Unfortunately, despite a lengthy validation process, I was unable to get the OXPHOS antibody cocktail to work with the samples. In addition, whilst the imaging protocol for MitoTracker was successfully validated and optimised, the

microscope and camera set up was incompatible with data collection. As the protocol uses permealised myotubes it is impossible to separate interfibrillar and subsarcolemmal mitochondria (IFM and SSM, respectively). It would be of interest to investigate whether the effects of VDR-KD are selective to a particular mitochondrial subpopulation, for example Dex has been shown to predominantly cause loss and dysfunction of IFM [447]. While high resolution respirometry can provide exceptionally useful data, the technique carries its own set of limitations. Use of a stirrer within each O2K chamber ensures even oxygenation of the medium and sample, yet this can generate shear forces that may potentially exert physiological stress upon the cells placed within the chamber. In addition, supraphysiological oxygen concentrations are required to overcome diffusion limitations. I ensured to treat all samples identically and use the same oxygen concentrations throughout, but it is important to consider that the experimental conditions do not necessarily match normal physiology.

Given that that differentiation was seemingly affected by VDR-KD, considerations must be made with regards to drawing comparisons between myoblasts and myotubes. In the VDR-KD cells, it can be assumed that as differentiation was impaired in the absence of VDR, there would be a greater number of myoblasts present. As the primary energy source shifts from glycolysis to OXPHOS during myogenic differentiation, the metabolic profiles of myoblasts and myotubes are, consequently, very different [464]Taking this into account, it is rational

to consider whether this could have somewhat contributed to the observed differences between NC and VDR-KD myotubes with regards to markers of cellular signalling and mitochondrial respiration [465,466]. Whilst this is an unavoidable limitation, given the nature of the knockdown model used, it is important to consider this when interpreting the results presented in this chapter.

Finally, and perhaps one of the biggest limitations of this chapter, is that it is unclear whether the conditions used did truly induce hypertrophy or atrophy. For both conditions, light microscopy images were taken of NC and VDR-KD from days 0 to 6 post-differentiation to ascertain whether myotubes were hypertrophic/atrophic, however, these images were lost due to corruption of my hard drive. This represents a huge flaw here as it meant that conclusions can be drawn based upon the gene and protein expression data only. Moving forwards, these experiments would need repeating with appropriate analysis of myotube images in order for true conclusions to be made with regards to hypertrophy and atrophy.

4.5 Conclusions

In this chapter, it was demonstrated that silencing of *Vdr* in C2C12 myotubes resulted in perturbed myogenic signalling and mitochondrial respiratory activity, therefore providing further evidence for a key regulatory role for VDR in skeletal muscle. VDR-KD myotubes were also exposed to IGF-1, dexamethasone, and lipopolysaccharides for 24 hours to generate models of hypertrophy, atrophy, and inflammation, respectively. In the absence of VDR, IGF-1 was unable to activate the PI3K/Akt/mTOR pathway and it appears that VDR is not involved in IGF-1 regulation of autophagy. Based on the current literature, it seems that this is the first report to demonstrate upregulation of *Vdr* by dexamethasone in C2C12 NC myotubes and the data presented here suggests that VDR may be a negative regulator of *Myf5* expression. This also represents the first line of evidence to suggest that LPS downregulates *Vdr* expression and DBP protein levels C2C12 myotubes which, based on the data presented here and previous reports, may contribute to the pro-inflammatory environment created by LPS in skeletal muscle. Finally, exposure of VDR-KD myotubes to each of the three conditions resulted in increased mitochondrial respiratory activity in primarily Complex I and Complexes I and II combined. Whilst unexpected, it is possible that this may be a compensatory mechanism to overcome increased ROS production and metabolic demand.

Chapter 5: Characterisation of loss of the vitamin D binding protein (DBP) gene (*Gc)* in C2C12 myotubes – a preliminary study.

5.1 Introduction

So far, the focus of this thesis has been on investigating the role of the vitamin D axis in skeletal muscle with **Chapter 4** concentrating upon determining the impact of silencing of the *Vdr* gene in C2C12 myotubes. However, data from **Chapter 3** indicated a novel relationship between genetic variation within the gene encoding the vitamin D binding protein (DBP; *GC*) and skeletal muscle physiology and function, thus raising an interesting question – does DBP have a regulatory role in skeletal muscle?

DBP acts as the major transport protein for circulating vitamin D metabolites due to the presence of a single vitamin D metabolite binding cleft in its A domain [26]. It is primarily synthesised by the liver but gene and protein expression of DBP has also been detected in other tissues, such as stomach, gall bladder, pancreas, and cardiac muscle [27–29]. Aside from transporting vitamin D metabolites, DBP also has a high affinity for monomeric actin (G-actin) which allows DBP to be classified as a positive acute phase reactant [46,467]. An influx of intracellular actin into the circulation is a common occurrence following major tissue injury and reduced serum DBP levels are frequently observed in cases of severe trauma and/or illness [43,46,442,468,469]. Therefore, it has been hypothesised that DBP acts to form actin-DBP complexes

that are rapidly cleared from the bloodstream, thus avoiding the hypercoagulable profile that is stimulated by heightened actin levels [43].

Recent evidence has suggested that the actin-binding property of DBP is not limited to actin scavenging in circulation as it appears that DBP is also able to bind actin intracellularly. Indeed, 25(OH)D_3-bound DBP (25(OH)D_3-DBP) is internalised into the cell via the two transmembrane transport proteins, megalin and cubilin, as demonstrated in C2C12 myotubes [255]. Once in the cell, the 25(OH)D_3-DBP complex binds intracellular actin via the actin-binding site of DBP, therefore forming high-affinity storage sites for 25(OH)D_3. As actin is found in abundance within skeletal muscle cells, particularly within cytoskeletal actomyosin or throughout the sarcoplasm, and DBP has been shown to have a short residence time in rabbit skeletal muscle, it has since been proposed that skeletal muscle acts in the maintenance of vitamin D status [299]. As such, this hypothesis may explain the prolonged half-life (15-50 days) of circulating 25(OH)D_3, as release of 25(OH)D_3 from DBP following proteolytic degradation of actin-bound DBP-25(OH)D_3 allows it to re-enter the circulation and be immediately re-bound to circulating free DBP [255].

Given that it was demonstrated that certain SNPs of the DBP gene (*GC*), were associated with alterations to muscle strength and size in **Chapter 3**, it is reasonable to consider the underlying mechanisms of this relationship and what roles DBP possesses in skeletal muscle beyond those already discussed. *In vitro* investigations have displayed involvement of DBP in regulation of cell

morphology and glucagon secretion in pancreatic-α cells, as DBP silencing lead to reductions in cell size and hyperplasia with altered distribution of filamentous actin (F-actin) microfilaments [345]. Fusion of myoblasts into multinucleated myotubes relies on dramatic remodelling of the actin cytoskeleton, a tightly regulated multi-step process that, if disrupted, could lead to incomplete fusion, abnormally shaped myotubes and, ultimately, myofibres that are incapable of complete and efficient contraction [470]. As loss of DBP leads to altered actin arrangement in pancreatic-α cells, it raises the question of its influence upon cytoskeletal actin within skeletal muscle, particularly given the previously discussed role of DBP binding intracellular actin to provide storage sites for 25(OH)D_3. Furthermore, mRNA expression of DBP has previously been documented in C2C12 myotubes which would suggest that it plays a direct role in skeletal muscle [143]. However, articles investigating DBP in the physiological setting of skeletal muscle are severely lacking with studies only examining the effects of exogenous DBP and, whilst a DBP knockout (DBP-KO) mouse model has been generated, nothing has been published in relation to the skeletal muscle physiology of these mice [471,472]. As DBP appears to have several other functions than those already mentioned, i.e. in binding of fatty acids, inflammation, and glucagon secretion, it is sensible to ponder whether it has a role in skeletal muscle cell function beyond storage of 25(OH)D_3 [49,473–475].

Here, this chapter aimed to use RNA interference (RNAi) to knockdown *DBP* expression (*Gc*; DBP-KD) in C2C12 myotubes to provide a characterisation of the role of DBP in skeletal muscle for the first time.

5.2 Methods

5.2.1 Cell Culture

Murine C2C12 myoblasts (ECACC, Salisbury, UK) were cultured and maintained in Dulbecco's Modified Eagle Medium (DMEM; Thermo Fisher Scientific) supplemented with 10% (v/v) fetal bovine serum (FBS), 1% (v/v) antibiotic-antimycotic solution, and 4mM L-Glutamine (all Sigma-Aldrich, UK) at 37°C with 5% CO_2. Cells (passage 8) were seeded onto 6-well plates (Nunclon™ Delta: Thermo Fisher Scientific) and upon reaching 70-80% confluency, differentiation was induced by switching to DMEM with reduced serum (2% FBS (v/v)). The day on which differentiation was induced is referred to as day 0. Media changes were performed every 48 hours.

5.2.2 RNA Interference

A small-interfering RNA (siRNA) sequence targeting vitamin D binding protein (DBP; *GC*) was used (Sigma Aldrich; EHU011421) and all knockdown experiments were performed in parallel with cells transfected with a Universal Negative Control siRNA (Sigma Aldrich; SIC001). At day 2 post-differentiation, cells were transfected with 25 pmol DBP or negative control (NC) siRNAs using the Lipofectamine RNAiMAX Transfection Reagent (Invitrogen) diluted in Opti-MEM (Gibco) following manufacturer's instructions.

The DBP eSIRNA sequence was as follows:

TGTGATCCAGGAAACACCAAAGTCATGGATAAGTATACATTTGAACTAAGCAGAAGGACTCATCTTCC
GGAAGTATTCCTCAGTAAGGTACTTGAGCCAACCCTAAAAAGCCTTGGTGAATGCTGTGATGTTGAAG
ACTCAACTACCTGTTTTAATGCTAAGGGCCCTCTACTAAAGAAGGAACTATCTTCTTTCATTGACAAGG

GACAAGAACTATGTGCAGATTATTCAGAAAATACATTTACTGAGTACAAGAAAAAACTGGCAGAGCG
ACTAAAAGCAAAATTGCCTGATGCCACACCCACGGAACTGGCAAAGCTGGTTAACAAGCACTCAGAC
TTTGCCTCCAACTGCTGTTCCATAAACTCACCTCCTCTTTACTGTGATTCAGAGATTGATGCTGAATTGA
AGAATATCCTGTAGTCCTGAAGCATGTTTATTAACTTTGACCAGAGTTGGAGCCACCCAGGGGAATGA
TCTCTGATGACCTAACCTAAGCAAAACCACTGAGCTTCTGGGA

5.2.3 Light Microscopy

Images of myotubes (magnification: 4x) were taken each day on an inverted light microscope (EVOS XL Core: Invitrogen), starting from day 0 of differentiation to day 5 post-differentiation, to determine the effect of DBP knockdown upon C2C12 myotube morphology. At least ten fields were taken per well and at least 60 images were captured per plate.

5.2.5 qRT-PCR

RNA was extracted using the phenol-chloroform method [371]. At day 5 post-differentiation, cells were scraped into 200 µl TRI reagent (Sigma Aldrich), and then incubated at room temperature and pressure (RTP) for 10 minutes. For the phase separation step, 40 µl chloroform (Fisher) was added and incubated for a further 10 minutes at RTP before samples were centrifuged at 12,000 rpm for 15 minutes at 4°C. The upper aqueous phase was transferred into a fresh Eppendorf (Eppendorf) and equal volume 100% isopropanol (Sigma) and 1 µl GlycoBlue (Invitrogen) were added to precipitate the RNA. Samples were centrifuged for 5 minutes at 7,000 rpm and 4°C, and the resulting RNA pellet was washed three times with 80% ethanol. Following removal of all ethanol

after the third and final wash, the pellet was left to air dry and subsequently resuspended in 20 µl Nuclease Free DEPC-treated water (Invitrogen). Sample concentration and purity (260/280 ratio) was determined using a Nanodrop 1000 (Thermo Scientific), and samples were stored at -80°C until further use.

Reverse transcription was performed using a High-Capacity cDNA Reverse Transcription kit (Applied Biosystems) and quantitative reverse transcriptase PCR (qRT-PCR) was subsequently performed on a ViiA7 Real-Time PCR system (Life Technologies) using SYBR Select Master Mix (Applied Biosystems) and primers designed in-house (**Table 5.1**). Thermal cycling conditions were as follows: 2 minutes at 50°C, 10 minutes at 95°C, 40 cycles of 15 seconds at 95°C, and 1 minute at 60°C. Samples were run in triplicate with two control samples, one without reverse transcriptase and one without cDNA, as negative controls. Gene expression (relative fold change) was quantified by normalising against GAPDH using the $2^{-\Delta\Delta CT}$ method [372].

Table 5.1. Primers used in qRT-PCR.

Gene Target	Forward Primer (5'-3')	Reverse Primer (5'-3')
Gapdh	TGGAAGGGCTCATGACCACAG	ACCAGTGGATGCAGGGATGA
Vdr	TCCCCCATCCCTAGAACCAGC	TCCTCATTGCTTGGGCTCTG
Foxo1	AACCAAAGCTTCCCACACAGT	AAGGACTTTTAAATGTAGCCTGC
Foxo3	GAAGGGAAGGAGCCGAGGTAG	TCCACTTCGAGCGGAGAGAG
Foxo4	TCATCAGCCAGGCCATTGAA	TTGTGACGGATGGAGTTCTTC
Mtor	TTCCTGAACAGCGAGCACAA	GTAGCGGATATCAGGGTCAGG
Eif4ebp1	GGTTGCTGGAGGGTCGTG	TAGATAATCCTGGTTCCTCCCG
Prkaa1	GGCAAAGTGAAGACTACCAGG	CTCTTCAACCCGCCCATGT
Tsc2	GAACTGAGTGGTGAATGCGG	CTCCACTGCATGCTCCTCAA
Pax7	TTCGATTAGCCCAGTGCTCA	ATCCAGACGGTTCCCTTTGT
Cubn	GGCTCCAAGTCCCATTGTCA	AATGTACGTCCACAACGGCT
Lrp2	GGCATAGGCCTCAGTGTTGT	GGGAAGGTAGGCACGTTTGA
Myh8	CACACCCTATCTCCGCCAAG	AGCCGAGGTTTCAGCTATGG
Myf5	TCAGGAATGCCATCCGCTAC	CCCGGCAGGCTGTAATAGTT
Slc2a1	CTTATGTTGGCCGTGGGAG	CTCTCCATAGCGGTGGTTCC
Slc2a4	GGCCATCGTCATTGGCATTC	TGTGAGAGCCAGAAGCAGTG
Mrf4	GAGATTCTGCGGAGTGCCAT	GCTCCTCCTTCCTTAGCAGT
Myh1	GCATCCCTAAAGGCAGGCTC	CAAACACCGATGACTTGGCG
Myh7	CCCAACCCTAAGGATGCCTG	GGCATCCTTAGGGTTGGGTAG
Rps6	CTTTTTCGTGACGCCTCCCA	ATCCGGACCACATAACCCTTC
Rps6kb1	TTATTTCGGGAGCAAGGGGG	ACAATGTTCCATGCCAAGTTCA
Hdac9	CTCACCGAATCCGCATGACT	ATTGGCTTTGTGAGGACGGT
Ppp3ca	AAAGCGCTACTGTTGAGGCT	GTCCGTGCCGTTAGTCTCTG
Myog	AGGAGATCATTTGCTCGCGG	ATCCTCCACCGTGATGCTGT
Myod1	TGCTCTGATGGCATGATGGAT	CACTGTAGTAGGCGGTGTCG

Ccnd1	**TCAAGTGACCCGGACTGC**	**CCTTGGGGTCGACGTTCTG**
Cdkn1a	**TTGTCGCTGTCTTGCACTCT**	**TTTCGGCCCTGAGATGTTCC**
Tuba1a	**AAGCAGCAACCATGCGTGA**	**CCTCCCCCAATGGTCTTGTC**
ActB	**TATAAAACCCGGCGGCGCA**	**GTCATCCATGGCGAACTGGTG**

Abbreviations*: Gapdh,* Glyceraldehyde 3-phosphate dehydrogenase; *Vdr,* vitamin D receptor; *Foxo1,* forkhead box protein O1; *Foxo3,* forkhead box protein O3; *Foxo4,* forkhead box protein O4; *Mtor,* mechanistic target of rapamycin; *Eif4ebp1,* Eukaryotic translation initiation factor 4E-binding protein 1*; Prkaa1,* AMP-Activated Protein Kinase, Catalytic, Alpha-1*; Tsc2,* tuberous sclerosis complex 2; *Pax7,* paired box protein 7; *Akt,* AKT serine/threonine kinase 1; *Cubn,* cubilin; *Lrp2,* megalin; *Myh8,* myosin heavy chain 8; *Myf5,* myogenic factor 5; *Slc2a1,* glucose transporter protein type 1 (GLUT1)*; Slc2a4,* glucose transporter protein type 4; *Mrf4,* myogenic regulatory factor 4; *Myh1,* myosin heavy chain 1; *Myh7,* myosin heavy chain 7; *Rps6,* ribosomal protein 6; *Rps6kb1,* ribosomal protein S6 kinase B1*; Hdac9,* histone deacetylase 9; *PPP3ca,* protein phosphatase 3 catalytic subunit alpha; *Myog,* myogenin; *Myod1,* myoblast determination protein 1; *Ccnd1,* Cyclin D1; *Cdkn1a,* cyclin dependent kinase inhibitor 1a; *Tuba1a,* α-tubulin; *ActB,* β-actin.

5.2.6 Western Blotting

At day 5 post-differentiation, cells were homogenised and scraped into ice-cold homogenisation buffer (10 mM β-glycerophosphate disodium salt, 50 mM NaF, 1 mM EGTA, 1 mM EDTA, 1 mM activated Na_3VO_4, and 50 mM Tris·HCl (pH 7.4)) followed by centrifugation of lysates at 11,000 *g* for 10 minutes at 4°C. The supernatant was removed to quantify protein content via Nanodrop. Depending on initial protein concentration, all samples were appropriately diluted in homogenisation buffer and 1x Laemmli buffer to the same concentration.

Samples were loaded onto a Criterion XT Bis-Tris 12% SDS-PAGE gel (Bio-Rad) and ran electrophoretically at 200V for one hour. The resulting separated proteins were then transferred onto a PVDF membrane at 100V for 45 minutes, followed by a one-hour blocking stage using 2.5% milk in 1x Tris buffered saline with 0.1% Tween-20 detergent (1x TBST) with gentle agitation. Membranes were subsequently incubated with their corresponding primary antibody solutions at 4°C overnight after which they were washed for five minutes three times with 1x TBST and incubated at RTP with the HRP-conjugated secondary antibody (anti-rabbit; Cell Signalling #7074S). After an hour, membranes were washed again three times for five minutes with 1x TBST and subsequently incubated in Millipore HRP reagent (Millipore) for five minutes at RTP. Membrane visualisation was performed with a Chemidoc XRS (BioRad), and bands were quantified using ImageLab software (Version 6.1).

Data was normalised to total loaded protein as visualised by staining with Coomassie brilliant blue (CBB) R250. Primary antibodies were all purchased from Cell Signalling (unless stated otherwise), diluted 1:2000, and were as follows: Total-ULK1 (#8054P), Total p70S6K (#9202S), Total Akt (#4685S), Total AMPKα (#5832P), phospho-EIF4E (p-EIF4E; #9741S), phospho-AMPKα (p-AMPKα; #2535S), phospho-4EBP1 (p-4EBP1; #2855S), phospho-Akt (p-Akt; #9271S), phospho-mTOR (p-mTOR; #2971S), phospho-p70S6K (p-p70S6K; #9234S), phospho-ULK1 (p-ULK1; #14202S), LC3B-II (#2775S), Beclin-1 (#3495T), β-Tubulin (#2128P), β-actin (#4968S), and GLUT4 (#2213S). VDR (ab109234) and DBP (ab65636) were both purchased from Abcam.

5.2.8 Statistical Analysis

For statistical comparisons, the D'Agostino and Pearson test was first performed to assess for normality. Statistical differences between groups were then assessed using either a Student T-test (for parametric factors) or a Mann Whitney U test (for non-parametric factors). All analyses were performed by a two-way ANOVA followed by post hoc testing for multiple comparisons. All data is represented as mean ± standard deviation (SD) of the mean. Statistical analysis was performed using GraphPad Prism statistical software (Version 7.0a) (La Jolie, CA, USA) with statistical significance set at * $p < 0.05$.

5.3 Results

5.3.1 Successful generation of DBP-KD C2C12 Myotubes.

To silence DBP, gene knockdown was performed via RNAi in C2C12 myoblasts at day 2 post-induction of differentiation. Following siRNA transfection, DBP protein levels were significantly reduced compared to the negative control (NC) by 68.61% (*P* = 0.0074; **Figure 5.1**).

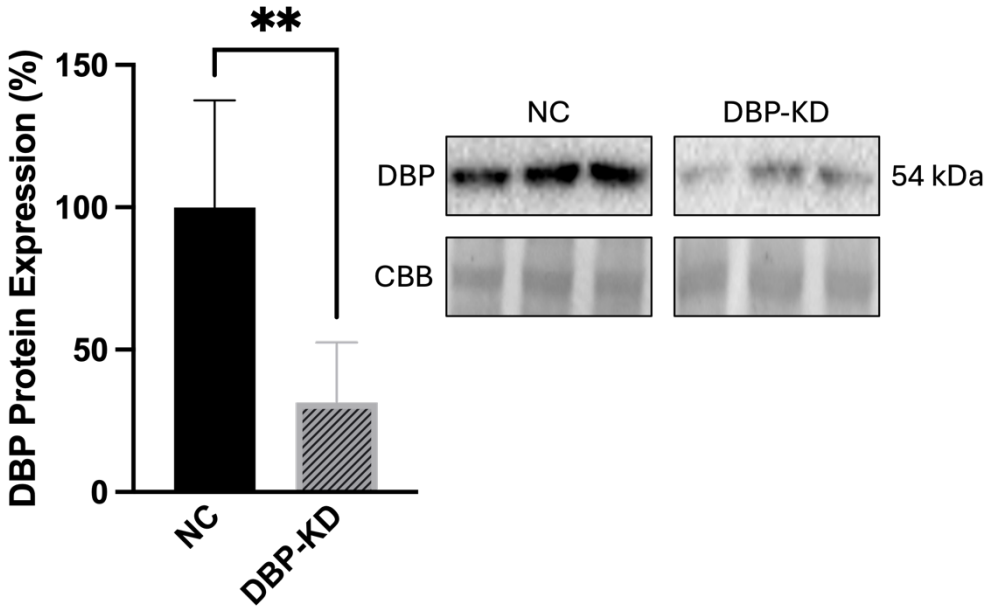


Figure 5.1. Successful generation of DBP-KD C2C12 myotubes. Representative western blot and quantification of KD. Data is shown as mean ± SD (n = 6). ** *P* < 0.01. Abbreviations: *%,* percent; *NC,* negative control; *DBP,* vitamin D binding protein; *KD,* knockdown; *CBB,* coomassie brilliant blue; *kDa,* kilodaltons.

5.3.2 Effect of DBP-KD upon C2C12 myotube morphology

Images were taken daily using an inverted light microscope from day 0 differentiation (when media was switched to differentiation media) to determine the influence of DBP-KD upon myotube morphology.

At day 5 differentiation, DBP-KD myotubes appeared dysmorphic and disorganised (**Figure 5.2**). NC myotubes were more unidirectional whilst DBP-KD resulted in areas of dense myotube overlapping with notable branching.

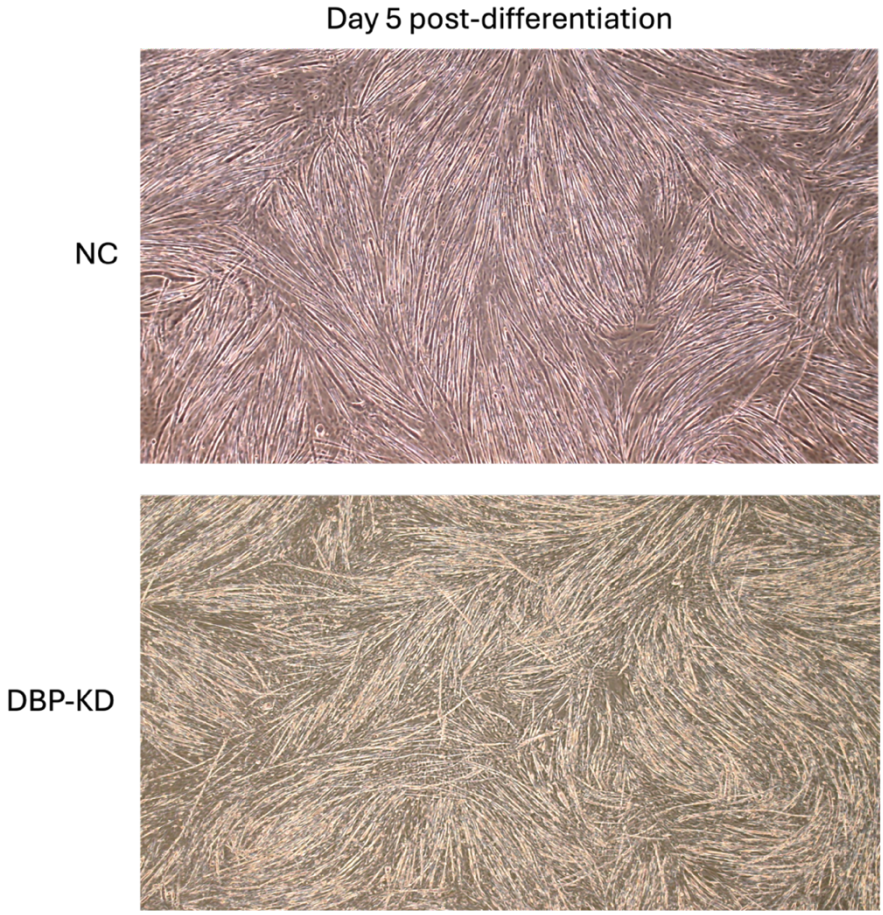


Figure 5.2. Light microscopy images of NC and DBP-KD C2C12 myotubes at day 5 differentiation displaying myotube disorganisation, branching, and overlapping in the DBP-KD group. Images were taken at 4x magnification. Abbreviations: *NC,* negative control; *DBP,* vitamin D binding protein; *KD,* knockdown.

5.3.3 Effect of DBP knockdown in C2C12 myotubes upon mRNA and protein expression of key metabolic targets.

To characterise the effects of DBP-KD in C2C12 myotubes, expression levels of key metabolic genes and proteins were quantified via qRT-PCR (**Figure 5.3**) and

western blotting (**Figure 5.4**), respectively. Values are compared to that of the negative control (NC) myotubes.

5.3.3.1 *Targets Related to Anabolism/Catabolism*

At mRNA level, altered gene expression of key anabolic targets was observed in DBP-KD myotubes with significant reductions in *Mtor* (P = 0.0285) and *Rps6kb1* (P = 0.0047), while *Eif4ebp1* (4EBP1) was significantly increased (P = 0.0115; **Figure 5.3**). When quantified at protein level, levels of the key anabolic targets p-4EBP1, p-EIF4E, and p-p70S6K were all significantly lower in DBP-KD myotubes compared to the NC (P = 0.0136, 0.0260, and <0.0001, respectively; **Figure 5.4**). Protein levels of T-ULK1, LC3B-II, and Beclin-1 were all significantly higher in DBP-KD myotubes (P = 0.0152, 0.0022, and 0.0107, respectively) but these myotubes also displayed lower levels of p-AMPKα (P = 0.0001; **Figure 5.4**).

5.3.3.2 *Metabolic-Related Targets*

Significant reductions in mRNA levels of the epigenetic factor *Hdac9,* the calcium (Ca^{2+}) handling gene, *Ppp3ca,* and the cell-cycle regulator *Cdkn1a* were observed in DBP-KD myotubes (P = <0.0001, 0.0003, <0.0001, respectively; **Figure 5.3**). In addition, DBP-KD was associated with significant declines in mRNA expression of *Foxo3* and *Foxo4* (P = 0.0006 and <0.0001, respectively; **Figure 5.3**).

5.3.3.3 *Myogenic*-Related *Targets*

Genes encoding the myogenic regulatory factors (MRFs), *Myf5* and *Mrf4*, were significantly increased following DBP-KD (*P* = 0.0056 and <0.0001, respectively), whilst expression of *Myod1* was significantly reduced (*P* = 0.0104; **Figure 5.3**).

5.3.3.4 *Cytoskeletal & Sarcomeric-Related Targets*

Intriguingly, mRNA expression of *Tuba1a* (α-tubulin) was significantly lower in DBP-KD myotubes (*P* = 0.0128; **Figure 5.3**) and, when examined at protein level, β-tubulin was increased following DBP-KD (*P* = 0.0295; **Figure 5.4**). No significant changes were seen in any of the sarcomeric-related genes investigated, i.e. *Myh1, Myh7,* and *Myh8.*

5.3.3.5 *Glucose Trafficking-Related Targets*

DBP-KD resulted in altered expression of targets related to glucose trafficking, with mRNA expression of *Slc2a1* (Glut1*)* and *Slc2a4 (*Glut4*)* being increased following DBP-KD (*P* = 0.0002 and <0.0001, respectively; **Figure 5.3**). However, protein levels of Glut4 were unaltered by DBP-KD (**Figure 5.4**).

5.3.3.6 *Vitamin D Axis-Related Targets*

Finally, whilst mRNA expression of *Vdr* was significantly reduced in DBP-KD myotubes (*P* = 0.0004; **Figure 5.3**), no changes were seen at protein level (**Figure 5.4**). In addition, DBP-KD displayed significantly lower *Cubn* mRNA expression (*P* = 0.0001) with *Lrp2* expression remaining unaltered (**Figure 5.3**).

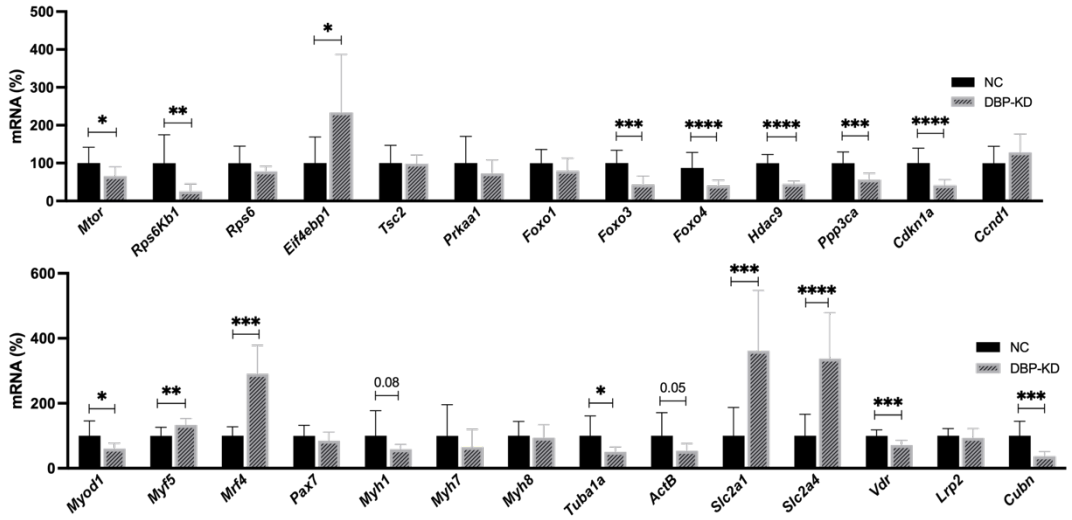


Figure 5.3. Effect of DBP-KD upon mRNA expression of key metabolic and myogenic targets as measured by qRT-PCR. Data is shown as mean ± SD (n = 6). * $P < 0.05$, ** $P < 0.01$, *** $P < 0.001$, **** $P < 0.0001$. Abbreviations: *mRNA,* messenger ribonucleic acid; *%,* percent; *Vdr,* vitamin D receptor; *Foxo1,* forkhead box protein O1; *Foxo3,* forkhead box protein O3; *Foxo4,* forkhead box protein O4; *Mtor,* mechanistic target of rapamycin; *Eif4ebp1,* Eukaryotic translation initiation factor 4E-binding protein 1*; Prkaa1,* AMP-Activated Protein Kinase, Catalytic, Alpha-1*; Tsc2,* tuberous sclerosis complex 2; *Pax7,* paired box protein 7; *Akt,* AKT serine/threonine kinase 1; *Cubn,* cubilin; *Lrp2,* megalin; *Myh8,* myosin heavy chain 8; *Myf5,* myogenic factor 5; *Slc2a1,* glucose transporter protein type 1 (GLUT1)*; Slc2a4,* glucose transporter protein type 4; *Mrf4,* myogenic regulatory factor 4; *Myh1,* myosin heavy chain 1; *Myh7,* myosin heavy chain 7; *Rps6,* ribosomal protein 6; *Rps6kb1,* Ribosomal Protein S6 Kinase B1*; Hdac9,* histone deacetylase 9; *PPP3ca,* protein phosphatase 3 catalytic subunit alpha; *Myog,* myogenin; *Myod1,* myoblast determination protein 1; *Ccnd1,* Cyclin D1; *Cdkn1a,* cyclin dependent kinase inhibitor 1a; *Tuba1a,* α-tubulin; *ActB,* β-actin; *NC,* negative control; *DBP,* vitamin D binding protein; *KD,* knockdown.

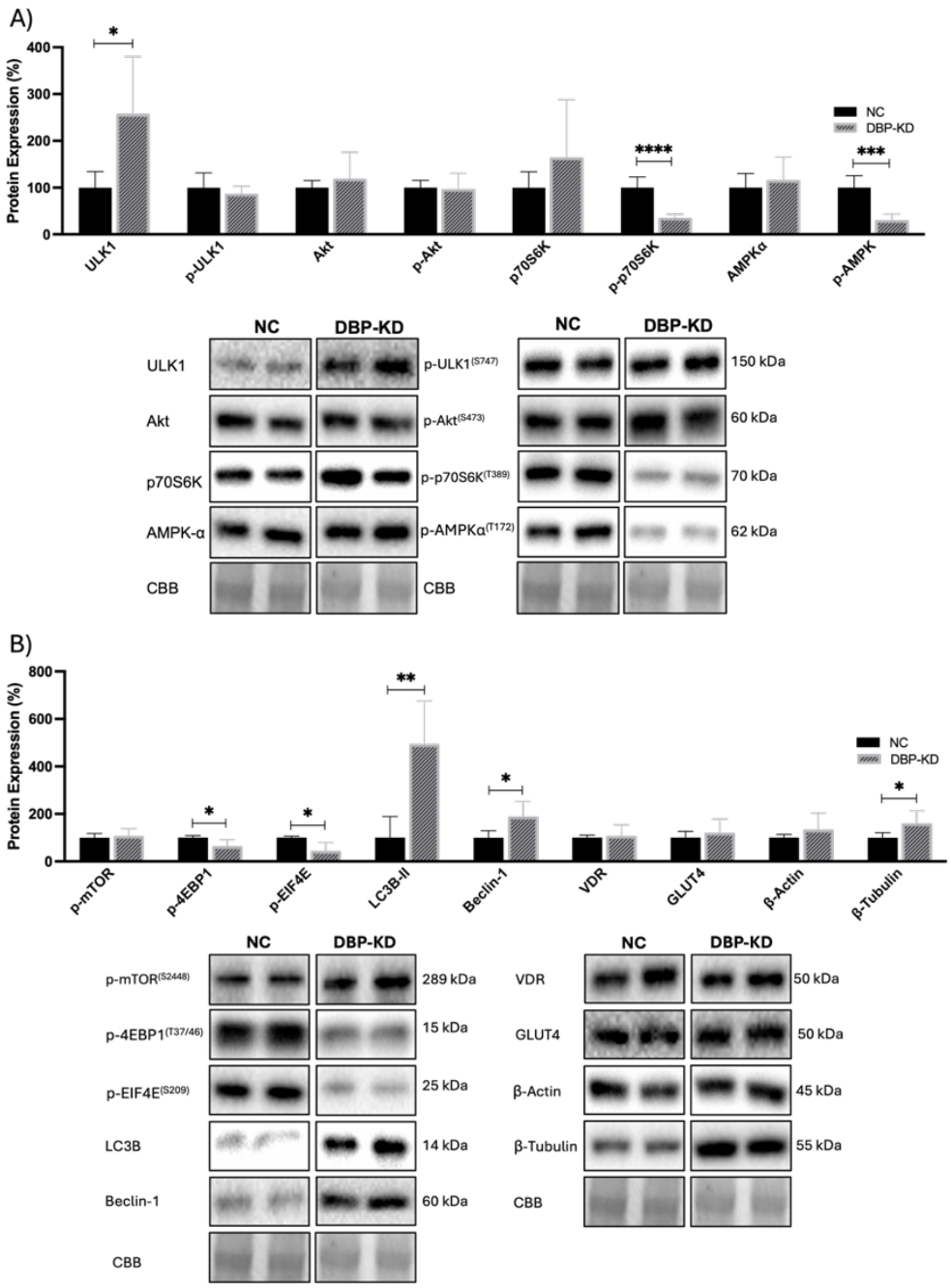


Figure 5.4. Effect of DBP-KD upon protein expression of (A) non-phosphorylated and phosphorylated forms of key anabolic and catabolic targets, and (B) key metabolic targets as measured by western blotting. Representative blots are displayed here, and data is shown as mean ± SD (n = 6). * $P < 0.05$, ** $P < 0.01$, *** $P < 0.001$, **** $P < 0.0001$. Abbreviations: *%,* percent; *p-,* phosphorylated; *ULK1*, unc-51-like autophagy-activating kinase 1; *p70S6K*, ribosomal protein S6 kinase β-1; *Akt*, AKT serine/threonine kinase 1; *AMPKα*, AMP-activated protein kinase; *EIF4E*, eukaryotic translation initiation factor 4E; *4EBP1*, eukaryotic translation

initiation factor 4E-binding protein 1; *mTOR*, mechanistic target of rapamycin; *LC3B-II*, microtubule-associated proteins 1A/1B light chain 3B; *GLUT4*, glucose transporter protein type 4; *VDR*, vitamin D receptor; *DBP*, vitamin D binding protein; *NC,* negative control; *KD,* knockdown; *CBB,* coomassie blue; *kDa,* kilodalton.

5.4 Discussion

To date, the relationship between DBP and skeletal muscle has only been researched in the context of maintenance of vitamin D status and no investigations have been made into whether DBP has a role in skeletal muscle beyond storage of $25(OH)D_3$. For the first time, in this chapter, DBP-KD myotubes were successfully generated by performing RNAi in C2C12 myotubes and demonstrated that loss of DBP results in perturbed expression of key metabolic and myogenic related targets at both mRNA and protein level. In addition, alterations to key targets involved in glucose uptake were observed, supporting previous reports of involvement of DBP in glucose homeostasis [345,475,476].

5.4.1 Effects of DBP-KD

Following RNAi, DBP protein levels were reduced by 68.61% compared to those transfected with NC siRNA, however, I was unable to detect DBP (*Gc*) mRNA. This is a direct contradiction of previous work demonstrating the presence of DBP (*Gc*) mRNA expression in C2C12 myotubes [143], but it is possible that this discrepancy may be due to experimental differences. In the work conducted for this chapter, all samples were collected at day 5 differentiation, whereas Girgis et al. only state that experiments were performed in myotubes and do not provide specific information with regards to what day post differentiation their experiments were performed at [143]. Another possibility is that DBP (*Gc*) mRNA levels may decline throughout the latter stages of myotube

differentiation to levels that are too low to detect but this is unlikely due to the high sensitivity of qRT-PCR.

Myotubes treated with DBP siRNA (DBP-KD) appeared dysmorphic with overlapping, branching, and growth in irregular directions (as opposed to being unidirectional), thus implying incomplete myoblast fusion. This is supported by altered mRNA expression of key myogenic targets that are imperative in the regulation of myogenic differentiation. As discussed in **Chapter 4**, myoblast determination protein (MYOD1) and myogenic factor 5 (MYF5) are both considered as "gatekeepers" in the commitment of stem stells to myogenic lineage, whilst myogenic regulator factor 4 (MRF4; also known as herculin or, in humans, MYF6) is required for stimulating the transition into multinucleated fibres. Following DBP-KD, mRNA expression of *Mrf4* and *Myf5* was upregulated whereas *Myod1* was downregulated. *Myf5* has been found to be upregulated in skeletal muscle of MYOD1-KO mice and it has been proposed that this increased *Myf5* mRNA acts to compensate for the reduced expression and proteolytic degradation of MYOD1 [477]. Impairment of MYOD1 signalling has also been previously documented to be associated with compromised differentiation in atrophic C2C12 myotubes, whilst MYOD1 overexpression (MYOD1-OE) appears to protect against myotube atrophy [478]. Comparatively, MRF4 appears to act as a negative regulator of skeletal muscle mass and it signals via an autoregulatory positive feedback mechanism, so it is perhaps unsurprising to see that it was upregulated in this instance [479,480]. Whilst

this evidence can be used in support of the observations of impaired myotube differentiation, it is tricky to determine exactly how DBP influences these MRFs as, until now, they have never been studied together.

It is possible that the influence of DBP-KD upon MRFs may be a downstream result of alterations to the cytoskeleton, as DBP-KD was associated with altered expression of the microtubular proteins, α- and β-tubulin. Functioning as an intracellular frame and a major site of intracellular trafficking, microtubules (MTs) are composed of α- and β-tubulin dimers that are polymerised and assembled into linear protofilaments [481]. Upon fusion of myoblasts into myotubes, stabilisation of MTs is imperative to ensure correct orientation of myotubes, so it can be assumed that disruption of microtubular proteins during this highly regulated process will result in the formation of dysmorphic myotubes [482]. Indeed, previous data has proposed MT disruption as a contributing factor to dysfunction in atrophic and dystrophic rodent skeletal muscle [483,484]. Following DBP-KD, mRNA expression of the gene encoding α-tubulin (*Tuba1a*) was reduced, while protein levels of β-tubulin were significantly increased.

Synthesis of tubulin proteins is under the control of an autoregulatory negative feedback mechanism in which a rise in the concentration of intracellular tubulin subunits will lead to targeted degradation of mRNAs encoding tubulin [485]. While mRNA expression of *Tuba1b* (β-tubulin) and protein levels of α-tubulin were not measured, it is still possible to hypothesise that DBP-KD lead

to MT disruption with subsequent release of free tubulin dimers and degradation of tubulin mRNA. Intriguingly, β-actin and the three investigated isoforms of myosin heavy chain (Myh1, Myh7, and Myh8) were not altered following DBP-KD. Considering that loss of DBP in pancreatic α-cells lead to altered G-actin content, it was anticipated that DBP-KD would result in similar effects in C2C12 myotubes [345]. While β-actin protein levels were unaltered, mRNA expression of its encoding gene, *ActB*, appeared to be reduced, however, statistical significance was not quite reached ($P = 0.0522$). These results would indicate that, in skeletal muscle, the relationship between DBP and actin does not extend beyond the actin-binding properties of DBP, but further study is needed for confirmation.

Signalling within key anabolic and catabolic pathways was also altered by DBP-KD, with certain autophagic targets being upregulated. Considering that perturbed proteostasis is a common feature of skeletal muscle atrophy, both *in vitro* and *in vivo*, it is perhaps unsurprising that key anabolic targets were suppressed in DBP-KD myotubes given that they displayed dysmorphic morphology [486,487]. mRNA expression of *Mtor* was reduced following DBP-KD yet protein levels of p-mTOR remained unchanged. It is possible that the reductions in *Mtor* mRNA were reflected in declines in levels of total-mTOR, however, as levels of phosphorylated mTOR were unaltered it is possible to place confidence in that DBP-KD did not influence mTOR activity. Nevertheless, *Rps6kb1,* p-EIF4E, p-4EBP1, p-p70S6K were all downregulated by DBP-KD, thus indicating suppression of anabolic signalling in the absence of DBP.

Comparatively, it appears that DBP-KD also resulted in perturbed catabolic signalling. mRNA expression of two transcription factors possessing key roles in muscle atrophy, the forkhead box proteins (FOXO) -3 and -4 (*Foxo3* and *Foxo4*, respectively) were downregulated following DBP-KD. Previous reports have demonstrated pro-atrophic effects of FOXO3 in skeletal muscle, such as activation of the key catabolic targets Atrogin-1 and Muscle RING-Finger protein-1 (MuRF1), yet FOXO3 activity appears to decline with age, hence previous suggestions for a cytoprotective role [488–491]. On the other hand, FOXO4 expression does not appear to change over time and its role in skeletal muscle is currently unknown, so the significance of its downregulation in this instance is unclear [492].

As FOXO3 is a well-documented activator of autophagy it was anticipated that markers of autophagy would remain unchanged, given its downregulation following DBP-KD, yet this was not the case [493]. In fact, protein levels of two definitive markers of autophagy, Beclin-1 and microtubule associated protein 1 light chain 3-β II (LC3B-II) were both significantly increased by DBP-KD. These autophagic markers are downstream targets of Unc-51-like autophagy activating kinase 1 (ULK1) which is necessary for the induction of autophagy. Phosphorylation of ULK1 at Ser 757 by mTOR inhibits its activity, whilst phosphorylation by 5' adenosine monophosphate-activated protein kinase α (AMPKα) at Ser 317 and/or Ser 777 acts to stimulate ULK1 activity [494]. As protein levels of p-ULK1 (Ser 757) were unchanged following DBP-KD and there were no significant differences between levels of p-mTOR, it can be

hypothesised that the activity of ULK1 was not being inhibited. DBP-KD was associated with reduced levels of T-ULK1, so it is possible that ULK1 was being phosphorylated at other sites by AMPKα (e.g. Ser 317 or Ser 777). However, given that the suppressed levels of p-AMPKα seen in DBP-KD myotubes imply reduced AMPKα activity, it is therefore unlikely that autophagy is being induced through the AMPKα-dependent pathway. Instead, it can be hypothesised that DBP-KD induced autophagy via another pathway, for example protein kinase C-α (PKCα) can also phosphorylate ULK1 (Ser 317, 555, and 777) and has previously been proposed to activate autophagy via an AMPKα-independent mechanism [495].

Considerations must also be made with regards to how the relationship between DBP and the microtubular protein, tubulin, could indirectly influence early stages of autophagy, especially in the context of DBP-KD. MT dynamics have been implicated in autophagosome formation as demonstrated by certain forms of LC3 being found in MT-containing subcellular fractions and certain markers of autophagosome formation (e.g. Beclin-1 and ULK1) have been associated with dynamic MTs [496,497]. As previously discussed, DBP-KD resulted in reduced mRNA expression of α-tubulin and increased protein levels of β-tubulin, which could be the result of microtubular rearrangement due to increased autophagy. Future work should aim to look at post-translational modifications of tubulin (e.g. acetylation) in the context of DBP-KD, as this could provide further information with regards to the specific impact and mechanisms underlying DBP-KD and MT dynamics.

Previous research has demonstrated an association between DBP and glucose homeostasis, with reduced DBP serum levels being inversely correlated with insulin levels and glucagon secretion being negatively impacted by loss of DBP in pancreatic α-cells [345,498]. Therefore, the effect of DBP-KD upon two major glucose-trafficking-related targets in skeletal muscle, glucose transporter-1 (GLUT1) and -4 (GLUT4), was also investigated. At mRNA level, both *Glut1* and *Glut4* (encoded by *Slc2a1* and *Slc2a4*, respectively) were upregulated following DBP-KD, but protein levels of GLUT4 remained unaltered. Primarily contributing to basal glucose transport across the sarcolemma, GLUT1 expression decreases throughout differentiation thereby reflecting the metabolic shift from glycolysis to OXPHOS that occurs as myoblasts differentiate into myotubes [499,500]. Upregulation of GLUT1 in DBP-KD cells would perhaps suggest the presence of myoblasts, despite the experimental time point of day 5 differentiation, which would support the previously discussed observations of DBP-KD seeming to impair myogenic differentiation. In comparison, GLUT4 is the most abundant GLUT isoform in skeletal muscle and primarily functions as the major transporter in intracellular insulin- and contraction-stimulated glucose uptake [501]. While GLUT1 is downregulated during differentiation, GLUT4 has been reported to follow an opposing expression pattern, with expression being upregulated following myoblast fusion into myotubes [502]. Considering that neither NC or DBP-KD myotubes were stimulated with insulin or electrical pulse stimulation (EPS; an inducer of contraction *in vitro*), it can be suggested that, in DBP-KD myotubes, GLUT4 is being upregulated via other means. However, why GLUT4 protein levels

remained unchanged despite the significant increase in *Slc2a4* mRNA is unclear. It may be due to experimental timings, as samples were only collected at one time point and further time points may better reflect changes that might be occurring at protein level. Conversely, it appears that the translation efficiency of *Slc2a4* mRNA is regulated via specific post-translational events that may explain the unchanged GLUT4 protein levels [503]. While DBP-KD did indeed result in increased mRNA expression of *Slc2a4,* it is possible that the poly(A) tails of these mRNA are shorter, therefore reducing translational efficiency; however, this hypothesis would require experimental confirmation before definitive conclusions can be made [503].

Finally, as it was demonstrated in **Chapter 4** that VDR was able to regulate DBP protein levels, it was also investigated whether loss of DBP would influence expression levels of VDR and other key targets related to the vitamin D axis. DBP-KD resulted in downregulation of *Vdr* mRNA expression, but protein levels of VDR remained unchanged. Surprisingly, despite the development and availability of the DBP-KO mouse, there is a notable absence of studies investigating the impact upon VDR in this scenario. As previously discussed in relation to other investigated targets, it may be that VDR protein levels do fall in reflection of the reductions in *Vdr* mRNA and additional experimental time points would be required to investigate this. It is possible to speculate that DBP can indirectly regulate VDR levels via its ability to bind $25(OH)D_3$ and $1,25(OH)_2D_3$ in circulation, yet this would still not explain the result due to the *in vitro* nature of the work.

Intriguingly, while DBP-KD had no effect upon mRNA expression of the endocytic receptor megalin (*Lrp2*), its closely associated fellow endocytic coreceptor cubilin (*Cubn)* was significantly downregulated. These transmembrane proteins are responsible for trafficking 25(OH)D_3-DBP complexes into myotubes as, although megalin directly binds the 25(OH)D_3-DBP complex, cubilin facilitates the mechanism of endocytosis by sequestering 25(OH)D_3-DBP complexes on the cell surface where they can then subsequently associate with megalin [504]. However, until now, they have never been investigated in a DBP-KO model. Given that cubilin dysfunction, by inhibition and/or genetic mutation, results in increased urinary excretion of 25(OH)D_3 and reduced serum 1,25$(OH)_2D_3$ levels, it would suggest involvement of cubilin in 25(OH)D_3 metabolism [504]. If DBP can indeed regulate *Cubn,* then it is possible that this could provide a mechanism for altered serum 25(OH)D_3 levels in individuals carrying certain *GC* (DBP) SNPs that have been reported, not only by us in **Chapter 3,** but also by several other groups [505,506]. These *GC* SNPs have been previously proposed to influence the binding affinity of DBP for 25(OH)D_3 so, when also taking the data presented herein into account, it is possible to suggest that they also affect *Cubn* expression [339]. Indeed, if serum levels of 25(OH)D_3 are altered due to an individual carrying certain *GC* SNPs, then perturbation of endocytic trafficking by dysregulated *Cubn* will only contribute further.

5.4.2. Limitations

As with any scientific study, it is important to consider the limitations of the work; of which there are several associated with the model and protocols used throughout this chapter.

Firstly, there have been reports of Lipofectamine transfection reagents exerting cytotoxic effects so a vehicle control group (Lipofectamine only) would have been useful to clarify whether transfection-mediated cytotoxicity, if any, may have influenced any of the investigated outcomes [463]. While siRNA is a useful gene editing tool, it does have its drawbacks as siRNA only provides transient suppression of DBP-mediated signalling while permanent transfection techniques, e.g. CRISPR, would permit DBP silencing throughout all stages of myogenesis. In addition, due to the nature of the siRNA technique, off-target effects cannot be eliminated. As previously discussed, DBP-KD was not possible to validate at mRNA level. It is possible that *Gc* expression is variable and changes throughout the different stages of myogenic differentiation, but experimental confirmation is required.

For the investigations into the influence upon cytoskeletal proteins, I had originally planned to also perform an actin stain in NC and DBP-KD myotubes. Whilst the imaging protocol for actin was successfully validated and optimised, the microscope and camera set up was incompatible with data collection. Myotube images were taken on a light microscope at 4x and 20x magnification, however following data corruption, only the images taken at 4x magnification

were salvageable. Sadly, this represents a big limitation of the work conducted in this chapter as the images at 20x magnification would have provided data on multiple myotube morphology parameters, such as number, length, width, and fusion index. In addition, only mRNA levels of α-tubulin and protein levels of β-tubulin were investigated, whereas it would have been useful to have mRNA and protein level data for both targets.

Finally, a glucose uptake assay was performed but the samples were unable to be run on the appropriate machines due to time restraints as a consequence of a high volume of users and large queues. It would have been of interest to compare glucose uptake between DBP-KD cells and the NC. In addition, the fact that DBP-KD seemed to alter myogenic differentiation should be taken into consideration when interpreting the results. Given that rates of glucose uptake have been shown to be 2-fold higher in myotubes compared to myoblasts and that DBP-KD appeared to impair differentiation, it is possible that myoblasts were still present in DBP-KD [507]. The presence of these two metabolically distinct cell types could potentially explain differences seen between the DBP-KD and NC groups, and it is important to take this into account when interpreting the results with regards to cellular signalling and markers of glucose trafficking.

5.4 Conclusions

In this chapter, the effect of loss of DBP in C2C12 myotubes was investigated to provide further information regarding potential mechanisms underlying the relationship between DBP (*Gc*) SNPs and skeletal muscle, as demonstrated in **Chapter 3**. DBP-KD lead to the formation of dysmorphic myotubes with overlapping and branching and altered expression of key myogenic regulatory factors (MRFs). Surprisingly, actin expression was unaltered following DBP-KD, whereas mRNA expression of α-tubulin and protein levels of β-tubulin were up- and downregulated, respectively. DBP-KD myotubes displayed impairment of anabolic signalling with upregulation of certain autophagic targets, e.g. Beclin-1 and LC3B-II, suggesting that loss of DBP results in a catabolic environment. Like other groups, the data in this chapter suggests a regulatory role for DBP in glucose handling as DBP-KD resulted in upregulation of GLUT1 and GLUT4. Finally, *Vdr* mRNA expression was reduced by DBP-KD, but no change was seen at protein level and, intriguingly, *Cubn (*cubilin) was downregulated in the absence of DBP with no change to its coreceptor *Lrp2* (megalin). The work conducted in this chapter represents the first time that loss of DBP has ever been functionally studied in the physiological setting of skeletal muscle. Further work is required to confirm the results and to expand on certain observations. Whilst the data presented in this chapter may be preliminary, it provides the first line of evidence to suggest a functional role for DBP in skeletal muscle beyond binding actin to provide storage sites for 25(OH)D_3.

Chapter 6: General Discussion

6.1 Overview of Aims

As demonstrated by the narrative literature review conducted in **Chapter 1**, there is a large body of evidence demonstrating a direct regulatory role for the vitamin D axis in skeletal muscle. However, the overall understanding of the mechanisms underlying this relationship remains unclear. Therefore, this thesis aimed to explore the impact of genetic variation within the vitamin D system upon skeletal muscle function and to investigate the potential underlying mechanisms *in vitro*.

6.2 Summary of Results

6.2.1. Chapter 2 – The impact of genetic variation within the vitamin D pathway upon skeletal muscle function: a systematic review.

The systematic review conducted in **Chapter 2** provides the most up to date and extensive overview of the current existing knowledge regarding the relationship between genetic variation of the vitamin D system and skeletal muscle. Following an extensive literature search, 21 articles were included in the final review, of which 20 only studied genetic variation of the *VDR* gene. Of the included articles, 81% solely included individuals aged 50 years or older, and of the 9 studies that did not only include White individuals, only 2 included Black participants. *VDR* SNPs were significantly associated with altered muscle function and phenotypes in two or more studies. Of note, A1012G was

consistently significantly associated with increased handgrip strength (HGS), whilst results for other SNPs varied across studies.

6.2.2. Chapter 3 – The association of vitamin D receptor (VDR) and vitamin D binding protein gene (GC) single nucleotide polymorphisms with skeletal muscle function and performance in elite master athletes – a candidate gene association study.

Based on the results of the systematic review conducted in **Chapter 2,** a candidate gene association study was subsequently conducted in **Chapter 3** to investigate key SNPs of the genes encoding *VDR* and DBP (*GC)* in relation to skeletal muscle function and performance in a cohort of elite master athletes (MA). Like several other groups, no differences were found in those carrying the *VDR* SNPs BsmI, FokI, and TaqI. In MA, A1012G was significantly associated with increased HGS, which is in support of the observations from **Chapter 2,** whilst it was also demonstrated that A1012G carrying controls displayed higher maximal velocity on tests for lower limb power and increased serum levels of serum hormone binding globulin (SHBG). With regards to the *GC* gene, rs4588 was associated with higher maximal knee extensor strength (KE MVC) and peak quadriceps cross-sectional area (CSA) in controls only. Comparatively, those carrying rs7041 displayed lower bone mineral density (BMD). Based on the current available literature, the work conducted in **Chapter 3** represents the first study to explore the impact of two key *GC* SNPs, rs4588 and rs7041, upon multiple parameters of musculoskeletal physiology. The findings confirm an association between A1012G and greater muscle/physical function, whilst

highlighting novel links between the vitamin D system and sex hormones in muscle.

6.2.3. Chapter 4 – VDR regulates myogenic/proteolytic signalling and mitochondrial respiration in response to anabolic, catabolic, and pro-inflammatory conditions in C2C12 myotubes.

As it was demonstrated in **Chapters 2** and **3** that genetic variation within the *VDR* gene was associated with altered skeletal muscle function and physiology, the aim of **Chapter 4** was to investigate potential underlying mechanisms by silencing *Vdr* (VDR-KD) in C2C12 myotubes. In comparison to the negative control (NC), VDR-KD resulted in altered myogenic signalling, as demonstrated by reduced mRNA expression of *Myog*, *Mrf4*, and *Myod1*, whilst anabolic targets were downregulated following VDR-KD, i.e. mTOR, rps6, Akt and p70S6K. In addition, loss of VDR impaired mitochondrial respiratory activity as initially anticipated. NC and VDR-KD myotubes were stimulated with insulin growth factor 1 (IGF-1), dexamethasone (Dex), and lipopolysaccharides (LPS; from E.coli) for 24 hours to induce hypertrophic, atrophic, and pro-inflammatory states, respectively. In the absence of VDR, IGF-1 was unable to activate the PI3K/Akt/mTOR pathway and it appears that VDR is not involved in IGF-1 regulation of autophagy. For the first time, it can be reported that Dex upregulates *Vdr* expression, as demonstrated in NC myotubes, plus the data also suggests that VDR may be a negative regulator of *Myf5* expression. In addition, *Vdr* expression and DBP protein levels were downregulated following LPS exposure which, based on the data presented in **Chapter 4** and previous

reports, may contribute to the pro-inflammatory environment generated by LPS in skeletal muscle. Finally, exposure of VDR-KD myotubes to each of the three conditions increased mitochondrial respiratory activity in Complex I and Complexes I and II combined. This result was unexpected, and it is possible that it may act as a compensatory mechanism to overcome increased cellular ROS production and to meet metabolic demand.

6.2.4 Chapter 5 – Characterisation of loss of the vitamin D binding protein (DBP) gene (Gc) in C2C12 myotubes – a preliminary study.

For the first time, results from **Chapter 3** indicated a novel relationship between two SNPs of the gene encoding DBP (*GC*) and musculoskeletal parameters, therefore raising the question of whether DBP has a regulatory role in skeletal muscle. To investigate this relationship further, the *Gc* gene was silenced (DBP-KD) in C2C12 myotubes in **Chapter 5**. Loss of DBP resulted in the formation of dysmorphic myotubes that were branched and displayed areas of dense overlapping. These observations were accompanied by altered expression of the key myogenic factors, *MyoD1, Myf5,* and *Mrf4*. Despite previous reports of loss of DBP negatively impacting actin in other tissue types, it was found that actin expression was unaltered following DBP-KD, but mRNA expression of α-tubulin and protein levels of β-tubulin were up- and downregulated, respectively. Anabolic signalling was impaired by DBP-KD with DBP-KD myotubes displaying elevated levels of certain autophagic targets, e.g. Beclin-1 and LC3B-II. The observations of *GLUT1* and *GLUT4* mRNA upregulation by DBP-KD are in support of previous reports indicating

involvement of DBP in glucose handling. Finally, it appears that DBP can regulate key gene targets within the vitamin D axis as both *Vdr* and *Cubn* (cubilin) were downregulated in the absence of DBP.

6.3 Future Directions

It is clear that changes are required moving forward to ensure that future work addresses key issues and topics that will both further our knowledge and make research more inclusive.

6.3.1 Genetic Association Studies

One of the most glaring issues raised by the systematic review conducted in **Chapter 2** was that only a very small proportion of studies investigating genetic variation of genes within the vitamin D axis included Black individuals and other people of colour. Whilst this racial bias is not restricted only to the study of the vitamin D system, it does represent a major issue within the field of genetic research. By ensuring that these populations are better represented, improve the representativeness of results can be improved and the field can also move towards fully understanding the genetic basis of human physiology and disease.

To date, many GWAS and candidate gene studies have reported vitamin D axis-related SNPs that are seemingly associated with not only skeletal muscle, but also disease and/or pathological outcomes, yet these articles very rarely explore the mechanisms underlying these SNPs. Functional studies are crucial moving forward, as they could provide explanations for the genetic-phenotype

associations that exist between these SNPs, and they could provide further information on the genetic basis of the vitamin D axis. In addition, as it was found in **Chapter 2** that the vast majority of studies have only investigated the *VDR* gene in relation to skeletal muscle, exploration of genetic variation within other vitamin D axis-related genes, e.g. megalin (*LRP2*), in the context of skeletal muscle is imperative. Not only would it further our understanding of vitamin D physiology in relation to skeletal muscle health but it may also synthesise novel relationships and/or mechanisms that have been missed thus far.

Finally, the work conducted in **Chapter 3** represents the first time that the *GC* SNPS, rs4588 and rs7041, have been explored in relation to multiple parameters of musculoskeletal physiology. While the cohort of elite MA offers a unique population to study the impact of genetic variation upon muscular outcomes but in an aged cohort, the sample size is a major limitation. Therefore, it would be useful if these investigations were repeated but with a much larger sample size.

6.3.2 Mechanistic Studies

While **Chapters 4** and **5** both provided novel information with regards to the impact of loss of the *Vdr* and *Gc* genes, respectively, in C2C12 myotubes, further experiments are required to confirm these observations and to provide further information.

It is important to acknowledge that the nature of the knockdown models used here for VDR-KD and DBP-KD may not fully recapitulate effects of the SNPs identified in **Chapters 2** and **3**. The ideal method for functional characterisation of these SNPs would be to compare isolated cells from genotyped donors and it represents a promising research topic moving forwards.

As with any scientific project, there were planned experiments that could not be included in this final thesis, be that for validation or optimisation reasons, and/or time constraints due to delays with reagents. Future work should endeavour to focus on imaging investigations, i.e. mitochondrial labelling in VDR-KD myotubes and staining of filamentous actin in DBP-KD, while performing a glucose uptake assay in DBP-KD myotubes would provide further information with regards to the impact of loss of DBP upon glucose trafficking. In addition, while high resolution respirometry was used to investigate mitochondrial respiratory activity within VDR-KD myotubes, this technique has the scope to provide an array of related measures, such as ROS production, ATP levels, and mitochondrial membrane potential.

For the presented investigations, the murine myoblast cell line, C2C12, was used. This cell line has been frequently used within *in vitro* skeletal muscle research, but it obviously has its limitations being an immortalised line. Future studies should aim to conduct the experiments performed here in human derived skeletal muscle cells, as this would improve translatability of the research. In addition, while we demonstrated that VDR- and DBP-KD impaired

myogenic differentiation, this comes with an important caveat in that it is tricky to determine whether the differences seen are a direct result of the gene knockdown itself or the result of impaired myogenesis.

Despite the development of a DBP-KO mouse model exists, yet its skeletal muscle has never been investigated or characterised. It would be of great interest to functionally characterise the impact of loss of DBP upon skeletal muscle in these animals. Finally, the DBP-KD experiments conducted here represent the first line of investigations in which DBP has been investigated in the context of skeletal muscle. The results generated by these experiments need validating and investigating further before any definitive conclusions can be made.

References

1. Bollen SE, Bass JJ, Fujita S, Wilkinson D, Hewison M, Atherton PJ. The Vitamin D/Vitamin D receptor (VDR) axis in muscle atrophy and sarcopenia. *Cell Signal*. 2022;**96**: 110355. doi:10.1016/j.cellsig.2022.110355

2. Bollen SE, Atherton PJ. Myogenic, genomic and non-genomic influences of the vitamin D axis in skeletal muscle. *Cell Biochem Funct*. 2020; cbf.3595. doi:10.1002/cbf.3595

3. Bollen SE, Bass JJ, Wilkinson DJ, Hewison M, Atherton PJ. The impact of genetic variation within the vitamin D pathway upon skeletal muscle function: A systematic review. *J Steroid Biochem Mol Biol*. 2023;**229**: 106266. doi:10.1016/j.jsbmb.2023.106266

4. Tsiaras W, Weinstock M. Factors Influencing Vitamin D Status. *Acta Dermato Venereologica*. 2011;**91**: 115–124. doi:10.2340/00015555-0980

5. Schmid A, Walther B. Natural Vitamin D Content in Animal Products. *Advances in Nutrition*. 2013;**4**: 453–462. doi:10.3945/an.113.003780

6. Bates B, Lennox A, Prentice A, Bates C, Page P, Nicholson S, Swan G. National Diet and Nutrition Survey Results from Years 1, 2, 3 and 4 (combined) of the Rolling Programme (2008/2009–2011/2012). 2014.

7. Holick F. McCollum Award Lecture, 1994: Vitamin D - new horizons for the 21st century. *American Journal for Clinical Nutrition*. 1994;**60**: 619–630.

8. Holick MF. Vitamin D: A millenium perspective. *J Cell Biochem*. 2003;**88**: 296–307. doi:10.1002/jcb.10338

9. Holick MF, Tian XQ, Allen M. Evolutionary importance for the membrane enhancement of the production of vitamin D3 in the skin of poikilothermic animals. *Proc Natl Acad Sci U S A*. 1995;**92**: 3124–3126. doi:10.1073/pnas.92.8.3124

10. Holick MF. The cutaneous photosynthesis of previtamin D3: A unique photoendocrine system. *Journal of Investigative Dermatology*. 1981;**77**: 51–58. doi:10.1111/1523-1747.ep12479237

11. Feldman D, J Malloy P. Mutations in the vitamin D receptor and hereditary vitamin D-resistant rickets. *Bonekey Rep*. 2014;**3**: 1–11. doi:10.1038/bonekey.2014.5

12. Javorsky BR, Maybee N, Padia SH, Dalkin AC. Vitamin D Deficiency in Gastrointestinal Disease. *Pract Gastroenterol*. 2006;**36**: 52–72.

13. Marshall WJ, Bangert SK. Clinical Chemistry. 6th ed. Elsevier Ltd; 2008.

14. Hewison M, Burke F, Evans KN, Lammas DA, Sansom DM, Liu P, Modlin RL, Adams JS. Extra-renal 25-hydroxyvitamin D3-1α-hydroxylase in human health and disease. *Journal of Steroid Biochemistry and Molecular Biology*. 2007;**103**: 316–321. doi:10.1016/j.jsbmb.2006.12.078

15. Holick MF. Vitamin D Status: Measurement, Interpretation, and Clinical Application. *Ann Epidemiol*. 2009;**19**: 73–78. doi:10.1016/j.annepidem.2007.12.001

16. Khundmiri SJ, Murray RD, Lederer E. PTH and Vitamin D. Comprehensive Physiology. Wiley; 2016. pp. 561–601. doi:10.1002/cphy.c140071

17. Latic N, Erben RG. FGF23 and Vitamin D Metabolism. *JBMR Plus*. 2021;**5**. doi:10.1002/jbm4.10558

18. Liu S, Tang W, Zhou J, Stubbs JR, Luo Q, Pi M, Quarles LD. Fibroblast Growth Factor 23 Is a Counter-Regulatory Phosphaturic Hormone for Vitamin D. *Journal of the American Society of Nephrology*. 2006;**17**: 1305–1315. doi:10.1681/ASN.2005111185

19. Janoušek J, Pilařová V, Macáková K, Nomura A, Veiga-Matos J, Silva DD da, Remião F, Saso L, Malá-Ládová K, Malý J, Nováková L, Mladěnka P. Vitamin D: sources, physiological role, biokinetics, deficiency, therapeutic use, toxicity, and overview of analytical methods for detection of vitamin D and its metabolites. *Crit Rev Clin Lab Sci*. 2022;**59**: 517–554. doi:10.1080/10408363.2022.2070595

20. Veldurthy V, Wei R, Campbell M, Lupicki K, Dhawan P, Christakos S. 25-Hydroxyvitamin D3 24-Hydroxylase: A Key Regulator of 1,25(OH)2D3 Catabolism and Calcium Homeostasis. 2016. pp. 137–150. doi:10.1016/bs.vh.2015.10.005

21. Zierold C, Darwish HM, DeLuca HF. Identification of a vitamin D-response element in the rat calcidiol (25-hydroxyvitamin D3) 24-hydroxylase gene. *Proceedings of the National Academy of Sciences*. 1994;**91**: 900–902. doi:10.1073/pnas.91.3.900

22. Wagner D, Hanwell HE, Schnabl K, Yazdanpanah M, Kimball S, Fu L, Sidhom G, Rousseau D, Cole DEC, Vieth R. The ratio of serum 24,25-

dihydroxyvitamin D3 to 25-hydroxyvitamin D3 is predictive of 25-hydroxyvitamin D3 response to vitamin D3 supplementation. *Journal of Steroid Biochemistry and Molecular Biology*. 2011;**126**: 72–77. doi:10.1016/j.jsbmb.2011.05.003

23. Tang JCY, Jackson S, Walsh NP, Greeves J, Fraser WD, Ball N, Dutton J, Nicholls H, Piec I, Washbourne CJ. The dynamic relationships between the active and catabolic vitamin D metabolites, their ratios, and associations with PTH. *Sci Rep*. 2019;**9**: 6974. doi:10.1038/s41598-019-43462-6

24. Wagner D, Hanwell HE, Schnabl K, Yazdanpanah M, Kimball S, Fu L, Sidhom G, Rousseau D, Cole DEC, Vieth R. The ratio of serum 24,25-dihydroxyvitamin D3 to 25-hydroxyvitamin D3 is predictive of 25-hydroxyvitamin D3 response to vitamin D3 supplementation. *Journal of Steroid Biochemistry and Molecular Biology*. 2011;**126**: 72–77. doi:10.1016/j.jsbmb.2011.05.003

25. Fabregat-Cabello N, Farre-Segura J, Huyghebaert L, Peeters S, Le Goff C, Souberbielle JC, Cavalier É. A fast and simple method for simultaneous measurements of 25(OH)D, 24,25(OH)2D and the Vitamin D Metabolite Ratio (VMR) in serum samples by LC-MS/MS. *Clinica Chimica Acta*. 2017;**473**: 116–123. doi:10.1016/j.cca.2017.08.024

26. Bouillon R, Schuit F, Antonio L, Rastinejad F. Vitamin D Binding Protein: A Historic Overview. *Front Endocrinol (Lausanne)*. 2020;**10**. doi:10.3389/fendo.2019.00910

27. Fagerberg L, Hallström BM, Oksvold P, Kampf C, Djureinovic D, Odeberg J, Habuka M, Tahmasebpoor S, Danielsson A, Edlund K, Asplund A, Sjöstedt E, Lundberg E, Szigyarto CA-K, Skogs M, Takanen JO, Berling H, Tegel H, Mulder J, Nilsson P, Schwenk JM, Lindskog C, Danielsson F, Mardinoglu A, Sivertsson Å, von Feilitzen K, Forsberg M, Zwahlen M, Olsson I, Navani S, Huss M, Nielsen J, Ponten F, Uhlén M. Analysis of the Human Tissue-specific Expression by Genome-wide Integration of Transcriptomics and Antibody-based Proteomics. *Molecular & Cellular Proteomics*. 2014;**13**: 397–406. doi:10.1074/mcp.M113.035600

28. Ardlie KG, Deluca DS, Segrè A V., Sullivan TJ, Young TR, Gelfand ET, Trowbridge CA, Maller JB, Tukiainen T, Lek M, Ward LD, Kheradpour P, Iriarte B, Meng Y, Palmer CD, Esko T, Winckler W, Hirschhorn JN, Kellis M, MacArthur DG, Getz G, Shabalin AA, Li G, Zhou Y-H, Nobel AB, Rusyn I, Wright FA, Lappalainen T, Ferreira PG, Ongen H, Rivas MA, Battle A, Mostafavi S, Monlong J, Sammeth M, Mele M, Reverter F, Goldmann JM, Koller D, Guigó R, McCarthy MI, Dermitzakis ET, Gamazon ER, Im HK, Konkashbaev A, Nicolae DL, Cox NJ, Flutre T, Wen X, Stephens M, Pritchard JK, Tu Z, Zhang B, Huang T, Long Q, Lin L, Yang J, Zhu J, Liu J,

Brown A, Mestichelli B, Tidwell D, Lo E, Salvatore M, Shad S, Thomas JA, Lonsdale JT, Moser MT, Gillard BM, Karasik E, Ramsey K, Choi C, Foster BA, Syron J, Fleming J, Magazine H, Hasz R, Walters GD, Bridge JP, Miklos M, Sullivan S, Barker LK, Traino HM, Mosavel M, Siminoff LA, Valley DR, Rohrer DC, Jewell SD, Branton PA, Sobin LH, Barcus M, Qi L, McLean J, Hariharan P, Um KS, Wu S, Tabor D, Shive C, Smith AM, Buia SA, Undale AH, Robinson KL, Roche N, Valentino KM, Britton A, Burges R, Bradbury D, Hambright KW, Seleski J, Korzeniewski GE, Erickson K, Marcus Y, Tejada J, Taherian M, Lu C, Basile M, Mash DC, Volpi S, Struewing JP, Temple GF, Boyer J, Colantuoni D, Little R, Koester S, Carithers LJ, Moore HM, Guan P, Compton C, Sawyer SJ, Demchok JP, Vaught JB, Rabiner CA, Lockhart NC, Ardlie KG, Getz G, Wright FA, Kellis M, Volpi S, Dermitzakis ET. The Genotype-Tissue Expression (GTEx) pilot analysis: Multitissue gene regulation in humans. *Science (1979)*. 2015;**348**: 648–660. doi:10.1126/science.1262110

29. Doll S, Dreßen M, Geyer PE, Itzhak DN, Braun C, Doppler SA, Meier F, Deutsch M-A, Lahm H, Lange R, Krane M, Mann M. Region and cell-type resolved quantitative proteomic map of the human heart. *Nat Commun*. 2017;**8**: 1469. doi:10.1038/s41467-017-01747-2

30. Cooke NE, Willard HF, David E V., George DL. Direct regional assignment of the gene for vitamin D binding protein (Gc-globulin) to human chromosome 4q11-q13 and identification of an associated DNA polymorphism. *Hum Genet*. 1986;**73**: 225–229. doi:10.1007/BF00401232

31. Bouillon R, Pauwels S. The Vitamin D-Binding Protein. Vitamin D. Elsevier; 2018. pp. 97–115. doi:10.1016/B978-0-12-809965-0.00007-0

32. Head JF, Swamy N, Ray R. Crystal Structure of the Complex between Actin and Human Vitamin D-Binding Protein at 2.5 Å Resolution ,. *Biochemistry*. 2002;**41**: 9015–9020. doi:10.1021/bi026054y

33. Feldman D, Krishnan A V., Swami S. Vitamin D: Biology, Actions, and Clinical Implications. Osteoporosis. Elsevier; 2013. pp. 283–328. doi:10.1016/B978-0-12-415853-5.00013-3

34. Cleve H, Constans J. The Mutants of the Vitamin-D-Binding Protein: More than 120 Variants of the GC/DBP System. *Vox Sang*. 1988;**54**: 215–225. doi:10.1111/j.1423-0410.1988.tb03908.x

35. Rozmus D, Płomiński J, Augustyn K, Cieślińska A. rs7041 and rs4588 Polymorphisms in Vitamin D Binding Protein Gene (VDBP) and the Risk of Diseases. *Int J Mol Sci*. 2022;**23**: 933. doi:10.3390/ijms23020933

36. Braun A, Bichlmaier R, Cleve H. Molecular analysis of the gene for the human vitamin-D-binding protein (group-specific component): allelic differences of the common genetic GC types. *Hum Genet*. 1992;**89**. doi:10.1007/BF00194311

37. Zhang Z, He J-W, Fu W-Z, Zhang C-Q, Zhang Z-L. An analysis of the association between the vitamin D pathway and serum 25-hydroxyvitamin D levels in a healthy Chinese population. *Journal of Bone and Mineral Research*. 2013;**28**: 1784–1792. doi:10.1002/jbmr.1926

38. Sollid ST, Hutchinson MYS, Berg V, Fuskevåg OM, Figenschau Y, Thorsby PM, Jorde R. Effects of vitamin D binding protein phenotypes and vitamin D supplementation on serum total 25(OH)D and directly measured free 25(OH)D. *Eur J Endocrinol*. 2016;**174**: 445–452. doi:10.1530/EJE-15-1089

39. Lauridsen AL, Vestergaard P, Hermann AP, Brot C, Heickendorff L, Mosekilde L, Nexo E. Plasma concentrations of 25-Hydroxy-Vitamin D and 1,25-Dihydroxy-Vitamin D are Related to the Phenotype of Gc (Vitamin D-Binding Protein): A Cross-sectional Study on 595 Early Postmenopausal Women. *Calcif Tissue Int*. 2005;**77**: 15–22. doi:10.1007/s00223-004-0227-5

40. Bikle DD, Schwartz J. Vitamin D Binding Protein, Total and Free Vitamin D Levels in Different Physiological and Pathophysiological Conditions. *Front Endocrinol (Lausanne)*. 2019;**10**. doi:10.3389/fendo.2019.00317

41. Van Baelen H, Bouillon R, De Moor P. Vitamin D-binding protein (Gc-globulin) binds actin. *J Biol Chem*. 1980;**255**: 2270–2.

42. Mc Leod JF, Kowalski MA, Haddad JG. Interactions among serum vitamin D binding protein, monomeric actin, profilin, and profilactin. *J Biol Chem*. 1989;**264**: 1260–7.

43. Coleman JR, Moore EE, Freeman K, Grubinger ND, Hennig GW, Cohen MJ, Samuels JM, Hansen K. Actin is associated with tissue injury in trauma patients and produces a hypercoagulable profile in vitro. *Journal of Trauma and Acute Care Surgery*. 2020;**89**: 87–95. doi:10.1097/TA.0000000000002739

44. Wang H, Cheng B, Chen Q, Wu S, Lv C, Xie G, Jin Y, Fang X. Time course of plasma gelsolin concentrations during severe sepsis in critically ill surgical patients. *Crit Care*. 2008;**12**: R106. doi:10.1186/cc6988

45. Epstein FH, Lee WM, Galbraith RM. The Extracellular Actin-Scavenger System and Actin Toxicity. *New England Journal of Medicine*. 1992;**326**: 1335–1341. doi:10.1056/NEJM199205143262006

46. Meng L, Wang X, Carson JL, Schlussel Y, Shapses SA. Vitamin D Binding Protein and Postsurgical Outcomes and Tissue Injury Markers After Hip Fracture: A Prospective Study. *J Clin Endocrinol Metab*. 2023;**109**: e18–e24. doi:10.1210/clinem/dgad502

47. Calvo M, Ena JoséM. Relations between vitamin D and fatty acid binding properties of vitamin D-binding protein. *Biochem Biophys Res Commun*. 1989;**163**: 14–17. doi:10.1016/0006-291X(89)92091-3

48. Williams MH, Van Alstyne EL, Galbraith RM. Evidence of a novel association of unsaturated fatty acids with Gc (Vitamin D-binding protein). *Biochem Biophys Res Commun*. 1988;**153**: 1019–1024. doi:10.1016/S0006-291X(88)81330-5

49. Bouillon R, Xiang DZ, Convents R, Van Baelen H. Polyunsaturated fatty acids decrease the apparent affinity of vitamin D metabolites for human vitamin D-binding protein. *J Steroid Biochem Mol Biol*. 1992;**42**: 855–861. doi:10.1016/0960-0760(92)90094-Y

50. DiMartino SJ, Trujillo G, McVoy LA, Zhang J, Kew RR. Upregulation of Vitamin D binding protein (Gc-globulin) binding sites during neutrophil activation from a latent reservoir in azurophil granules. *Mol Immunol*. 2007;**44**: 2370–2377. doi:10.1016/j.molimm.2006.10.011

51. Binder R, Kress A, Kan G, Herrmann K, Kirschfink M. Neutrophil priming by cytokines and vitamin D binding protein (Gc-globulin): impact on C5a-mediated chemotaxis, degranulation and respiratory burst. *Mol Immunol*. 1999;**36**: 885–892. doi:10.1016/S0161-5890(99)00110-8

52. McVoy LA, Kew RR. CD44 and Annexin A2 Mediate the C5a Chemotactic Cofactor Function of the Vitamin D Binding Protein. *The Journal of Immunology*. 2005;**175**: 4754–4760. doi:10.4049/jimmunol.175.7.4754

53. Yamamoto N. Structural definition of a potent macrophage activating factor derived from vitamin D3-binding protein with adjuvant activity for antibody production. *Mol Immunol*. 1996;**33**: 1157–1164. doi:10.1016/S0161-5890(96)00081-8

54. Yamamoto N, Homma S. Vitamin D3 binding protein (group-specific component) is a precursor for the macrophage-activating signal factor from lysophosphatidylcholine-treated lymphocytes. *Proceedings of the*

National Academy of Sciences. 1991;**88**: 8539–8543. doi:10.1073/pnas.88.19.8539

55. Swamy N, Ghosh S, Schneider GB, Ray R. Baculovirus-expressed vitamin D-binding protein-macrophage activating factor (DBP-maf) activates osteoclasts and binding of 25-hydroxyvitamin D3 does not influence this activity. *J Cell Biochem*. 2001;**81**: 535–546. doi:10.1002/1097-4644(20010601)81:3<535::AID-JCB1067>3.0.CO;2-6

56. Schneider GB, Benis KA, Flay NW, Ireland RA, Popoff SN. Effects of vitamin D binding protein-macrophage activating factor (DBP-MAF) infusion on bone resorption in two osteopetrotic mutations. *Bone*. 1995;**16**: 657–662. doi:10.1016/8756-3282(95)00118-W

57. Ames BN, Grant WB, Willett WC. Does the High Prevalence of Vitamin D Deficiency in African Americans Contribute to Health Disparities? *Nutrients*. 2021;**13**: 499. doi:10.3390/nu13020499

58. G R, Gupta A. Vitamin D Deficiency in India: Prevalence, Causalities and Interventions. *Nutrients*. 2014;**6**: 729–775. doi:10.3390/nu6020729

59. Arabi A, El Rassi R, El-Hajj Fuleihan G. Hypovitaminosis D in developing countries—prevalence, risk factors and outcomes. *Nat Rev Endocrinol*. 2010;**6**: 550–561. doi:10.1038/nrendo.2010.146

60. Webb A, Kazantzidis A, Kift R, Farrar M, Wilkinson J, Rhodes L. Colour Counts: Sunlight and Skin Type as Drivers of Vitamin D Deficiency at UK Latitudes. *Nutrients*. 2018;**10**: 457. doi:10.3390/nu10040457

61. Powe CE, Evans MK, Wenger J, Zonderman AB, Berg AH, Nalls M, Tamez H, Zhang D, Bhan I, Karumanchi SA, Powe NR, Thadhani R. Vitamin D–Binding Protein and Vitamin D Status of Black Americans and White Americans. *New England Journal of Medicine*. 2013;**369**: 1991–2000. doi:10.1056/NEJMoa1306357

62. Hsu S, Hoofnagle AN, Gupta DK, Gutierrez OM, Peralta CA, Shea S, Allen NB, Burke G, Michos ED, Ix JH, Siscovick D, Psaty BM, Watson KE, Kestenbaum B, de Boer IH, Robinson-Cohen C. Race, Ancestry, and Vitamin D Metabolism: The Multi-Ethnic Study of Atherosclerosis. *J Clin Endocrinol Metab*. 2020;**105**: e4337–e4350. doi:10.1210/clinem/dgaa612

63. Haussler MR, Norman AW. CHROMOSOMAL RECEPTOR FOR A VITAMIN D METABOLITE. *Proceedings of the National Academy of Sciences*. 1969;**62**: 155–162. doi:10.1073/pnas.62.1.155

64. Bouillon R, Carmeliet G, Verlinden L, van Etten E, Verstuyf A, Luderer HF, Lieben L, Mathieu C, Demay M. Vitamin D and Human Health: Lessons from Vitamin D Receptor Null Mice. *Endocr Rev*. 2008;**29**: 726–776. doi:10.1210/er.2008-0004

65. Taymans SE, Pack S, Pak E, Orban Z, Barsony J, Zhuang Z, Stratakis CA. The Human Vitamin D Receptor Gene (VDR) Is Localized to Region 12cen-q12 by Fluorescent In Situ Hybridization and Radiation Hybrid Mapping: Genetic and Physical VDR Map. *Journal of Bone and Mineral Research*. 1999;**14**: 1163–1166. doi:10.1359/jbmr.1999.14.7.1163

66. Zenata O, Vrzal R. Fine tuning of vitamin D receptor (VDR) activity by post-transcriptional and post-translational modifications. *Oncotarget*. 2017;**8**: 35390–35402. doi:10.18632/oncotarget.15697

67. Jurutka PW, Remus LS, Whitfield GK, Thompson PD, Hsieh J-C, Zitzer H, Tavakkoli P, Galligan MA, Dang HTL, Haussler CA, Haussler MR. The Polymorphic N Terminus in Human Vitamin D Receptor Isoforms Influences Transcriptional Activity by Modulating Interaction with Transcription Factor IIB. *Molecular Endocrinology*. 2000;**14**: 401–420. doi:10.1210/mend.14.3.0435

68. Rochel N. Vitamin D and Its Receptor from a Structural Perspective. *Nutrients*. 2022;**14**: 2847. doi:10.3390/nu14142847

69. Haussler MR, Whitfield GK, Haussler CA, Hsieh JC, Thompson PD, Selznick SH, Dominguez CE, Jurutka PW. The nuclear vitamin D receptor: Biological and molecular regulatory properties revealed. *Journal of Bone and Mineral Research*. 1998;**13**: 325–349. doi:10.1359/jbmr.1998.13.3.325

70. Christakos S, Ajibade D V., Dhawan P, Fechner AJ, Mady LJ. Vitamin D: Metabolism. *Endocrinol Metab Clin North Am*. 2010;**39**: 243–253. doi:10.1016/j.ecl.2010.02.002

71. Bouillon R, Bischoff-Ferrari H, Willett W. Vitamin D and health: Perspectives from mice and man. *Journal of Bone and Mineral Research*. 2008;**23**: 974–979. doi:10.1359/jbmr.080420

72. Wang T-Tian, Tavera-Mendoza LE, Laperriere D, Libby E, MacLeod NB, Nagai Y, Bourdeau V, Konstorum A, Lallemant B, Zhang R, Mader S, White JH. Large-Scale in Silico and Microarray-Based Identification of Direct 1,25-Dihydroxyvitamin D3 Target Genes. *Molecular Endocrinology*. 2005;**19**: 2685–2695.

73. Hii CS, Ferrante A. The non-genomic actions of vitamin D. *Nutrients*. 2016;**8**: 1–14. doi:10.3390/nu8030135

74. Fleet JC. Rapid, Membrane-Initiated Actions of 1,25 Dihydroxyvitamin D: What Are They and What Do They Mean? *J Nutr*. 2004;**134**: 3215–3218. doi:10.1093/jn/134.12.3215

75. Baskin KK, Winders BR, Olson EN. Muscle as a "Mediator" of Systemic Metabolism. *Cell Metab*. 2015;**21**: 237–248. doi:10.1016/j.cmet.2014.12.021

76. Cruz-Jentoft AJ, Bahat G, Bauer J, Boirie Y, Bruyère O, Cederholm T, Cooper C, Landi F, Rolland Y, Sayer AA, Schneider SM, Sieber CC, Topinkova E, Vandewoude M, Visser M, Zamboni M, Bautmans I, Baeyens J-P, Cesari M, Cherubini A, Kanis J, Maggio M, Martin F, Michel J-P, Pitkala K, Reginster J-Y, Rizzoli R, Sánchez-Rodríguez D, Schols J. Sarcopenia: revised European consensus on definition and diagnosis. *Age Ageing*. 2019;**48**: 16–31. doi:10.1093/ageing/afy169

77. Rudrappa SS, Wilkinson DJ, Greenhaff PL, Smith K, Idris I, Atherton PJ. Human Skeletal Muscle Disuse Atrophy: Effects on Muscle Protein Synthesis, Breakdown, and Insulin Resistance—A Qualitative Review. *Front Physiol*. 2016;**7**. doi:10.3389/fphys.2016.00361

78. Fernando R, Drescher C, Nowotny K, Grune T, Castro JP. Impaired proteostasis during skeletal muscle aging. *Free Radic Biol Med*. 2019;**132**: 58–66. doi:10.1016/j.freeradbiomed.2018.08.037

79. Sartori R, Romanello V, Sandri M. Mechanisms of muscle atrophy and hypertrophy: implications in health and disease. *Nat Commun*. 2021;**12**: 330. doi:10.1038/s41467-020-20123-1

80. Holick MF. Vitamin D Deficiency. *New England Journal of Medicine*. 2007;**357**: 266–281. doi:10.1056/NEJMra070553

81. Prokopidis K, Giannos P, Katsikas Triantafyllidis K, Kechagias KS, Mesinovic J, Witard OC, Scott D. Effect of vitamin D monotherapy on indices of sarcopenia in community-dwelling older adults: a systematic review and meta-analysis. *J Cachexia Sarcopenia Muscle*. 2022. doi:10.1002/jcsm.12976

82. NICE (National Institute for Health and Care Excellence). Vitamin D deficiency in adults. 2022 [cited 5 Mar 2022]. Available: https://cks.nice.org.uk/topics/vitamin-d-deficiency-in-adults/

83. Bischoff-Ferrari H, Borchers M, Gudat F, Dürmüller U, Stähelin H, Dick W. Vitamin D Receptor Expression in Human Muscle Tissue Decreases With Age. *Journal of Bone and Mineral Research*. 2004;**19**: 265–269. doi:10.1359/jbmr.2004.19.2.265

84. MacLaughlin J, Holick MF. Aging decreases the capacity of human skin to produce vitamin D3. *Journal of Clinical Investigation*. 1985;**76**: 1536–1538. doi:10.1172/JCI112134

85. Srikuea R, Hirunsai M, Charoenphandhu N. Regulation of vitamin D system in skeletal muscle and resident myogenic stem cell during development, maturation, and ageing. *Sci Rep*. 2020;**10**: 8239. doi:10.1038/s41598-020-65067-0

86. Si Y, Kazamel M, Kwon Y, Lee I, Anderson T, Zhou S, Bamman M, Wiggins D, Kwan T, King PH. The vitamin D activator CYP27B1 is upregulated in muscle fibers in denervating disease and can track progression in amyotrophic lateral sclerosis. *Journal of Steroid Biochemistry and Molecular Biology*. 2020;**200**: 105650. doi:10.1016/j.jsbmb.2020.105650

87. Girgis CM, Mokbel N, DiGirolamo DJ. Therapies for Musculoskeletal Disease: Can we Treat Two Birds with One Stone? *Curr Osteoporos Rep*. 2014;**12**: 142–153. doi:10.1007/s11914-014-0204-5

88. Li W, Qin X, Poon CC, Wong M, Feng R, Wang J, Lin F, Sun Y, Liu S, Wang Y, Zhang Y. Vitamin D Receptor Signaling Attenuates Skeletal Muscle Atrophy by Suppressing Renin-Angiotensin System. *Journal of Bone and Mineral Research*. 2022;**37**: 121–136. doi:10.1002/jbmr.4441

89. Mendoza-Garcés L, Velázquez-Alva MC, Cabrer-Rosales MF, Arrieta-Cruz I, Gutiérrez-Juárez R, Irigoyen-Camacho ME. Vitamin D Deficiency is Associated with Handgrip Strength, Nutritional Status and T2DM in Community-Dwelling Older Mexican Women: A Cross-Sectional Study. *Nutrients*. 2021;**13**: 736. doi:10.3390/nu13030736

90. Haslam A, Johnson MA, Hausman DB, Cress ME, Houston DK, Davey A, Poon LW, Georgia Centenarian Study. Vitamin D Status Is Associated With Grip Strength in Centenarians. *J Nutr Gerontol Geriatr*. 2014;**33**: 35–46. doi:10.1080/21551197.2013.867825

91. Wang J, Wang X, Gu Y, Liu M, Chi VTQ, Zhang Q, Liu L, Meng G, Yao Z, Wu H, Bao X, Zhang S, Wang Y, Lu Z, Wang L, Zheng L, Wang X, Tian C, Fu J, Sun S, Zhou M, Jia Q, Song K, Huang J, Huo J, Zhang B, Ding G, Niu K. Vitamin D is related to handgrip strength in adult men aged 50 years and over: A population study from the TCLSIH cohort study. *Clin Endocrinol (Oxf)*. 2019;**90**: 753–765. doi:10.1111/cen.13952

92. Kalliokoski P, Bergqvist Y, Löfvander M. Physical performance and 25-hydroxyvitamin D: a cross-sectional study of pregnant Swedish and

Somali immigrant women and new mothers. *BMC Pregnancy Childbirth*. 2013;**13**: 237. doi:10.1186/1471-2393-13-237

93. GRIMALDI AS, PARKER BA, CAPIZZI JA, CLARKSON PM, PESCATELLO LS, WHITE MC, THOMPSON PD. 25(OH) Vitamin D Is Associated with Greater Muscle Strength in Healthy Men and Women. *Med Sci Sports Exerc*. 2013;**45**: 157–162. doi:10.1249/MSS.0b013e31826c9a78

94. Toffanello ED, Perissinotto E, Sergi G, Zambon S, Musacchio E, Maggi S, Coin A, Sartori L, Corti M-C, Baggio G, Crepaldi G, Manzato E. Vitamin D and Physical Performance in Elderly Subjects: The Pro.V.A Study. Ruiz JR, editor. *PLoS One*. 2012;**7**: e34950. doi:10.1371/journal.pone.0034950

95. Orces CH. Prevalence of clinically relevant muscle weakness and its association with vitamin D status among older adults in Ecuador. *Aging Clin Exp Res*. 2017;**29**: 943–949. doi:10.1007/s40520-016-0678-3

96. Michael YL, Smit E, Seguin R, Curb JD, Phillips LS, Manson JE. Serum 25-Hydroxyvitamin D and Physical Performance in Postmenopausal Women. *J Womens Health*. 2011;**20**: 1603–1608. doi:10.1089/jwh.2010.2606

97. Aspell N, Laird E, Healy M, Lawlor B, O'Sullivan M. Vitamin D Deficiency Is Associated With Impaired Muscle Strength And Physical Performance In Community-Dwelling Older Adults: Findings From The English Longitudinal Study Of Ageing. *Clin Interv Aging*. 2019;**Volume 14**: 1751–1761. doi:10.2147/CIA.S222143

98. Dam T-TL, von Mühlen D, Barrett-Connor EL. Sex-specific association of serum vitamin D levels with physical function in older adults. *Osteoporosis International*. 2009;**20**: 751–760. doi:10.1007/s00198-008-0749-1

99. Bischoff-Ferrari HA, Dietrich T, Orav EJ, Hu FB, Zhang Y, Karlson EW, Dawson-Hughes B. Higher 25-hydroxyvitamin D concentrations are associated with better lower-extremity function in both active and inactive persons aged ≥60 y. *Am J Clin Nutr*. 2004;**80**: 752–758. doi:10.1093/ajcn/80.3.752

100. Levinger P, Begg R, Sanders KM, Nagano H, Downie C, Petersen A, Hayes A, Cicuttini F. The effect of vitamin D status on pain, lower limb strength and knee function during balance recovery in people with knee osteoarthritis: an exploratory study. *Arch Osteoporos*. 2017;**12**: 83. doi:10.1007/s11657-017-0378-4

101. Sohl E, van Schoor NM, de Jongh RT, Visser M, Deeg DJH, Lips P. Vitamin D Status Is Associated With Functional Limitations and Functional Decline in Older Individuals. *J Clin Endocrinol Metab*. 2013;**98**: E1483–E1490. doi:10.1210/jc.2013-1698

102. Iolascon G, de Sire A, Calafiore D, Moretti A, Gimigliano R, Gimigliano F. Hypovitaminosis D is associated with a reduction in upper and lower limb muscle strength and physical performance in post-menopausal women: a retrospective study. *Aging Clin Exp Res*. 2015;**27**: 23–30. doi:10.1007/s40520-015-0405-5

103. Granic A, Hill T, Davies K, Jagger C, Adamson A, Siervo M, Kirkwood T, Mathers J, Sayer A. Vitamin D Status, Muscle Strength and Physical Performance Decline in Very Old Adults: A Prospective Study. *Nutrients*. 2017;**9**: 379. doi:10.3390/nu9040379

104. Salminen M, Saaristo P, Salonoja M, Vaapio S, Vahlberg T, Lamberg-Allardt C, Aarnio P, Kivelä S-L. Vitamin D status and physical function in older Finnish people: A one-year follow-up study. *Arch Gerontol Geriatr*. 2015;**61**: 419–424. doi:10.1016/j.archger.2015.08.014

105. Scott D, Ebeling PR, Sanders KM, Aitken D, Winzenberg T, Jones G. Vitamin D and Physical Activity Status: Associations With Five-Year Changes in Body Composition and Muscle Function in Community-Dwelling Older Adults. *J Clin Endocrinol Metab*. 2015;**100**: 670–678. doi:10.1210/jc.2014-3519

106. Houston DK, Tooze JA, Davis CC, Chaves PHM, Hirsch CH, Robbins JA, Arnold AM, Newman AB, Kritchevsky SB. Serum 25-Hydroxyvitamin D and Physical Function in Older Adults: The Cardiovascular Health Study All Stars. *J Am Geriatr Soc*. 2011;**59**: 1793–1801. doi:10.1111/j.1532-5415.2011.03601.x

107. Visser M, Deeg DJH, Lips P. Low Vitamin D and High Parathyroid Hormone Levels as Determinants of Loss of Muscle Strength and Muscle Mass (Sarcopenia): The Longitudinal Aging Study Amsterdam. *J Clin Endocrinol Metab*. 2003;**88**: 5766–5772. doi:10.1210/jc.2003-030604

108. Hirani V, Cumming RG, Naganathan V, Blyth F, Le Couteur DG, Hsu B, Handelsman DJ, Waite LM, Seibel MJ. Longitudinal Associations Between Vitamin D Metabolites and Sarcopenia in Older Australian men: The Concord Health and Aging in Men Project. *The Journals of Gerontology: Series A*. 2018;**73**: 131–138. doi:10.1093/gerona/glx086

109. Wicherts IS, van Schoor NM, Boeke AJP, Visser M, Deeg DJH, Smit J, Knol DL, Lips P. Vitamin D Status Predicts Physical Performance and Its

Decline in Older Persons. *J Clin Endocrinol Metab*. 2007;**92**: 2058–2065. doi:10.1210/jc.2006-1525

110. Luo S, Chen X, Hou L, Yue J, Liu X, Wang Y, Xia X, Dong B. The Relationship between Sarcopenia and Vitamin D Levels in Adults of Different Ethnicities: Findings from the West China Health and Aging Trend Study. *J Nutr Health Aging*. 2021;**25**: 909–913. doi:10.1007/s12603-021-1645-z

111. Yoo J, Chung HJ, Kim BG, Jung Y, Baek K, Song M, Cho M. Comparative analysis of the association between various serum vitamin D biomarkers and sarcopenia. *J Clin Lab Anal*. 2021;**35**. doi:10.1002/jcla.23946

112. Snijder MB, van Schoor NM, Pluijm SMF, van Dam RM, Visser M, Lips P. Vitamin D Status in Relation to One-Year Risk of Recurrent Falling in Older Men and Women. *J Clin Endocrinol Metab*. 2006;**91**: 2980–2985. doi:10.1210/jc.2006-0510

113. Ceglia L, Niramitmahapanya S, da Silva Morais M, Rivas DA, Harris SS, Bischoff-Ferrari H, Fielding RA, Dawson-Hughes B. A Randomized Study on the Effect of Vitamin D 3 Supplementation on Skeletal Muscle Morphology and Vitamin D Receptor Concentration in Older Women. *J Clin Endocrinol Metab*. 2013;**98**: E1927–E1935. doi:10.1210/jc.2013-2820

114. Agergaard J, Trøstrup J, Uth J, Iversen JV, Boesen A, Andersen JL, Schjerling P, Langberg H. Does vitamin-D intake during resistance training improve the skeletal muscle hypertrophic and strength response in young and elderly men? – a randomized controlled trial. *Nutr Metab (Lond)*. 2015;**12**: 32. doi:10.1186/s12986-015-0029-y

115. YOSHIKAWA S, NAKAMURA T, TANABE H, IMAMURA T. Osteomalacic Myopathy. *Endocrinol Jpn*. 1979;**26**: 65–72. doi:10.1507/endocrj1954.26.Supplement_65

116. Tanganelli F, Meinke P, Hofmeister F, Jarmusch S, Baber L, Mehaffey S, Hintze S, Ferrari U, Neuerburg C, Kammerlander C, Schoser B, Drey M. Type-2 muscle fiber atrophy is associated with sarcopenia in elderly men with hip fracture. *Exp Gerontol*. 2021;**144**: 111171. doi:10.1016/j.exger.2020.111171

117. Snijder MB, van Schoor NM, Pluijm SMF, van Dam RM, Visser M, Lips P. Vitamin D Status in Relation to One-Year Risk of Recurrent Falling in Older Men and Women. *J Clin Endocrinol Metab*. 2006;**91**: 2980–2985. doi:10.1210/jc.2006-0510

118. Suzuki T, Kwon J, Kim H, Shimada H, Yoshida Y, Iwasa H, Yoshida H. Low Serum 25-Hydroxyvitamin D Levels Associated With Falls Among Japanese Community-Dwelling Elderly. *Journal of Bone and Mineral Research*. 2008;**23**: 1309–1317. doi:10.1359/jbmr.080328

119. Boersma D, Demontiero O, Amiri ZM, Hassan S, Suarez H, Geisinger D, Suriyaarachchi P, Sharma A, Duque G. Vitamin D status in relation to postural stability in the elderly. *J Nutr Health Aging*. 2012;**16**: 270–275. doi:10.1007/s12603-011-0345-5

120. Flicker L, Mead K, MacInnis RJ, Nowson C, Scherer S, Stein MS, Thomasx J, Hopper JL, Wark JD. Serum Vitamin D and Falls in Older Women in Residential Care in Australia. *J Am Geriatr Soc*. 2003;**51**: 1533–1538. doi:10.1046/j.1532-5415.2003.51510.x

121. Shimizu Y, Kim H, Yoshida H, Shimada H, Suzuki T. Serum 25-hydroxyvitamin D level and risk of falls in Japanese community-dwelling elderly women: a 1-year follow-up study. *Osteoporosis International*. 2015;**26**: 2185–2192. doi:10.1007/s00198-015-3130-1

122. Ceglia L, Niramitmahapanya S, da Silva Morais M, Rivas DA, Harris SS, Bischoff-Ferrari H, Fielding RA, Dawson-Hughes B. A Randomized Study on the Effect of Vitamin D 3 Supplementation on Skeletal Muscle Morphology and Vitamin D Receptor Concentration in Older Women. *J Clin Endocrinol Metab*. 2013;**98**: E1927–E1935. doi:10.1210/jc.2013-2820

123. Agergaard J, Trøstrup J, Uth J, Iversen JV, Boesen A, Andersen JL, Schjerling P, Langberg H. Does vitamin-D intake during resistance training improve the skeletal muscle hypertrophic and strength response in young and elderly men? – a randomized controlled trial. *Nutr Metab (Lond)*. 2015;**12**: 32. doi:10.1186/s12986-015-0029-y

124. El Hajj C, Fares S, Chardigny JM, Boirie Y, Walrand S. Vitamin D supplementation and muscle strength in pre-sarcopenic elderly Lebanese people: a randomized controlled trial. *Arch Osteoporos*. 2019;**14**: 4. doi:10.1007/s11657-018-0553-2

125. BRAY NW, DOHERTY TJ, MONTERO-ODASSO M. THE EFFECT OF HIGH DOSE VITAMIN D3 ON PHYSICAL PERFORMANCE IN FRAIL OLDER ADULTS. A FEASIBILITY STUDY. *J Frailty Aging*. 2018; 1–7. doi:10.14283/jfa.2018.18

126. Saito K, Miyakoshi N, Matsunaga T, Hongo M, Kasukawa Y, Shimada Y. Eldecalcitol improves muscle strength and dynamic balance in postmenopausal women with osteoporosis: an open-label randomized

controlled study. *J Bone Miner Metab*. 2016;**34**: 547–554. doi:10.1007/s00774-015-0695-x

127. Zhu K, Austin N, Devine A, Bruce D, Prince RL. A Randomized Controlled Trial of the Effects of Vitamin D on Muscle Strength and Mobility in Older Women with Vitamin D Insufficiency. *J Am Geriatr Soc*. 2010;**58**: 2063–2068. doi:10.1111/j.1532-5415.2010.03142.x

128. Cangussu LM, Nahas-Neto J, Orsatti CL, Bueloni-Dias FN, Nahas EAP. Effect of vitamin D supplementation alone on muscle function in postmenopausal women: a randomized, double-blind, placebo-controlled clinical trial. *Osteoporosis International*. 2015;**26**: 2413–2421. doi:10.1007/s00198-015-3151-9

129. Anek A, Bunyaratavej N, Jittivilai T. Effects of Short-Term Vitamin D Supplementation on Musculoskeletal and Body Balance for Prevention of Falling in Postmenopausal Women. *J Med Assoc Thai*. 2015;**98 Suppl 8**: S26-31.

130. Close GL, Russell J, Cobley JN, Owens DJ, Wilson G, Gregson W, Fraser WD, Morton JP. Assessment of vitamin D concentration in non-supplemented professional athletes and healthy adults during the winter months in the UK: implications for skeletal muscle function. *J Sports Sci*. 2013;**31**: 344–353. doi:10.1080/02640414.2012.733822

131. Iolascon G, Moretti A, de Sire A, Calafiore D, Gimigliano F. Effectiveness of Calcifediol in Improving Muscle Function in Post-Menopausal Women: A Prospective Cohort Study. *Adv Ther*. 2017;**34**: 744–752. doi:10.1007/s12325-017-0492-0

132. Moreira-Pfrimer LDF, Pedrosa MAC, Teixeira L, Lazaretti-Castro M. Treatment of Vitamin D Deficiency Increases Lower Limb Muscle Strength in Institutionalized Older People Independently of Regular Physical Activity: A Randomized Double-Blind Controlled Trial. *Ann Nutr Metab*. 2009;**54**: 291–300. doi:10.1159/000235874

133. Shea MK, Fielding RA, Dawson-Hughes B. The effect of vitamin D supplementation on lower-extremity power and function in older adults: a randomized controlled trial. *Am J Clin Nutr*. 2019;**109**: 369–379. doi:10.1093/ajcn/nqy290

134. Wood AD, Secombes KR, Thies F, Aucott LS, Black AJ, Reid DM, Mavroeidi A, Simpson WG, Fraser WD, Macdonald HM. A parallel group double-blind RCT of vitamin D3 assessing physical function: is the biochemical response to treatment affected by overweight and obesity? *Osteoporosis International*. 2014;**25**: 305–315. doi:10.1007/s00198-013-2473-8

135. Janssen HCJP, Samson MM, Verhaar HJJ. Muscle strength and mobility in vitamin D-insufficient female geriatric patients: a randomized controlled trial on vitamin D and calcium supplementation. *Aging Clin Exp Res*. 2010;**22**: 78–84. doi:10.1007/BF03324819

136. Hansen KE, Johnson RE, Chambers KR, Johnson MG, Lemon CC, Vo TNT, Marvdashti S. Treatment of Vitamin D Insufficiency in Postmenopausal Women. *JAMA Intern Med*. 2015;**175**: 1612. doi:10.1001/jamainternmed.2015.3874

137. Kenny AM, Biskup B, Robbins B, Marcella G, Burleson JA. Effects of Vitamin D Supplementation on Strength, Physical Function, and Health Perception in Older, Community-Dwelling Men. *J Am Geriatr Soc*. 2003;**51**: 1762–1767. doi:10.1046/j.1532-5415.2003.51561.x

138. Glendenning P, Zhu K, Inderjeeth C, Howat P, Lewis JR, Prince RL. Effects of three-monthly oral 150,000 IU cholecalciferol supplementation on falls, mobility, and muscle strength in older postmenopausal women: A randomized controlled trial. *Journal of Bone and Mineral Research*. 2012;**27**: 170–176. doi:10.1002/jbmr.524

139. Brunner RL, Cochrane B, Jackson RD, Larson J, Lewis C, Limacher M, Rosal M, Shumaker S, Wallace R. Calcium, Vitamin D Supplementation, and Physical Function in the Women's Health Initiative. *J Am Diet Assoc*. 2008;**108**: 1472–1479. doi:10.1016/j.jada.2008.06.432

140. Levis S, Gómez-Marín O. Vitamin D and Physical Function in Sedentary Older Men. *J Am Geriatr Soc*. 2017;**65**: 323–331. doi:10.1111/jgs.14510

141. Ensrud KE, Ewing SK, Fredman L, Hochberg MC, Cauley JA, Hillier TA, Cummings SR, Yaffe K, Cawthon PM. Circulating 25-Hydroxyvitamin D Levels and Frailty Status in Older Women. *J Clin Endocrinol Metab*. 2010;**95**: 5266–5273. doi:10.1210/jc.2010-2317

142. Dokoh S, Donaldson CA, Haussler MR. Influence of 1,25-Di hydroxy vitamin D3 on Cultured Osteogenic Sarcoma Cells: Correlation with the 1,25-Dihydroxyvitamin D3 Receptor. *Cancer Res*. 1984;**44**: 2103–2109.

143. Girgis CM, Clifton-Bligh RJ, Mokbel N, Cheng K, Gunton JE. Vitamin D signaling regulates proliferation, differentiation, and myotube size in C2C12 skeletal muscle cells. *Endocrinology*. 2014;**155**: 347–357. doi:10.1210/en.2013-1205

144. van der Meijden K, Bravenboer N, Dirks NF, Heijboer AC, den Heijer M, de Wit GMJ, Offringa C, Lips P, Jaspers RT. Effects of 1,25(OH)2D3 and 25(OH)D3 on C2C12 Myoblast Proliferation, Differentiation, and

Myotube Hypertrophy. *J Cell Physiol*. 2016;**231**: 2517–2528. doi:10.1002/jcp.25388

145. Camperi A, Pin F, Costamagna D, Penna F, Menduina ML, Aversa Z, Zimmers T, Verzaro R, Fittipaldi R, Caretti G, Baccino FM, Muscaritoli M, Costelli P. Vitamin D and VDR in cancer cachexia and muscle regeneration. *Oncotarget*. 2017;**8**: 21778–21793. doi:10.18632/oncotarget.15583

146. Wang Y, Becklund BR, DeLuca HF. Identification of a highly specific and versatile vitamin D receptor antibody. *Arch Biochem Biophys*. 2010;**494**: 166–177. doi:10.1016/j.abb.2009.11.029

147. Girgis CM, Cha KM, So B, Tsang M, Chen J, Houweling PJ, Schindeler A, Stokes R, Swarbrick MM, Evesson FJ, Cooper ST, Gunton JE. Mice with myocyte deletion of vitamin D receptor have sarcopenia and impaired muscle function. *J Cachexia Sarcopenia Muscle*. 2019;**10**: 1228–1240. doi:10.1002/jcsm.12460

148. Wang Y, DeLuca HF. Is the Vitamin D Receptor Found in Muscle? *Endocrinology*. 2011;**152**: 354–363. doi:10.1210/en.2010-1109

149. Sandgren ME, Brönnegärd M, DeLuca HF. Tissue distribution of the 1,25-dihydroxyvitamin D3 receptor in the male rat. *Biochem Biophys Res Commun*. 1991;**181**: 611–616. doi:10.1016/0006-291X(91)91234-4

150. Makanae Y, Ogasawara R, Sato K, Takamura Y, Matsutani K, Kido K, Shiozawa N, Nakazato K, Fujita S. Acute bout of resistance exercise increases vitamin D receptor protein expression in rat skeletal muscle. *Exp Physiol*. 2015;**100**: 1168–1176. doi:10.1113/EP085207

151. Srikuea R, Zhang X, Park-Sarge O-K, Esser KA. VDR and CYP27B1 are expressed in C2C12 cells and regenerating skeletal muscle: potential role in suppression of myoblast proliferation. *American Journal of Physiology-Cell Physiology*. 2012;**303**: C396–C405. doi:10.1152/ajpcell.00014.2012

152. Srikuea R, Hirunsai M. Effects of intramuscular administration of 1α,25(OH)2D3 during skeletal muscle regeneration on regenerative capacity, muscular fibrosis, and angiogenesis. *J Appl Physiol*. 2016;**120**: 1381–1393. doi:10.1152/japplphysiol.01018.2015

153. Allbrook DB, Han MF, Hellmuth AE. Population of muscle satellite cells in relation to age and mitotic activity. *Pathology*. 1971;**3**: 233–243. doi:10.1080/00313027109073739

154. Fu X, Wang H, Hu P. Stem cell activation in skeletal muscle regeneration. *Cellular and Molecular Life Sciences*. 2015;**72**: 1663–1677. doi:10.1007/s00018-014-1819-5

155. Garcia LA, Ferrini MG, Norris KC, Artaza JN. 1,25(OH)2 vitamin D3 Enhances Myogenic Differentiation by Modulating the Expression of Key Angiogenic Growth factors and Angiogenic Inhibitors in C2C12 Skeletal Muscle Cells. *Journal of Steroid Biochemistry and Molecular Biology*. 2013;**133**: 1–11. doi:10.1038/jid.2014.371

156. Garcia LA, King KK, Ferrini MG, Norris KC, Artaza JN. 1,25(OH)2vitamin D3 stimulates myogenic differentiation by inhibiting cell proliferation and modulating the expression of promyogenic growth factors and myostatin in C2C12 skeletal muscle cells. *Endocrinology*. 2011;**152**: 2976–2986. doi:10.1210/en.2011-0159

157. Okuno H, Kishimoto KN, Hatori M, Itoi E. 1α,25-dihydroxyvitamin D 3 enhances fast-myosin heavy chain expression in differentiated C2C12 myoblasts . *Cell Biol Int*. 2012;**36**: 441–447. doi:10.1042/cbi20100782

158. Irazoqui AP, Boland RL, Buitrago CG. Actions of 1,25(OH)2-vitamin D3 on the cellular cycle depend on VDR and p38 MAPK in skeletal muscle cells. *J Mol Endocrinol*. 2014;**53**: 331–343. doi:10.1530/JME-14-0102

159. Rohan JNP, Weigel NL. 1α,25-Dihydroxyvitamin D 3 Reduces c-Myc Expression, Inhibiting Proliferation and Causing G 1 Accumulation in C4-2 Prostate Cancer Cells. *Endocrinology*. 2009;**150**: 2046–2054. doi:10.1210/en.2008-1395

160. André LM, Ausems CRM, Wansink DG, Wieringa B. Abnormalities in Skeletal Muscle Myogenesis, Growth, and Regeneration in Myotonic Dystrophy. *Front Neurol*. 2018;**9**. doi:10.3389/fneur.2018.00368

161. Yoshiko Y, Hirao K, Maeda N. Differentiation in C2C12 myoblasts depends on the expression of endogenous IGFs and not serum depletion. *American Journal of Physiology-Cell Physiology*. 2002;**283**: C1278–C1286. doi:10.1152/ajpcell.00168.2002

162. Braga M, Simmons Z, Norris KC, Ferrini MG, Artaza JN. Vitamin D induces myogenic differentiation in skeletal muscle derived stem cells. *Endocr Connect*. 2017;**6**: 139–150. doi:10.1530/ec-17-0008

163. Endo I, Inoue D, Mitsui T, Umaki Y, Akaike M, Yoshizawa T, Kato S, Matsumoto T. Deletion of Vitamin D Receptor Gene in Mice Results in Abnormal Skeletal Muscle Development with Deregulated Expression of Myoregulatory Transcription Factors. *Endocrinology*. 2003;**144**: 5138–5144. doi:10.1210/en.2003-0502

164. Minasyan A, Keisala T, Zou J, Zhang Y, Toppila E, Syvälä H, Lou Y-R, Kalueff A V., Pyykkö I, Tuohimaa P. Vestibular dysfunction in vitamin D receptor mutant mice. *J Steroid Biochem Mol Biol*. 2009;**114**: 161–166. doi:10.1016/j.jsbmb.2009.01.020

165. Burne THJ, Johnston ANB, McGrath JJ, Mackay-Sim A. Swimming behaviour and post-swimming activity in Vitamin D receptor knockout mice. *Brain Res Bull*. 2006;**69**: 74–78. doi:10.1016/j.brainresbull.2005.10.014

166. Girgis CM, Cha KM, Houweling PJ, Rao R, Mokbel N, Lin M, Clifton-Bligh RJ, Gunton JE. Vitamin D Receptor Ablation and Vitamin D Deficiency Result in Reduced Grip Strength, Altered Muscle Fibers, and Increased Myostatin in Mice. *Calcif Tissue Int*. 2015;**97**: 602–610. doi:10.1007/s00223-015-0054-x

167. Domingues-Faria C, Chanet A, Salles J, Berry A, Giraudet C, Patrac V, Denis P, Bouton K, Goncalves-Mendes N, Vasson MP, Boirie Y, Walrand S. Vitamin D deficiency down-regulates Notch pathway contributing to skeletal muscle atrophy in old wistar rats. *Nutr Metab (Lond)*. 2014;**11**: 1–13. doi:10.1186/1743-7075-11-47

168. Bjornson CRR, Cheung TH, Liu L, Tripathi P V., Steeper KM, Rando TA. Notch Signaling Is Necessary to Maintain Quiescence in Adult Muscle Stem Cells. *Stem Cells*. 2012;**30**: 232–242. doi:10.1002/stem.773

169. Grimm M, Thiel A, Lauer A, Winkler J, Lehmann J, Regner L, Nelke C, Janitschke D, Benoist C, Streidenberger O, Stötzel H, Endres K, Herr C, Beisswenger C, Grimm H, Bals R, Lammert F, Hartmann T. Vitamin D and Its Analogues Decrease Amyloid-β (Aβ) Formation and Increase Aβ-Degradation. *Int J Mol Sci*. 2017;**18**: 2764. doi:10.3390/ijms18122764

170. Kato S, Takeyama K, Kitanaka S, Murayama A, Sekine K, Yoshizawa T. In vivo function of VDR in gene expression-VDR knock-out mice. *J Steroid Biochem Mol Biol*. 1999;**69**: 247–251. doi:10.1016/S0960-0760(99)00042-4

171. Lau SL, Stokes RA, Ng B, Cheng K, Clifton-Bligh R, Gunton JE. Metabolic changes in vitamin D receptor knockout mice. Bader M, editor. *PLoS One*. 2022;**17**: e0267573. doi:10.1371/journal.pone.0267573

172. Bouillon R, Bischoff-Ferrari H, Willett W. Vitamin D and health: Perspectives from mice and man. *Journal of Bone and Mineral Research*. 2008;**23**: 974–979. doi:10.1359/jbmr.080420

173. Hassan-Smith ZK, Jenkinson C, Smith DJ, Hernandez I, Morgan SA, Crabtree NJ, Gittoes NJ, Keevil BG, Stewart PM, Hewison M. 25-hydroxyvitamin D3 and 1,25-dihydroxyvitamin D3 exert distinct effects on human skeletal muscle function and gene expression. Campbell M, editor. *PLoS One*. 2017;**12**: e0170665. doi:10.1371/journal.pone.0170665

174. Ryan ZC, Craig TA, Folmes CD, Wang X, Lanza IR, Schaible NS, Salisbury JL, Nair KS, Terzic A, Sieck GC, Kumar R. 1α,25-Dihydroxyvitamin D3 Regulates Mitochondrial Oxygen Consumption and Dynamics in Human Skeletal Muscle Cells. *Journal of Biological Chemistry*. 2016;**291**: 1514–1528.

175. Bonaldo P, Sandri M. Cellular and molecular mechanisms of muscle atrophy. *Dis Model Mech*. 2013;**6**: 25–39.

176. Chen S, Villalta SA, Agrawal DK. FOXO1 Mediates Vitamin D Deficiency-Induced Insulin Resistance in Skeletal Muscle. *Journal of Bone and Mineral Research*. 2016;**31**: 585–595. doi:10.1002/jbmr.2729

177. An B-Soo, Tavera-Mendoza LE, Dimitrov Vassil, Wang X, Calderon MR, Wang H-Jun, White JH. Stimulation of Sirt1-Regulated FoxO Protein Function by the Ligand-Bound Vitamin D Receptor. *Mol Cell Biol*. 2010;**30**: 4890–4900.

178. Duan C, Ren H, Gao S. Insulin-like growth factors (IGFs), IGF receptors, and IGF-binding proteins: roles in skeletal muscle growth and differentiation. *Gen Comp Endocrinol*. 2010;**167**: 344–351.

179. Ren H, Yin P, Duan C. IGFBP-5 regulates muscle cell differentiation by binding to IGF-II and switching on the IGF-II auto-regulation loop. *Journal of Cell Biology*. 2008;**182**: 979–991.

180. Schedlich LJ, Muthukaruppan A, O'Han MK, Baxter RC. Insulin-Like Growth Factor Binding Protein-5 Interacts with the Vitamin D Receptor and Modulates the Vitamin D Response in Osteoblasts. *Molecular Endocrinology*. 2007;**21**: 2378–2390.

181. Matilainen M, Malinen M, Saavalainen K, Carlberg C. Regulation of multiple insulin-like growth factor binding protein genes by 1α,25-dihydroxyvitamin D3. *Nucleic Acids Res*. 2005;**33**: 5521–5532.

182. Schiaffino S, Mammucari C. Regulation of skeletal muscle growth by the IGF1-Akt/PKB pathway: insights from genetic models. *Skelet Muscle*. 2011;**1**: 1–14.

183. Wang J, Fry CME, Walker CL. Carboxyl-terminal modulator protein regulates Akt signaling during skeletal muscle atrophy in vitro and a mouse model of amyotrophic lateral sclerosis. *Sci Rep*. 2019;**9**: 1–10.

184. Wang Q, He Y, Shen Y, Zhang Q, Chen D, Zuo C, Qin J, Wang H, Wang J, Yu Y. Vitamin D Inhibits COX-2 Expression and Inflammatory Response by Targeting Thioesterase Superfamily Member 4. *Journal of Biological Chemistry*. 2014;**289**: 11681–11694.

185. Partridge L, Gems D. Mechanisms of Ageing: Public or Private? *Nat Rev Genet*. 2002;**3**: 165–175.

186. Mera P, Laue K, Ferron M, Confavreux C, Wei J, Galán-Diez M, Lacampagne A, Mitchell SJ, Mattison JA, Chen Y, Bacchetta J, Szulc P, Kitis RN, de Cabo R, Friedman RA, Torsitano C, McGraw TE, Puchowicz M, Kurland I, Karsenty G. Osteocalcin signaling in myofibers is necessary and sufficient for optimum adaptation to exercise. *Cell Metab*. 2017;**23**: 1078–1092.

187. Lisse TS, Liu T, Irmler M, Beckers J, Chen H, Adams JS, Hewison Martin. Gene targeting by the vitamin D response element binding protein reveals a role for vitamin D in osteoblast mTOR signaling. *The FASEB Journal*. 2011;**25**: 937–947.

188. Clemens TL, Karsenty G. The osteoblast: an insulin target cell controlling glucose homeostasis. *Journal of Bone and Mineral Research*. 2011;**26**: 677–680.

189. Sims NA, White CP, Sunn KL, Thomas GP, Drummond ML, Morrison NA, Eisman JA, Gardiner EM. Human and murine Osteocalcin gene expression: conserved tissue restricted expression and divergent responses to 1,25-dihydroxyvitamin D3 in vivo. *Molecular Endocrinology*. 1997;**11**: 1695–1708.

190. Oury F, Khrimian L, Denny CA, Gardin A, Chamouni A, Goeden N, Huang Y, Lee H, Srinivas Prashanth, Gao X-Bing, Suyama S, Langer T, Mann JJ, Horvath TL, Bonnin A, Karsenty G. Maternal and offspring pools of osteocalcin influence brain development and functions. *Cell*. 2013;**155**.

191. Liu H, Niu A, Chen S-Ei, Li Y-Ping. Beta3-integrin Mediates Satellite Cell Differentiation in Regenerating Mouse Muscle. *FASEB Journal*. 2011;**25**: 1914–1921.

192. Alberts B, Johnson A, Lewis J, Raff M, Roberts K, Walter P. Molecular Biology of the Cell. 2008.

193. Posa F, Di Benedetto A, Cavalcanti-Adam EA, Colaianni G, Porro C, Trotta T, Brunetti G, Lo Muzio L, Grano M, Mori G. Vitamin D Promotes MSC Osteogenic Differentiation Stimulating Cell Adhesion and α V β 3 Expression. *Stem Cells Int*. 2018;**2018**: 1–9. doi:10.1155/2018/6958713

194. Breen L, Phillips SM. Skeletal muscle protein metabolism in the elderly: Interventions to counteract the "anabolic resistance" of ageing. *Nutr Metab (Lond)*. 2011;**8**: 68. doi:10.1186/1743-7075-8-68

195. Tipton KD, Hamilton DL, Gallagher IJ. Assessing the Role of Muscle Protein Breakdown in Response to Nutrition and Exercise in Humans. *Sports Medicine*. 2018;**48**: 53–64. doi:10.1007/s40279-017-0845-5

196. Bhat M, Kalam R, Syh Qadri S, Madabushi S, Ismail A. Vitamin D deficiency-induced muscle wasting occurs through the ubiquitin proteasome pathway and is partially corrected by calcium in male rats. *Endocrinology*. 2013;**154**: 4018–4029. doi:10.1210/en.2013-1369

197. Bhat M, Ismail A. Vitamin D treatment protects against and reverses oxidative stress induced muscle proteolysis. *J Steroid Biochem Mol Biol*. 2015;**152**: 171–179. doi:10.1016/j.jsbmb.2015.05.012

198. Bard JAM, Goodall EA, Greene ER, Jonsson E, Dong KC, Martin A. Structure and Function of the 26S Proteasome. *Annu Rev Biochem*. 2018;**87**: 697–724. doi:10.1146/annurev-biochem-062917-011931

199. Lecker SH, Solomon V, Mitch WE, Goldberg AL. Muscle Protein Breakdown and the Critical Role of the Ubiquitin-Proteasome Pathway in Normal and Disease States. *J Nutr*. 1999;**129**: 227S-237S. doi:10.1093/jn/129.1.227S

200. Clavel S, Coldefy A-S, Kurkdjian E, Salles J, Margaritis I, Derijard B. Atrophy-related ubiquitin ligases, atrogin-1 and MuRF1 are up-regulated in aged rat Tibialis Anterior muscle. *Mech Ageing Dev*. 2006;**127**: 794–801. doi:10.1016/j.mad.2006.07.005

201. Brunet A, Bonni A, Zigmond MJ, Lin MZ, Juo P, Hu LS, Anderson MJ, Arden KC, Blenis J, Greenberg ME. Akt Promotes Cell Survival by Phosphorylating and Inhibiting a Forkhead Transcription Factor. *Cell*. 1999;**96**: 857–868. doi:10.1016/S0092-8674(00)80595-4

202. HAYAKAWA N, FUKUMURA J, YASUNO H, FUJIMOTO-OUCHI K, KITAMURA H. 1α,25(OH)2D3 downregulates gene expression levels of muscle ubiquitin ligases MAFbx and MuRF1 in human myotubes. *Biomedical Research*. 2015;**36**: 71–80. doi:10.2220/biomedres.36.71

203. Hirose Y, Onishi T, Miura S, Hatazawa Y, Kamei Y. Vitamin D attenuates FOXO1-target atrophy gene expression in C2C12 muscle cells. *J Nutr Sci Vitaminol (Tokyo)*. 2018;**64**: 229–232. doi:10.3177/jnsv.64.229

204. Dzik KP, Skrobot W, Kaczor KB, Flis DJ, Karnia MJ, Libionka W, Antosiewicz J, Kloc W, Kaczor JJ. Vitamin D Deficiency Is Associated with Muscle Atrophy and Reduced Mitochondrial Function in Patients with Chronic Low Back Pain. *Oxid Med Cell Longev*. 2019;**2019**: 1–11. doi:10.1155/2019/6835341

205. Cheung WW, Hao S, Wang Z, Ding W, Zheng R, Gonzalez A, Zhan J, Zhou P, Li S, Esparza MC, Hoffman HM, Lieber RL, Mak RH. Vitamin D repletion ameliorates adipose tissue browning and muscle wasting in infantile nephropathic cystinosis-associated cachexia. *J Cachexia Sarcopenia Muscle*. 2020;**11**: 120–134. doi:10.1002/jcsm.12497

206. Gopinath SD. Inhibition of Stat3 signaling ameliorates atrophy of the soleus muscles in mice lacking the vitamin D receptor. *Skelet Muscle*. 2017;**7**: 2. doi:10.1186/s13395-017-0121-2

207. Lyons C, Roche H. Nutritional Modulation of AMPK-Impact upon Metabolic-Inflammation. *Int J Mol Sci*. 2018;**19**: 3092. doi:10.3390/ijms19103092

208. Vilchinskaya N, Krivoi I, Shenkman B. AMP-Activated Protein Kinase as a Key Trigger for the Disuse-Induced Skeletal Muscle Remodeling. *Int J Mol Sci*. 2018;**19**: 3558. doi:10.3390/ijms19113558

209. Chang E, Kim Y. Vitamin D Ameliorates Fat Accumulation with AMPK/SIRT1 Activity in C2C12 Skeletal Muscle Cells. *Nutrients*. 2019;**11**: 2806. doi:10.3390/nu11112806

210. Manna P, Achari AE, Jain SK. Vitamin D supplementation inhibits oxidative stress and upregulate SIRT1/AMPK/GLUT4 cascade in high glucose-treated 3T3L1 adipocytes and in adipose tissue of high fat diet-fed diabetic mice. *Arch Biochem Biophys*. 2017;**615**: 22–34. doi:10.1016/j.abb.2017.01.002

211. LI A, SHEN P, LIU S, WANG J, ZENG J, DU C. Vitamin D alleviates skeletal muscle loss and insulin resistance by inducing vitamin D receptor expression and regulating the AMPK/SIRT1 signaling pathway in mice. *Food Science and Technology*. 2022;**42**. doi:10.1590/fst.47921

212. Das A, Gopinath SD, Arimbasseri GA. Systemic ablation of vitamin D receptor leads to skeletal muscle glycogen storage disorder in mice. *J Cachexia Sarcopenia Muscle*. 2022;**13**: 467–480. doi:10.1002/jcsm.12841

213. Bass JJ, Kazi AA, Deane CS, Nakhuda A, Ashcroft SP, Brook MS, Wilkinson DJ, Phillips BE, Philp A, Tarum J, Kadi F, Andersen D, Garcia AM, Smith K, Gallagher IJ, Szewczyk NJ, Cleasby ME, Atherton PJ. The mechanisms of skeletal muscle atrophy in response to transient knockdown of the vitamin D receptor in vivo. *J Physiol*. 2021;**599**: 963–979. doi:10.1113/JP280652

214. Yuk J-M, Shin D-M, Lee H-M, Yang C-S, Jin HS, Kim K-K, Lee Z-W, Lee S-H, Kim J-M, Jo E-K. Vitamin D3 Induces Autophagy in Human Monocytes/Macrophages via Cathelicidin. *Cell Host Microbe*. 2009;**6**: 231–243. doi:10.1016/j.chom.2009.08.004

215. Jang W, Kim HJ, Li H, Jo KD, Lee MK, Song SH, Yang HO. 1,25-Dyhydroxyvitamin D3 attenuates rotenone-induced neurotoxicity in SH-SY5Y cells through induction of autophagy. *Biochem Biophys Res Commun*. 2014;**451**: 142–147. doi:10.1016/j.bbrc.2014.07.081

216. Buitrago CG, González Pardo V, De Boland AR, Boland R. Activation of Raf-1 through Ras and protein kinase Cα mediates 1α,25(OH)2-vitamin D3 regulation of the mitogen-activated protein kinase pathway in muscle cells. *Journal of Biological Chemistry*. 2003;**278**: 2199–2205. doi:10.1074/jbc.M205732200

217. Buitrago C, Pardo VG, Boland R. Role of VDR in 1α,25-dihydroxyvitamin D3-dependent non-genomic activation of MAPKs, Src and Akt in skeletal muscle cells. *Journal of Steroid Biochemistry and Molecular Biology*. 2013;**136**: 125–130. doi:10.1016/j.jsbmb.2013.02.013

218. Choi M, Park H, Cho S, Lee M. Vitamin D 3 supplementation modulates inflammatory responses from the muscle damage induced by high-intensity exercise in SD rats. *Cytokine*. 2013;**63**: 27–35. doi:10.1016/j.cyto.2013.03.018

219. Shi H, Scheffler JM, Zeng C, Pleitner JM, Hannon KM, Grant AL, Gerrard DE. Mitogen-activated protein kinase signaling is necessary for the maintenance of skeletal muscle mass. *American Journal of Physiology-Cell Physiology*. 2009;**296**: C1040–C1048. doi:10.1152/ajpcell.00475.2008

220. Buitrago C, Boland R. Caveolae and caveolin-1 are implicated in 1α,25(OH)2-vitamin D3-dependent modulation of Src, MAPK cascades and VDR localization in skeletal muscle cells. *J Steroid Biochem Mol Biol*. 2010;**121**: 169–175. doi:10.1016/j.jsbmb.2010.03.002

221. Capiati D, Benassati S, Boland RL. 1,25(OH)2-vitamin D3 induces translocation of the vitamin D receptor (VDR) to the plasma membrane

in skeletal muscle cells. *J Cell Biochem*. 2002;**86**: 128–135. doi:10.1002/jcb.10191

222. Ge Y, Wu A-L, Warnes C, Liu J, Zhang C, Kawasome H, Terada N, Boppart MD, Schoenherr CJ, Chen J. mTOR regulates skeletal muscle regeneration in vivo through kinase-dependent and kinase-independent mechanisms. *Am J Physiol Cell Physiol*. 2009;**297**.

223. Sandri M, Sandri C, Gilbert A, Skurk C, Calabria E, Picard A, Walsh K, Schiaffino S, Lecker SH, Goldberg AL. Foxo transcription factors induce the atrophy-related ubiquitin ligase atrogin-1 and cause skeletal muscle atrophy. *Cell*. 2004;**117**: 399–412. doi:10.1016/s0092-8674(04)00400-3

224. Gogulothu R, Nagar D, Gopalakrishnan S, Garlapati VR, Kallamadi PR, Ismail A. Disrupted expression of genes essential for skeletal muscle fibre integrity and energy metabolism in Vitamin D deficient rats. *Journal of Steroid Biochemistry and Molecular Biology*. 2020;**197**: 105525. doi:10.1016/j.jsbmb.2019.105525

225. Salles J, Chanet A, Giraudet C, Patrac V, Pierre P, Jourdan M, Luiking YC, Verlaan S, Migné C, Boirie Y, Walrand S. 1,25(OH)2-vitamin D3 enhances the stimulating effect of leucine and insulin on protein synthesis rate through Akt/PKB and mTOR mediated pathways in murine C2C12 skeletal myotubes. *Mol Nutr Food Res*. 2013;**57**: 2137–2146. doi:10.1002/mnfr.201300074

226. Schuelke M, Wagner KR, Stolz LE, Hübner C, Riebel T, Kömen W, Braun T, Tobin JF, Lee S-J. Myostatin Mutation Associated with Gross Muscle Hypertrophy in a Child. *New England Journal of Medicine*. 2004;**350**: 2682–2688. doi:10.1056/NEJMoa040933

227. McPherron AC, Lawler AM, Lee S-J. Regulation of skeletal muscle mass in mice by a new TGF-beta superfamily member. *Nature*. 1997;**387**: 83–90. doi:10.1038/387083a0

228. Lopez JR, Kaura V, Diggle CP, Hopkins PM, Allen PD. Malignant hyperthermia, environmental heat stress, and intracellular calcium dysregulation in a mouse model expressing the p.G2435R variant of RYR1. *Br J Anaesth*. 2018;**121**: 953–961. doi:10.1016/j.bja.2018.07.008

229. Capiati DA, Vazquez G, Tellez Iñón MT, Boland RL. Role of protein kinase C in 1,25(OH)2-vitamin D3 modulation of intracellular calcium during development of skeletal muscle cells in culture. *J Cell Biochem*. 2000;**77**: 200–212. doi:10.1002/(SICI)1097-4644(20000501)77:2<200::AID-JCB4>3.0.CO;2-5

230. Capiati DA, Vazquez G, Boland RL. Protein Kinase C α Modulates the Ca2+ Influx Phase of the Ca2+ Response to 1α,25-Dihydroxy-Vitamin-D3 in Skeletal Muscle Cells. *Hormone and Metabolic Research*. 2001;**33**: 201–206. doi:10.1055/s-2001-14950

231. Boyan BD, Sylvia VL, McKinney N, Schwartz Z. Membrane actions of vitamin D metabolites 1,25(OH)2D3 and 24R,25(OH)2D3 are retained in growth plate cartilage cells from vitamin D receptor knockout mice. *J Cell Biochem*. 2003;**90**: 1207–1223. doi:10.1002/jcb.10716

232. Vazquez Guillermo, de Boland ARusso, Boland RL. 1α,25-Dihydroxy-vitamin-D 3 -induced Store-operated Ca 2+ Influx in Skeletal Muscle Cells. *Journal of Biological Chemistry*. 1998;**273**: 33954–33960. doi:10.1074/jbc.273.51.33954

233. Santillán G, Katz S, Vazquez G, Boland RL. TRPC3-like protein and Vitamin D receptor mediate 1α,25(OH)2D3-induced SOC influx in muscle cells. *Int J Biochem Cell Biol*. 2004;**36**: 1910–1918. doi:10.1016/j.biocel.2004.01.027

234. Zanou N, Schakman O, Louis P, Ruegg UT, Dietrich A, Birnbaumer L, Gailly P. Trpc1 Ion Channel Modulates Phosphatidylinositol 3-Kinase/Akt Pathway during Myoblast Differentiation and Muscle Regeneration. *Journal of Biological Chemistry*. 2012;**287**: 14524–14534. doi:10.1074/jbc.M112.341784

235. Zhang C, Liu Z, Xie Z. 1,25-Dihydroxyvitamin D promotes calcium influx in human skeletal muscle myotubes. *Osteoporos Sarcopenia*. 2017;**3**.

236. Constantin B, Cognard C, Raymond G. Myoblast fusion requires cytosolic calcium elevation but not activation of voltage-dependent calcium channels. *Cell Calcium*. 1996;**19**: 365–374. doi:10.1016/S0143-4160(96)90109-8

237. Hindi SM, Tajrishi MM, Kumar A. Signaling Mechanisms in Mammalian Myoblast Fusion. *Science Signalling*. 2013;**6**: 1–18. doi:10.1038/jid.2014.371

238. Pleasure D, Wyszynski B, Sumner A, Schotland D, Feldmann B, Nugent N, Hitz K, Goodman DBP. Skeletal Muscle Calcium Metabolism and Contractile Force in Vitamin D-deficient Chicks. *Journal of Clinical Investigation*. 1979;**64**: 1157–1167. doi:10.1172/JCI109569

239. Rodman JS, Baker T. Changes in the kinetics of muscle contraction in vitamin D-depleted rats. *Kidney Int*. 1978;**13**: 189–193. doi:10.1038/ki.1978.28

240. Zhou J, Dhakal K, Yi J. Mitochondrial Ca2+ uptake in skeletal muscle health and disease. *Sci China Life Sci*. 2016;**59**: 770–776. doi:10.1007/s11427-016-5089-3

241. Mukherjee A, Zetwekh JE, Nicar MJ, McCoy K, Buja LM. Effect of chronic vitamin D deficiency on chick heart mitochondrial oxidative phosphorylation. *J Mol Cell Cardiol*. 1981;**13**: 171–183. doi:10.1016/0022-2828(81)90214-5

242. Latham CM, Brightwell CR, Keeble AR, Munson BD, Thomas NT, Zagzoog AM, Fry CS, Fry JL. Vitamin D Promotes Skeletal Muscle Regeneration and Mitochondrial Health. *Front Physiol*. 2021;**12**. doi:10.3389/fphys.2021.660498

243. Ashcroft SP, Fletcher G, Philp AM, Atherton PJ, Philp A. Diet-induced vitamin D deficiency results in reduced skeletal muscle mitochondrial respiration in C57BL/6J mice. *bioRxiv*. 2020. doi:10.1101/2020.05.15.098087

244. Ashcroft SP, Bass JJ, Kazi AA, Atherton PJ, Philp A. The vitamin D receptor regulates mitochondrial function in C2C12 myoblasts. *American Journal of Physiology-Cell Physiology*. 2020;**318**: C536–C541. doi:10.1152/ajpcell.00568.2019

245. Silvagno F, Consiglio M, Foglizzo V, Destefanis M, Pescarmona G. Mitochondrial Translocation of Vitamin D Receptor Is Mediated by the Permeability Transition Pore in Human Keratinocyte Cell Line. Makishima M, editor. *PLoS One*. 2013;**8**: e54716. doi:10.1371/journal.pone.0054716

246. Romeu Montenegro K, Carlessi R, Cruzat V, Newsholme P. Effects of vitamin D on primary human skeletal muscle cell proliferation, differentiation, protein synthesis and bioenergetics. *Journal of Steroid Biochemistry and Molecular Biology*. 2019;**193**: 105423. doi:10.1016/j.jsbmb.2019.105423

247. Schnell DM, Walton RG, Vekaria HJ, Sullivan PG, Bollinger LM, Peterson CA, Thomas DT. Vitamin D produces a perilipin 2-dependent increase in mitochondrial function in C2C12 myotubes. *J Nutr Biochem*. 2019;**65**: 83–92. doi:10.1016/J.JNUTBIO.2018.11.002

248. Sinha A, Hollingsworth KG, Ball S, Cheetham T. Improving the Vitamin D Status of Vitamin D Deficient Adults Is Associated With Improved Mitochondrial Oxidative Function in Skeletal Muscle. *J Clin Endocrinol Metab*. 2013;**98**: E509–E513. doi:10.1210/jc.2012-3592

249. Silvagno F, Pescarmona G. Spotlight on vitamin D receptor, lipid metabolism and mitochondria: Some preliminary emerging issues. *Mol Cell Endocrinol*. 2017;**450**: 24–31. doi:10.1016/j.mce.2017.04.013

250. Muñoz García A, Eijssen LM, Kutmon M, Sarathy C, Cengo A, Hewison M, Evelo CT, Lenz M, Coort SL. A bioinformatics workflow to decipher transcriptomic data from vitamin D studies. *Journal of Steroid Biochemistry and Molecular Biology*. 2019;**189**: 28–35. doi:10.1016/j.jsbmb.2019.01.003

251. Ricca C, Aillon A, Bergandi L, Alotto D, Castagnoli C, Silvagno F. Vitamin D Receptor Is Necessary for Mitochondrial Function and Cell Health. *Int J Mol Sci*. 2018;**19**: 1672. doi:10.3390/ijms19061672

252. Abboud M, Puglisi DA, Davies BN, Rybchyn M, Whitehead NP, Brock KE, Cole L, Gordon-Thomson C, Fraser DR, Mason RS. Evidence for a Specific Uptake and Retention Mechanism for 25-Hydroxyvitamin D (25OHD) in Skeletal Muscle Cells. *Endocrinology*. 2013;**154**: 3022–3030. doi:10.1210/en.2012-2245

253. Otterbein LR, Cosio C, Graceffa P, Dominguez R. Crystal structures of the vitamin D-binding protein and its complex with actin: Structural basis of the actin-scavenger system. *Proceedings of the National Academy of Sciences*. 2002;**99**: 8003–8008. doi:10.1073/pnas.122126299

254. Clements MR, Fraser DR. Vitamin D supply to the rat fetus and neonate. *Journal of Clinical Investigation*. 1988;**81**: 1768–1773. doi:10.1172/JCI113518

255. Mason RS, Rybchyn MS, Abboud M, Brennan-Speranza TC, Fraser DR. The Role of Skeletal Muscle in Maintaining Vitamin D Status in Winter. *Curr Dev Nutr*. 2019;**3**. doi:10.1093/cdn/nzz087

256. Khanal P, He L, Herbert AJ, Stebbings GK, Onambele-Pearson GL, Degens H, Morse CI, Thomis M, Williams AG. The Association of Multiple Gene Variants with Ageing Skeletal Muscle Phenotypes in Elderly Women. *Genes (Basel)*. 2020;**11**: 1459. doi:10.3390/genes11121459

257. Appel M, Zentgraf K, Krüger K, Alack K. Effects of Genetic Variation on Endurance Performance, Muscle Strength, and Injury Susceptibility in Sports: A Systematic Review. *Front Physiol*. 2021;**12**. doi:10.3389/fphys.2021.694411

258. Tikkanen E, Gustafsson S, Amar D, Shcherbina A, Waggott D, Ashley EA, Ingelsson E. Biological Insights Into Muscular Strength: Genetic Findings

in the UK Biobank. *Sci Rep*. 2018;**8**: 6451. doi:10.1038/s41598-018-24735-y

259. Uitterlinden AG, Fang Y, van Meurs JBJ, Pols HAP, van Leeuwen JPTM. Genetics and biology of vitamin D receptor polymorphisms. *Gene*. 2004;**338**: 143–156. doi:10.1016/j.gene.2004.05.014

260. Scimeca M, Centofanti F, Celi M, Gasbarra E, Novelli G, Botta A, Tarantino U. Vitamin D receptor in muscle atrophy of elderly patients: A key element of osteoporosis-sarcopenia connection. *Aging Dis*. 2018;**9**: 952–964. doi:10.14336/AD.2018.0215

261. Roth SM, Zmuda JM, Cauley JA, Shea PR, Ferrell RE. Vitamin D Receptor Genotype Is Associated With Fat-Free Mass and Sarcopenia in Elderly Men. *J Gerontol A Biol Sci Med Sci*. 2004;**59**: B10–B15. doi:10.1093/gerona/59.1.B10

262. Bass JJ, Kazi AA, Deane CS, Nakhuda A, Ashcroft SP, Brook MS, Wilkinson DJ, Phillips BE, Philp A, Tarum J, Kadi F, Andersen D, Garcia AM, Smith K, Gallagher IJ, Szewczyk NJ, Cleasby ME, Atherton PJ. The mechanisms of skeletal muscle atrophy in response to transient knockdown of the vitamin D receptor in vivo. *J Physiol*. 2021;**599**: 963–979. doi:10.1113/JP280652

263. Liberati A, Altman DG, Tetzlaff J, Mulrow C, Gotzsche PC, Ioannidis JPA, Clarke M, Devereaux PJ, Kleijnen J, Moher D. The PRISMA statement for reporting systematic reviews and meta-analyses of studies that evaluate healthcare interventions: explanation and elaboration. *BMJ*. 2009;**339**: b2700–b2700. doi:10.1136/bmj.b2700

264. Sohani ZN, Meyre D, de Souza RJ, Joseph PG, Gandhi M, Dennis BB, Norman G, Anand SS. Assessing the quality of published genetic association studies in meta-analyses: the quality of genetic studies (Q-Genie) tool. *BMC Genet*. 2015;**16**: 50. doi:10.1186/s12863-015-0211-2

265. Cohen J, Attenasio A, Swenson S, Gu A, Gordish-Dressman H, Floor M, Harmon B, Hoffman E, Hittel D, Knoblach S, Devaney JM, Tosi LL. Vitamin D Receptor Polymorphisms are Associated with Baseline Muscle Strength and Response to Strength Training. 2017.

266. Grundberg E, Brändström H, Ribom EL, Ljunggren O, Mallmin H, Kindmark A. Genetic variation in the human vitamin D receptor is associated with muscle strength, fat mass and body weight in Swedish women. *Eur J Endocrinol*. 2004;**150**: 323–328. doi:10.1530/eje.0.1500323

267. Bahat G, Saka B, Erten N, Ozbek U, Coskunpinar E, Yildiz S, Sahinkaya T, Karan MA. BsmI polymorphism in the vitamin D receptor gene is associated with leg extensor muscle strength in elderly men. *Aging Clin Exp Res*. 2010;**22**: 198–205. doi:10.1007/BF03324797

268. Onder G, Capoluongo E, Danese P, Settanni S, Russo A, Concolino P, Bernabei R, Landi F. Vitamin D receptor polymorphisms and falls among older adults living in the community: Results from the ilSIRENTE study. *Journal of Bone and Mineral Research*. 2008;**23**: 1031–1036. doi:10.1359/jbmr.080225

269. Yao X, Yang L, Li M, Xiao H. Relationship of vitamin D receptor gene polymorphism with sarcopenia and muscle traits based on propensity score matching. *J Clin Lab Anal*. 2020;**34**: 1–8. doi:10.1002/jcla.23485

270. Bozsodi A, Boja S, Szilagyi A, Somhegyi A, Varga PP, Lazary A. Muscle strength is associated with vitamin D receptor gene variants. *Journal of Orthopaedic Research*. 2016;**34**: 2031–2037. doi:10.1002/jor.23220

271. Björk A, Ribom E, Johansson G, Scragg R, Mellström D, Grundberg E, Ohlsson C, Karlsson M, Ljunggren, Kindmark A. Variations in the vitamin D receptor gene are not associated with measures of muscle strength, physical performance, or falls in elderly men. Data from MrOS Sweden. *Journal of Steroid Biochemistry and Molecular Biology*. 2019;**187**: 160–165. doi:10.1016/j.jsbmb.2018.11.014

272. Hopkinson NS, Ka WL, Kehoe A, Humphries SE, Roughton M, Moxham J, Montgomery H, Polkey MI. Vitamin D receptor genotypes influence quadriceps strength in chronic obstructive pulmonary disease. *American Journal of Clinical Nutrition*. 2008;**87**: 385–390. doi:10.1093/ajcn/87.2.385

273. Walsh S, Ludlow AT, Metter EJ, Ferrucci L, Roth SM. Replication study of the vitamin D receptor (VDR) genotype association with skeletal muscle traits and sarcopenia. *Aging Clin Exp Res*. 2016;**28**: 435–442. doi:10.1007/s40520-015-0447-8

274. Xia Z, Man Q, Li L, Song P, Jia S, Song S, Meng L, Zhang J. Vitamin D receptor gene polymorphisms modify the association of serum 25-hydroxyvitamin D levels with handgrip strength in the elderly in Northern China. *Nutrition*. 2019;**57**: 202–207. doi:10.1016/j.nut.2018.05.025

275. Barr R, Macdonald H, Stewart A, McGuigan F, Rogers A, Eastell R, Felsenberg D, Glüer C, Roux C, Reid DM. Association between vitamin D receptor gene polymorphisms, falls, balance and muscle power: results

from two independent studies (APOSS and OPUS). *Osteoporosis International*. 2010;**21**: 457–466. doi:10.1007/s00198-009-1019-6

276. Gussago C, Arosio B, Guerini FR, Ferri E, Costa AS, Casati M, Bollini EM, Ronchetti F, Colombo E, Bernardelli G, Clerici M, Mari D. Impact of vitamin D receptor polymorphisms in centenarians. *Endocrine*. 2016;**53**: 558–564. doi:10.1007/s12020-016-0908-7

277. Wu FY, Liu CS, Liao LN, Li CI, Lin CH, Yang CW, Meng NH, Lin WY, Chang CK, Hsiao JH, Li TC, Lin CC. Vitamin D receptor variability and physical activity are jointly associated with low handgrip strength and osteoporosis in community-dwelling elderly people in Taiwan: The Taichung Community Health Study for Elders (TCHS-E). *Osteoporosis International*. 2014;**25**: 1917–1929. doi:10.1007/s00198-014-2691-8

278. Windelinckx A, De Mars G, Beunen G, Aerssens J, Delecluse C, Lefevre J, Thomis MAI. Polymorphisms in the vitamin D receptor gene are associated with muscle strength in men and women. *Osteoporosis International*. 2007;**18**: 1235–1242. doi:10.1007/s00198-007-0374-4

279. Van Pottelbergh I, Goemaere S, De Bacquer D, De Paepe A, Kaufman M. Vitamin D receptor gene allelic variants, bone density, and bone turnover in community-dwelling men. *Bone*. 2002;**31**: 631–637. doi:10.1016/S8756-3282(02)00867-0

280. Wang P, Ma LH, Wang HY, Zhang W, Tian Q, Cao DN, Zheng GX, Sun YL. Association between polymorphisms of vitamin D receptor gene ApaI, BsmI and TaqI and muscular strength in young Chinese women. *Int J Sports Med*. 2006;**27**: 182–186. doi:10.1055/s-2005-865626

281. Jolliffe DA, James WY, Hooper RL, Barnes NC, Greiller CL, Islam K, Bhowmik A, Timms PM, Rajakulasingam RK, Choudhury AB, Simcock DE, Hyppönen E, Walton RT, Corrigan CJ, Griffiths CJ, Martineau AR. Prevalence, determinants and clinical correlates of vitamin D deficiency in patients with Chronic Obstructive Pulmonary Disease in London, UK. *Journal of Steroid Biochemistry and Molecular Biology*. 2018;**175**: 138–145. doi:10.1016/j.jsbmb.2017.01.019

282. Garnero P, Munoz F, Borel O, Sornay-Rendu E, Delmas PD. Vitamin D receptor gene polymorphisms are associated with the risk of fractures in postmenopausal women, independently of bone mineral density. *Journal of Clinical Endocrinology and Metabolism*. 2005;**90**: 4829–4835. doi:10.1210/jc.2005-0364

283. Iki M, Saito Y, Dohi Y, Kajita E, Nishino H, Yonemasu K, Kusaka Y. Greater trunk muscle torque reduces postmenopausal bone loss at the spine independently of age, body size, and vitamin D receptor

genotype in Japanese women. *Calcif Tissue Int*. 2002;**71**: 300–307. doi:10.1007/s00223-001-2109-4

284. Murakami S-I, Otsuki T, Maeda M, Miura Y, Morii S, Kiyokane K, Hayakawa S-I, Maeda A, Imakawa T, Harada S, Handa T, Nishimura Y, Murakami S, Kumagai N, Hayashi H, Chen Y, Suemori S-I, Fukushima Y, Nishida S, Fukushima K. Effects of vitamin D receptor gene polymorphisms on low-resistance training using exercise machines: The 'Power Rehabilitation' program. *Int J Mol Med*. 2009;**23**: 81–88. doi:10.3892/ijmm

285. Bozsodi A, Boja S, Szilagyi A, Somhegyi A, Varga PP, Lazary A. Muscle strength is associated with vitamin D receptor gene variants. *Journal of Orthopaedic Research*. 2016;**34**.

286. Gross C, Krishnan A V., Malloy PJ, Eccleshall TR, Zhao X-Y, Feldman D. The Vitamin D Receptor Gene Start Codon Polymorphism: A Functional Analysis of FokI Variants. *Journal of Bone and Mineral Research*. 1998;**13**: 1691–1699. doi:10.1359/jbmr.1998.13.11.1691

287. Arai H, Miyamoto K-I, Taketani Y, Yamamoto H, Iemori Y, Morita K, Tonai T, Nishisho T, Mori S, Takeda E. A Vitamin D Receptor Gene Polymorphism in the Translation Initiation Codon: Effect on Protein Activity and Relation to Bone Mineral Density in Japanese Women. *Journal of Bone and Mineral Research*. 1997;**12**: 915–921. doi:10.1359/jbmr.1997.12.6.915

288. Halsall JA, Osborne JE, Potter L, Pringle JH, Hutchinson PE. A novel polymorphism in the 1A promoter region of the vitamin D receptor is associated with altered susceptibilty and prognosis in malignant melanoma. *Br J Cancer*. 2004;**91**: 765–770. doi:10.1038/sj.bjc.6602006

289. Lee SH, Gong HS. Measurement and Interpretation of Handgrip Strength for Research on Sarcopenia and Osteoporosis. *J Bone Metab*. 2020;**27**: 85. doi:10.11005/jbm.2020.27.2.85

290. Pratt J, Boreham C, Ennis S, Ryan AW, De Vito G. Genetic Associations with Aging Muscle: A Systematic Review. *Cells*. 2019;**9**: 1–31. doi:10.3390/cells9010012

291. Sirugo G, Williams SM, Tishkoff SA. The Missing Diversity in Human Genetic Studies. *Cell*. 2019;**177**: 26–31. doi:10.1016/j.cell.2019.02.048

292. Cruz-Jentoft AJ, Sayer AA. Sarcopenia. *The Lancet*. 2019;**393**: 2636–2646. doi:10.1016/S0140-6736(19)31138-9

293. Hwang J, Park S. Gender-Specific Risk Factors and Prevalence for Sarcopenia among Community-Dwelling Young-Old Adults. *Int J Environ Res Public Health*. 2022;**19**: 7232. doi:10.3390/ijerph19127232

294. Walston JD. Sarcopenia in older adults. *Curr Opin Rheumatol*. 2012;**24**: 623–627. doi:10.1097/BOR.0b013e328358d59b

295. Girgis CM, Mokbel N, Cha KM, Houweling PJ, Abboud M, Fraser DR, Mason RS, Clifton-Bligh RJ, Gunton JE. The Vitamin D Receptor (VDR) Is Expressed in Skeletal Muscle of Male Mice and Modulates 25-Hydroxyvitamin D (25OHD) Uptake in Myofibers. *Endocrinology*. 2014;**155**: 3227–3237. doi:10.1210/en.2014-1016

296. Bass JJ, Nakhuda A, Deane CS, Brook MS, Wilkinson DJ, Phillips BE, Philp A, Tarum J, Kadi F, Andersen D, Garcia AM, Smith K, Gallagher IJ, Szewczyk NJ, Cleasby ME, Atherton PJ. Overexpression of the vitamin D receptor (VDR) induces skeletal muscle hypertrophy. *Mol Metab*. 2020;**42**: 101059. doi:10.1016/j.molmet.2020.101059

297. Miyamoto K, Kesterson RA, Yamamoto H, Taketani Y, Nishiwaki E, Tatsumi S, Inoue Y, Morita K, Takeda E, Pike JW. Structural Organization of the Human Vitamin D Receptor Chromosomal Gene and Its Promoter. *Molecular Endocrinology*. 1997;**11**: 1165–1179. doi:10.1210/mend.11.8.9951

298. Fang Y, van Meurs JBJ, D'Alesio A, Jhamai M, Zhao H, Rivadeneira F, Hofman A, van Leeuwen JPT, Jehan F, Pols HAP, Uitterlinden AG. Promoter and 3'-Untranslated-Region Haplotypes in the Vitamin D Receptor Gene Predispose to Osteoporotic Fracture: The Rotterdam Study. *The American Journal of Human Genetics*. 2005;**77**: 807–823. doi:10.1086/497438

299. Rybchyn MS, Abboud M, Puglisi DA, Gordon-Thomson C, Brennan-Speranza TC, Mason RS, Fraser DR. Skeletal Muscle and the Maintenance of Vitamin D Status. *Nutrients*. 2020;**12**: 3270. doi:10.3390/nu12113270

300. Fu L, Yun F, Oczak M, Wong BYL, Vieth R, Cole DEC. Common genetic variants of the vitamin D binding protein (DBP) predict differences in response of serum 25-hydroxyvitamin D [25(OH)D] to vitamin D supplementation. *Clin Biochem*. 2009;**42**: 1174–1177. doi:10.1016/j.clinbiochem.2009.03.008

301. Perna L, Felix JF, Breitling LP, Haug U, Raum E, Burwinkel B, Schöttker B, Brenner H. Genetic Variations in the Vitamin D Binding Protein and Season-Specific Levels of Vitamin D Among Older Adults. *Epidemiology*. 2013;**24**: 104–109. doi:10.1097/EDE.0b013e318276c4b0

302. Lafi ZM, Irshaid YM, El-Khateeb M, Ajlouni KM, Hyassat D. Association of rs7041 and rs4588 Polymorphisms of the Vitamin D Binding Protein and the rs10741657 Polymorphism of CYP2R1 with Vitamin D Status Among Jordanian Patients. *Genet Test Mol Biomarkers*. 2015;**19**: 629–636. doi:10.1089/gtmb.2015.0058

303. Deere KC, Hannam K, Coulson J, Ireland A, McPhee JS, Moss C, Edwards MH, Dennison E, Cooper C, Sayers A, Lipperts M, Grimm B, Tobias JH. Quantifying Habitual Levels of Physical Activity According to Impact in Older People: Accelerometry Protocol for the VIBE Study. *J Aging Phys Act*. 2016;**24**: 290–295. doi:10.1123/japa.2015-0066

304. Piasecki J, McPhee JS, Hannam K, Deere KC, Elhakeem A, Piasecki M, Degens H, Tobias JH, Ireland A. Hip and spine bone mineral density are greater in master sprinters, but not endurance runners compared with non-athletic controls. *Arch Osteoporos*. 2018;**13**: 72. doi:10.1007/s11657-018-0486-9

305. Maden-Wilkinson TM, McPhee JS, Rittweger J, Jones DA, Degens H. Thigh muscle volume in relation to age, sex and femur volume. *Age (Omaha)*. 2014;**36**: 383–393. doi:10.1007/s11357-013-9571-6

306. Hannam K, Hartley A, Clark EM, Aihie Sayer A, Tobias JH, Gregson CL. Feasibility and acceptability of using jumping mechanography to detect early components of sarcopenia in community-dwelling older women. *J Musculoskelet Neuronal Interact*. 2017;**17**: 246–257.

307. Crossland H, Piasecki J, McCormick D, Phillips BE, Wilkinson DJ, Smith K, McPhee JS, Piasecki M, Atherton PJ. Targeted genotype analyses of GWAS-derived lean body mass and handgrip strength-associated single-nucleotide polymorphisms in elite master athletes. *Am J Physiol Regul Integr Comp Physiol*. 2020;**319**: R184–R194. doi:10.1152/ajpregu.00110.2020

308. Ye S. An efficient procedure for genotyping single nucleotide polymorphisms. *Nucleic Acids Res*. 2001;**29**: 88e–888. doi:10.1093/nar/29.17.e88

309. Kazemi SM, Esmaieli-bandboni A, Malekshahi ZV, Sardood MS, Hashemi M, Majidzadeh K, Kadkhodazadeh M, Esmaili R, Negahdari B. Vitamin D receptor gene polymorphisms and risk of breast cancer in Iranian women. *Annals of Medicine & Surgery*. 2022;**73**. doi:10.1016/j.amsu.2021.103150

310. Chatterjee S, Pal JK. Role of 5'- and 3'-untranslated regions of mRNAs in human diseases. *Biol Cell*. 2009;**101**: 251–262. doi:10.1042/BC20080104

311. Bergquist R, Weber M, Schwenk M, Ulseth S, Helbostad JL, Vereijken B, Taraldsen K. Performance-based clinical tests of balance and muscle strength used in young seniors: a systematic literature review. *BMC Geriatr*. 2019;**19**: 9. doi:10.1186/s12877-018-1011-0

312. Araujo CG, de Souza e Silva CG, Laukkanen JA, Fiatarone Singh M, Kunutsor SK, Myers J, Franca JF, Castro CL. Successful 10-second one-legged stance performance predicts survival in middle-aged and older individuals. *Br J Sports Med*. 2022;**56**: 975–980. doi:10.1136/bjsports-2021-105360

313. Fang Y, Van Meurs JB, Bergink AP, Hofman A, Van Duijn CM, Van Leeuwen JP, Pols HA, Uitterlinden AG. Cdx-2 Polymorphism in the Promoter Region of the Human Vitamin D Receptor Gene Determines Susceptibility to Fracture in the Elderly. *Journal of Bone and Mineral Research*. 2003;**18**: 1632–1641. doi:10.1359/jbmr.2003.18.9.1632

314. Arai H, Miyamoto K-I, Yoshida M, Yamamoto H, Taketani Y, Morita K, Kubota M, Yoshida S, Ikeda M, Watabe F, Kanemasa Y, Takeda E. The Polymorphism in the Caudal-Related Homeodomain Protein Cdx-2 Binding Element in the Human Vitamin D Receptor Gene. *Journal of Bone and Mineral Research*. 2001;**16**: 1256–1264. doi:10.1359/jbmr.2001.16.7.1256

315. Moreno Lima R, de Abreu BS, Gentil P, de Lima Lins TC, Grattapaglia D, Pereira RW, de Oliveira RJ. Lack of Association Between Vitamin D Receptor Genotypes and Haplotypes With Fat-Free Mass in Postmenopausal Brazilian Women. *J Gerontol A Biol Sci Med Sci*. 2007;**62**: 966–972. doi:10.1093/gerona/62.9.966

316. Vimaleswaran KS, Cavadino A, Berry DJ, Whittaker JC, Power C, Järvelin M-R, Hyppönen E. Genetic association analysis of vitamin D pathway with obesity traits. *Int J Obes*. 2013;**37**: 1399–1406. doi:10.1038/ijo.2013.6

317. Gu J, Xiao W, He J, Zhang H, Hu W, Hu Y, Li M, Liu Y, Fu W, Yu J, Gao G, Yue H, Ke Y, Zhang Z. Association between VDR and ESR1 gene polymorphisms with bone and obesity phenotypes in Chinese male nuclear families. *Acta Pharmacol Sin*. 2009;**30**: 1634–1642. doi:10.1038/aps.2009.169

318. Shere C, Fuggle NR, Edward MH, Parsons CM, Jameson KA, Cooper C, Dennison EM, Ward KA. Jumping Joints: The Complex Relationship

Between Osteoarthritis and Jumping Mechanography. *Calcif Tissue Int*. 2020;**106**: 115–123. doi:10.1007/s00223-019-00622-0

319. BELLINGER P, BOURNE MN, DUHIG S, LIEVENS E, KENNEDY B, MARTIN A, COOPER C, TREDREA M, RICE H, DERAVE W, MINAHAN C. Relationships between Lower Limb Muscle Characteristics and Force–Velocity Profiles Derived during Sprinting and Jumping. *Med Sci Sports Exerc*. 2021;**53**: 1400–1411. doi:10.1249/MSS.0000000000002605

320. Fitts RH, McDonald KS, Schluter JM. The determinants of skeletal muscle force and power: Their adaptability with changes in activity pattern. *J Biomech*. 1991;**24**: 111–122. doi:10.1016/0021-9290(91)90382-W

321. James R, Kazenwadel J. Homeobox gene expression in the intestinal epithelium of adult mice. *J Biol Chem*. 1991;**266**: 3246–51.

322. Morita A, Iki M, Dohi Y, Ikeda Y, Kagamimori S, Kagawa Y, Yoneshima H. Effects of the Cdx-2 Polymorphism of the Vitamin D Receptor Gene and Lifestyle Factors on Bone Mineral Density in a Representative Sample of Japanese Women: The Japanese Population-based Osteoporosis (JPOS) Study. *Calcif Tissue Int*. 2005;**77**: 339–347. doi:10.1007/s00223-005-0047-2

323. Boroňová I, Bernasovská J, Mačeková S, Kľoc J, Tomková Z, Bernasovský I, Šeliga P, Petrejčíková E, Zigová M, Blaščáková MM, Majherová M, Grejtáková D, Klamárová T. Association between vitamin D receptor gene polymorphisms (Fok I, Cdx-2) and bone mineral density in Slovak postmenopausal women. *Anthropologischer Anzeiger*. 2020;**77**: 195–203. doi:10.1127/anthranz/2020/1048

324. Kostik MM, Smirnov AM, Demin GS, Scheplyagina LA, Larionova VI. Juvenile idiopathic arthritis patients and their skeletal status: possible role of vitamin D receptor gene polymorphism. *Mol Biol Rep*. 2014;**41**: 1937–1943. doi:10.1007/s11033-014-3040-x

325. Chin K-Y, Ima-Nirwana S, Wan Ngah WZ. Vitamin D is significantly associated with total testosterone and sex hormone-binding globulin in Malaysian men. *The Aging Male*. 2015;**18**: 175–179. doi:10.3109/13685538.2015.1034686

326. Wang N, Han B, Li Q, Chen Y, Chen Y, Xia F, Lin D, Jensen MD, Lu Y. Vitamin D is associated with testosterone and hypogonadism in Chinese men: Results from a cross-sectional SPECT-China study. *Reproductive Biology and Endocrinology*. 2015;**13**: 74. doi:10.1186/s12958-015-0068-2

327. Zhao D, Ouyang P, de Boer IH, Lutsey PL, Farag YMK, Guallar E, Siscovick DS, Post WS, Kalyani RR, Billups KL, Michos ED. Serum vitamin D and sex hormones levels in men and women: The Multi-Ethnic Study of Atherosclerosis (MESA). *Maturitas*. 2017;**96**: 95–102. doi:10.1016/j.maturitas.2016.11.017

328. Kuhr DL, Sjaarda LA, Alkhalaf Z, Omosigho UR, Connell MT, Silver RM, Kim K, Perkins NJ, Holland TL, Plowden TC, Schisterman EF, Mumford SL. Vitamin D is associated with bioavailability of androgens in eumenorrheic women with prior pregnancy loss. *Am J Obstet Gynecol*. 2018;**218**: 608.e1-608.e6. doi:10.1016/j.ajog.2018.03.012

329. Braga V, Sangalli A, Malerba G, Mottes M, Mirandola S, Gatti D, Rossini M, Zamboni M, Adami S. Relationship Among VDR (BsmI and FokI), COLIA1, and CTR Polymorphisms with Bone Mass, Bone Turnover Markers, and Sex Hormones in Men. *Calcif Tissue Int*. 2002;**70**: 457–462. doi:10.1007/s00223-001-1088-9

330. Ranjzad F, Mahban A, Irani Shemirani A, Mahmoudi T, Vahedi M, Nikzamir A, Zali MR. Influence of gene variants related to calcium homeostasis on biochemical parameters of women with polycystic ovary syndrome. *J Assist Reprod Genet*. 2011;**28**: 225–232. doi:10.1007/s10815-010-9506-4

331. d'Alésio A, Garabédian M, Sabatier JP, Guaydier-Souquières G, Marcelli C, Lemaçon A, Walrant-Debray O, Jehan F. Two single-nucleotide polymorphisms in the human vitamin D receptor promoter change protein–DNA complex formation and are associated with height and vitamin D status in adolescent girls. *Hum Mol Genet*. 2005;**14**: 3539–3548. doi:10.1093/hmg/ddi382

332. Rengarajan J, Szabo SJ, Glimcher LH. Transcriptional regulation of Th1/Th2 polarization. *Immunol Today*. 2000;**21**: 479–483. doi:10.1016/S0167-5699(00)01712-6

333. Richetta AG, Silvestri V, Giancristoforo S, Rizzolo P, D'Epiro S, Graziano V, Mattozzi C, Navazio AS, Campoli M, D'Amico C, Scarnò M, Calvieri S, Ottini L. A-1012G Promoter Polymorphism of Vitamin D Receptor Gene Is Associated with Psoriasis Risk and Lower Allele-Specific Expression. *DNA Cell Biol*. 2014;**33**: 102–109. doi:10.1089/dna.2013.2217

334. Gardiner EM, Esteban LM, Fong C, Allison SJ, Flanagan JL, Kouzmenko AP, Eisman JA. Vitamin D receptor B1 and exon 1d: functional and evolutionary analysis. *J Steroid Biochem Mol Biol*. 2004;**89–90**: 233–238. doi:10.1016/j.jsbmb.2004.03.078

335. Batai K, Murphy AB, Shah E, Ruden M, Newsome J, Agate S, Dixon MA, Chen HY, Deane LA, Hollowell CMP, Ahaghotu C, Kittles RA. Common vitamin D pathway gene variants reveal contrasting effects on serum vitamin D levels in African Americans and European Americans. *Hum Genet*. 2014;**133**: 1395–1405. doi:10.1007/s00439-014-1472-y

336. Elkum N, Alkayal F, Noronha F, Ali MM, Melhem M, Al-Arouj M, Bennakhi A, Behbehani K, Alsmadi O, Abubaker J. Vitamin D Insufficiency in Arabs and South Asians Positively Associates with Polymorphisms in GC and CYP2R1 Genes. Katoh M, editor. *PLoS One*. 2014;**9**: e113102. doi:10.1371/journal.pone.0113102

337. Engelman CD, Fingerlin TE, Langefeld CD, Hicks PJ, Rich SS, Wagenknecht LE, Bowden DW, Norris JM. Genetic and Environmental Determinants of 25-Hydroxyvitamin D and 1,25-Dihydroxyvitamin D Levels in Hispanic and African Americans. *J Clin Endocrinol Metab*. 2008;**93**: 3381–3388. doi:10.1210/jc.2007-2702

338. Gaffney-Stomberg E, Lutz LJ, Shcherbina A, Ricke DO, Petrovick M, Cropper TL, Cable SJ, McClung JP. Association Between Single Gene Polymorphisms and Bone Biomarkers and Response to Calcium and Vitamin D Supplementation in Young Adults Undergoing Military Training. *Journal of Bone and Mineral Research*. 2017;**32**: 498–507. doi:10.1002/jbmr.3008

339. Arnaud J, Constans J. Affinity differences for vitamin D metabolites associated with the genetic isoforms of the human serum carrier protein (DBP). *Hum Genet*. 1993;**92**. doi:10.1007/BF00219689

340. Carter GD, Phinney KW. Assessing Vitamin D Status: Time for a Rethink? *Clin Chem*. 2014;**60**: 809–811. doi:10.1373/clinchem.2013.219386

341. Powe CE, Evans MK, Wenger J, Zonderman AB, Berg AH, Nalls M, Tamez H, Zhang D, Bhan I, Karumanchi SA, Powe NR, Thadhani R. Vitamin D–Binding Protein and Vitamin D Status of Black Americans and White Americans. *New England Journal of Medicine*. 2013;**369**: 1991–2000. doi:10.1056/NEJMoa1306357

342. Bikle D, Bouillon R, Thadhani R, Schoenmakers I. Vitamin D metabolites in captivity? Should we measure free or total 25(OH)D to assess vitamin D status? *J Steroid Biochem Mol Biol*. 2017;**173**: 105–116. doi:10.1016/j.jsbmb.2017.01.007

343. Ashraf AP, Huisingh C, Alvarez JA, Wang X, Gower BA. Insulin Resistance Indices Are Inversely Associated With Vitamin D Binding

Protein Concentrations. *J Clin Endocrinol Metab*. 2014;**99**: 178–183. doi:10.1210/jc.2013-2452

344. Kuliczkowska-Plaksej J, Pasquali R, Milewicz A, Lwow F, Jedrzejuk D, Bolanowski M. Serum Vitamin D Binding Protein Level Associated with Metabolic Cardiovascular Risk Factors in Women with the Polycystic Ovary Syndrome. *Hormone and Metabolic Research*. 2019;**51**: 54–61. doi:10.1055/a-0759-7533

345. Viloria K, Nasteska D, Briant LJB, Heising S, Larner DP, Fine NHF, Ashford FB, da Silva Xavier G, Ramos MJ, Hasib A, Cuozzo F, Manning Fox JE, MacDonald PE, Akerman I, Lavery GG, Flaxman C, Morgan NG, Richardson SJ, Hewison M, Hodson DJ. Vitamin-D-Binding Protein Contributes to the Maintenance of α Cell Function and Glucagon Secretion. *Cell Rep*. 2020;**31**: 107761. doi:10.1016/j.celrep.2020.107761

346. Borges CR, Jarvis JW, Oran PE, Nelson RW. Population Studies of Vitamin D Binding Protein Microheterogeneity by Mass Spectrometry Lead to Characterization of its Genotype-Dependent O-Glycosylation Patterns. *J Proteome Res*. 2008;**7**: 4143–4153. doi:10.1021/pr8002936

347. Cui C-Y, Ferrucci L. Macrophages in skeletal muscle aging. *Aging*. 2020;**12**: 3–4. doi:10.18632/aging.102740

348. Bai J, Liu F. The Yin-Yang functions of macrophages in metabolic disorders. *Life Medicine*. 2022;**1**: 319–332. doi:10.1093/lifemedi/lnac035

349. Lopez DV, Al-Jaberi FAH, Woetmann A, Ødum N, Bonefeld CM, Kongsbak-Wismann M, Geisler C. Macrophages Control the Bioavailability of Vitamin D and Vitamin D-Regulated T Cell Responses. *Front Immunol*. 2021;**12**. doi:10.3389/fimmu.2021.722806

350. Gressner OA, Lahme B, Gressner AM. Gc-globulin (vitamin D binding protein) is synthesized and secreted by hepatocytes and internalized by hepatic stellate cells through Ca2+-dependent interaction with the megalin/gp330 receptor. *Clinica Chimica Acta*. 2008;**390**: 28–37. doi:10.1016/j.cca.2007.12.011

351. Boutin B, Galbraith RM, Arnaud P. Comparative affinity of the major genetic variants of human group-specific component (vitamin D-binding protein) for 25-(OH) vitamin D3. *J Steroid Biochem*. 1989;**32**: 59–63. doi:10.1016/0022-4731(89)90014-9

352. Pedersen JT, Østergaard J, Houen G, Heegaard NHH. Affinity capillary electrophoresis for identification and investigation of human Gc-

globulin (vitamin D-binding protein) and its isoforms interacting with G-actin. *Electrophoresis*. 2008;**29**: 1723–1733. doi:10.1002/elps.200700618

353. Rivera-Paredez B, Hidalgo-Bravo A, León-Reyes G, Antuna-Puente B, Flores YN, Salmerón J, Velázquez-Cruz R. Association of GC Variants with Bone Mineral Density and Serum VDBP Concentrations in Mexican Population. *Genes (Basel)*. 2021;**12**: 1176. doi:10.3390/genes12081176

354. Wang Y, Zhu J, DeLuca HF. Where is the vitamin D receptor? *Arch Biochem Biophys*. 2012;**523**: 123–133. doi:10.1016/j.abb.2012.04.001

355. Brennan-Speranza TC, Mor D, Mason RS, Bartlett JR, Duque G, Levinger I, Levinger P. Skeletal muscle vitamin D in patients with end stage osteoarthritis of the knee. *J Steroid Biochem Mol Biol*. 2017;**173**: 180–184. doi:10.1016/j.jsbmb.2017.01.022

356. Rana P, Marwaha RK, Kumar P, Narang A, Devi MM, Tripathi RP, Khushu S. Effect of vitamin D supplementation on muscle energy phospho-metabolites: a 31 P magnetic resonance spectroscopy-based pilot study. *Endocr Res*. 2014;**39**: 152–156. doi:10.3109/07435800.2013.865210

357. Sadra V, Khabbazi A, Kolahi S, Hajialiloo M, Ghojazadeh M. Randomized double-blind study of the effect of dexamethasone and methylprednisolone pulse in the control of rheumatoid arthritis flare-up: a preliminary study. *Int J Rheum Dis*. 2014;**17**: 389–393. doi:10.1111/1756-185X.12278

358. Group TRC. Dexamethasone in Hospitalized Patients with Covid-19. *New England Journal of Medicine*. 2021;**384**: 693–704. doi:10.1056/NEJMoa2021436

359. Schakman O, Kalista S, Barbé C, Loumaye A, Thissen JP. Glucocorticoid-induced skeletal muscle atrophy. *Int J Biochem Cell Biol*. 2013;**45**: 2163–2172. doi:10.1016/j.biocel.2013.05.036

360. Li W, Qin X, Poon CC, Wong M, Feng R, Wang J, Lin F, Sun Y, Liu S, Wang Y, Zhang Y. Vitamin D/Vitamin D Receptor Signaling Attenuates Skeletal Muscle Atrophy by Suppressing Renin-Angiotensin System. *Journal of Bone and Mineral Research*. 2022;**37**: 121–136. doi:10.1002/jbmr.4441

361. Krzysztofik, Wilk, Wojdała, Gołaś. Maximizing Muscle Hypertrophy: A Systematic Review of Advanced Resistance Training Techniques and Methods. *Int J Environ Res Public Health*. 2019;**16**: 4897. doi:10.3390/ijerph16244897

362. Fink J, Schoenfeld BJ, Nakazato K. The role of hormones in muscle hypertrophy. *Phys Sportsmed*. 2018;**46**: 129–134. doi:10.1080/00913847.2018.1406778

363. Rommel C, Bodine SC, Clarke BA, Rossman R, Nunez L, Stitt TN, Yancopoulos GD, Glass DJ. Mediation of IGF-1-induced skeletal myotube hypertrophy by PI(3)K/Akt/mTOR and PI(3)K/Akt/GSK3 pathways. *Nat Cell Biol*. 2001;**3**: 1009–1013. doi:10.1038/ncb1101-1009

364. Latres E, Amini AR, Amini AA, Griffiths J, Martin FJ, Wei Y, Lin HC, Yancopoulos GD, Glass DJ. Insulin-like Growth Factor-1 (IGF-1) Inversely Regulates Atrophy-induced Genes via the Phosphatidylinositol 3-Kinase/Akt/Mammalian Target of Rapamycin (PI3K/Akt/mTOR) Pathway. *Journal of Biological Chemistry*. 2005;**280**: 2737–2744. doi:10.1074/jbc.M407517200

365. Frost RA, Nystrom GJ, Lang CH. Lipopolysaccharide regulates proinflammatory cytokine expression in mouse myoblasts and skeletal muscle. *American Journal of Physiology-Regulatory, Integrative and Comparative Physiology*. 2002;**283**: R698–R709. doi:10.1152/ajpregu.00039.2002

366. Bivona III JJ, Mank MM, Stapleton RD, Files DC, Toth MJ, Poynter ME. Skeletal Muscle Myofibers Directly Contribute to LPS-Induced Systemic Inflammatory Tone. *Front Pharmacol*. 2022;**13**. doi:10.3389/fphar.2022.917917

367. Nonaka K, Akiyama J, Yoshikawa Y, Une S, Ito K. 1,25-Dihydroxyvitamin D3 Inhibits Lipopolysaccharide-Induced Interleukin-6 Production by C2C12 Myotubes. *Medicina (B Aires)*. 2020;**56**: 450. doi:10.3390/medicina56090450

368. Gatera VA, Lesmana R, Musfiroh I, Judistiani RTD, Setiabudiawan B, Abdulah R. Vitamin D Inhibits Lipopolysaccharide (LPS)-Induced Inflammation in A549 Cells by Downregulating Inflammatory Cytokines. *Med Sci Monit Basic Res*. 2021;**27**. doi:10.12659/MSMBR.931481

369. Ge X, Wang L, Li M, Xu N, Yu F, Yang F, Li R, Zhang F, Zhao B, Du J. Vitamin D/VDR signaling inhibits LPS-induced IFNγ and IL-1β in Oral epithelia by regulating hypoxia-inducible factor-1α signaling pathway. *Cell Communication and Signaling*. 2019;**17**: 18. doi:10.1186/s12964-019-0331-9

370. Du J, Jiang S, Hu Z, Tang S, Sun Y, He J, Li Z, Yi B, Wang J, Zhang H, Li YC. Vitamin D receptor activation protects against lipopolysaccharide-induced acute kidney injury through suppression of tubular cell

apoptosis. *American Journal of Physiology-Renal Physiology*. 2019;**316**: F1068–F1077. doi:10.1152/ajprenal.00332.2018

371. Rio DC, Ares M, Hannon GJ, Nilsen TW. Purification of RNA Using TRIzol (TRI Reagent). *Cold Spring Harb Protoc*. 2010;**2010**: pdb.prot5439. doi:10.1101/pdb.prot5439

372. Schmittgen TD, Livak KJ. Analyzing real-time PCR data by the comparative CT method. *Nat Protoc*. 2008;**3**: 1101–1108. doi:10.1038/nprot.2008.73

373. Bass JJ, Kazi AA, Deane CS, Nakhuda A, Ashcroft SP, Brook MS, Wilkinson DJ, Phillips BE, Philp A, Tarum J, Kadi F, Andersen D, Garcia AM, Smith K, Gallagher IJ, Szewczyk NJ, Cleasby ME, Atherton PJ. The mechanisms of skeletal muscle atrophy in response to transient knockdown of the vitamin D receptor in vivo. *J Physiol*. 2021;**599**: 963–979. doi:10.1113/JP280652

374. Olsson K, Saini A, Strömberg A, Alam S, Lilja M, Rullman E, Gustafsson T. Evidence for Vitamin D receptor expression and direct effects of 1α,25(OH)2D3 in human skeletal muscle precursor cells. Endocrinology. 2016. pp. 98–111. doi:10.1210/en.2015-1685

375. Chen H, Hu X, Yang R, Wu G, Tan Q, Goltzman D, Miao D. SIRT1/FOXO3a axis plays an important role in the prevention of mandibular bone loss induced by 1,25(OH) 2 D deficiency. *Int J Biol Sci*. 2020;**16**: 2712–2726. doi:10.7150/ijbs.48169

376. Jia J, Tao X, Tian Z, Liu J, Ye X, Zhan Y. Vitamin D receptor deficiency increases systolic blood pressure by upregulating the renin-angiotensin system and autophagy. *Exp Ther Med*. 2022;**23**: 314. doi:10.3892/etm.2022.11243

377. Tavera-Mendoza LE, Westerling T, Libby E, Marusyk A, Cato L, Cassani R, Cameron LA, Ficarro SB, Marto JA, Klawitter J, Brown M. Vitamin D receptor regulates autophagy in the normal mammary gland and in luminal breast cancer cells. *Proceedings of the National Academy of Sciences*. 2017;**114**. doi:10.1073/pnas.1615015114

378. Zhang Z, Zhang L, Zhou Y, Li L, Zhao J, Qin W, Jin Z, Liu W. Increase in HDAC9 suppresses myoblast differentiation via epigenetic regulation of autophagy in hypoxia. *Cell Death Dis*. 2019;**10**: 552. doi:10.1038/s41419-019-1763-2

379. Tanaka M, Kishimoto KN, Okuno H, Saito H, Itoi E. Vitamin D receptor gene silencing effects on differentiation of myogenic cell lines. *Muscle Nerve*. 2014;**49**: 700–708. doi:10.1002/mus.23950

380. Hawke TJ, Meeson AP, Jiang N, Graham S, Hutcheson K, DiMaio JM, Garry DJ. p21 is essential for normal myogenic progenitor cell function in regenerating skeletal muscle. *American Journal of Physiology-Cell Physiology*. 2003;**285**: C1019–C1027. doi:10.1152/ajpcell.00055.2003

381. Pickholtz I, Saadyan S, Keshet GI, Wang VS, Cohen R, Bouwman P, Jonkers J, Byers SW, Papa MZ, Yarden RI. Cooperation between BRCA1 and vitamin D is critical for histone acetylation of the p21waf1 promoter and for growth inhibition of breast cancer cells and cancer stem-like cells. *Oncotarget*. 2014;**5**: 11827–11846. doi:10.18632/oncotarget.2582

382. Pajalunga D, Puggioni EMR, Mazzola A, Leva V, Montecucco A, Crescenzi M. DNA Replication Is Intrinsically Hindered in Terminally Differentiated Myotubes. Blagosklonny M V., editor. *PLoS One*. 2010;**5**: e11559. doi:10.1371/journal.pone.0011559

383. Stuart CA, Stone WL, Howell MEA, Brannon MF, Hall HK, Gibson AL, Stone MH. Myosin content of individual human muscle fibers isolated by laser capture microdissection. *American Journal of Physiology-Cell Physiology*. 2016;**310**: C381–C389. doi:10.1152/ajpcell.00317.2015

384. Resnicow DI, Deacon JC, Warrick HM, Spudich JA, Leinwand LA. Functional diversity among a family of human skeletal muscle myosin motors. *Proceedings of the National Academy of Sciences*. 2010;**107**: 1053–1058. doi:10.1073/pnas.0913527107

385. Watson EL, Wilkinson TJ, O'Sullivan TF, Baker LA, Gould DW, Xenophontos S, Graham-Brown M, Major R, Jenkinson C, Hewison M, Philp A, Smith AC. Association between vitamin D deficiency and exercise capacity in patients with CKD, a cross-sectional analysis. *J Steroid Biochem Mol Biol*. 2021;**210**: 105861. doi:10.1016/j.jsbmb.2021.105861

386. Jiang Z, Zhang L, Yao Z, Cao W, Ma S, Chen Y, Guang L, Zheng Z, Li C, Yu K, Shyh-Chang N. Machine learning-based phenotypic screening for postmitotic growth inducers uncover vitamin D3 metabolites as small molecule ribosome agonists. *Cell Prolif*. 2022;**55**. doi:10.1111/cpr.13214

387. Szabadkai G, Duchen MR. Mitochondria: The Hub of Cellular Ca 2+ Signaling. *Physiology*. 2008;**23**: 84–94. doi:10.1152/physiol.00046.2007

388. Miyazaki M, McCarthy JJ, Esser KA. Insulin like growth factor-1-induced phosphorylation and altered distribution of tuberous sclerosis complex

(TSC)1/TSC2 in C2C12 myotubes. *FEBS Journal*. 2010;**277**: 2180–2191. doi:10.1111/j.1742-4658.2010.07635.x

389. Gou Z, Li F, Qiao F, Maimaititusvn G, Liu F. Causal associations between insulin-like growth factor 1 and vitamin D levels: a two-sample bidirectional Mendelian randomization study. *Front Nutr*. 2023;**10**. doi:10.3389/fnut.2023.1162442

390. Witkowska-Sędek E, Kucharska A, Rumińska M, Pyrżak B. Relationship Between 25(OH)D and IGF-I in Children and Adolescents with Growth Hormone Deficiency. 2016. pp. 43–49. doi:10.1007/5584_2016_212

391. Song Y, Fleet JC, Kato S. Vitamin D Receptor (VDR) Knockout Mice Reveal VDR-Independent Regulation of Intestinal Calcium Absorption and ECaC2 and Calbindin D9k mRNA. *J Nutr*. 2003;**133**: 374–380. doi:10.1093/jn/133.2.374

392. Ameri P, Giusti A, Boschetti M, Murialdo G, Minuto F, Ferone D. Interactions between vitamin D and IGF-I: from physiology to clinical practice. *Clin Endocrinol (Oxf)*. 2013;**79**: 457–463. doi:10.1111/cen.12268

393. Buitrago CG, Arango NS, Boland RL. 1α,25(OH) 2D 3-dependent modulation of Akt in proliferating and differentiating C2C12 skeletal muscle cells. *J Cell Biochem*. 2012;**113**: 1170–1181. doi:10.1002/jcb.23444

394. Cui Q-L, Zheng W-H, Quirion R, Almazan G. Inhibition of Src-like Kinases Reveals Akt-dependent and -independent Pathways in Insulin-like Growth Factor I-mediated Oligodendrocyte Progenitor Survival. *Journal of Biological Chemistry*. 2005;**280**: 8918–8928. doi:10.1074/jbc.M414267200

395. Nakashima K, Ishida A. Regulation of Autophagy in Chick Myotubes: Effects of Insulin, Insulin-Like Growth Factor-I, and Amino Acids. *J Poult Sci*. 2018;**55**: 257–262. doi:10.2141/jpsa.0170196

396. O'Neill BT, Lee KY, Klaus K, Softic S, Krumpoch MT, Fentz J, Stanford KI, Robinson MM, Cai W, Kleinridders A, Pereira RO, Hirshman MF, Abel ED, Accili D, Goodyear LJ, Nair KS, Kahn CR. Insulin and IGF-1 receptors regulate FoxO-mediated signaling in muscle proteostasis. *Journal of Clinical Investigation*. 2016;**126**: 3433–3446. doi:10.1172/JCI86522

397. Stitt TN, Drujan D, Clarke BA, Panaro F, Timofeyva Y, Kline WO, Gonzalez M, Yancopoulos GD, Glass DJ. The IGF-1/PI3K/Akt Pathway Prevents Expression of Muscle Atrophy-Induced Ubiquitin Ligases by

Inhibiting FOXO Transcription Factors. *Mol Cell*. 2004;**14**: 395–403. doi:10.1016/S1097-2765(04)00211-4

398. Coleman ME, DeMayo F, Yin KC, Lee HM, Geske R, Montgomery C, Schwartz RJ. Myogenic Vector Expression of Insulin-like Growth Factor I Stimulates Muscle Cell Differentiation and Myofiber Hypertrophy in Transgenic Mice. *Journal of Biological Chemistry*. 1995;**270**: 12109–12116. doi:10.1074/jbc.270.20.12109

399. Lin Y-A, Li Y-R, Chang Y-C, Hsu M-C, Chen S-T. Activation of IGF-1 pathway and suppression of atrophy related genes are involved in Epimedium extract (icariin) promoted C2C12 myotube hypertrophy. *Sci Rep*. 2021;**11**: 10790. doi:10.1038/s41598-021-89039-0

400. Das S, Morvan F, Morozzi G, Jourde B, Minetti GC, Kahle P, Rivet H, Brebbia P, Toussaint G, Glass DJ, Fornaro M. ATP Citrate Lyase Regulates Myofiber Differentiation and Increases Regeneration by Altering Histone Acetylation. *Cell Rep*. 2017;**21**: 3003–3011. doi:10.1016/j.celrep.2017.11.038

401. Trappe S, Trappe T, Gallagher P, Harber M, Alkner B, Tesch P. Human single muscle fibre function with 84 day bed-rest and resistance exercise. *J Physiol*. 2004;**557**: 501–513. doi:10.1113/jphysiol.2004.062166

402. Andersen JL, Aagaard P. Myosin heavy chain IIX overshoot in human skeletal muscle. *Muscle Nerve*. 2000;**23**: 1095–1104. doi:10.1002/1097-4598(200007)23:7<1095::AID-MUS13>3.0.CO;2-O

403. Kim R, Kim H, Im M, Park SK, Han HJ, An S, Kang J-S, Lee S-J, Bae G-U. BST204 Protects Dexamethasone-Induced Myotube Atrophy through the Upregulation of Myotube Formation and Mitochondrial Function. *Int J Environ Res Public Health*. 2021;**18**: 2367. doi:10.3390/ijerph18052367

404. Kim J, Park MY, Kim HK, Park Y, Whang K-Y. Cortisone and dexamethasone inhibit myogenesis by modulating the AKT/mTOR signaling pathway in C2C12. *Biosci Biotechnol Biochem*. 2016;**80**: 2093–2099. doi:10.1080/09168451.2016.1210502

405. Wang H, Kubica N, Ellisen LW, Jefferson LS, Kimball SR. Dexamethasone Represses Signaling through the Mammalian Target of Rapamycin in Muscle Cells by Enhancing Expression of REDD1. *Journal of Biological Chemistry*. 2006;**281**: 39128–39134. doi:10.1074/jbc.M610023200

406. Hidalgo AA, Deeb KK, Pike JW, Johnson CS, Trump DL. Dexamethasone Enhances 1α,25-Dihydroxyvitamin D3 Effects by Increasing Vitamin D

Receptor Transcription. *Journal of Biological Chemistry*. 2011;**286**: 36228–36237. doi:10.1074/jbc.M111.244061

407. Akeno N, Matsunuma A, Maeda T, Kawane T, Horiuchi N. Regulation of vitamin D-1alpha-hydroxylase and -24-hydroxylase expression by dexamethasone in mouse kidney. *Journal of Endocrinology*. 2000;**164**: 339–348. doi:10.1677/joe.0.1640339

408. Zhang Y, Leung DYM, Goleva E. Vitamin D Enhances Glucocorticoid Action in Human Monocytes. *Journal of Biological Chemistry*. 2013;**288**: 14544–14553. doi:10.1074/jbc.M112.427054

409. Noh KK, Chung KW, Choi YJ, Park MH, Jang EJ, Park CH, Yoon C, Kim ND, Kim MK, Chung HY. β–Hydroxy β–Methylbutyrate Improves Dexamethasone-Induced Muscle Atrophy by Modulating the Muscle Degradation Pathway in SD Rat. Gallouzi IE, editor. *PLoS One*. 2014;**9**: e102947. doi:10.1371/journal.pone.0102947

410. Syverud BC, VanDusen KW, Larkin LM. Effects of Dexamethasone on Satellite Cells and Tissue Engineered Skeletal Muscle Units. *Tissue Eng Part A*. 2016;**22**: 480–489. doi:10.1089/ten.tea.2015.0545

411. Lin J-W, Huang Y-M, Chen Y-Q, Chuang T-Y, Lan T-Y, Liu Y-W, Pan H-W, You L-R, Wang Y-K, Lin K, Chiou A, Kuo J-C. Dexamethasone accelerates muscle regeneration by modulating kinesin-1-mediated focal adhesion signals. *Cell Death Discov*. 2021;**7**: 35. doi:10.1038/s41420-021-00412-4

412. Sun L, Trausch-Azar JS, Muglia LJ, Schwartz AL. Glucocorticoids differentially regulate degradation of MyoD and Id1 by N-terminal ubiquitination to promote muscle protein catabolism. *Proceedings of the National Academy of Sciences*. 2008;**105**: 3339–3344. doi:10.1073/pnas.0800165105

413. Furlow JD, Watson ML, Waddell DS, Neff ES, Baehr LM, Ross AP, Bodine SC. Altered gene expression patterns in muscle ring finger 1 null mice during denervation- and dexamethasone-induced muscle atrophy. *Physiol Genomics*. 2013;**45**: 1168–85. doi:10.1152/physiolgenomics.00022.2013

414. Llano-Diez M, Fury W, Okamoto H, Bai Y, Gromada J, Larsson L. RNA-sequencing reveals altered skeletal muscle contraction, E3 ligases, autophagy, apoptosis, and chaperone expression in patients with critical illness myopathy. *Skelet Muscle*. 2019;**9**: 9. doi:10.1186/s13395-019-0194-1

415. Beharry AW, Judge AR. Differential expression of HDAC and HAT genes in atrophying skeletal muscle. *Muscle Nerve*. 2015;**52**: 1098–1101. doi:10.1002/mus.24912

416. Macpherson PCD, Farshi P, Goldman D. Dach2-Hdac9 signaling regulates reinnervation of muscle endplates. *Development*. 2015. doi:10.1242/dev.125674

417. Reed SA, Sandesara PB, Senf SM, Judge AR. Inhibition of FoxO transcriptional activity prevents muscle fiber atrophy during cachexia and induces hypertrophy. *The FASEB Journal*. 2012;**26**: 987–1000. doi:10.1096/fj.11-189977

418. Kang S-H, Lee H-A, Kim M, Lee E, Sohn UD, Kim I. Forkhead box O3 plays a role in skeletal muscle atrophy through expression of E3 ubiquitin ligases MuRF-1 and atrogin-1 in Cushing's syndrome. *American Journal of Physiology-Endocrinology and Metabolism*. 2017;**312**: E495–E507. doi:10.1152/ajpendo.00389.2016

419. Bodine SC, Baehr LM. Skeletal muscle atrophy and the E3 ubiquitin ligases MuRF1 and MAFbx/atrogin-1. *American Journal of Physiology-Endocrinology and Metabolism*. 2014;**307**: E469–E484. doi:10.1152/ajpendo.00204.2014

420. Doyle A, Zhang G, Fattah EAA, Eissa NT, Li Y. Toll-like receptor 4 mediates lipopolysaccharide-induced muscle catabolism via coordinate activation of ubiquitin-proteasome and autophagy-lysosome pathways. *The FASEB Journal*. 2011;**25**: 99–110. doi:10.1096/fj.10-164152

421. Jin B, Li Y. Curcumin prevents lipopolysaccharide-induced atrogin-1/MAFbx upregulation and muscle mass loss. *J Cell Biochem*. 2007;**100**: 960–969. doi:10.1002/jcb.21060

422. Premer DM, Goertz R, Georgieff MK, Mammel MC, Schwarzenberg SJ. Muscle proteolysis and weight loss in a neonatal rat model of sepsis syndrome. *Inflammation*. 2002;**26**: 97–101. doi:10.1023/a:1014840412552

423. Dehoux MJM, van Beneden RP, Fernández-Celemín L, Lause PL, Thissen J-PM. Induction of MafBx and Murf ubiquitin ligase mRNAs in rat skeletal muscle after LPS injection. *FEBS Lett*. 2003;**544**: 214–217. doi:10.1016/S0014-5793(03)00505-2

424. Tarabees R, Hill D, Rauch C, Barrow PA, Loughna PT. Endotoxin transiently inhibits protein synthesis through Akt and MAPK mediating pathways in C2C12 myotubes. *American Journal of Physiology-Cell Physiology*. 2011;**301**: C895–C902. doi:10.1152/ajpcell.00387.2010

425. Pramanik R, Asplin JR, Lindeman C, Favus MJ, Bai S, Coe FL. Lipopolysaccharide negatively modulates vitamin D action by down-regulating expression of vitamin D-induced VDR in human monocytic THP-1 cells. *Cell Immunol*. 2004;**232**: 137–143. doi:10.1016/j.cellimm.2005.03.004

426. Zhao B, Li R, Yang F, Yu F, Xu N, Zhang F, Ge X, Du J. LPS-induced Vitamin D Receptor Decrease in Oral Keratinocytes Is Associated With Oral Lichen Planus. *Sci Rep*. 2018;**8**: 763. doi:10.1038/s41598-018-19234-z

427. Mokhtari-Zaer A, Hosseini M, Salmani H, Arab Z, Zareian P. Vitamin D3 attenuates lipopolysaccharide-induced cognitive impairment in rats by inhibiting inflammation and oxidative stress. *Life Sci*. 2020;**253**: 117703. doi:10.1016/j.lfs.2020.117703

428. Chen Y-H, Yu Z, Fu L, Wang H, Chen X, Zhang C, Lv Z-M, Xu D-X. Vitamin D3 inhibits lipopolysaccharide-induced placental inflammation through reinforcing interaction between vitamin D receptor and nuclear factor kappa B p65 subunit. *Sci Rep*. 2015;**5**: 10871. doi:10.1038/srep10871

429. Li H, Malhotra S, Kumar A. Nuclear factor-kappa B signaling in skeletal muscle atrophy. *J Mol Med*. 2008;**86**: 1113–1126. doi:10.1007/s00109-008-0373-8

430. Pan M, Liu J, Huang D, Guo Y, Luo K, Yang M, Gao W, Xu Q, Zhang W, Mai K. FoxO3 Modulates LPS-Activated Hepatic Inflammation in Turbot (Scophthalmus maximus L.). *Front Immunol*. 2021;**12**. doi:10.3389/fimmu.2021.679704

431. Yin Y, Wang J, Zhao X, Wu X, Zou H, Qin Z, Cao J. Overexpressed FOXO3 improves inflammatory status in mice by affecting NLRP3-mediated cell coronation in necrotizing colitis mice. *Biomedicine & Pharmacotherapy*. 2020;**125**: 109867. doi:10.1016/j.biopha.2020.109867

432. Liu Y-M, Lv J, Zeng Q-L, Shen S, Xing J-Y, Zhang Y-Y, Zhang Z-H, Yu Z-J. AMPK activation ameliorates D-GalN/LPS-induced acute liver failure by upregulating Foxo3A to induce autophagy. *Exp Cell Res*. 2017;**358**: 335–342. doi:10.1016/j.yexcr.2017.07.008

433. He Y, She H, Zhang T, Xu H, Cheng L, Yepes M, Zhao Y, Mao Z. p38 MAPK inhibits autophagy and promotes microglial inflammatory responses by phosphorylating ULK1. *Journal of Cell Biology*. 2018;**217**: 315–328. doi:10.1083/jcb.201701049

434. Jin L, Li J, Yang S, Zhang R, Hu C, Chen Y, Tian Z, Ma W, Feng Y, Liu N, Liu J, Yang Y, Chen T, Zhao Y, He Y, Yan T. MAPK p38/Ulk1 pathway inhibits autophagy and induces IL-1β expression in hepatic stellate cells. *American Journal of Physiology-Gastrointestinal and Liver Physiology*. 2022;**322**: G360–G367. doi:10.1152/ajpgi.00230.2021

435. She H, He Y, Zhao Y, Mao Z. Autophagy in inflammation: the p38α MAPK-ULK1 axis. *Macrophage (Houst)*. 2018;**5**.

436. Ono Y, Sakamoto K. Lipopolysaccharide inhibits myogenic differentiation of C2C12 myoblasts through the Toll-like receptor 4-nuclear factor-κB signaling pathway and myoblast-derived tumor necrosis factor-α. Asakura A, editor. *PLoS One*. 2017;**12**: e0182040. doi:10.1371/journal.pone.0182040

437. Shi L-L, Zhu K-C, Wang H-L. Characterization of myogenic regulatory factors, myod and myf5 from Megalobrama amblycephala and the effect of lipopolysaccharide on satellite cells in skeletal muscle. *Gene*. 2022;**834**: 146608. doi:10.1016/j.gene.2022.146608

438. Sattari M, Masoudnia M, Mashayekhi K, Hashemi SM, Khannazer N, Sattari S, Mohammadian Haftcheshmeh S, Momtazi-Borojeni AA. Evaluating the effect of <scp>LPS</scp> from periodontal pathogenic bacteria on the expression of senescence-related genes in human dental pulp stem cells. *J Cell Mol Med*. 2022;**26**: 5647–5656. doi:10.1111/jcmm.17594

439. Ring RH, Valo Z, Gao C, Barish ME, Singer-Sam J. The Cdkn1a gene (p21Waf1/Cip1) is an inflammatory response gene in the mouse central nervous system. *Neurosci Lett*. 2003;**350**: 73–76. doi:10.1016/S0304-3940(03)00883-8

440. Chen J, Chen XY, Cong XX, Wang S, Xu SB, Sun YT, Zhou YT, Zheng LL, Huang M. CELLULAR SENESCENCE IMPLICATED IN SEPSIS-INDUCED MUSCLE WEAKNESS AND AMELIORATED WITH METFORMIN. *Shock*. 2023;**59**: 646–656. doi:10.1097/SHK.0000000000002086

441. Xiao K, Zhang D-C, Hu Y, Song L-C, Xu J-Q, He W-X, Pan P, Wang Y-W, Xie L-X. Potential roles of vitamin D binding protein in attenuating liver injury in sepsis. *Mil Med Res*. 2022;**9**: 4. doi:10.1186/s40779-022-00365-4

442. Dahl B, Schiødt F V., Ott P, Wians F, Lee WM, Balko J, O'Keefe GE. Plasma concentration of Gc-globulin is associated with organ dysfunction and sepsis after injury. *Crit Care Med*. 2003;**31**: 152–156. doi:10.1097/00003246-200301000-00024

443. Suberviola B, Lavin BA, Jimenez AF, Perez-San Martin S, Garcia-Unzueta M, Santibañez M. Vitamin D binding protein, but not vitamin D or vitamin D-related peptides, is associated with septic shock mortality. *Enfermedades infecciosas y microbiologia clinica (English ed)*. 2019;**37**: 239–243. doi:10.1016/j.eimce.2018.06.007

444. Jeng L, Yamshchikov A V, Judd SE, Blumberg HM, Martin GS, Ziegler TR, Tangpricha V. Alterations in vitamin D status and anti-microbial peptide levels in patients in the intensive care unit with sepsis. *J Transl Med*. 2009;**7**: 28. doi:10.1186/1479-5876-7-28

445. Guan X, Yan Q, Wang D, Du G, Zhou J. IGF-1 Signaling Regulates Mitochondrial Remodeling during Myogenic Differentiation. *Nutrients*. 2022;**14**: 1249. doi:10.3390/nu14061249

446. Pharaoh G, Owen D, Yeganeh A, Premkumar P, Farley J, Bhaskaran S, Ashpole N, Kinter M, Van Remmen H, Logan S. Disparate Central and Peripheral Effects of Circulating IGF-1 Deficiency on Tissue Mitochondrial Function. *Mol Neurobiol*. 2020;**57**: 1317–1331. doi:10.1007/s12035-019-01821-4

447. Liu J, Peng Y, Wang X, Fan Y, Qin C, Shi L, Tang Y, Cao K, Li H, Long J, Liu J. Mitochondrial Dysfunction Launches Dexamethasone-Induced Skeletal Muscle Atrophy via AMPK/FOXO3 Signaling. *Mol Pharm*. 2016;**13**: 73–84. doi:10.1021/acs.molpharmaceut.5b00516

448. Huang Y, Chen K, Ren Q, Yi L, Zhu J, Zhang Q, Mi M. Dihydromyricetin Attenuates Dexamethasone-Induced Muscle Atrophy by Improving Mitochondrial Function via the PGC-1α Pathway. *Cellular Physiology and Biochemistry*. 2018;**49**: 758–779. doi:10.1159/000493040

449. Mitsui T, Azuma H, Nagasawa M, Iuchi T, Akaike M, Odomi M, Matsumoto T. Chronic corticosteroid administration causes mitochondrial dysfunction in skeletal muscle. *J Neurol*. 2002;**249**: 1004–1009. doi:10.1007/s00415-002-0774-5

450. Trzeciak S, McCoy J V., Phillip Dellinger R, Arnold RC, Rizzuto M, Abate NL, Shapiro NI, Parrillo JE, Hollenberg SM. Early increases in microcirculatory perfusion during protocol-directed resuscitation are associated with reduced multi-organ failure at 24 h in patients with sepsis. *Intensive Care Med*. 2008;**34**: 2210–2217. doi:10.1007/s00134-008-1193-6

451. Sun H, Huang Y, Yin C, Guo J, Zhao R, Yang X. Lipopolysaccharide markedly changes glucose metabolism and mitochondrial function in the longissimus muscle of pigs. *Animal*. 2016;**10**: 1204–1212. doi:10.1017/S1751731116000100

452. Hansen ME, Simmons KJ, Tippetts TS, Thatcher MO, Saito RR, Hubbard ST, Trumbull AM, Parker BA, Taylor OJ, Bikman BT. Lipopolysaccharide Disrupts Mitochondrial Physiology in Skeletal Muscle via Disparate Effects on Sphingolipid Metabolism. *Shock*. 2015;**44**: 585–592. doi:10.1097/SHK.0000000000000468

453. Frisard MI, Wu Y, McMillan RP, Voelker KA, Wahlberg KA, Anderson AS, Boutagy N, Resendes K, Ravussin E, Hulver MW. Low Levels of Lipopolysaccharide Modulate Mitochondrial Oxygen Consumption in Skeletal Muscle. *Metabolism*. 2015;**64**: 416–427. doi:10.1016/j.metabol.2014.11.007

454. Ascenzi F, Barberi L, Dobrowolny G, Villa Nova Bacurau A, Nicoletti C, Rizzuto E, Rosenthal N, Scicchitano BM, Musarò A. Effects of IGF-1 isoforms on muscle growth and sarcopenia. *Aging Cell*. 2019;**18**. doi:10.1111/acel.12954

455. Handayaningsih A-E, Iguchi G, Fukuoka H, Nishizawa H, Takahashi M, Yamamoto M, Herningtyas E-H, Okimura Y, Kaji H, Chihara K, Seino S, Takahashi Y. Reactive Oxygen Species Play an Essential Role in IGF-I Signaling and IGF-I-Induced Myocyte Hypertrophy in C2C12 Myocytes. *Endocrinology*. 2011;**152**: 912–921. doi:10.1210/en.2010-0981

456. Park C-M, Kim MJ, Kim S-M, Park J-H, Kim Z-H, Choi Y-S. Umbilical cord mesenchymal stem cell-conditioned media prevent muscle atrophy by suppressing muscle atrophy-related proteins and ROS generation. *In Vitro Cell Dev Biol Anim*. 2016;**52**: 68–76. doi:10.1007/s11626-015-9948-1

457. Ulla A, Uchida T, Miki Y, Sugiura K, Higashitani A, Kobayashi T, Ohno A, Nakao R, Hirasaka K, Sakakibara I, Nikawa T. Morin attenuates dexamethasone-mediated oxidative stress and atrophy in mouse C2C12 skeletal myotubes. *Arch Biochem Biophys*. 2021;**704**: 108873. doi:10.1016/j.abb.2021.108873

458. Zheng Z, Xie J, Ma L, Hao Z, Zhang W, Li L. Vitamin D Receptor Activation Targets ROS-Mediated Crosstalk Between Autophagy and Apoptosis in Hepatocytes in Cholestasic Mice. *Cell Mol Gastroenterol Hepatol*. 2023;**15**: 887–901. doi:10.1016/j.jcmgh.2022.10.011

459. Chen L, Yang R, Qiao W, Zhang W, Chen J, Mao L, Goltzman D, Miao D. 1,25-Dihydroxyvitamin D exerts an antiaging role by activation of Nrf2-antioxidant signaling and inactivation of p16/p53-senescence signaling. *Aging Cell*. 2019;**18**: e12951. doi:10.1111/acel.12951

460. Ray PD, Huang B-W, Tsuji Y. Reactive oxygen species (ROS) homeostasis and redox regulation in cellular signaling. *Cell Signal*. 2012;**24**: 981–990. doi:10.1016/j.cellsig.2012.01.008

461. Redza-Dutordoir M, Averill-Bates DA. Activation of apoptosis signalling pathways by reactive oxygen species. *Biochimica et Biophysica Acta (BBA) - Molecular Cell Research*. 2016;**1863**: 2977–2992. doi:10.1016/j.bbamcr.2016.09.012

462. Okoye CN, Koren SA, Wojtovich AP. Mitochondrial complex I ROS production and redox signaling in hypoxia. *Redox Biol*. 2023;**67**: 102926. doi:10.1016/j.redox.2023.102926

463. Berardo C, Siciliano V, Di Pasqua LG, Richelmi P, Vairetti M, Ferrigno A. Comparison between Lipofectamine RNAiMAX and GenMute transfection agents in two cellular models of human hepatoma. *European Journal of Histochemistry*. 2019;**63**. doi:10.4081/ejh.2019.3048

464. Lyons CN, Leary SC, Moyes CD. Bioenergetic remodeling during cellular differentiation: changes in cytochrome *c* oxidase regulation do not affect the metabolic phenotype. *Biochemistry and Cell Biology*. 2004;**82**: 391–399. doi:10.1139/o04-040

465. Kraft CS, LeMoine CMR, Lyons CN, Michaud D, Mueller CR, Moyes CD. Control of mitochondrial biogenesis during myogenesis. *American Journal of Physiology-Cell Physiology*. 2006;**290**: C1119–C1127. doi:10.1152/ajpcell.00463.2005

466. Leary SC, Battersby BJ, Hansford RG, Moyes CD. Interactions between bioenergetics and mitochondrial biogenesis. *Biochimica et Biophysica Acta (BBA) - Bioenergetics*. 1998;**1365**: 522–530. doi:10.1016/S0005-2728(98)00105-4

467. Dahl B, Gehrchen, F.V. Schiødt PM, Kiær, J. Ramlau T. Gc-globulin is an acute phase reactant and an indicator of muscle injury after spinal surgery. *Inflammation Research*. 2001;**50**: 39–43. doi:10.1007/s000110050722

468. Sudakov NP, Klimenkov I V., Byvaltsev VA, Nikiforov SB, Konstantinov YuM. Extracellular actin in health and disease. *Biochemistry (Moscow)*. 2017;**82**: 1–12. doi:10.1134/S0006297917010011

469. Yuan C, Song M, Zhang Y, Wolpin BM, Meyerhardt JA, Ogino S, Hollis BW, Chan AT, Fuchs CS, Wu K, Wang M, Smith-Warner SA, Giovannucci EL, Ng K. Prediagnostic Circulating Concentrations of Vitamin D Binding Protein and Survival among Patients with Colorectal Cancer. *Cancer*

Epidemiology, Biomarkers & Prevention. 2020;**29**: 2323–2331. doi:10.1158/1055-9965.EPI-20-0291

470. Lehka L, Rędowicz MJ. Mechanisms regulating myoblast fusion: A multilevel interplay. *Semin Cell Dev Biol*. 2020;**104**: 81–92. doi:10.1016/j.semcdb.2020.02.004

471. Kew RR, Tabrizian T, Vosswinkel JA, Davis JE, Jawa RS. Vitamin D–binding protein deficiency in mice decreases systemic and select tissue levels of inflammatory cytokines in a murine model of acute muscle injury. *Journal of Trauma and Acute Care Surgery*. 2018;**84**: 847–854. doi:10.1097/TA.0000000000001875

472. Raiteri T, Reano S, Scircoli A, Zaggia I, Prodam F, Filigheddu N. THU515 Vitamin D Binding Protein Induces Skeletal Muscle Atrophy And Contributes To Cancer-associated Muscle Wasting. Journal of the Endocrine Society. 2023. doi:10.1210/jendso/bvad114.2143

473. Swamy N, Ray R. Fatty acid-binding site environments of serum vitamin D-binding protein and albumin are different. *Bioorg Chem*. 2008;**36**: 165–8. doi:10.1016/j.bioorg.2008.02.002

474. Kew RR. The Vitamin D Binding Protein and Inflammatory Injury: A Mediator or Sentinel of Tissue Damage? *Front Endocrinol (Lausanne)*. 2019;**10**. doi:10.3389/fendo.2019.00470

475. Viloria K, Nasteska D, Ast J, Hasib A, Cuozzo F, Heising S, Briant LJB, Hewison M, Hodson DJ. GC-Globulin/Vitamin D–Binding Protein Is Required for Pancreatic α-Cell Adaptation to Metabolic Stress. *Diabetes*. 2023;**72**: 275–289. doi:10.2337/db22-0326

476. Wang G, Li Y, Li L, Yu F, Cui L, Ba Y, Li W, Wang C. Association of the vitamin D binding protein polymorphisms with the risk of type 2 diabetes mellitus: a meta-analysis. *BMJ Open*. 2014;**4**: e005617. doi:10.1136/bmjopen-2014-005617

477. Sabourin LA, Girgis-Gabardo A, Seale P, Asakura A, Rudnicki MA. Reduced Differentiation Potential of Primary MyoD −/− Myogenic Cells Derived from Adult Skeletal Muscle. *J Cell Biol*. 1999;**144**: 631–643. doi:10.1083/jcb.144.4.631

478. Lagirand-Cantaloube J, Cornille K, Csibi A, Batonnet-Pichon S, Leibovitch MP, Leibovitch SA. Inhibition of Atrogin-1/MAFbx Mediated MyoD Proteolysis Prevents Skeletal Muscle Atrophy In Vivo. Parise G, editor. *PLoS One*. 2009;**4**: e4973. doi:10.1371/journal.pone.0004973

479. Moretti I, Ciciliot S, Dyar KA, Abraham R, Murgia M, Agatea L, Akimoto T, Bicciato S, Forcato M, Pierre P, Uhlenhaut NH, Rigby PWJ, Carvajal JJ, Blaauw B, Calabria E, Schiaffino S. MRF4 negatively regulates adult skeletal muscle growth by repressing MEF2 activity. *Nat Commun*. 2016;**7**: 12397. doi:10.1038/ncomms12397

480. Pavlath GK, Dominov JA, Kegley KM, Miller JB. Regeneration of Transgenic Skeletal Muscles with Altered Timing of Expression of the Basic Helix-Loop-Helix Muscle Regulatory Factor MRF4. *Am J Pathol*. 2003;**162**: 1685–1691. doi:10.1016/S0002-9440(10)64303-9

481. Lucas L, Cooper TA. Insights into Cell-Specific Functions of Microtubules in Skeletal Muscle Development and Homeostasis. *Int J Mol Sci*. 2023;**24**: 2903. doi:10.3390/ijms24032903

482. Chang W, Webster DR, Salam AA, Gruber D, Prasad A, Eiserich JP, Bulinski JC. Alteration of the C-terminal Amino Acid of Tubulin Specifically Inhibits Myogenic Differentiation. *Journal of Biological Chemistry*. 2002;**277**: 30690–30698. doi:10.1074/jbc.M204930200

483. Sakurai T, Fujita Y, Ohto E, Oguro A, Atomi Y. The decrease of the cytoskeleton tubulin follows the decrease of the associating molecular chaperone αB-crystallin in unloaded soleus muscle atrophy without stretch. *The FASEB Journal*. 2005;**19**: 1199–1201. doi:10.1096/fj.04-3060fje

484. Khairallah RJ, Shi G, Sbrana F, Prosser BL, Borroto C, Mazaitis MJ, Hoffman EP, Mahurkar A, Sachs F, Sun Y, Chen Y-W, Raiteri R, Lederer WJ, Dorsey SG, Ward CW. Microtubules Underlie Dysfunction in Duchenne Muscular Dystrophy. *Sci Signal*. 2012;**5**. doi:10.1126/scisignal.2002829

485. Theodorakis NG, Cleveland DW. Physical evidence for cotranslational regulation of beta-tubulin mRNA degradation. *Mol Cell Biol*. 1992;**12**: 791–799. doi:10.1128/MCB.12.2.791

486. Agrawal A, Rathor R, Kumar R, Suryakumar G, Ganju L. Role of altered proteostasis network in chronic hypobaric hypoxia induced skeletal muscle atrophy. Kumar A, editor. *PLoS One*. 2018;**13**: e0204283. doi:10.1371/journal.pone.0204283

487. Lu S, Li Y, Shen Q, Zhang W, Gu X, Ma M, Li Y, Zhang L, Liu X, Zhang X. Carnosol and its analogues attenuate muscle atrophy and fat lipolysis induced by cancer cachexia. *J Cachexia Sarcopenia Muscle*. 2021;**12**: 779–795. doi:10.1002/jcsm.12710

488. Girón MD, Vílchez JD, Shreeram S, Salto R, Manzano M, Cabrera E, Campos N, Edens NK, Rueda R, López-Pedrosa JM. β-Hydroxy-β-Methylbutyrate (HMB) Normalizes Dexamethasone-Induced Autophagy-Lysosomal Pathway in Skeletal Muscle. Kumar A, editor. *PLoS One*. 2015;**10**: e0117520. doi:10.1371/journal.pone.0117520

489. Zhang S-F, Zhang Y, Li B, Chen N. Physical inactivity induces the atrophy of skeletal muscle of rats through activating AMPK/FoxO3 signal pathway. *Eur Rev Med Pharmacol Sci*. 2018;**22**: 199–209. doi:10.26355/eurrev_201801_14118

490. Jing Y, Zuo Y, Yu Y, Sun L, Yu Z, Ma S, Zhao Q, Sun G, Hu H, Li J, Huang D, Liu L, Li J, Xin Z, Huang H, Izpisua Belmonte JC, Zhang W, Wang S, Qu J, Liu G-H. Single-nucleus profiling unveils a geroprotective role of the FOXO3 in primate skeletal muscle aging. *Protein Cell*. 2022. doi:10.1093/procel/pwac061

491. Léger B, Derave W, De Bock K, Hespel P, Russell AP. Human Sarcopenia Reveals an Increase in SOCS-3 and Myostatin and a Reduced Efficiency of Akt Phosphorylation. *Rejuvenation Res*. 2008;**11**: 163-175B. doi:10.1089/rej.2007.0588

492. Cho JE, Fournier M, Da X, Lewis MI. Time course expression of Foxo transcription factors in skeletal muscle following corticosteroid administration. *J Appl Physiol*. 2010;**108**: 137–145. doi:10.1152/japplphysiol.00704.2009

493. Zhao J, Brault JJ, Schild A, Cao P, Sandri M, Schiaffino S, Lecker SH, Goldberg AL. FoxO3 Coordinately Activates Protein Degradation by the Autophagic/Lysosomal and Proteasomal Pathways in Atrophying Muscle Cells. *Cell Metab*. 2007;**6**: 472–483. doi:10.1016/j.cmet.2007.11.004

494. Kim J, Kundu M, Viollet B, Guan K-L. AMPK and mTOR regulate autophagy through direct phosphorylation of Ulk1. *Nat Cell Biol*. 2011;**13**: 132–141. doi:10.1038/ncb2152

495. Wang T, Liu C, Jia L. The roles of PKCs in regulating autophagy. *J Cancer Res Clin Oncol*. 2018;**144**: 2303–2311. doi:10.1007/s00432-018-2731-4

496. Geeraert C, Ratier A, Pfisterer SG, Perdiz D, Cantaloube I, Rouault A, Pattingre S, Proikas-Cezanne T, Codogno P, Poüs C. Starvation-induced Hyperacetylation of Tubulin Is Required for the Stimulation of Autophagy by Nutrient Deprivation. *Journal of Biological Chemistry*. 2010;**285**: 24184–24194. doi:10.1074/jbc.M109.091553

497. Köchl R, Hu XW, Chan EYW, Tooze SA. Microtubules Facilitate Autophagosome Formation and Fusion of Autophagosomes with Endosomes. *Traffic*. 2006;**7**: 129–145. doi:10.1111/j.1600-0854.2005.00368.x

498. Setayesh L, Casazza K, Moradi N, Mehranfar S, Yarizadeh H, Amini A, Yekaninejad MS, Mirzaei K. Association of vitamin D-binding protein and vitamin D3 with insulin and homeostatic model assessment (HOMA-IR) in overweight and obese females. *BMC Res Notes*. 2021;**14**: 193. doi:10.1186/s13104-021-05608-6

499. Mitsumoto Y, Burdett E, Grant A, Klip A. Differential expression of the GLUT1 and GLUT4 glucose transporters during differentiation of L6 muscle cells. *Biochem Biophys Res Commun*. 1991;**175**: 652–659. doi:10.1016/0006-291X(91)91615-J

500. Al-Khalili L, Chibalin A V., Kannisto K, Zhang BB, Permert J, Holman GD, Ehrenborg E, Ding VDH, Zierath JR, Krook A. Insulin action in cultured human skeletal muscle cells during differentiation: assessment of cell surface GLUT4 and GLUT1 content. *Cellular and Molecular Life Sciences*. 2003;**60**: 991–998. doi:10.1007/s00018-003-3001-3

501. Pereira LO, Lancha AH. Effect of insulin and contraction up on glucose transport in skeletal muscle. *Prog Biophys Mol Biol*. 2004;**84**: 1–27. doi:10.1016/S0079-6107(03)00055-5

502. Guillet-Deniau I, Leturque A, Girard J. Expression and cellular localization of glucose transporters (GLUT1, GLUT3, GLUT4) during differentiation of myogenic cells isolated from rat fœtuses. *J Cell Sci*. 1994;**107**: 487–496. doi:10.1242/jcs.107.3.487

503. Seraphim PM, Nunes MT, Giannocco G, Machado UF. Age related obesity-induced shortening of GLUT4 mRNA poly(A) tail length in rat gastrocnemius skeletal muscle. *Mol Cell Endocrinol*. 2007;**276**: 80–87. doi:10.1016/j.mce.2007.07.004

504. Nykjaer A, Fyfe JC, Kozyraki R, Leheste J-R, Jacobsen C, Nielsen MS, Verroust PJ, Aminoff M, de la Chapelle A, Moestrup SK, Ray R, Gliemann J, Willnow TE, Christensen EI. Cubilin dysfunction causes abnormal metabolism of the steroid hormone 25(OH) vitamin D 3. *Proceedings of the National Academy of Sciences*. 2001;**98**: 13895–13900. doi:10.1073/pnas.241516998

505. Sinotte M, Diorio C, Bérubé S, Pollak M, Brisson J. Genetic polymorphisms of the vitamin D binding protein and plasma concentrations of 25-hydroxyvitamin D in premenopausal women. *Am J Clin Nutr*. 2009;**89**: 634–640. doi:10.3945/ajcn.2008.26445

506. Braithwaite VS, Jones KS, Schoenmakers I, Silver M, Prentice A, Hennig BJ. Vitamin D binding protein genotype is associated with plasma 25OHD concentration in West African children. *Bone*. 2015;**74**: 166–170. doi:10.1016/j.bone.2014.12.068

507. Guillet-Deniau I, Leturque A, Girard J. Expression and cellular localization of glucose transporters (GLUT1, GLUT3, GLUT4) during differentiation of myogenic cells isolated from rat fœtuses. *J Cell Sci*. 1994;**107**: 487–496. doi:10.1242/jcs.107.3.487

508. MitoPedia - Bioblast. Available: https://wiki.oroboros.at/index.php/SUIT-008_O2_ce-pce_D025